MICROGLIAL PHAGOCYTOSIS OF BACTERIA AND SYNAPSES

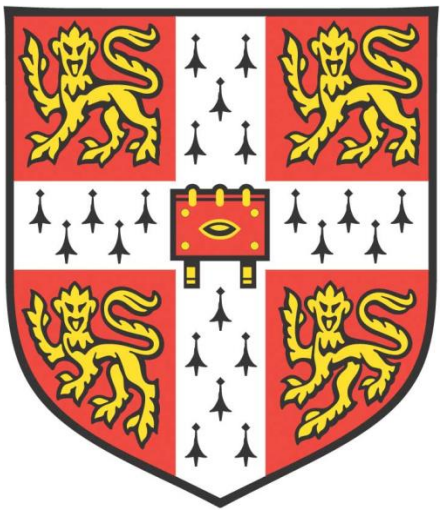

Thomas Oliver John Cockram

Downing College

Department of Biochemistry

University of Cambridge

This thesis is submitted for the degree of Doctor of Philosophy

December 2019

MICROGLIAL PHAGOCYTOSIS OF BACTERIA AND SYNAPSES

THOMAS OLIVER JOHN COCKRAM

ABSTRACT

Microglia, the resident brain macrophage, are essential for maintaining normal brain homeostasis through removal of pathogens - including bacteria and fungi - via phagocytosis. However, the mechanisms that regulate these phagocytic events are not clear. In this work, involvement of calreticulin, galectin-3, apolipoprotein E and β-amyloid in microglial phagocytosis of bacteria were studied. Microglia activated with bacterial endotoxin upregulated and released extracellular calreticulin and galectin-3 in culture, and both proteins could bind the surface of the gram-negative bacteria *E. coli*. Moreover, association of these proteins with the bacteria opsonised them for phagocytosis by microglia. This opsonisation was inhibitable by sugars, or by blocking microglial receptors MerTK or LRP1. LPS-activated microglia phagocytosed more *E. coli* than unactivated microglia, and this phagocytic induction was inhibited by an antibody against calreticulin, sugars, blocking MerTK or LRP1, or simply exchanging the cellular media. Thus, calreticulin and galectin-3 are bacterial opsonins, which may play an important role in immune responses to bacteria in the brain. Apolipoprotein E and β-amyloid – both of which are known to circulate extracellularly in the brain - also bound and opsonised *E. coli* for phagocytosis by microglia, and may further contribute to bacterial clearance in the brain.

Extracellular nucleotides mediate a variety of microglial functions by binding receptors exposed by the microglia, including the phagocytic receptor $P2Y_6R$ and the chemotactic receptor $P2Y_{12}R$. Both *E. coli* and inflammatory-activated microglia released extracellular agonist of $P2Y_6R$, as did non-activated microglia, astrocytes and pheochromocytoma under specific experimental conditions. Exogenous UDP induced microglial phagocytosis of the bacteria in a time-sensitive manner, and this effect was inhibitable by blocking $P2Y_6R$, suggesting that $P2Y_6R$ signalling regulates bacterial phagocytosis. Furthermore, LPS-induction of phagocytosis was inhibited by apyrase, or by blocking $P2Y_6R$, indicating that LPS-induced phagocytosis is mediated by microglial $P2Y_6R$. Moreover, exogenous ADP

(which activates $P2Y_{12}R$) inhibited *E. coli* phagocytosis by microglia, as did blocking $P2Y_{12}R$, consistent with a role for ADP- $P2Y_{12}R$ signalling in microglial chemotaxis toward bacteria.

In addition to eliminating pathogens, microglial phagocytosis of synapses is a crucial facilitator of the 'synaptic pruning' that occurs in the developing brain, but this regulation is poorly understood. Here, the mechanisms that regulate microglial phagocytosis of synapses were studied. Calreticulin and galectin-3 opsonised isolated synapses, or 'synaptosomes', in a similar fashion to the bacteria, suggesting diverse regulatory functions for these proteins. Microglial phagocytosis of synaptosomes was also enhanced by apolipoprotein E and extracellular tau, which may play a role in pathological synaptic loss during neurodegeneration. In addition, blocking $P2Y_6R$ or $P2Y_{12}R$ inhibited microglial phagocytosis of synaptosomes. Through a novel model of inflammatory synaptic loss in cerebellar neuronal cultures, LPS was found to induce synaptic loss without neuronal loss, which was mediated by microglia and consistent with microglial phagocytosis of the synapses. Such synaptic loss was absent in cultures lacking $P2Y_6R$, and in cultures treated with a $P2Y_{12}R$ antagonist – further implicating both $P2Y_6R$ and $P2Y_{12}R$ in microglial phagocytosis of synapses.

Taken together, these findings provide insights into novel mechanisms through which microglial phagocytosis of two diverse targets – bacteria and synapses - is regulated.

ACKNOWLEDGEMENTS

I would first like to thank Professor Guy Brown - for allowing me to work in his lab, for countless scientific discussions, and for his continued and tireless supervision and guidance, particularly during the write-up phase of my thesis.

I would also like to thank members of the Brown Lab, past and present, for their endless support, motivation and friendship over the course of my PhD. In particular, I would like to thank Mar Puigdellivol, David Allendorf, Claire Butler, Anna Vilalta, Alma Popescu, Michael Baumgartner, Stefan Milde, Miguel Burguillos, Jeff Lee and Michiko Inouye. I would like to extend a special thanks to Mar Puigdellivol, Anna Vilalta and Stefan Milde for their guidance and instruction on the bench. Together, these wonderful people contributed to a fantastic working environment, and were a reliable and much-needed source of encouragement throughout. I would also like to extend this thanks to other members of the Skylab – particularly Samantha Salvage, Johanna Rees, Jenny Jeffreys, Kerry Price, Susanne Mesøy, Bijun Tang, Ana Couto and Steven Devenish.

I also want to thank everyone with whom I shared such amazing times at 27 Ross Street – particularly my 'little' housemate. In these people, I was always able to find encouragement and motivation when things were looking bleak, and with them, I was also able to share the happier moments when things were going well. They were truly my family in Cambridge, and without them I don't believe this work would have been possible.

Finally, I would like to thank my family – especially my sister Hannah, for her assistance with the drawing of schematics – my mum and my dad, and all extended family, just for always being there.

I also acknowledge and thank the BBSRC for funding this work and me for the duration of my PhD, and also the PHAGO consortium for further funding the work.

CONTENTS

LIST OF TABLES AND FIGURES

LIST OF ABBREVIATIONS AND ACRONYMS

Abbreviations used within this thesis are listed below. Abbreviations for chemicals and reagents included in Chapter 3 (Materials and Methods) are listed in pages 92-96. Note that all abbreviations are also outlined in the text.

AD	Alzheimer's disease
ADP	Adenosine-5'-diphosphate
ALS	Amyotrophic lateral sclerosis
ANOVA	Analysis of variance
APC	Antigen presenting cell
ApoE	Apolipoprotein E
APP	Amyloid precursor protein
ATP	Adenosine-5'-triphosphate
BAI-1	Brain angiogenesis inhibitor 1
BDNF	Brain-derived neurotrophic factor
CD47	Cluster of differentiation 47
CGC	Cerebellar granule cell
CNS	Central nervous system
CR3	Complement receptor 3
CSF	Cerebrospinal fluid
DAM	Disease-associated microglia
DAMP	Damage-associated molecular pattern
DNA	Deoxyribonucleic acid
ECM	Extracellular matrix
EGF	Epidermal growth factor
ER	Endoplasmic reticulum
FFA	Flufenamic acid
FCγR	Fragment-crystallisable γ receptor
FTD	Frontotemporal dementia

GPCR	G-protein coupled receptor
GTP	Guanosine-5’-triphosphate
IGF-1	Insulin-like growth factor 1
IgG	Immunoglobulin G
IFN-γ	Interferon γ
IL	Interleukin
IRF	Interferon-regulatory factor
KO	Knock-out
kDa	Kilodalton
LPS	Lipopolysaccharide
LTA	Lipoteichoic acid
LTD	Long-term depression
LTP	Long-term potentiation
LRP1	LDL-receptor related protein 1
M-CSF	Macrophage-stimulating colony factor
MerTK	Mer tyrosine kinase
MFG-E8	Milk fat globule-EGF factor 8
MHC	Major histocompatibility complex
mRNA	Messenger RNA
MS	Multiple sclerosis
NFT	Neurofibrillary tangle
NGF	Nerve growth factor
NO	Nitric oxide
NPC	Neural progenitor cell
NSPC	Neural stem precursor cell
PAMP	Pathogen-associated molecular pattern
PBD	Probenecid
PD	Parkinson’s disease
PtdSer	Phosphatidylserine
PMA	Phorbol 12-myristate 13-acetate

PNA	Peanut agglutinin
PRR	Pattern recognition receptor
PSD-95	Post-synaptic density 95
qPCR	Quantitative polymerase chain reaction
RAP	Receptor-associated protein
RGC	Retinal ganglion cell
RONS	Reactive oxygen and nitrogen species
RNA	Ribonucleic acid
R/T	Room temperature
SIGLEC	Sialic acid-binding immunoglobulin-type lectin
STAT	Signal-transducer and activator of transcription
SIRPα	Signal regulatory protein α
TBI	Traumatic brain injury
TGF-β	Transforming growth factor β
TIM-4	T-cell membrane protein 4
TLR	Toll-like receptor
TNF-α	Tumour-necrosis factor α
TREM2	Triggering receptor expressed on myeloid cells 2
UDP	Uridine-5'-diphosphate
UMP	Uridine-5'-monophosphate
UTP	Uridine-5'-triphosphate
VNR	Vitronectin receptor
WNV	West Nile virus

CHAPTER I

INTRODUCTION PART I - PHAGOCYTOSIS

Arguably the most impactful means by which cells manipulate their external environment is via phagocytosis. Phagocytosis is the process whereby cells engulf and biochemically degrade extracellular material, which can include other cells or cellular debris, subcellular organelles, pathogenic material or proteinaceous plaques. Originally described by Ilya Metchnikoff (1845-1916), who observed partially ingested cells within starfish larvae[1], phagocytosis is believed to have evolutionary roots tracing back billions of years to pre-eukaryotic archaeans[2,3]. Whatever the original function of phagocytosis might have been in these cells (possibly as a source of nutrition), that function diversified substantially through the evolution of multicellular metazoans. In such organisms, phagocytosis is known to play fundamental roles in organism development, tissue homeostasis, and both innate and adaptive immunity. In mammals – including humans – phagocytosis is a primary function of several immune cell-types known collectively as 'professional phagocytes', which include macrophages, monocytes and dendritic cells resident throughout the mammalian system. However, phagocytic functions have been described in a much wider array of cell-types ('non-professional phagocytes') and in various physiological contexts, and so can be considered a common cellular function[4]. The importance of phagocytosis to human physiology is emphasised by the myriad diseases, both genetic and acquired, that are linked to some defect in the phagocytic mechanism – from immunodeficiencies resulting from ineffective clearance of pathogens[5], to tumourigenesis and cancer growth caused by impaired cell turnover[6], and the aberrant elimination of healthy cells that can promote neuronal loss and brain atrophy characteristic of several neurodegenerative pathologies[7]. In this chapter, the diverse functionalities and cellular mechanisms of phagocytosis will be reviewed, with particular emphasis on mammalian systems.

1.1. Evolutionary origins of phagocytosis

1.1.1. Pre-eukaryotic archaeans

The earliest organisms hypothesised as capable of performing phagocytosis are the pre-eukaryotic archaeans, or the 'primitive phagocyte'[2,3]. Comparative proteomic analyses have identified prokaryotic homologues to two protein families fundamental to eukaryotic phagocytosis: the actin-related family, and the Ras superfamily of small GTPases[8]. A subset of archaeal actins was found to not only be monophyletic with their eukaryotic homologues (Arp2/3), but also share structural features known to be crucial for filamentous branching and remodelling intrinsic to the phagocytic process in eukaryotes[8]. If such protein structures had indeed evolved a phagocytic function in these primitive organisms, it is unclear what purpose this phagocytosis may have had, although it has been suggested that it served a nutritional role[3]. Indeed, such a form of phagocytosis has been speculated as responsible for the acquisition of mitochondria into the proto-eukaryotic endosymbiont, widely accepted to have triggered eukaryogenesis[8].

1.1.2. Protozoans

Phagocytosis has been demonstrated as essential for providing nutrients for various protozoan species, known as phagoprotozoans[9]. Diverse genera of protozoa, including amoeba, paramecia and tetrahymena, have comparable mechanisms through which target cells - such as bacteria and other protozoa - are phagocytosed for nutrients (reviewed in[3]). After positioning proximal to the target cell, the protozoan engulfs the cell, which is incorporated into an internal food vacuole homologous to the eukaryotic phagosome. The vacuole subsequently undergoes maturation, during which hydrolytic enzymes acquired from the lysosome degrade the target and from which nutrients are ingested, with waste expelled extracellularly[9].

1.1.3. Invertebrates

Phagocytic functionality experienced substantial diversification within the animal kingdom, and invertebrates (that is, all animals outside the subphylum Vertebrata[10]) evolved several new roles for the phagocytic mechanism of cell removal in addition to simple ingestion of

foreign unicellular organisms for feeding. Two well studied invertebrate models – *Caenorhabditis elegans* and *Drosophila melanogaster* – provide insights into such novel roles[3]. *C. elegans* develop phagocytic cells capable of recognising and swiftly eliminating apoptotic host cells via surface-exposure of phosphatidylserine, thus aiding tissue homeostasis[11]. Endodermal cells in *C. elegans* have been shown to actively engulf and remodel primordial germ cells during embryonic development – a phenomenon labelled 'intercellular cannibalism'[12]. In *D. melanogaster*, phagocytes called haemocytes (also present in a variety of other insects) engulf and eliminate apoptotic host cells and virally-infected host cells, as well as foreign pathogens such as *Staphylococcus aureus,* via overlapping receptor-mediated mechanisms[13,14]. Thus, phagocytosis expanded its physiological portfolio in invertebrates to roles in development, tissue homeostasis, and innate immunity.

1.1.4. Vertebrates

Non-mammalian vertebrates utilise phagocytosis for all aforementioned roles employed by invertebrates (with the possible exception of nutrition), in addition to a novel role in adaptive immunity. The adaptive immune system evolved around 500 million years ago in ectothermic vertebrates[15], and differs from innate immunity fundamentally through its ability to acquire novel immune defences (that were not present innately) for the host against foreign insults[16]. Taxonomic classes as distantly related to Mammalia as the Chondrichthyes (cartilaginous fish) reveal several cellular and molecular features homologous to the adaptive immune system, including B and T cells, immunoglobulins and major histocompatibility complex (MHC) class II[15]. In such species, phagocytosis of a foreign particle, such as a bacterium, generates peptides from enzymatic cleavage of bacterial protein, which are then loaded onto MHC class II receptors within the phagosome. Subsequently, such antigen-presenting receptors are translocated to the cell surface, where they initiate paracrine adaptive immune responses culminating in antibody production against the bacterial species originally phagocytosed[15]. The role of phagocytosis in facilitating adaptive immune responses in mammalian vertebrates has been studied extensively, and is reviewed in section 1.2.4.

1.2. Physiological functions of phagocytosis in mammals

1.2.1. Phagocytosis in development

In all vertebrates studied, embryonic development involves a progressive and highly regulated cycle of cell genesis, differentiation and death (i.e. turnover) to allow tissue remodelling and organ growth[17]. From early stages of embryonic development in mice, macrophage progenitor cells exist within the yolk sac, although these differ substantially from the differentiated macrophages found within the adult, and are functionally immature[17,18]. However, phagocytic cells from the yolk sac possess a complement of lysosomal enzymes and can phagocytose erythrocytes[19], indicating an early role for phagocytosis in embryonic development. After liver haematopoiesis, macrophages dramatically increase in number in the developing embryo, taking up residence in all developing tissues and organs (and in some organs, constituting as much as 15% of total cell number)[17]. As macrophage-like cells undergo spatiotemporal expansion, they become predominant in regions undergoing extensive cell death and active tissue remodelling[20], notably around the pharyngeal arches (tissue bands under the early brain) and the dorsal midline[21]. Phagocytes line the ventricular surface of the developing mouse brain, and at later stages, associate with brain regions including the choroid plexus, corpus callosum, leptomeninges and developing cortex[22], further supporting a role for their phagocytic activity in developmental remodelling.

From embryonic development through to adulthood, apoptosis (a form of programmed cell-death) is considered a crucial facilitator of normal mammalian development, as well as development of all metazoans[23]. Equally crucial is the phagocytic removal of apoptotic cells by 'professional scavengers' such as macrophages[24]. Removal of apoptotic cells via phagocytosis is typically anti-inflammatory[25]. However, apoptotic cells that are not efficiently cleared progress to a secondary necrotic state[26,27], which can be pro-inflammatory and contribute to autoimmune disease[24]. The role of apoptosis in structural development is especially well documented in the interdigital zone of the mammalian footpad, as well as in developing retinal tissue, a part of the central nervous system (CNS)[20,28,29]. Indeed, the role of phagocytosis in the developing CNS, including the brain, is of special relevance to this thesis. Microglia, derived from yolk sac macrophages which invade the brain parenchyma during

early development[30], are the resident macrophages of the brain. Within neurogenic niches, neural progenitor cells (NPCs) are generated in excess, with the majority undergoing rapid apoptosis[31]. Microglia within the subgranular and subventricular zones are required to phagocytose apoptotic NPCs from early development and throughout adulthood[31]. In addition to the phagocytic removal of whole cells, microglial phagocytosis of neurites and synapses – also known as synaptophagy – has been well documented in several mammalian models as essential for orthodox neural circuitry development by contributing to synaptic pruning (the targeted elimination of synapses). As with the NPCs, synaptic connections between neurons are generated in excess, and supernumerary synapses are rapidly eliminated via synaptophagy. Whilst the mechanisms that regulate developmental synaptophagy are not fully characterised, they are known to overlap with immune signalling pathways (e.g. via complement signalling)[32]. Indeed, microglial phagocytosis of synapses is a focal topic of this thesis, and will be discussed in depth in section 2.1.1.

1.2.2. Phagocytosis in tissue homeostasis

As well as occurring in mammalian development, cell apoptosis is a fundamental mechanism to optimise cell turnover during normal tissue homeostasis and is observed in all organs and tissues, with levels reaching 300 billion per day in humans[27,33]. B-cell maturation in the peripheral immune system, essential for generating target-specific antibodies in adaptive immunity[34], involves the rapid elimination of millions of immature B cells and thymocytes via apoptosis[27]. In the testes of biologically adult males, germ cells are continuously generated via spermatogenesis with large numbers eliminated through apoptosis[27], and in the lactating mammary gland of biologically adult females, alveolar epithelial cells undergo rapid programmed cell-death *en masse*[35]. Adult neurogenesis produces thousands of differentiated neural precursor cells in various regions of the brain, including the hippocampus and olfactory bulb, with only a small fraction being retained and incorporated in the neural circuitry[36,37]. In all cases, removal of cells committed to death via apoptosis (or otherwise) is facilitated through their phagocytosis by tissue-resident phagocytes[27]. In addition to phagocytosis of whole cells, phagocytic removal of subcellular structures also facilitates tissue homeostasis - as exemplified in the central nervous system, where the developmental synaptophagy essential for neural circuitry development continues into adulthood, as demonstrated by *in vivo* imaging of dentate granule cells from adult mice[38]. The repertoire of phagocytic cells in the mammalian body is wide and diverse, with tissue-specific

heterogeneity in cell-type and context-dependent specificity of the phagocytic mechanism, both of which are reviewed in greater depth in sections 1.3 and 1.4, respectively.

1.2.3. Phagocytosis in innate immunity

In non-sterile conditions, mammals are continuously exposed to microorganisms including bacteria, protozoa, fungi and viruses - infection by which can cause deleterious effects that vary in terms of type, location and severity[39]. The first line of defence against such insults – broadly classified as innate immunity – encompasses the recognition and phagocytic removal of such microorganisms by phagocytic cells. Phagocytosis of the pathogenic target is initiated after recognition of so-called pathogen-associated molecular patterns (PAMPs): pathogenic stimuli including bacterial endotoxins (such as lipopolysaccharide or LPS from gram-negative bacteria[40], and lipotechoic acid or LTA from gram-positive bacteria[41]), fungal-exposed β-glucan sugars such as zymosan[42], and viral RNA[43]. Pathogenic ligands are identified by a range of germline-encoded pattern-recognition receptors (PRRs), typically expressed on the outer membrane of the phagocytic host immune cell but also in endosomal membranes and within the cytosol[39,44]. PRRs include the toll-like receptors (TLRs), nucleotide oligomerisation domain-like receptors (NLRs), c-type lectin receptors (CLRs), RIG-like receptors (RLRs) and the cytosolic DNA-sensing receptors[44,45]. Importantly, such detection mechanisms exhibit a high degree of specificity between pathogen and host-cell recognition[46], although substantial overlap between the phagocytosis of pathogens and host cells in homeostasis and development is increasingly documented[47].

Following recognition of pathogenic ligands and phagocytic receptor clustering[48], engulfment of the foreign target is initiated and a stepwise process of cytoskeletal rearrangement, target internalisation and degradation follows, discussed further in section 1.4. The importance of phagocytosis during innate immune responses to pathogenic invasion is highlighted by immunodeficiency and increased morbidity of mammals congenitally deficient in key components of the phagocytic machinery[49] - for example via polymorphisms of the Fcγ receptor[50,51] - as well as by the increased susceptibility to infection and reduced survival rates of several animal knockout models deficient in phagocytosis, such as mice lacking complement components C3 and/or C4[52,53,54].

1.2.4. Phagocytosis in adaptive immunity

The ability for mammals to develop pathogen-specific immune defences is attributable to their adaptive (or acquired) immunity, for which the phagocytic process is key, as the relay of structural and biochemical information from the invading microbe to T and B cells in order to generate complementary anti-microbial immunoglobulins depends on it. Microbial (and viral) entities internalised within the phagosome are subjected to a variety of host-generated insults to induce protein degradation, including low pH (~4.5)[55], hydrolytic enzymes such as cathepsins, proteases and lipases[56], and reactive oxygen species (ROS) generated by NADPH oxidase[57,58]. In such harsh environmental conditions, pathogenic peptides are generated, which can bind membrane-bound MHC class II molecules in a process called antigen-loading[59]. It is interesting to note that microbes capable of interfering with phagosome maturation likely limit antigen presentation by the host, as indicated by studies on *Mycobacterium tuberculosis* - where a reduction in antigen-MHC class II complex formation was observed with live bacteria when compared with the same bacteria that had been heat-inactivated[60].

Following antigen loading, antigen-MHC class II complexes are trafficked to the cell surface for presentation to T helper cells expressing the glycoproteins CD4 (otherwise known as $CD4^+$ T cells), thus stimulating their proliferation and cytokine release and ultimately inducing antigen-specific immunoglobulin production by B cells[59]. It is of relevance to note that, as well as being expressed on the cell-surface, B cells also secrete immunoglobulins in soluble form, which can coat other pathogens of the same type and opsonise them for phagocytosis by binding surface-expressed Fc receptors on macrophages[61].

1.3. Phagocytic effector cells

The capacity for phagocytosis is shared by a large and diverse range of mammalian cell-types. However, there are substantial differences in the efficiency by which this can be achieved, in the plurality of targets vulnerable to it and in the importance of the process to functionality of the cell-type as a whole. Thus, cells proficient in phagocytosis can be subdivided into two major groups. Immune cells for which phagocytosis is imperative for general functionality (and so have evolved mechanisms to phagocytose a wide range of targets and with high efficiency) are known as 'professional' phagocytes - a group of myeloid

cells of hematopoietic origin that includes monocytes, macrophages, dendritic cells, neutrophils, osteoclasts and eosinophils[1]. Cells for which phagocytosis is not a primary function - but for which phagocytic functionality has been observed in various developmental and homeostatic contexts - are classed as 'non-professional' phagocytes, and comprise cells of diverse lineage including epithelial, endothelial and fibroblast cells found throughout the mammalian system[4].

1.3.1. 'Professional' phagocytes

1.3.1.1. Monocytes

Monocytes are myeloid cells derived from bone marrow[62], which circulate in blood but also reside in the spleen and bone marrow[63]. Monocytes express a range of chemokine and pattern-recognition receptors[63] and can directly phagocytose pathogenic material, as well as host cells[64] and cellular debris[65]. Other innate immune functions of monocytes include inflammatory cytokine release and antigen presentation[65]. After migrating to infected or otherwise damaged tissue, local inflammatory factors induce their differentiation into macrophages or dendritic cells, a process which is considered inflammation-specific[63,65,66].

1.3.1.2. Macrophages

Macrophages exist in all vertebrates studied[39], and in mammals, derive either from monocytes circulating within the blood ('recruited' macrophages) or from erythromyeloid progenitors originating in the yolk sac or foetal liver ('tissue-resident' macrophages)[67]. Tissue-resident macrophages reside in lymphoid and non-lymphoid tissues throughout the body[63] – including the brain (microglia), liver (Kupfer cells[68]), skin (Langerhans cells & dermal macrophages[69], intestine (Lamina Propria macrophages, submucosa macrophages & muscularis macrophages[70]), lung (alveolar macrophages & interstitial macrophages[71]) and spleen (marginal metallophillic macrophages & marginal zone macrophages[72]) – and exhibit a high degree of spatial heterogeneity[67].

Like monocytes (from which many macrophages directly originate), macrophages are equipped with a portfolio of chemokine, cytokine and pattern-recognition receptors, and are

highly efficient in phagocytic elimination of both foreign pathogens and host cells, as well as subcellular material[67]. They can also initiate and perpetuate an inflammatory response through production and release of extracellular cytokine, chemokines and growth factors[67]. However, in contrast to monocytes, their phagocytic activity is employed commonly in the absence of inflammation, to clear senescent (i.e. apoptotic) cells in so-called 'steady-state' tissue homeostasis[63]. They are also typically the first responders to pathogenic presence[73].

1.3.1.3. Dendritic cells

Traditionally, dendritic cells have been understood to originate exclusively from common myeloid progenitor cells within the bone marrow (which also give rise to monocytes and macrophages)[63] but distinct groups have more recently been revealed to display markers of lymphoid origin[74]. Two major subsets have been characterised in mammalian systems: the classical dendritic cell (CDC) and the plasmocytoid dendritic cell (PDC)[74]. CDCs, also known as myeloid dendritic cells, circulate in the blood but are also present within tissue and lymphoid organs, achieved via their high capacity for migration[63]. CDCs are short-lived cells that are continuously replaced by precursors from blood[75], and combine high phagocytic capacity with specialised antigen-processing capabilities, so are key antigen-presenting cells in the adaptive immune system[63]. PDCs are the most common blood dendritic cell type[74] but also reside in a range of mammalian organs at low levels, as well as within bone marrow[63]. PDCs have a relatively low turnover rate compared to CDCs, and are important in innate immune responses to viral infection due to rapid production of type I interferon[76]. However, more recent evidence has demonstrated their capacity for phagocytosis of virally-infected apoptotic cells and subsequent antigen-presentation to T cells[77], thus outlining their importance in adaptive immunity.

1.3.1.4. Neutrophils

One of the four major granulocytes of myeloblast origin, along with eosinophils, basophils and mast cells[78], the mature neutrophil is the most abundant leukocyte in peripheral blood circulation in humans[79]. Neutrophils are best characterised in terms of their ability to recognise and respond to microbial invasion and tissue damage[80]. Circulating neutrophils express a range of chemotactic ligand receptors, which are activated in response to tissue infection or injury and induce neutrophil migration and endothelial extravasation[79]. After

tissue infiltration, they combine forces with macrophages to directly eliminate microorganisms and cellular debris via phagocytosis[80]. Their importance in phagocytic elimination of both foreign and host cellular material in inflamed tissue is emphasised by the fact that approximately 20% of congenital immunodeficiency disorders in humans are linked to abnormal neutrophil abundance or functionality[79].

1.3.1.5. Osteoclasts

Although they share a common myeloid progenitor with macrophages, monocytes and dendritic cells, osteoclasts are a phagocytic cell type distinguished by their multinucleated morphology, which results from direct fusion of multiple osteoclast precursor cells[81]. Osteoclasts are essential for skeletal development and maintenance throughout the mammalian lifespan, which is achieved via their primary function of lacunar bone resorption[81,82]. Osteoclasts are demonstrated as capable of phagocytosing latex beads and red blood cells[83]. The extent to which this phagocytosis is required for their function is not clear. However, findings that individuals with pycnodysostosis – a lysosomal storage disease resulting from deficiency of cathepsin K, an osteoclast-specific lysosomal protease[84] – contain osteoclasts filled with undegraded bone collagen fibrils (which were not present in osteoclasts from healthy individuals[85]) hint at the importance of phagocytosis for their function.

1.3.1.6. Eosinophils

Eosinophils are granulocytes with a similar haematopoietic lineage to neutrophils[78]. Like neutrophils, eosinophils are key cellular players in the response to infection by pathogens ranging from bacteria and viruses to parasitic worms (helminths)[86], notably in the gastrointestinal tract but also in lymphoid organs including the thymus and spleen[87]. Eosinophils are well characterised for their cytotoxic effector functions[86], for example through the release of cytotoxic granules containing a plethora of enzymatic and non-enzymatic cationic proteins to degrade pathogenic targets extracellularly[88]. Importantly, eosinophils have been shown to phagocytose a wide range of pathogenic material including yeast[89], gram-negative and gram-positive bacteria[90] and parasitic protozoa[91]; however, phagocytosis by eosinophils is generally less efficient compared to neutrophils, and is triggered by distinct molecular mechanisms[86].

1.3.2. 'Non-professional' phagocytes

1.3.2.1. Endothelial cells

As crucial structural components of the mammalian vasculature, endothelial cells protect proximal tissue against pathogens and toxins circulating within the bloodstream[92]. In addition to providing a physically protective barrier, endothelial cells can adhere to and phagocytose both pathogenic and non-pathogenic bacteria through molecular mechanisms distinct from this employed by macrophages[92]. Furthermore, endothelial cells can internalise and remove extracellular fibrin clots within blood[93], thus maintaining tissue homeostasis and facilitating normal circulation[92].

1.3.2.2. Epithelial cells

The epithelium is one of the four major tissue types found in mammals, and demarcates and protects organs, tissues and vessels throughout the body[94]. Given such global presence, epithelial cells (which constitute epithelia) are unsurprisingly heterogeneous in terms of phenotype and physiological function. Whilst phagocytosis is not considered the primary function of any single epithelial cell-type, epithelial phagocytosis is documented in diverse physiological contexts and performs several biological roles. In the lactating mammary gland, for example, programmed death of alveolar epithelial cells that have lost the capacity for milk production occurs at very high rates, and rapid gland involution (removal of such redundant cells) is attained via phagocytosis of the apoptotic cells by both macrophages and also mammary epithelial cells, or MECs[35,95]. Phagocytic elimination of the cells by MECs is achieved using many receptor-signalling systems shared with macrophage phagocytosis, although phagocytosis of apoptotic cells by MECs is much less efficient[35].

1.3.2.3. Fibroblasts

The most common cell-type present in mammalian connective tissue, fibroblasts are responsible for the production of myriad structural and adhesive proteins essential for formation of the extracellular matrix (ECM), as well as maintenance of its structural integrity[96] - notably type I collagen, the most abundant protein in the human body[97]. As well as ECM production, fibroblasts are also crucial for ECM resorption - differing markedly from

the bone, where bone production and resorption activities are separated between the osteoblasts and osteoclasts, respectively[96]. Fibroblast-mediated degradation of collagen fibrils, both in normal physiology and in pathological fibrosis, is achieved by i) extracellular release of matrix-degrading enzymes[96], and ii) direct phagocytosis of the collagen[98], dependent upon collagen-specific receptors expressed by the fibroblast[99]. Thus, fibroblast phagocytosis plays a critical role in ECM remodelling and homeostasis throughout the mammalian body. In addition, fibroblasts have been shown as capable of phagocytically eliminating apoptotic neutrophils[100], further implicating fibroblast phagocytosis in tissue homeostasis.

1.4. Phagocytic regulation and execution

The human body turns over approximately 1,000,000 cells each second - in contexts of tissue development, cell-density maintenance, neutrophil & erythrocyte turnover, cellular damage and microbial infection - and a primary means by which these cells are eliminated is phagocytically, meaning phagocytosis happens constantly and on a mass scale[101]. However, it is clearly imperative that such phagocytic activity can differentiate between cells intended for removal (foreign or host) and cells that are physiologically indispensable. Accordingly, phagocytosis is strictly regulated by a plethora of pro- and anti-phagocytic signals, and the molecular mechanisms that induce initiation, progression and execution of phagocytosis can be both target- and context-specific. Such mechanisms are here reviewed.

1.4.1. Target recognition

1.4.1.1. 'Find-me' signals

In many scenarios, the migration of phagocytically proficient cells toward cells that are dying (through apoptosis or otherwise) may not be paramount, as neighbouring cells may be sufficiently phagocytic to eliminate the cell completely[101] – for example, in the epithelial layers of the lung alveoli or the gastrointestinal tract[27]. Indeed, in such locations, access by migratory phagocytes is limited, and phagocytic removal depends entirely on neighbouring epithelia. However, certain cases may benefit from recruitment of professional phagocytes with increased phagocytic efficiency and comprehensive immune functions, particularly

where local neighbours have no phagocytic capacity at all (in the thymus gland for example, where thymocytes cannot phagocytically eliminate their dying neighbours)[102]. The ability for host cells to release extracellular signals that trigger chemotactic responses from migratory phagocytes has been well documented in mammalian systems, and such signals come in variety of chemical forms – including protein, lipid and nucleotide (Figure 1.1, page 34).

1.4.1.1.1. Fractalkine (CX_3CL1)

Ubiquitous throughout the mammalian body, fractalkine is expressed in organs as diverse as brain, lung and skin, as well as in endocrine and lymphoid tissue[103]. A chemokine, fractalkine is a 90 kDa peptide which can be enzymatically cleaved to a 60 kDa form and released extracellularly from a variety of cells undergoing apoptosis (such as lymphocytes[104] and germinal B cells[105]) to induce migration of macrophages or monocytes. Chemotactic responses to fractalkine have also been demonstrated by natural killer (NK) cells and T-cells[106]. Fractalkine can exist extracellularly either in a soluble form[107], or in a membrane-anchored form as part of an apoptotic microparticle, which are released during the membrane blebbing process[102]. The chemokine is a ligand for the CX_3CR1 receptor, a G protein-coupled receptor (GPCR) expressed by a number of phagocytic effector cells including macrophages, natural killer cells, T cells and circulating monocytes[108]. In the latter, expression is downregulated following differentiation into macrophages or dendritic cells[108] which occurs after entry to infected or damaged tissue), and so likely acts to prevent subsequent chemotactic distraction from the site of injury.

In the brain, fractalkine is constitutively expressed by neurons, and the fractalkine receptor exclusively expressed by microglia, the resident macrophages[109]. Here, fractalkine is not only employed as a chemotactic agent toward dying cells during tissue homeostasis, but also toward developing neurites to influence synaptic pruning by the microglia during circuitry development[110,111]. This phenomenon will be further reviewed in section 2.1.1.

1.4.1.1.2. Lysophosphatidylcholine

Lysophosphatidylcholines (LPCs) describe a family of lipids that derive from the partial hydrolysis of phosphatidylcholine precursors via phospholipase A_2, or through the chemical

transfer of free fatty acids to cholesterol by a cholesterol acyl-transferase, and are ubiquitous throughout mammalian tissue[112]. LPCs can be released from apoptotic cells to induce phagocyte migration[113]. Chemotactic induction has been suggested to signal agonistically via the GPCR G2A[114], although this has been questioned by findings that LPC can act antagonistically on G2A in certain contexts[115]. The inability for chemically similar lysophospholipids or LPS-derived compounds to trigger phagocyte migration emphases the structural specificity of the signal for chemotactic function[114].

1.4.1.1.3. Sphingosine-1-phosphate

Chemically similar to LPC, sphingosine-1-phosphate (S1P) is actively released by apoptotic cells to trigger phagocyte migration[116]. S1P has known binding affinity with 5 distinct GPCRs, $S1P_{1-5}$ – although which specific receptor(s) is (are) required for S1P-mediated chemotaxis is unclear. Indeed, phagocytes can express several such receptors simultaneously, meaning S1P-signalling may occur through multiple receptors and be context-specific[102].

1.4.1.1.4. Nucleotides

The nucleotides adeonise-5'-triphosphate (ATP) and uridine-5'-triphosphate (UTP) are released from a variety of cells undergoing apoptosis, including thymocytes and T-cells[117], and these extracellular nucleotides can promote migration of monocytes, macrophages and neutrophils to the apoptotic cell *in vitro* and *in vivo*[36,118]. Nucleotide release from apoptotic cells with intact membranes is mediated via specific channels called pannexons, whose permeability is influenced by caspase-dependent cleavage of an obstructive C-terminal tail[119,120]. Phagocytes express a range of surface receptors for extracellular nucleotides from the ionotropic P2X and metabotropic P2Y receptor sub-families[121], and such receptors are implicated in mediating full migratory responses from phagocytes along extracellular nucleotide gradients. Macrophages lacking the $P2Y_2$ receptor have been shown as deficient in both their migration toward supernatant from apoptotic T cells, and in their clearance of apoptotic thymocytes *in vitro*[117]. Genetic knockout of the ATP-sensing $P2Y_{12}$ receptor in microglia abolished their ability to migrate or extend processes toward nucleotides *in vitro*, and also inhibited their process extension toward sites of cortical damage *in vivo*[118].

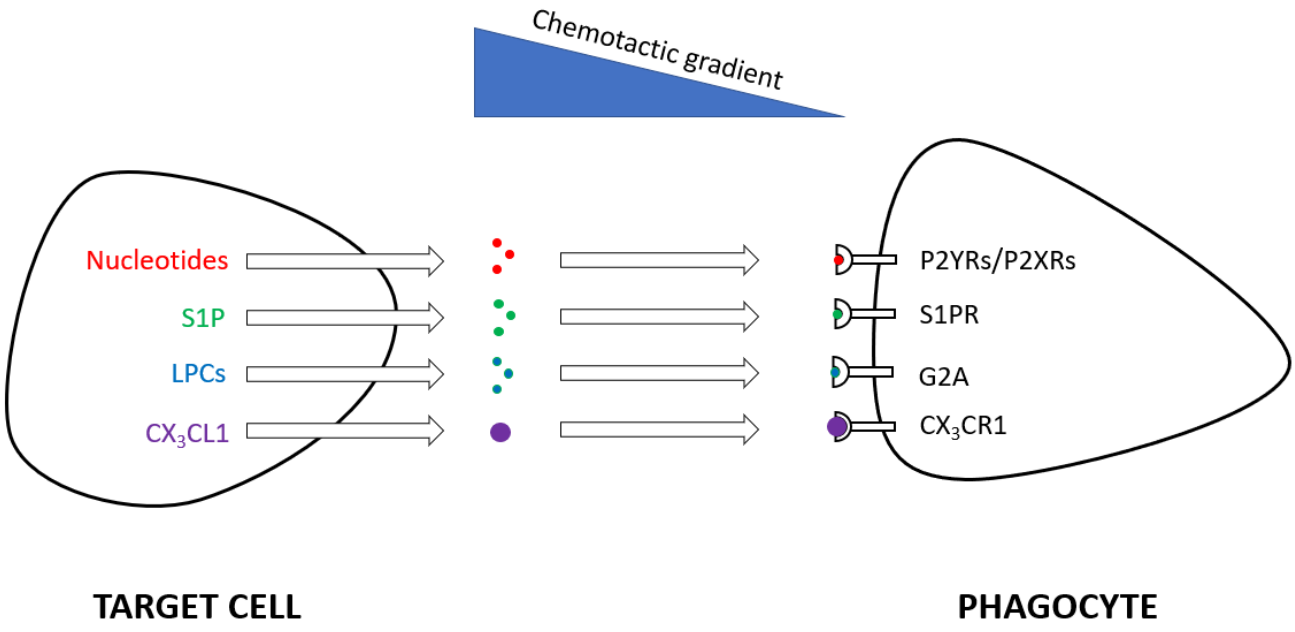

Figure 1.1. 'Find-me' signalling in mammalian phagocytosis. Phagocytosis is facilitated initially by 'find-me' signalling, which promotes migration of the phagocyte to the target cell. S1P: sphingosine-1-phosphate. LPC: lysophosphatidylcholine.

1.4.1.2. 'Eat-me' signals

'Find-me' and 'eat-me' signals both ultimately contribute to phagocytosis of cellular (or sub-cellular) targets. However, whilst 'find-me' signals are released extracellularly by the target and promote a migratory response from the phagocyte along a chemotactic gradient, 'eat-me' signals are molecules that are exposed on the surface of the target cell to directly induce phagocytosis by a proximal phagocyte[122]. Cellular exposure of 'eat-me' signals is strictly regulated, so that physiologically indispensable cells – which may outnumber local cells intended for phagocytic removal by some margin – are not inadvertently phagocytosed by scavenger phagocytes that may reside locally or have migrated[123]. There is much variation in the literature regarding the classification of 'eat-me' signals, which is commonly used as an umbrella term to describe all membrane-anchored molecules as well as soluble bridging molecules (i.e. opsonins) that bind the target surface from the extracellular space to induce phagocytosis. Here, such terms will be distinguished as follows – 'eat-me' signals (including phosphatidylserine and calreticulin) will be defined as any signal normally located

intracellularly, whose exposure on the cell surface is recognised by phagocytes and induces phagocytic engulfment of that target cell. Opsonins (including complement, immunoglobulins, collectins, ficolins and pentraxins) will be defined as any soluble protein that can be released extracellularly from cells – often immune cells that have been inflammatory activated[124] – and that when bound to the surface of a target cell induces phagocytosis of that cell. Established 'eat-me' signalling mechanisms are depicted schematically in Figure 1.2 (page 36).

1.4.1.2.1. Phosphatidylserine

By far the best characterised 'eat-me' signal[36,123], surface exposure of phosphatidylserine (PtdSer) occurs early in the apoptotic process, within 1 or 2 hours[125]. Given its observation in different cell-types undergoing various forms of apoptosis, PtdSer exposure is considered a universal apoptotic marker[126]. Healthy, non-apoptotic cells expose negligible PtdSer on their outer surface, maintained via an active process of phosphatidylserine internalisation by aminophospholipid translocases[127]. During apoptosis, translocase activity diminishes whilst the activity of phospholipid scramblases – proteins that promote phosphatidylserine externalisation to the outer surface - increases, resulting in a net increase in PtdSer exposure[127,128]. Indeed, increases in exposed PtdSer by 280-fold have been observed in apoptotic Jurkat T cells[125]. Early studies investigating the involvement of apoptotic PtdSer exposure in macrophage phagocytosis showed that blocking PtdSer exposed by apoptotic erythrocytes or lymphocytes with annexin V completely abolished their phagocytosis by a range of macrophage cell-types[129] - indicating that PtdSer exposure is both required and sufficient for phagocytosis. However, more recent studies have brought the singular importance of PtdSer into question[36], and it is likely that PtdSer is recognised in conjunction with other eat-me signals to induce apoptosis.

Several surface receptors for PtdSer exist and are expressed by a range of phagocytic cells[36] to mediate PtdSer-dependent phagocytosis of the target. Many such receptors bind exposed PtdSer directly, such as T-cell immunoglobulin and mucin family (TIM) family receptors TIM-1, TIM-3 and TIM-4, brain angiogenesis inhibitor 1 (BAI1) and stabilin-2[36]. Other receptors for PtdSer bind indirectly via intermediate bridging molecules, or opsonins, which

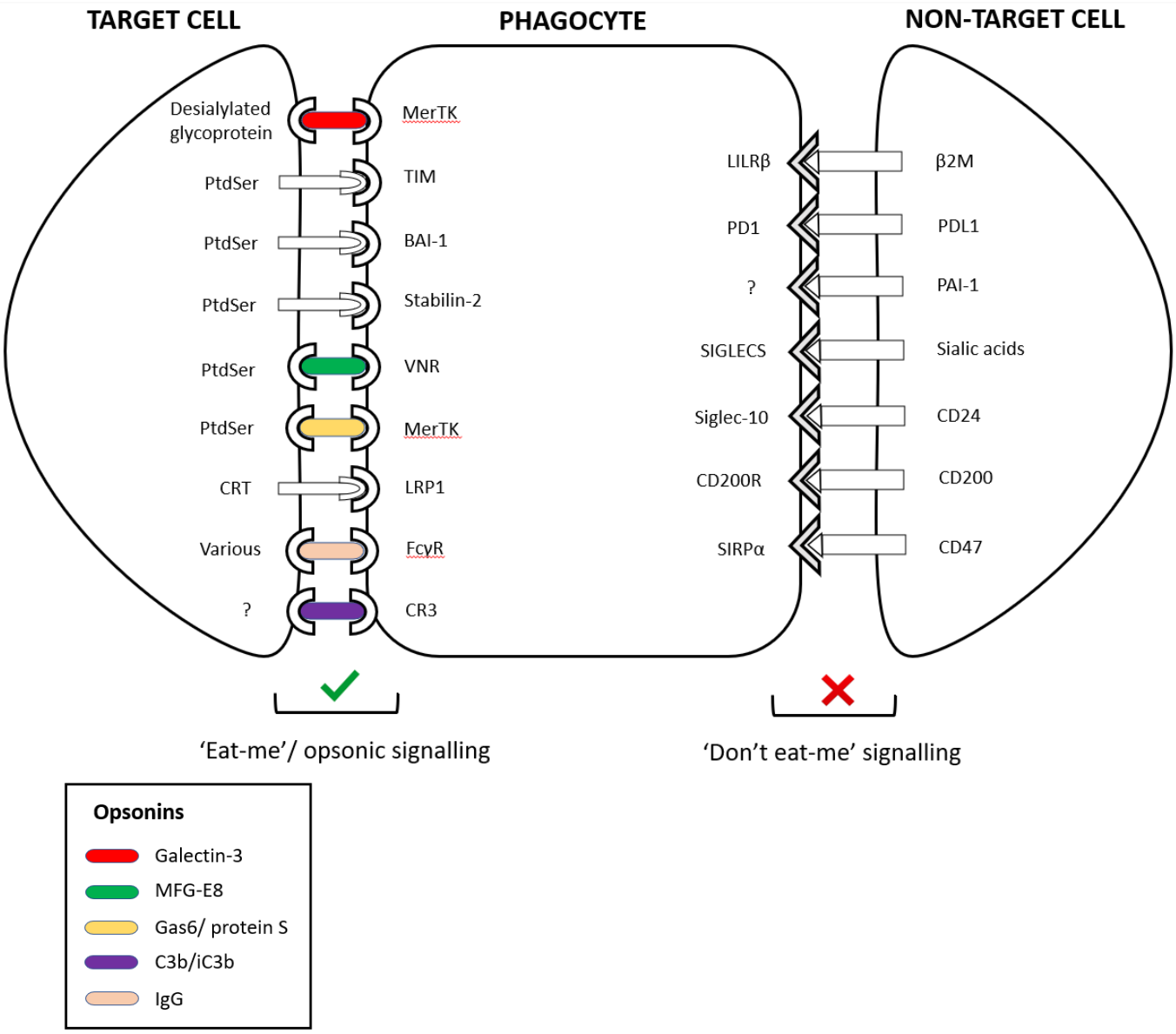

Figure 1.2. 'Eat-me' signalling in mammalian phagocytosis. Following migration of the phagocyte to the target cell, the initial steps in phagocytosis are regulated by 'eat-me' signalling, which facilitates the initial steps in phagocytosis of the target cell by the phagocyte. 'Eat-me' and opsonic signals are exposed on the surface of the target cell and bound by receptors on the phagocyte (either directly e.g. when LRP1 binds surface-bound calreticulin, or indirectly e.g. when VNR binds PtdSer via the opsonin MFG-E8). 'Don't eat-me' signalling inhibits phagocytosis of the target cell. Like with 'eat-me' signals, 'don't eat-me' signals are exposed on the surface of the target cell and are bound by receptors on the phagocyte. PtdSer: phospatidylserine. CRT: calreticulin. MerTK: Mer receptor tyrosine kinase. TIM: T-cell membrane protein. BAI-1: brain angiogenesis inhibitor 1. VNR: vitronectin receptor. LRP1: low-density lipoprotein receptor-related protein 1. CR3: complement receptor 3. FcγR; fragment-crystallisable-gamma receptor. LILRβ: leukocyte immunoglobulin-like receptor B1. PD-L1: programmed cell death ligand 1. β2M: β-2 microglobulin subunit of the major histocompatibility class I complex. PAI-1: plasminogen activator inhibitor 1. SIGLEC: sialic acid-binding immunoglobulin-type lectin. CD24: cluster of differentiation 24. SIRPα: signal regulatory protein α.

are reviewed in section 1.4.1.3. Examples of such receptors include the αvβ3 receptor, also known as the vitronectin receptor (VNR), through which PtdSer signals via the opsonin MFG-E8[130], and the MerTK receptor, through which PtdSer signals via gas6, protein S or galectin-3[131,132]. It remains unclear why such a range of receptors for the same signalling ligand exist, but their differential activation may be context-dependent.

1.4.1.2.2. Calreticulin

Calreticulin is a 46 kDa lectin (carbohydrate-binding protein) that is constitutively expressed in virtually all mammalian cell-types[133]. Calreticulin typically resides within the endoplasmic reticulum (ER) where it functions as a molecular chaperone, binding to glucose residues present on the developing glycan chains of nascent polypeptides[134]. During conditions of apoptosis or ER stress, calreticulin can be translocated to the surface of the cell[135,136]. At the cell surface, calreticulin can act as an 'eat-me' signal to local phagocytes, such as macrophages, through signalling via the phagocytic LDL receptor-related protein 1 (LRP1) receptor[135,137,138,139]. Calreticulin can bind PtdSer directly[140], and so may signal to phagocytes alone or in association with exposed PtdSer. It should be noted that calreticulin can also function as a phagocytic co-receptor - for example during the phagocytosis of apoptotic T cells by macrophages, via complex formation with macrophage-exposed LRP1 and surfactant proteins SP-A and SP-D[141] and/or C1q[64]. Indeed, calreticulin is a well-documented receptor for C1q, and is alternatively known as C1qR[142].

More recently, calreticulin has been shown by us[124] and others[143] to be secreted by inflammatory-activated macrophages into the extracellular space, where it can opsonise target cells for macrophage phagocytosis, for example in the opsonisation of neutrophils for phagocytosis by peritoneal macrophages[143]. Indeed, the additional role of calreticulin as an opsonin, as well as an ‘eat-me’ signal, is of special relevance to this thesis and further reviewed in Chapters 4 and 6.

1.4.1.3. Opsonins

Commonly classed as 'eat-me' signals, opsonins are soluble, extracellular proteins that can circulate freely during the steady-state and/or be released from mammalian cells, often immune cells subjected to an inflammatory stimulus[124,144]. Evolution of mammalian systems has generated a range of soluble proteins capable of opsonising both foreign (i.e. pathogenic) and host targets for phagocytic elimination, in contexts of infection or tissue homeostasis and development. Indeed, many proteins originally designated as opsonins for pathogens – such as complement and immunoglobulin proteins – now reveal multi-functional roles in apoptotic cell clearance, tissue remodelling and developmental shaping of neural circuitry[144,145]. Established mammalian opsonins are here reviewed, and summarised in Figure 1.2 (page 36) and Table 1 (page 44).

1.4.1.3.1. Complement

The complement system comprises over 30 distinct proteins, which together account for approximately 15% of total globular proteins in plasma[146], and is one of the most evolutionarily ancient components of the eukaryotic defence against pathogens[147]. Anti-pathogenic mechanisms employed by the complement system are varied: from the pro-inflammatory mediation of the anaphylatoxins, to targeted osmolysis of pathogenic cells via complement-complex formation of porous membrane attack complexes (MACs), to target opsonisation for phagocytosis by host cells[147]. Of all the complement component proteins, microbial opsonisation is known to occur via C3b (and its cleavage products iC3b, C3c and C3dg), C4b and C1q[147], which bind the microbial surface through unclear means (possibly via LPS[148,149]), thus tagging the target microbe for immune recognition. Such tags are recognised by a range of complement receptors including CR1, CR2, CR3, CR4 and CRIg expressed by several phagocytes; notably neutrophils[150], monocytes[150,151,152] and macrophages[152,153,154].

As well as targeting microbes, complement can tag host cells and sub-cellular structures for phagocytosis, which is important in tissue homeostasis and remodelling[144]. How complement components bind host cells for removal is not entirely clear, but may occur through association with PtdSer, an interaction which has been observed in the early stages of apoptosis[155]. Deficiency of complement component C1q inhibits clearance of apoptotic cells

in mice[156], and confers increased risk in humans of systemic lupus erythematosus (SLE)[157], an autoimmune disease characterised by ineffective apoptotic cell clearance and inflammation[158]. Complement is also a key tag for synapses undergoing phagocytic pruning in the CNS[145], a topic that will be discussed in greater depth in section 2.1.1. Specific ligands and receptors for the different complement components – as well as specific opsonisation roles for the proteins in different contexts – are listed in Table 1.

1.4.1.3.2. Antibodies (immunoglobulins)

A crucial component of the adaptive immune system in mammals, antibody production is achieved by mature B cells exposed to antigen presented by other immune cells (such as dendritic cells), Through a process of antibody selection, this exposure results in a predominance of functional antibodies capable of binding specifically to the original antigen to elicit downstream immune responses, including target phagocytosis. All professional phagocytes express receptors for the Fc portion of antibodies called Fcγ receptors[159]. The major Fcγ receptors that promote phagocytosis of antibody-coated targets are FcγRI, FcγRIIA and FcγRIII[160]. Fc receptors bind monomeric immunoglobulin with relatively low affinity, but immunoglobulin aggregated on antibody-coated particles with much higher affinity[159], thus minimising their activation from freely circulating immunoglobulins not coating pathogen. Genetic truncation of the Fcγ receptor inhibits macrophage phagocytosis of IgG-coated particles *in vitro*[161], and causes immunodeficiency in multiple models of infection[162,163]. Thus, antibody opsonisation of microbial targets via Fcγ receptor signalling is an important anti-microbial mechanism in adaptive immunity.

Given the virtually infinite target specificity antibodies can possess, undesirable generation of antibodies that bind host epitopes (autoantibodies)[164] is possible, and indeed features commonly in autoimmune disease[144]. However, recent evidence indicates that autoantibodies may play beneficial physiological roles. IgGs have been shown to opsonise apoptotic neutrophils for macrophage phagocytosis via FcγRIIa signalling[165], whilst IgMs (but not IgGs) have been shown to opsonise apoptotic microparticles for phagocytosis by macrophages[166], and are implicated in the opsonisation of apoptotic lymphocytes[167]. Furthermore, anti-phospholipid autoantibodies have been shown to bind apoptotic thymocytes but not healthy thymocytes, and such binding is mediated indirectly via the PtdSer-binding protein β2-glycoprotein I[164], indicating that apoptotic cell markers may

present a natural immunogen for autoantibody-dependent opsonisation by phagocytes. It should be noted that IgA- and IgE-type antibodies have either not been reported as opsonins, or have been demonstrated to have little or no opsonisation capacity[168].

1.4.1.3.3. Collectins

Collectins are a family of carbohydrate-binding proteins belonging to the calcium-dependent (C-type) lectin superfamily[169], which circulate freely and bind a wide range of sugar residues via their carbohydrate recognition domain (CBD)[170]. Several types of collectins have been described, of which the best characterised are the mannan binding lectin (MBL, also known as the mannose-binding lectin), and surfactant proteins A (SP-A) and D (SP-D)[170]. Collectins can be subdivided based on the nature of their 3-residue sugar-binding motif: Glu-Pro-Asn (found in MBL and SP-D) which binds with high affinity to mannose, or Gln-Pro-Asp (found in SP-D), which binds more favourably to galactose[171]. Such differences confer variable binding specificities to the collectins, but they are broadly capable of binding a wide range of sugars including glucose, N-acetylglucosamine and N-acetylmannosamine, as well as galactose and mannose[170].

Through their lectin domain, collectins exhibit affinity for mannan and high-mannose containing structures (as present in the cell walls of yeast), as well as bacterial lipopolysaccharide, and have been demonstrated to bind directly to both bacteria and fungi[170]. Collectins can indirectly induce phagocytosis of microbes through activation of the complement system, whereby deposition of complement components C3b and C4b on the microbial surface promotes phagocytosis of the microbe via corresponding complement receptors on the phagocyte[172,173]. They can also opsonise microbes directly[174], although the receptor-mediated mechanisms involved in this opsonisation are not clear[144].

In addition to pathogens, increasing evidence implicates collectins as capable of targeting host cells for phagocytic elimination in homeostatic contexts. MBL has been documented to bind the surface of apoptotic cells along with C1q, which together can undergo complex formation with calreticulin and CD91 present on the surface of local phagocytes to induce engulfment of the apoptotic cell[64]. SP-A and SP-D have both been shown to induce phagocytosis of apoptotic neutrophils by alveolar macrophages, further implicating collectins in apoptotic cell removal. Indeed, mutation frequencies in the MBL gene are significantly

higher in populations suffering from autoimmune diseases such as rheumatoid arthritis and SLE, where apoptotic cell clearance is deficient[158].

1.4.1.3.4. Ficolins

Like collectins, ficolins are a group of proteins characterised by a C-terminal lectin domain[175], expressed by various cell-types, including monocytes[170]. The lectin domain confers sugar-binding capacity to ficolins, which have demonstrated binding affinity for yeast mannan[176], as well as bacterial lipotechoic acid (LTA)[177] and LPS[178], and so can bind to both gram-positive and gram-negative bacteria. Two ficolins were originally identified in human serum – H-ficolin and L-ficolin[179]. L-ficolin can opsonise microbial targets including *S. typhimurium* for phagocytosis by monocytes[180], and *M. tuberculosis* for phagocytosis by macrophages[181], thus contributing to innate immune responses. Any opsonisation capacity for H-ficolin is not clear, but considered likely given structural and functional similarities to L-ficolin[179]. A third human ficolin, M-ficolin, has been shown to be produced by peripheral blood monocytes[182] and can opsonise *E. coli* for phagocytosis by the human monocyte cell-line U937[183].

1.4.1.3.5. Pentraxins

An evolutionary ancient protein family, mammalian pentraxins exist as pentameric structures that function as pattern recognition molecules[184]. Two major classical pentraxin proteins have been documented: the C-reactive protein (CRP) and the serum amyloid P component (SAP)[184]. CRP, named after early identification of its affinity for C-polysaccharide present in the cell wall of *S. pneumoniae*[185], binds phosphocholine moieties of lipotechoic acid (LTA) present on the surface of gram-positive bacteria[186], but also various other pathogenic organisms[184]. Phosphocholine groups are not typically exposed on the surface of healthy mammalian cells; however, CRP can bind phosphatidylcholine residues exposed by cells stressed via enzymatic damage or complement attack[187], indicating that CRP may target dead or dying host cells for immune processing. SAP differs in its ligand-binding affinity, as it is incapable of binding phosphocholine but has a notable binding affinity for lipopolysaccharides and other carbohydrates present on the bacteria *N. meningitidis* and *S. pyogenes*[188,189], as well as for amyloid fibrils[190].

Both CRP and SAP can opsonise targets for phagocytosis by monocytes, macrophages, neutrophils and dendritic cells, either through direct interaction via Fcγ receptors on the phagocyte surface[191], or indirectly through association with complement component C1q and subsequent initiation of the complement cascade[192]. Such targets include gram-negative and gram-positive bacteria [184], the euglenozoan parasite *L. donovani*[193], and mammalian cells such as apoptotic human lymphocytes[191,194] - implicating pentraxins in apoptotic cell clearance as well as innate immune protection against pathogenic infection.

1.4.1.3.6. Milk fat globule-EGF factor 8 (MFG-E8)

MFG-E8 is a soluble 46 kDa protein expressed in various cell-types and tissues, including gastrointestinal, mammary alveolar and retinal pigment epithelia, skin and brain[195]. MFG-E8 is secreted peripherally from dendritic cells[196] and macrophages[195,197] in response to diverse stimuli including amyloid[197], granulocyte-macrophage colony-stimulating factor (GM-CSF)[198] and CX_3CL1[199]. MFG-E8 is best characterised as an efferocytic opsonin - that is, an opsonin that tags apoptotic cells for phagocytic removal[195]. Soluble MFG-E8 binds exposed PtdSer on the surface of apoptotic cells[200], and also the αvβ3 (vitronectin) receptor expressed on the surface of activated macrophages[201], thus promoting signal transduction that ultimately leads to cytoskeletal rearrangements and target engulfment. MFG-E8 has been shown to enhance apoptotic cell phagocytosis when applied exogenously at nanomolar levels[202], whilst MFG-E8 containing a single point mutation that precludes vitronectin (but not PtdSer) binding can inhibit phagocytosis of apoptotic cells by masking exposed PtdSer[203], resulting in autoantibody production. MFG-E8 promotes phagocytosis of defective red blood cells (sickle cells) by macrophages[204], and is also implicated in the clearance of excess collagen by alveolar macrophages in lung tissue[205].

1.4.1.3.7. Gas6

The protein product of growth arrest-specific gene 6, gas6 is a cell-secreted glycoprotein and known ligand for the phagocytic receptor MerTK (as well as for other TAM members Tyro3 and Axl)[206], and can directly bind PtdSer[207]. Gas6 stimulates phagocytosis of apoptotic thymocytes by bone marrow-derived macrophages, and this stimulation is abolished by genetic deletion of MerTK[208], indicating that Gas6 opsonises PtdSer-exposing apoptotic cells

for phagocytosis via macrophage-expressed MerTK. Indeed, MerTK activation by PtdSer-exposing liposomes (but not phosphatidylcholine-exposing liposomes) is dramatically enhanced by gas6[209], further supporting the idea that gas6 can bridge PtdSer exposed on cells to MerTK exposed on phagocytes. Gas6 also induces phagocytosis of fluorescent microspheres and apoptotic Jurkat cells by microglia[210], implicating gas6 as a regulator of phagocytosis within the unique environment of the mammalian brain.

1.4.1.3.8. Galectin-3

Galectin-3 is a β-galactoside-binding protein highly expressed by several myeloid cells including macrophages, monocytes, dendritic cells and neutrophils, and is found in tissues throughout the mammalian system[211]. Galectin-3 has been detected both intracellularly and extracellularly, and can be released from cells following stimulation, such as BV-2 microglial cells stimulated by bacterial LPS[212]. Galectin-3 can bind with high affinity to N-acetyl-lactosamine – a disaccharide prevalent on glycan chains of glycoproteins and gangliosides[213,214] – and this capacity for binding sugars is fundamental to its ability to opsonise cells for phagocytosis. Galectin-3 has been shown to enhance the uptake of apoptotic neutrophils by monocyte-derived macrophages, and this increased uptake was completely blocked by lactose, which competes for sugar binding[215]. Whilst it usually exists as a monomer, binding to N-acetyl-lactosamine induces crosslinking of the protein (via its N-terminal domain) to other galectin-3 monomers, which may facilitate the bridging between phagocytes and target cells during phagocytosis[213,214].

Galectin-3 can directly bind the phagocytic receptor MerTK, and stimulation of macrophage phagocytosis of apoptotic Jurkat cells by galectin-3 is prevented by a function-blocking antibody against MerTK[216] - indicating that MerTK is a phagocytic receptor that mediates galectin-3 opsonisation. Galectin-3 has also been shown to induce phagocytosis of cellular debris and neuron-like PC12 cells by microglia, which is inhibited by blocking MerTK[212]. In the same study, galectin-3 binding to both PC12s (the target cell) and BV-2s (the phagocyte) was enhanced dramatically by enzymatically removing surface sialic acid residues (‘don’t eat-me’ signals, section 1.4.1.4) via application of the sialidase neuraminidase, which also enhanced phagocytosis of the PC12s in the presence of galectin-3 - indicating that galectin-3 opsonisation of cells is prevented by sialic acids[212].

Table 1: List of known mammalian opsonins.

Opsonin type	Opsonin	Ligand(s)	Receptor(s)	Opsonisation roles
Complement	C1q	PtdSer[155], C1qR (CRT)[217], bacterial membrane proteins[218]	CR1[219], C1qR (CRT)[220], LRP1[64]	Phagocytosis of apoptotic cells by monocytes and macrophages[64,217], phagocytosis of neurites and synapses by microglia[221,222], phagocytosis of bacteria by macrophages[223,224]
Complement	C3b/iC3b	LPS[148,149], zymosan[225], bacterial membrane proteins[226]	CR1, CR2, CR3, CR4, CRIg[227,154]	Phagocytosis of apoptotic cells by macrophages[228], phagocytosis of synapses by microglia[32], phagocytosis of bacteria by macrophages[229], phagocytosis of fungi by neutrophils[230]
Complement	C4b	Bacterial membrane proteins[226]	CR1[231]	Phagocytosis of bacteria?[226]
Antibody	IgG	Various	FcγRI, FcγRIIA, FcγRIII[160]	Phagocytosis of diverse microbes by leukocytes[232], phagocytosis of red blood cells by macrophages[166], phagocytosis of apoptotic neutrophils by macrophages[165]
Antibody	IgM	Various	CR3[233], FCMR[234]	Phagocytosis of diverse microbes by leukocytes[166], phagocytosis of apoptotic microparticles by macrophages[166]
Collectin	MBL (mannan binding lectin)	Yeast mannan[176], GlcNAc in bacterial peptidoglycan[235], LPS[170], LTA[236], PtdSer[237]	C1qR (CRT)[64,238], CR1[239]	Phagocytosis of T cells by monocytes[64], phagocytosis of bacteria by macrophages, monocytes and neutrophils[174,240], phagocytosis of fungi by polymorphonuclear leukocytes[241]

Collectin	SP-A	PtdSer[242], lipids[243], LPS[244]	CRT/LRP1 [238,245,141]	Phagocytosis of bacteria by monocytes and macrophages[246,247], phagocytosis of apoptotic neutrophils by macrophages[248]
Collectin	SP-D	Bacterial peptidoglycan and LTA[249], LPS[244], yeast β-glucan[250]	CRT/LRP1 [141]	Phagocytosis of apoptotic neutrophils by macrophages[248], phagocytosis of bacteria by macrophages[251,252], phagocytosis of fungi by macrophages[253]
Ficolin	L-ficolin	Yeast mannan and GlcNAc[176], LTA[177], LPS[178]	CRT/LRP1 [254]	Phagocytosis of bacteria by monocytes and macrophages[176,180,181]
Ficolin	M-ficolin	Sialic acid (on the phagocyte membrane)[255], GlcNAc and other acetylated glycans[177], yeast glycans[256], bacterial polysaccharide [257]	GPCR43[258]	Phagocytosis of *E. coli* by monocytes[183]
Pentraxin	CRP (C-reactive protein)	LTA[186], phosphatidyl-choline on pathogenic and mammalian cell membranes[184], C1q[192]	FcγRI[259], FcγRIIa[260], FcαRI	Phagocytosis of apoptotic T cells by macrophages[191], phagocytosis of bacteria by neutrophils[261], phagocytosis of zymosan particles by macrophages[262,263]
Pentraxin	SAP (serum amyloid P component)	LPS[264], bacterial glycans[265], amyloid fibrils[190], C1q[266]	FcγRI[263], FcγRIIa[262], FcγRIII[191]	Phagocytosis of apoptotic neutrophils and T cells by macrophages[191], phagocytosis of zymosan particles by macrophages [262] and neutrophils [263]

?	MFG-E8 (milk fat globule-EGF factor 8)	PtdSer[200]	VNR[201]	Phagocytosis of apoptotic cells by macrophages[202], phagocytosis of red blood cells by macrophages[204], phagocytosis of neurons by microglia[197]
?	Gas6	PtdSer[207]	MerTK[206]	Phagocytosis of apoptotic thymocytes by macrophages[208], phagocytosis of apoptotic T cells by microglia[210]
?	Protein S	PtdSer[267]	MerTK[268]	Phagocytosis of apoptotic lymphoma cells by macrophages[267]
?	Tubby	?	MerTK[132]	Phagocytosis of apoptotic cells by macrophages[269,270]
?	Galectin-3	Asialoglycans[212]	MerTK[216]	Phagocytosis of apoptotic neutrophils and T cells by macrophages[215,216], phagocytosis of cell debris and pheochromocytoma cells by microglia[212]
?	Calreticulin	Asialoglycans[143]	LRP1[135]	Phagocytosis of neutrophils by macrophages[143]

1.4.1.4. 'Don't eat-me' signals

Scavenger cells like macrophages possess potent phagocytic capacity in the steady-state. Thus, without established defence mechanisms, the majority of mammalian cells would be vulnerable to phagocytic elimination at any given time. However, just as cells destined for phagocytic elimination (such as apoptotic cells) express 'eat-me' signals on their surface to promote engulfment by resident phagocytes, other cells are protected through exposure of 'don't eat-me' signals, which ward off their removal by phagocytically active cells. Such anti-phagocytic signals are of particular relevance in the context of autoimmunity, as well as in tumorigenesis and cancer progression. The ability for any apoptotic cell to hide their protective signalling mechanisms is mediated via either i) downregulation and/or internalisation of such 'don't eat-me' signals, or ii) modification of the signal such that its

protective functionality is removed[271] – for example, in the enzymatic desialylation of various surface glycoproteins, which will be discussed[245]. Established 'don't eat-me' signalling mechanisms are depicted schematically in Figure 1.2 (page 36).

1.4.1.4.1. Cluster of differentiation 47 (CD47)

CD47 is a highly glycosylated protein within the immunoglobulin superfamily, and is ubiquitously expressed by cells throughout the mammalian system[271]. CD47 employs a range of functions in different cell-types, with roles in proliferation, cell-cell adhesion, migration, and importantly in regulating a cell's vulnerability to engulfment by resident phagocytes[271]. Regarding phagocytosis, CD47 acts as a marker in two fundamental contexts: during microbial infection, to mark the cell as 'self', and in normal homeostasis, to protect the cell from efferocytosis[271].

CD47 signals *in trans* to resident phagocytes via the phagocytic inhibitory receptor signal regulatory protein α (SIRPα)[135].Upon activation by CD47, an intracellular signalling cascade is initiated which ultimately results in inhibition of myosin recruitment at the interface between the effector and target cell, thus preventing the cytoskeletal rearrangements necessary for engulfment[272]. In experimental systems, blocking the interaction between CD47 and SIRPα can induce phagocytosis of perfectly viable cells[135] (a phenomenon known as phagoptosis[7]), and CD47-deficient mice exhibit symptoms of autoimmune disease[273]. Exposure of CD47 on red blood cells has been shown to prevent their phagocytosis by circulating splenic red-pulp macrophages, which otherwise rapidly eliminate cells that do not expose CD47[274], demonstrating importance of the signal in normal tissue homeostasis. However, CD47-mediated inhibition of cell clearance can also be detrimental to health: such mechanisms are upregulated during various cancers to facilitate tumour cell perpetuation[271]. Elevated CD47 levels have been documented in ovarian cancer[275], acute lymphoblastic leukemia (ALL)[276], multiple myeloma (MM)[277], acute myeloid leukemia[278] and non-Hodgekin lymphoma[138], and CD47 is expressed on all documented solid tumour cells[279]. Thus, CD47 presents as a promising therapeutic target in diverse oncological indications.

1.4.1.4.2. Cluster of differentiation 200 (CD200)

CD200 is a ~45 kDa protein commonly expressed by cells of hematopoietic origin, including macrophages, neutrophils, dendritic cells, B and T cells[280]. CD200 is also expressed by various non-hematopoietic cells, notably brain cells such as neurons, astrocytes, oligodendrocytes and endothelial cells[280]. The cognate receptor of CD200 (CD200R) is expressed predominantly by myeloid cells such as macrophages, including microglia[280]. CD200 has been described as a 'don't eat-me' signal[7], and is implicated in precluding macrophage phagocytosis of oligodendrocyte precursor cells[281]. Furthermore, decreased CD200 presence around myelinating plaques in multiple sclerosis (MS) was correlated with increased microglial activation[282], and microglia from mice deficient in CD200 reveal markers of activation including increased proliferation and nitric oxide synthase (NOS) expression[283], suggesting that CD200 influences phagocytosis and general activation status of resident phagocytes. Accordingly, CD200 is classed as a neuroimmunoregulatory protein (NIReg), along with CD47[284]. However, CD200 expression has been shown to increase in certain cells undergoing apoptosis, and such increased expression inhibited generation of pro-inflammatory cytokines by proximal dendritic cells[285]. Thus, the role of CD200 is ambiguous, and may reduce phagocytic clearance of cells indirectly by promoting an anti-inflammatory extracellular environment.

1.4.1.4.3. Cluster of differentiation 24 (CD24)

CD24 is a highly glycosylated surface protein expressed at particularly high levels in the kidney and bladder, with lower levels documented in endocrine and pancreatic tissue[103]. CD24 is known to directly interact with immune cells via surface-expressed sialic acid-binding immunoglobulin-type lectin 10 (Siglec-10), thus promoting various anti-inflammatory responses in the immune cell, including the inhibition of target phagocytosis, achieved through inhibition of the cytoskeletal rearrangements required for target engulfment[286]. CD24 is of particular relevance in ovarian and breast cancer, as such tumour cells overexpress CD24 (concurrent with overexpression of Siglec-10 in tumour-associated macrophages)[286]. Interfering with CD24/Siglec-10 signalling via either genetic ablation of the proteins or via pharmacological blockade increased phagocytosis of a range of CD24-expressing tumour cells from humans[286], emphasising the importance of CD24 as a 'don't eat-me' signal in certain cancers.

1.4.1.4.4. Plasminogen activator inhibitor 1 (PAI-1)

A member of the superfamily of serpins (serine-protease inhibitors), PAI-1 is a crucial homeostatic regulator of blood clot degradation as the main inhibitor of plasminogen, a zymogen that circulates in the bloodstream and is enzymatically processed to plasmin during fibrinolysis[287]. PAI-1 is upregulated during the inflammatory response resulting from sepsis[288], acute lung injury[289] or myocardial infarction[290]. However, surface-expression of the protein is decreased on neutrophils undergoing death by apoptosis[291], indicating that PAI-1 may protect healthy cells from phagocytic clearance. Phagocytosis of neutrophils has been shown to increase with genetic deletion of the gene encoding PAI-1, or in the presence of anti-PAI-1 antibodies, and such increase depends on calreticulin/LRP1 signalling[291]. Conversely, neutrophil phagocytosis was inhibited by exogenous application of PAI-1 to the cells[291]. The phagocytosis of zymosan particles by microglial can also be inhibited with PAI-1[292], suggesting that the presence of PAI-1 on the surface of diverse phagocytic targets is sufficient to inhibit their phagocytic elimination.

1.4.1.4.5. Programmed cell death ligand 1 (PD-L1)

PD-L1 is a membrane-bound protein of particular interest in cancer research, due to observations that it is upregulated at the surface of cancer cells[293]. Its cognate receptor PD-1 (also known as CD279) is well characterised in regulating T cell activity[294], but is also expressed by various types of macrophages, and such expression is upregulated during pathogenic infection and in sepsis[295,296]. PD-1 is expressed by tumour-associated macrophages in both mouse and human cancers, and correlates negatively with phagocytic capacity of the macrophages against tumour cells requiring phagocytic elimination[294]. Importantly, disruption of the PD-L1/PD-1 signalling pathway enhanced macrophage-mediated phagocytosis of the cells and limited tumour growth *in vivo*[294]. Thus, PD-L1 is currently being targeted as an anti-cancer therapeutic to mitigate tumour growth.

1.4.1.4.6. β-2 microglobulin subunit of the major histocompatibility class I complex (β2M)

β2M is a 12 kDa protein component of the MHC class I complex that is expressed in virtually all nucleated cells[297]. Like PD-L1, β2M is implicated in cancer development, and its expression in various cancer cell lines is positively correlated with resistance to macrophage-mediated phagocytosis[298]. β2M on the surface of cancer cells is recognised by the leukocyte

immunoglobulin-like receptor B1 (LILR-B1), which is expressed at the macrophage surface and, once bound to its ligand, initiates an intracellular signalling cascade that suppresses initiation of the phagosome, thus inhibiting phagocytosis[298].

1.4.1.4.7. *Sialic acid*

Sialic acids are a family of negatively-charged monosaccharides ubiquitously located at the terminus of glycan chains present on proteins and lipids in all major mammalian cell-types[299,300]. Sialylation of glycan chains is an enzymatic process catalysed by Golgi-resident sialyltransferases (STs) which covalently link a single sialic acid residue to N-terminal glycans[301]. Sialic acid residues perform myriad functions in eukaryotes, including roles in regulating cell-cell signalling, cell adhesion and glycoprotein stability[299], and their importance is emphasised by the fact that homozygous mutants deficient in sialic acid production die early during embryogenesis[302].

A crucial function of surface-expressed sialic acids is in modulation of the immune system. Sialic acids generated by mammalian systems and used to decorate glycan chains are distinct from similar sugars found in microbial pathogens, and so sialic acids exposed on the cell surface aid in the discrimination between 'self' and 'non-self' by cells of the innate and adaptive immune systems[303]. Surface-exposed sialic acids are recognised by sialic acid-binding immunoglobulin type lectins (SIGLECs) expressed by all major myeloid cells including monocytes, macrophages, dendritic cells, neutrophils and eosinophils[303]. The binding of sialic acid residues to SIGLECs inhibits phagocytosis[304], and desialylation of N-glycans - for example via enzymatic activity of the lysosomal human sialidase neuraminidase 1[300], which can be secreted to the cell surface during inflammation[305] - has been shown to promote phagocytosis of platelets by peripheral macrophages[306], of sperm cells by peritoneal macrophages[307], and of neuron-like PC12 cells by microglia[212].

1.4.2. Target internalisation

Following migration to and recognition of a target, the phagocyte is ready to engage in the step-wise processes of phagosome formation and phagosome maturation into the phagolysosome, which ultimately leads to phagocytic elimination of the target[232]. Such processes will now be described, and are depicted schematically in Figure 1.3 (page 54).

1.4.2.1. Phagosome formation

How the initial recognition of pro-phagocytic signals by phagocytes is translated into the signalling cascades that initiate the first step of engulfment – formation of the phagosome - has been intently studied in recent years, with particular emphasis on those regulated by Fcγ receptors and complement receptor 3 (CR3) expressed on the phagocyte surface[232].

The binding of pro-phagocytic Fcγ receptor aggregates to target-exposed IgG leads to FcγR activation, which promotes phosphorylation of their cytoplasmic immunoreceptor tyrosine-based activation (ITAM) motifs, achieved by Src-family kinases[232]. This in turn provides a docking site for the tyrosine kinase Syk, which can then phosphorylate ITAMs through a positive feedback process[58]. Syk also phosphorylates the guanine nucleotide exchange factor (GEF) Vav, which then activates the GTPases Rho, Rac and Cdc42[232]. Together, these GTPases facilitate actin polymerisation via Arp2/3, which generates localised actin fibres and drives the pseudopod extension that begins the phagosome[232]. CR3-mediated phagocytosis also involves the phosphorylation and activation of Syk[308]. However, the procession of phagosome formation initiated by CR3 activation is distinguished from that mediated by Fcγ receptors through the involvement of microtubule-mediated (as well as actin-mediated) cytoskeletal rearrangements[309,310].

Actin (and microtubule) remodelling facilitates extension of the pseudopodia that can rapidly engulf the target, and such remodelling involves multiple important steps: i) disruption of the membrane-associated cytoskeleton; ii) actin filament nucleation and polymerisation; and iii) actin depolymerisation and phagosome sealing[58]. In both Fcγ- and CR-mediated engulfment, the pre-existing cytoskeletal organisation responsible for the 'resting' morphology of the phagocyte is disrupted by a group of actin-debranching proteins, known as coronins[311], as well as the actin-severing proteins cofilin[312] and gelsolin[313]. Accumulation of coronin-1 at the base of the nascent phagocytic cup causes localised debranching of F-actin, generating fibres that are severed by cofilin and gelsolin. Such destruction of the local actin cytoskeleton generates a dip in the phagocyte surface which initiates the phagosome, and also enhances association of pro-phagocytic surface receptors with ligands on the target. Furthermore, this depolymerisation increases levels of monomeric actin that can be incorporated into new filaments[58].

Following disruption of the pre-existing cytoskeletal network, the next step in the engulfment process requires the creation of novel cytoskeletal processes to wrap around the target, which is achieved via nucleation of actin filaments and filament polymerisation[58]. Actin nucleation depends upon recruitment of the Arp2/3 complex, the activity of which is stimulated by various regulatory proteins including Cdc42, Rho and Rac via intermediary signalling cascades that differ between Fcγ- and CR-mediated engulfment[58]. Finally, sealing of the phagosome is achieved through both the collapse of F-actin at the base of the phagocytic cup, and the fusion of membrane extensions at the distal end, thus generating a fully enclosed nascent phagosome[58].

1.4.2.2. Phagosome maturation

Phagosome maturation describes the process through which the nascent phagosome undergoes successive fusion and fission events with early and late endosomes, and finally lysosomes, to generate the mature phagolysosome[314]. The phagosome undergoes its first membrane fusion events with sorting and recycling endosomes[315], during which the luminal acidification process is initiated via accumulation of V-ATPases within the phagosome membrane, which translocate protons across the membrane in an ATP-hydrolysing process[55]. Such fusion events are regulated by the small GTPase Rab5, which is subsequently replaced by Rab7 to promote fusion with late endosomes[316], so generating the late phagosome. Rab7 also recruits new proteins to the phagosome membrane - importantly, the Rab-interacting lysosomal protein (RILP)[317], which indirectly interacts with the microtubules that draw in proximal lysosomes for phagosome fusion[318]. Following fusion, the phagosome is transformed into the phagolysosome, a severely inhospitable environment for biological material. Along with lysosomes, phagolyosomes are the most acidic organelles known, with a pH as low as 4.5 attained through extensive V-ATPase activity[55]. Hydrolytic enzymes sourced from the now fused lysosomes include various proteases, cathepsins, lipases and lysozymes, and these assist in the degradation of proteinaceous components of the target[58]. The phagolysosome also contains antimicrobial molecules such as lactoferrin[319], which sequesters the iron on which many bacterial proteins and enzymes depend[320]. Generation of reactive oxygen species via NADPH oxidase activity - such as hydroxyl radicals and singlet oxygen - further assist in the degradation of both pathogenic and host cellular targets[321].

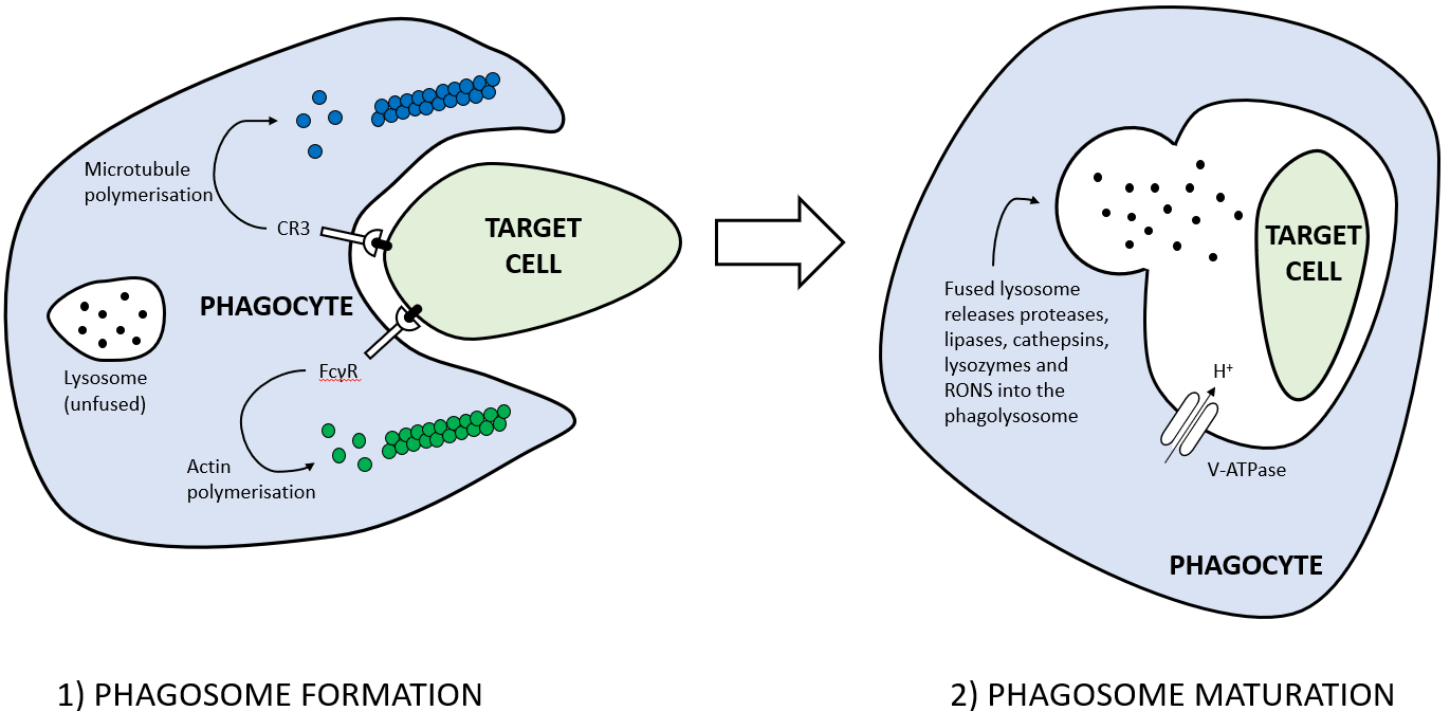

Figure 1.3. Phagosome formation and maturation. Activation of Fcγ and CR3 receptors on the phagocyte trigger actin and microtubule polymerisation respectively, which drive the cytoskeletal rearrangements that engulf the target and form the phagosome (1). Lysosomes containing cathepsins, proteases, lipases, lysozymes and RONS fuse with phagosome to facilitate degradation of the target, and thus create the mature phagolysosome (2). Target degradation is also facilitated by acidification of the phagolysosome, mediated by membrane VTPases. CR3: complement receptor 3. FcγR; fragment-crystallisable-gamma receptor. RONS: reactive oxygen or nitrogen species.

CHAPTER II

INTRODUCTION PART II – MICROGLIA

Microglia are the predominant non-neuronal immune cell type in the CNS, constituting between 10-20% of the total cell population[322,323]. From the earliest stages of CNS development, microglial progenitors that originate in the yolk sac invade the CNS, where they differentiate into mature microglia and distribute throughout the brain parenchyma[324]. Since their identification, various immune functions have been ascribed to microglia in both physiological and pathological contexts. Like other macrophages, microglia exhibit phagocytic activity and can phagocytose diverse targets - including neurons (and non-neuronal cells), subcellular neuronal components like axons and synapses, neuronal debris, axonal myelin, and toxic extracellular protein aggregates such as amyloid plaques[325,326,327]. These phagocytic activities play fundamental roles in CNS development, homeostasis, and neuroprotection during pathology, and the spatiotemporal heterogeneity in microglial function is mediated through adoption of distinct microglial phenotypes[328] - although the precise conditions and mechanisms that regulate such phenotypes are far from clear. The physiological importance of microglial function, particularly phagocytosis, is emphasised by the myriad neurological diseases in which microglial dysfunction is implicated[329]. In this chapter, the roles and regulatory mechanisms of this microglial phagocytosis in contexts of development, tissue homeostasis and pathology will be reviewed, with particular emphasis on microglial phagocytosis of bacteria and synapses - both of special relevance to this thesis.

2.1. Microglial functions in the brain

2.1.1. Microglia in CNS development

Microglia originate from yolk sac-derived myeloid progenitors which infiltrate the developing brain parenchyma in early embryonic development, and this colonisation continues well into the postnatal period[330]. Microglia remain in the brain throughout the mammalian lifespan via continual self-renewal, with only a minor contribution to microglial

density being provided by circulating blood monocytes[331]. Crucially, they constitute the single glial cell population for a significant portion of the prenatal developmental period, as astrocytes and oligodendrocytes (the other major CNS immune cells) arrive later, through differentiation from neural progenitor cells[332]. Accordingly, microglia have been described to play several fundamental roles during early development. Indeed, microglia have been demonstrated as essential for regulating the differentiation of other immune cells such as oligodendrocytes, and can directly induce oligodendrocyte myelinogenesis through release of the insulin-like growth factor 1 (IGF-1)[333]. *In vitro* evidence also indicates microglial-released factors, including interleukin 6 (IL-6) and leukaemia inhibitory factor (LIF), can stimulate the differentiation of astrocytes from neural stem precursor cells (NSPCs)[334].

Microglia exploit their dual capacity for phagocytosis and release of soluble, diffusible factors (trophic or otherwise) in brain development[335]. In the cerebral cortex of rodents and primates, microglia present in the subventricular zone (SVZ) and neocortex directly regulate neuronal density through targeted phagocytosis of neural progenitor cells (NPCs), thus limiting excessive neurogenesis[336]. Microglia also eliminate differentiated neurons in the developing cerebellum, inducing apoptosis in cerebellar Purkinje cells via superoxide release, and subsequently clearing the dying cells via phagocytosis - highlighting that microglia *per se* can be sufficient to induce developmental neuronal loss[337]. However, developmental turnover of cells by microglia is not restricted to neurons, as microglial phagocytosis of oligodendrocytes has been observed in developing white matter[338]. In contrast, microglia present in white matter can provide trophic support (in the form of IGF-1) to layer V cortical neurons during postnatal development[339]. Without such support, the pyramidal neurons undergo apoptosis, indicating that microglia can promote cell survival as well as removal in distinct developmental contexts. Microglial invasion and distribution within the cerebral cortex is highly dynamic[340], and during cortical layer development, microglia have been shown to promote correct positioning of cortical interneurons within the cortical plate by facilitating their migration from neocortical locations outside the plate[341]. As well as regulating appropriate neuronal migration, microglia can stimulate axonal outgrowth and neurite development – notably during embryonic formation of the corpus callosum[342] and the prosencephalon (early forebrain)[341] – and also dendritic spine formation and generation of functional synapses[343,344], which together help establish the earliest connections in the neural circuitry.

Perhaps the best characterised developmental function of microglia is the phenomenon of phagocytosis of synapses, also known as synaptophagy[122]. Synaptogenesis in postnatal mammals is well known to generate an excess number of synaptic connections, which peaks at levels significantly greater than those in adults, before gradually declining[345]. In the mouse hippocampus, spine density analyses have identified rapid spine formation between postnatal days 6 to 15 in CA1 and CA3 pyramidal neurons and dentate granule cells, before a subsequent drop in density by P45[346]. In humans, this transition from net production to net elimination of synapses has also been observed, and occurs at different timepoints across different cortical regions[347]. Such developmental 'synaptic pruning' may be critical for experience-dependent neural circuitry formation, as disruptions in its regulation are linked to developmental disorders such as autism[348]. One of the fundamental mechanisms through which supernumerary synapses are pruned is through phagocytosis, which is primarily attributed to microglia as the resident brain macrophage (although synaptophagy by astrocytes is increasingly documented as critical to the pruning process[349]).

Microglia express a range of receptors capable of sensing synaptic activity - including those for neurotransmitters, neuropeptides and neuromodulators[350,351] - and have been demonstrated to engage in brief yet repetitive interactions with neuronal synapses in the somatosensory and visual cortex, which occurs in an activity-dependent manner[352,353]. Indeed, in the visual cortex specifically, over 90% of microglial processes have been shown to interact with synaptic elements at any given time[353]. Microglial phagocytosis of synapses in the developing brain was first established in the mouse hippocampus, where synaptic markers were found internalised within microglial vesicles during a period of high synaptic turnover, at postnatal day 15[354]. Mice lacking the fractalkine receptor CX_3CR1 - a microglial-specific receptor that mediates chemotaxis and microglial migration[351] - contained neurons with significantly higher synaptic and dendritic spine densities in the CA1 hippocampal region, implicating microglial phagocytosis of synapses in developmental synaptic pruning[354]. Furthermore, electrophysiological recording of these neurons revealed deficits in spontaneous excitatory post-synaptic current (sEPSC) generation, suggesting that microglia-mediated phagocytosis is required for normal signalling activity and maturation of neural connectivity. Such findings were supported by independent demonstration that genetic deletion of CX_3CR1 inhibited

microglial entry into barrel-centres within the somatosensory cortex at crucial stages of early postnatal development, which was associated with impaired functional maturation of thalamocortical synapses within the region[110]. Studies on the mouse retinogeniculate (RGC) system provide further evidence for microglial phagocytosis of synaptic inputs during periods of robust synaptic pruning[32]. Again, significant levels of internalised synapses were observed within microglia at early postnatal stages (P5), and this internalisation was not observed at later stages (P30) indicating that i) such synapses had been phagocytosed, and ii) this microglial phagocytosis of synapses is temporally regulated[32]. The same study also demonstrated that engulfment of retinal ganglion cell (RGC) inputs by microglia was influenced by neuronal activity, consistent with previous findings that interactions between synapses and microglial processes was activity-dependent[352,353].

Regarding the molecular mechanisms that regulate synaptic pruning by microglia, several lines of evidence have revealed the importance of complement signalling to this process. C1q has long been known to localise at synapses in the postnatal CNS, and mice deficient in C1q or C3 exhibit substantial defects in synapse elimination in the RGC system[145], opening the possibility that complement proteins opsonise the synapses for phagocytosis. Microglial phagocytosis of pre-synaptic components within the RGC system later established by Schafer *et al*[32] was found to occur in a complement-dependent manner, as mice deficient in CR3, C3 or C1q revealed reduced synaptic pruning - consistent with microglia mediating the complement-dependent synapse elimination during development identified previously[145]. Moreover, astrocyte-secreted transforming growth factor (TGF)-β has been shown to induce upregulation of C1q by RGC neurons and increased synaptic tagging by C1q, and mice deficient in TGF-β reveal reduced presence of C1q at the neurons, as well as reduced microglial engulfment of RCG terminals at developmental stage P5[222]. Tagging of neurites by complement has been shown to be influenced by surface desialylation i.e. enzymatic removal of sialic acid residues (well characterised 'don't eat-me' signals as described in section 1.4.1.4) enhances complement binding and synaptic engulfment by microglia[221,355]. Recent evidence also reveals the microglial receptor TREM2 (described in section 2.3.1.8) as a key regulator of developmental synaptic pruning by microglia both *in vitro* and *in vivo*[356]. Furthermore, CD47 (a known 'don't eat-me' signal – section 1.4.1.4.1) has been found to localise at synapses during periods of developmental synaptic pruning, where it inhibits microglial synaptophagy by signalling via the anti-phagocytic receptor SIRPα, which is

enriched in microglia during pruning[357]. Moreover, CD47 was found to accumulate at more active synapses, and thus CD47-SIRPα signalling is implicated in protecting more active synapses from phagocytic elimination by microglia[357].

Since deficient synaptic pruning by microglia is associated with social behaviour abnormalities and increased repetitive behaviours in mice[356,358], defective microglial pruning during development may feature in neurodevelopmental disorders such as autism, highlighting its importance to normal CNS development.

2.1.2. Microglia in CNS homeostasis

The dual capacity for phagocytosis and release of soluble factors by microglia extends beyond the perinatal period, where such activities remain crucial for tissue homeostasis throughout the brain. As the resident macrophage of the brain parenchyma, microglia are directly responsible for phagocytically clearing dead or dying neurons (apoptotic or otherwise), as well as neuronal debris[122], and the molecular mechanisms that regulate this phagocytosis are reviewed in section 2.3. Whilst astrocytes are also phagocytically proficient immune cells in the brain, they exhibit significantly less efficient phagocytosis of apoptotic cells compared to microglia[359], and so are unlikely to play as vital a role in apoptotic cell-clearance. Following acute CNS injury, for example during stroke or traumatic brain injury (TBI)[360], an initial wave of inflammation is mitigated by microglial phagocytosis of apoptotic cells coupled with release of anti-inflammatory cytokines[361], which prevents chronic inflammation and restores tissue homeostasis. Microglial phagocytosis of apoptotic neural progenitor cells observed in the developing brain has also been described in adulthood: the majority of new-born NPCs in the subventricular zone and the hippocampal dentate gyrus in adult mice undergo apoptotic death during their transition into neuroblasts (primitive neurons), and such apoptotic cells are rapidly scavenged by resident microglia[362]. Microglia can also phagocytose myelin[361], which is essential in the elimination of myelin debris that accumulates during normal ageing[363], and may also play a homeostatic role in axonal maintenance. Independent to their phagocytic capacity, microglia contribute to tissue homeostasis through release of various soluble and diffusible molecular components, which have been ascribed to several homeostatic functions[364]. In the hippocampus of adult rats, microglial released IGF-1 stimulates oligodendrocyte production through differentiation of

hippocampal-derived NPCs[365]. Microglia throughout the brain also release several trophic factors to maintain neuronal survival and facilitate normal neuronal function, including nerve growth factor (NGF), brain-derived neurotrophic factor (BDNF) and epidermal growth factor (EGF)[364].

As well as in early development, microglial modulation of synapses in healthy adults is increasingly documented. Microglia continue to survey the brain parenchyma into adulthood through dynamic process extension, which again occurs in an activity-dependent manner. In the adult retina, for example, agonisation of neuronal α-amino-3-hydroxy-5-methyl-4-isoxazolepropionic acid (AMPA) receptors stimulates microglial process extension in mechanisms that depend on ATP[366]. In hippocampal slices taken from adult mice, application of N-Methyl-d-aspartate (NMDA) to NMDA receptors triggered microglial process outgrowth, which was again mediated by extracellular ATP[367]. Glutamate-induced microglial process extension has also been reported in the somatosensory cortex of 1-2 month old mice *in vivo*[368]. Such activity-dependent interactions have implicated microglia in both the developing and adult CNS as key regulators of synaptic plasticity (i.e. the long-term potentiation (LTP) or long-term depression (LTD) of synapses to modulate firing propensity[351]), which mediate information processing and storage in the brain[369]. BDNF released by microglia has been shown to regulate expression of the post-synaptic glutamate receptors GluN2B and GluA2[344]. Genetic deletion of BDNF (or selective depletion of microglia) decreased expression of these receptors at synapses without promoting a decrease in neuronal densities in the hippocampus or cortex[344]. Importantly, proper maintenance of such glutamate receptors is necessary for synaptic plasticity[370]. Microglial release of the soluble cytokine tumour necrosis factor-α (TNF-α) has been shown to modulate AMPAR- and NMDAR-mediated synaptic currents and so regulate 'synaptic scaling', the uniform modulation of all synapses within a single neuron (distinct from LTP or LTD, which is specific to individual synapses)[371]. Whilst TNF-α release in the brain is typically associated with neuroinflammation, circulating TNF-α has also been detected under physiological conditions, albeit at lower concentrations[351], meaning TNF-α may regulate homeostatic synaptic scaling[371]. Together, these findings indicate that microglial-release of soluble factors, including growth factors and cytokines, can modulate synapses.

Synaptic plasticity modulation via phagocytosis of synapses by microglia has also been suggested: in the mouse visual cortex, monocular deprivation (i.e. forced closure of a single eye in the animal) triggered increased microglial interactions with, and phagocytosis of, synapses in corresponding cortical regions[372]. Such effects were absent in animals lacking $P2Y_{12}R$, a chemotactic receptor expressed at high levels in homeostatic (unactivated) microglia[372]. However, as most of the literature pertains to perinatal animal models, the extent to which synaptic pruning by microglia mediates plasticity across the adult brain is unclear, and requires investigation. Furthermore, findings that basal synaptic transmission and function is unaffected in mice deficient in chemotactic migration through deletion of CX_3CR1 [373], or in mice deficient in microglia altogether[374], question the role of microglial activity in regulating baseline synaptic activity in the absence of plasticity[325].

2.1.3. Microglia in immunity

Historically, the brain has been considered a sterile and immune-privileged environment, where microbial presence is exclusively associated with pathological infection and/or immunocompromised hosts[375]. However, the presence of bacteria within the brain parenchyma in non-pathological contexts is being increasingly documented. Bacterially-encoded RNA has been detected in the white matter of both pathologically normal and abnormal human brains[376], and Roberts *et al* observed bacterial cells within neurons and glia across various regions of post-mortem brain tissue, including the hippocampus, cortex and substantia nigra[377]. Bacteria cells have also been observed in similar regions in mouse brains fixed immediately after death, but not in germ-free mice processed identically[377], indicating that such bacterial presence is not an experimental artefact. In healthy individuals, the mammalian brain is highly protected against microbial infiltration (relative to other organs) by the blood-brain barrier, a layer of endothelial cells connected by tight intercellular junctions[378]. Such barriers form an effective obstacle to microbial penetration; however, bacteria have evolved several mechanisms that enable them to infect the brain. *Streptococcus pneumoniae*, the causative agent of community-acquired pneumonia, release the toxin pneumolysin which directly damages endothelial cells, generating holes in the barrier[379]. Pathogenic entry through junctions between endothelial cells (paracellular traversal), or through cells via endocytic mechanisms (transcellular traversal), have also been documented[378,380].

Microglia, as the brain-resident macrophage, are the major immune cell-type within the brain that can directly recognise and eliminate invading pathogens. Thus, microglia are crucial components of the innate immune system of the brain. Recognition of pathogenic material (PAMPs) by microglia is achieved through binding to germ-line encoded PRRs, many of which are shared commonly by tissue-resident macrophages throughout the body. Some of the best characterised PRRs include the toll-like receptors (TLRs)[378]. Microglia are known to express TLR1-9, which together bind a wide range of highly conserved pathogenic motifs[381]. For example, TLR4 binds LPS present on the surface of gram-negative bacteria[382], whilst TLR2 binds LTA, a constituent of the cell wall of gram-positive bacteria[383]. Both receptors signal intracellularly via the adaptor protein myeloid differentiation factor 88 (MyD88), and functional MyD88 is essential for mammalian resistance to infection by bacterial species including *E. coli*[384], *S. aureus*[385] and *S. pneumoniae*[386], or by the protozoan parasite *T. gondii*[387]. TLR3 detects virally-encoded double-stranded RNA (dsRNA), activation of which triggers an intracellular signalling cascade involving Toll/interleukin-1 (IL-1) receptor domain-containing adaptor molecule 1 (TICAM-1)[388]. Microglial TLR3-TICAM-1 signalling has been implicated in prevention of CNS infection by Poliovirus[388,389] and West Nile virus (WNV)[390]. Furthermore, TLR recognition of various fungal species has also been reported, including *Candida albicans, Cryptococcus neoformans* and A*spergillus fumigatus*[391]. Other PRRs include the NLRs, RLRs and CLRs which recognise a wide range of PAMPs originating from diverse bacterial and fungal species, as well as viruses[378,392]. Microglia also express a range of receptors that respond to pathogenic infection indirectly by recognising host-derived distress signals, or 'damage-associated molecular patterns' (DAMPs). Such receptors include purinergic receptors, cannabinoid receptors, tachykinin receptors and estrogen receptors, and evoke inflammatory responses in microglia upon activation[393].

In microglia, activation of PRRs induces a variety of downstream effects including extracellular cytokine and chemokine release, reactive oxygen/nitrogen species (RO/NS) generation and release, and increased phagocytosis of microbes[378]. Microglia treated with agonists for TLRs 2, 4 or 9 release nitric oxide (NO), which can directly damage bacteria[394], and cytokines including TNF-α and IL-6 that trigger pro-inflammatory responses from other immune cells to facilitate pathogen clearance[395]. Such stimulants also induce an

inflammatory-activated ('M1') microglial phenotype (reviewed further in section 2.2.2), enhancing microglial phagocytosis of gram-negative and gram-positive bacteria *in vitro* [396,397,398,399]. It is not entirely clear how this microglial activation promotes increased microbial phagocytosis, although it is likely facilitated by microbial opsonisation via complement and immunoglobulins (reviewed in sections 1.4.1.3.1 and 1.4.1.3.2, respectively). Indeed, microglia (as well as astrocytes, neurons and oligodendrocytes) secrete complement components including C1q and C3[400], and such secretion is dramatically increased during inflammation[145,401]. Inflammatory-activated microglia also upregulate complement receptors 3 (CR3) and 4 (CR4)[402], thus enabling phagocytosis of microbial targets opsonised by secreted complement. Bacterial opsonisation by immunoglobulins such as IgG and IgM also promotes microglial phagocytosis of the bacteria, through binding to surface-expressed Fcγ and also complement receptors[403]. Inflammatory-activated microglia also upregulate Fcγ receptors including FcγRIII and FcγRIV[404], again facilitating phagocytosis of Ig-opsonised pathogens during inflammation. The importance of microglial activation in the context of pathogenic infection is highlighted by studies in which genetic deletion of various TLRs (including TLR2, TLR4 and TLR9) results in impaired host defence against bacterial and fungal infection in mice[391,405], and also by findings that pre-treatment of mice with the TLR agonists can enhance their survival after infection, such as by experimental meningitis[406].

Like tissue-resident macrophages in peripheral organs throughout the body, microglia are key players in adaptive immunity within the brain[407]. Microglia are antigen-presenting cells (APCs), and express both MHC classes I and II to present antigen (generated through phagocytosis of microbes, as reviewed in section 1.2.4) to $CD8^+$ and $CD4^+$ T cells. Microglia have not been observed to migrate outside the brain to draining lymph nodes to activate naïve T cells (a role ascribed to monocyte-derived dendritic cells[408]), but their presentation of antigen is considered important in perpetuation and/or reactivation of primed $CD4^+$ T cells that have already infiltrated the brain parenchyma[407]. In homeostatic conditions, microglial expression of MHCII is low, but is significantly upregulated during inflammation, for example in response to bacterial LPS[409,410]. Inflammatory-activated microglia also release T cell-activating cytokines such as IL-12[411]. Microglial-activated T cells are subsequently involved in a downstream immune signalling network that leads to recruitment and activation of antibody-secreting B cells, as described in 1.2.4.

2.2. Microglial phenotypes

From early stages in embryonic development and throughout the mammalian lifespan, microglia exist within the brain to perform myriad functions in developmental, homeostatic and pathological contexts, and such activities are spatiotemporally regulated. This heterogeneity is permitted by the various activation phenotypes microglia are known to adopt, as revealed by decades of biochemical and genetic characterisation of microglia isolated from various brain regions and at different developmental stages, and also of macrophages generally[328,412]. The original dichotomous classification of microglia into either 'resting' or 'activated' states is now considered an oversimplification, so such classifications have expanded to encompass the sub-types of microglial activation including the 'classically activated' (M1) and 'alternatively activated' (M2) phenotypes, with several sub-sub-types also described[328,412]. These classifications can be useful for predicting microglial activities in different contexts based on differential marker expression. However, more recent data from single-cell sequencing of thousands of individual microglia from different brain regions in mice, and from mice at different ages (from postnatal to old age), reveal substantially more transcriptional heterogeneity than previously reported[413]. Thus, the plurality of phenotypes microglia adopt in different physiological and pathological contexts is far more diverse than previously thought, and is a focus of intense research and debate. This section aims to describe three 'umbrella' phenotypes adopted by microglial populations - including the resting 'M0' phenotype, the classically activated 'M1' phenotype, and the alternatively activated 'M2' phenotype - and also the recent evidence regarding phenotype heterogeneity of microglia at the single-cell level.

2.2.1. Resting 'M0' microglia

The 'resting' microglial state, also known as the 'M0', 'homeostatic', 'quiescent' or 'steady' state[414], describes the phenotype commonly adopted by microglia in conditions that are physiologically 'normal' i.e. in the absence of neuroinflammation or neuropathology. In the healthy and uninflamed brain, M0 microglia exhibit small and static cell bodies with highly ramified processes that actively extend into and patrol their surrounding environment[327,415]. Resting microglia were originally considered passive bystanders within the brain, whose

primary functions manifest during inflammation or injury. However, resting microglia are now known to actively regulate and manipulate the CNS during development and normal homeostasis through direct cell-cell interactions, secretion of soluble factors, and phagocytosis, as reviewed in sections 2.1.1 and 2.1.2.

To perpetuate their resting phenotype in normal physiology, microglia recognise various inhibitory and immunosuppressive factors that circulate constitutively within the CNS, such as transforming growth factor β (TGF-β)[416]. Lack of TGF-β expression in the mouse brain causes significant microgliosis (microglial proliferation) and associated neuronal degeneration[417]. Inhibitory signals are also received via cell-cell interactions between microglia and neurons, for example through interactions between neuronal-expressed CD200 (or OX2) and microglial-expressed CD200R, interference of which is also associated with microgliosis and microglial activation[418]. Under homeostatic conditions, microglia constitutively express a range of proteins unique within the CNS, together referred to as the 'homeostatic microglial signature genes'[328]. Whilst independently obtained transcriptomic profiles differ due to variations in microglial source, isolation technique and analytical methods, commonly identified homeostatic genes include *P2ry12, Trem2, Tmem119, Cx3cr1, MerTK, SiglecH* and *Gpr43*[328], which have been ascribed to various homeostatic functions including signal detection, migration and immunosuppression. Resting microglia release a variety of non-inflammatory and trophic factors in different developmental and homeostatic contexts, including IGF-1, NGF, EGF and BDNF[364]. On the contrary, expression and secretion of pro-inflammatory cytokines such as IL-6, IL-12 and TNF-α is relatively low compared to the 'classically activated' M1 state (see section 2.2.2)[419]. However, resting microglia do constitutively express pattern recognition receptors including the TLRs 1-9 (as well as their downstream signalling adaptor molecules), which can polarise the microglia to an activated phenotype in response to pathogenic stimuli or inflammation[420].

Ambiguity in the classification of 'resting' microglia is highlighted by reports of various microglial activities and markers characteristic of an 'activated' phenotype, but in the absence of inflammation or injury, particularly during CNS development. For example, during development microglia express several markers associated with activation including CD11c[421], CR3[32], CD68[32,356] and MHCII[356], and also increased transcription of inflammatory

molecules such as *Tnf* and *Il1b*[356] but reduced transcription of homeostatic genes such as *P2ry12, MafB and Tmem119*[335,356]. Microglia in various stages of prenatal and postnatal development exhibit morphological traits commonly associated with activation, including an amoeboid cell-body with minimal ramification[335]. Such phenotypes may be essential for normal developmental processes, like phagocytosis of synapses to shape neural circuitry[356], and phagocytosis of whole neurons during developmental cell turnover[337]. Furthermore, simplification of homeostatic microglia into a single 'resting' phenotype is problematic as single-cell transcriptome analyses of microglia reveal substantial spatiotemporal heterogeneity in different environmental niches and across different stages of the CNS lifespan[413,422] (described further in section 2.2.4).

2.2.2. Classically activated 'M1' microglia

Polarisation of microglia to the classically activated 'M1' phenotype is induced by a variety of pathogenic and inflammatory stimuli including LPS[412], interferon γ (IFN-γ) (released from activated immune cells like T cells[423]), reactive oxygen or nitrogen species (RONS), and the extracellular protein aggregates α-synuclein or β-amyloid[421]. M1 microglia are most commonly described in terms of an increased capacity for release of inflammatory molecules such as cytokines, chemokines and RONS, and increased phagocytosis of cells, including foreign pathogens[7] but also viable host cells[326]. M1 polarisation of microglia involves a dramatic modulation of the transcriptome. A variety of stimuli can induce a similar M1 phenotype in microglia, due to overlap in the transcription factors that are activated. For example, LPS-mediated activation via TLR4 induces an intracellular signalling cascade that promotes nuclear translocation of transcriptional activators such as nuclear factor kappa light-chain enhancer of activated B cells (NF-κB), interferon-regulatory factor (IRF) and signal-transducer and activator of transcription (STAT)[424]. IFN-γ activation occurs via surface-expressed IFN-γ receptors, which also induce transcriptional changes by activating STAT and IRF proteins[425]. Such transcriptional changes include the upregulation of multiple pro-inflammatory chemokines and cytokines including IL-6, TNF-α, IL-12, IFN-γ, CCL2 and CCL20, which are then released extracellularly to promote recruitment and activation of other immune cells[421]. Cytokine generation can also result from activation of the NOD-like receptor family pyrin domain-containing (NLRP) inflammasome complexes, which in turn activate caspases to proteolytically activate cytokine precursor proteins[414]. For example,

NLRP3 activation promotes caspase-1-dependent production of IL-18 and IL-1β from their respective precursor proteins[426]. Thus, cytokine upregulation/activation and release by microglia both initiates and perpetuates inflammatory responses within the CNS. M1-polarisation also upregulates proteins that generate RONS, such as inducible nitric oxide synthase (iNOS) (which generates NO)[427] and NADPH oxidase (which generates superoxide[428]). RONS generation is a key mechanism of target-cell degradation in the phagosome, as described in section 1.4.2.2. Other upregulated proteins in M1 microglia include: MHC class II and CD86, which permit antigen-presentation to lymphocytes[414,429]; CR3[403], $P2Y_6R$[430], MerTK[212] and multiple FcγRs[431], which facilitate microglial phagocytosis; and CD40 and COX-2, which promote downstream inflammatory immune responses and are considered markers of the classically activated M1 phenotype[432,433].

Classical activation of microglia is of great therapeutic interest as the collateral tissue damage that results from the release of inflammatory agents and RONS - as well as through the aberrant phagocytosis of otherwise healthy neurons (phagoptosis)[7] - is implicated in neurodegenerative pathologies including Alzheimer's disease, Parkinson's disease, motor neuron disease, as well as stroke, brain trauma and multiple psychiatric disorders[412,434]. However, such sophisticated mechanisms of phenotype manipulation by microglia did not evolve to promote host damage. Inflammatory activation of microglia is crucial in response to brain injury and pathogenic infection, as highlighted by studies that show deficiencies in the M1-activation pathway result in impaired host defences against infection by diverse bacterial and fungal species[391,405]. M1-polarisation enhances microglial killing of bacteria via phagocytosis, as demonstrated *in vitro* with a range of bacterial species including *E. coli, S. pneumoniae* and *M. tuberculosis*[378]. Induction of M1-polarisation via the TLR-9 agonist cytosine-guanine oligodeoxynucleotide 1668 (CpG) strongly enhanced survival rates of mice infected with *E. coli* in experimental meningitis[406]. The enhanced capacity to eliminate pathogenic infection that results from M1-polarisation is attributed to various factors, including the upregulation of PRRs to rapidly recognise proximal pathogens, release of extracellular complement components that lyse and/or opsonise pathogens[400], and increased surface-expression of phagocytic receptors including CR3[402], FcγRIII and FcγRIV[404], which enhance phagocytosis of the pathogens. Such mechanisms of pathogenic clearance by M1 microglia are reviewed in section 2.3. M1 microglial activation is also important for the

activation of effector T cells, which activate the adaptive immune response against pathogenic infection in the CNS[414], as described in section 1.2.4.

2.2.3. Alternatively activated 'M2' microglia

Whilst microglial transition to the M1 phenotype is associated with pro-inflammatory activities, polarisation to an alternatively activated anti-inflammatory ('M2') phenotype is well documented in microglia, although more extensively characterised in peripheral macrophages[414]. Ascribed roles of the M2 macrophage phenotype include suppression of local inflammation, tissue remodelling, wound healing and matrix deposition; and for microglia specifically, in neuroprotection and restoring brain tissue homeostasis after neuroinflammation or injury[328,435]. Stimuli known to induce an M2 phenotype in macrophages include the cytokines IL-4, IL-10 and IL-13[436,437], macrophage colony stimulating factor (M-CSF)[437], and glucocorticoid hormones from the adrenal gland[438], which modulate gene transcription through regulation of diverse transcriptional activators including members of the STAT and NF-κB families, as well as glucocorticoid receptor (GR) complex and specific protein 1 (Sp1)[437]. Indeed, such diversity in transcriptomic and phenotypic changes induced by different environmental stimuli and for different physiological functions has led to subdivision of the M2 state into 4 sub-states: 2a, 2b, 2c and 2d, although all are associated with anti-inflammatory functions and inhibition of the M1-associated transcriptional activator NF-κB[439].

The extent to which stimuli that polarise peripheral macrophages to the M2 phenotype are also capable of (or indeed relevant for) polarising microglia is not completely clear. IL-4, IL-13 and IL-10 all exist in the CNS, in part through secretion by microglia themselves[440], and each can induce polarisation of microglia to an M2 phenotype[439,441]. The fact that microglia (activated or otherwise) can release such cytokines themselves emphasises their capacity to dictate their own polarisation, which is considered crucial in their conversion from an immunoinflammatory (M1) to immunosuppressive (M2) state over the course of brain tissue damage or infection[442]. Activation by IL-4 and/or IL-13 induces polarisation to a specific microglial phenotype characterised by tissue repair and regeneration activities, known as M2a[439]. Such activation promotes several transcriptomic and proteomic changes, including inhibition of NF-κB, activation of transcriptional activators Stat1, 3 and 6, and upregulation

of arginase 1 and multiple phagocytic 'scavenger' receptors[441,443,444]. IL-4 can decrease TNFα expression but increase IGF-1 expression in microglia[445], and also decrease production of NO[446]. The importance of IL-4 in suppressing neuroinflammation is demonstrated by studies in which genetic deletion of IL-4 is associated with increased neuroinflammation in response to LPS[447]. On the other hand, IL-10 polarises microglia to an M2c phenotype, associated with microglial deactivation and a return to M0[439]. IL-10 also induces transcriptional modulation through members of the STAT family, and results in downregulation of MHCII and suppression of cytokine production[441]. General markers for an M2 phenotype include the type 1 mannose receptor CD206, and the scavenger receptor CD163, both of which are expressed in the M2a and M2c states[439].

The beneficial role of microglial polarisation to an anti-inflammatory M2 phenotype in various brain pathologies - including infection, stroke, traumatic brain injury and spinal cord injury - has been well documented[444]. However, M2 polarisation can also be harmful: for example in gliomas, where tumour cells actively recruit microglia and induce their M2 polarisation to suppress local immune responses against the tumour[448]. Thus, the mechanisms that regulate M2 polarisation and mediate its diverse cellular functions in different contexts are of great therapeutic interest.

2.2.4. M0/M1/M2 – an outdated paradigm?

As mentioned, the classification of microglia into 'resting' and 'activated' phenotypic states - and even the re-classification between M1 and M2 activation states – has long been controversial within the scientific community, and criticised for being an over-simplification of the true biological complexity of microglia. Indeed, much of our understanding of microglial phenotypes has been derived through extrapolation from peripheral macrophages[361]. However, this is problematic because i) microglia are ontologically distinct from peripheral macrophages[30] (see section 2.1.1), and ii) microglia operate in the highly unique environment of the brain parenchyma, which has conferred on them unique and specialised roles relating to neurodevelopment and homeostasis[449]. Such criticism has increased further in recent years, as more sophisticated experimental methods – particularly single-cell based techniques – have better elucidated the transcriptomic and proteomic heterogeneity of microglia depending on their cellular environment and specific anatomical

and developmental niche. By analysing single-cell RNA expression patterns from thousands of individual microglia across various timepoints of the mouse lifespan, from different brain regions, and from both healthy and injured brains, Hammond *et al*[413] identified no fewer than 9 transcriptionally-distinct microglial states. Strikingly, the plurality in states adopted by microglia was also found to be temporally regulated – heterogeneity in microglial states was highest during early development, but then reduced in adulthood, before expanding again during ageing. Moreover, states that were minimally adopted in homeostatic conditions were found to emerge substantially following brain injury[413]. Such findings emphasise the notion that the M0/M1/M2 paradigm of transcriptional states is indeed an oversimplification. However, they do support the idea that microglia can be subcategorised into specific phenotypes (although this is more precisely achieved through a single-cell approach), and this precise categorisation may be useful for targeting distinct microglial populations for therapeutic intervention against brain pathology, for example neurodegenerative pathology.

In support of this idea, Keren-Shaul *et al*[450] identified (via single-cell RNA sequencing) a novel microglial subtype in a genetic mouse model of AD – called 'disease-associated microglia' (DAM) - which revealed a specific gene-expression signature that was distinct from that of other cells isolated from the same brain, and absent from healthy control brains. DAM were found to be enriched around amyloid plaques in the AD mouse brains, and were also found to be conserved in humans, where again they were enriched around amyloid plaques in AD brains (but absent in non-AD control brains). Moreover, DAM were also detected in a mouse model of (ALS), suggesting that these microglia may be of relevance to neurodegenerative pathologies generally[450]. More recently, DAM enrichment has been directly associated with neuronal loss and amyloid deposition in human AD brains[451], suggesting that these microglia contribute to pathology, and providing further promise that targeted modulation of disease-associated microglia may be therapeutically beneficial.

2.3. Microglial phagocytosis

As for phagocytes throughout the mammalian system, the ability to phagocytose extracellular material provides microglia with a powerful means to dramatically alter their environment. Accordingly, in healthy individuals, phagocytosis by microglia is strictly regulated. Microglia

express a range of pro- and anti-phagocytic receptors, which are typically not unique to the brain-resident macrophage population. However, the unique environment of the brain parenchyma has conferred on them highly specific developmental, homeostatic and protective roles: notably in neuroprotection, modelling of axonal myelin, clearance of neuronal debris and extracellular amyloid aggregates, as well as in developmental synaptic pruning[361]. This section focuses on the major microglial phagocytic receptors that have been documented, with a particular emphasis on those relevant to this thesis. A schematic of microglial phagocytosis of diverse targets, and key signalling mechanisms known to regulate such phagocytosis, is shown in Figure 2.1 (page 72). A more comprehensive list of known phagocytic receptors in microglia, and also macrophages generally, is reviewed by Sierra *et al* [361].

2.3.1. Pro-phagocytic receptors

2.3.1.1. Brain angiogenesis inhibitor 1 (BAI-1)

BAI-1 is a G-protein coupled receptor (GPCR) highly expressed in the brain - by microglia[452] but also by neurons[453] and astrocytes[454]. BAI-1 has been described as an engulfment receptor for phagocytosis of apoptotic cells by macrophages, capable of binding exposed phosphatidylserine[455]. In zebrafish microglia, BAI-1 has been implicated in the phagosome formation step of phagocytosis of apoptotic neurons[452]. BAI-1 has also been suggested to promote phagocytosis of axons by microglial BV-2 cells[456]. More recently, however, the physiological expression of BAI-1 in microglia (and macrophages in general) has been questioned, as has it's biological relevance *in vivo*[457].

2.3.1.2. Complement receptor 3 (CR3)

Also known as Mac-1, CR3 is a $\alpha_M\beta_2$ integrin receptor consisting of CD11b and CD18 and expressed by several mammalian leukocytes[458]. CR3 is considered specific to microglia within the brain[459]. CR3 is a well characterised microglial phagocytic receptor[460], which is activated by complement components such as C3[326] but also immunoglobulin M (IgM)[403].

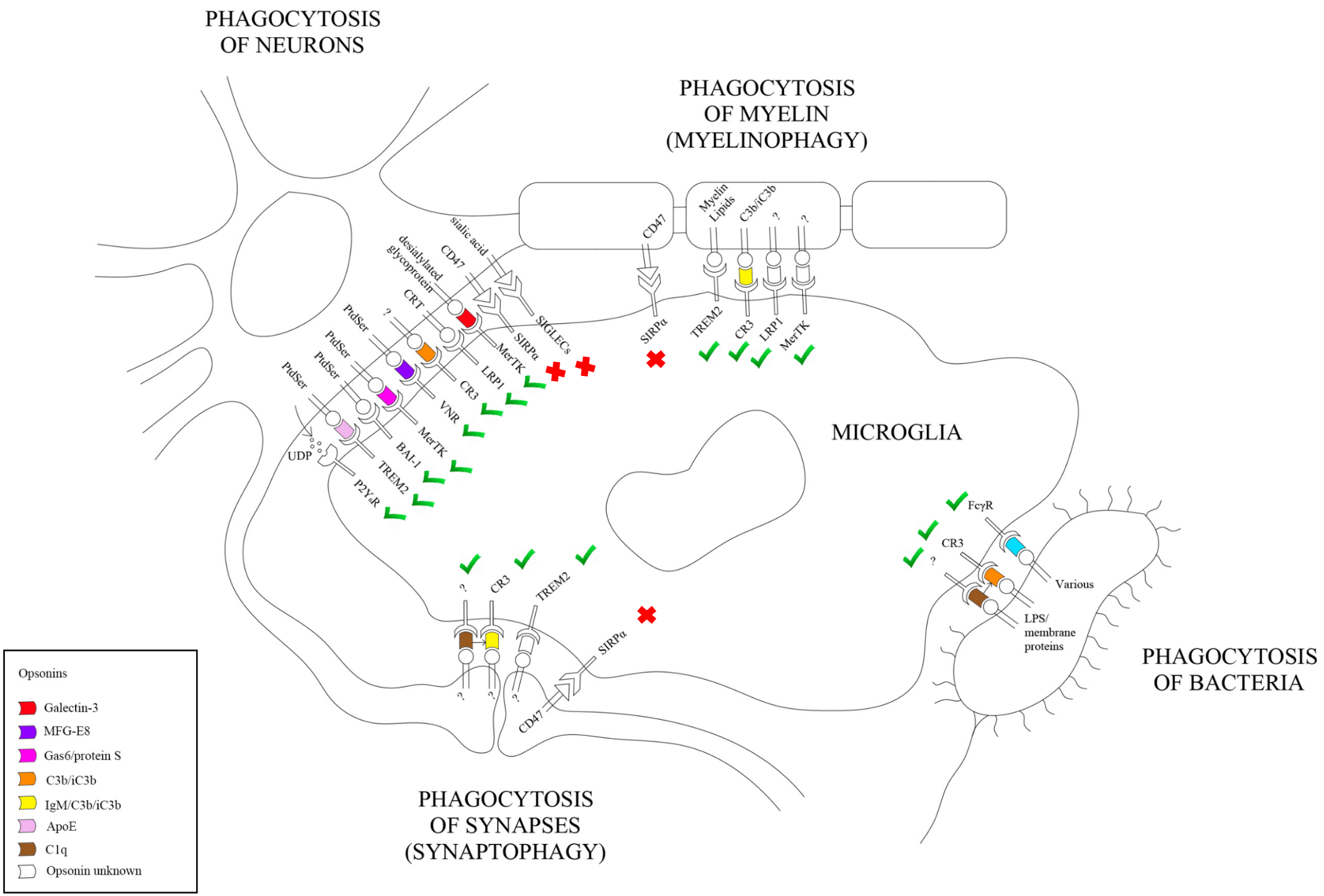
PHAGOCYTOSIS OF NEURONS
PHAGOCYTOSIS OF MYELIN (MYELINOPHAGY)
MICROGLIA
PHAGOCYTOSIS OF SYNAPSES (SYNAPTOPHAGY)
PHAGOCYTOSIS OF BACTERIA
sialic acid
desialylated glycoprotein
CD47
CRT
PtdSer
?
SIRPα
SIGLECs
MerTK
LRP1
CR3
VNR
BAI-1
TREM2
P2Y6R
UDP
Myelin Lipids
C3b/iC3b
TREM2
CR3
LRP1
MerTK
FcγR
Various
LPS/ membrane proteins
Opsonins
Galectin-3
MFG-E8
Gas6/protein S
C3b/iC3b
IgM/C3b/iC3b
ApoE
C1q
Opsonin unknown

Figure 2.1. Regulation of microglial phagocytosis. The phagocytosis of diverse targets by microglia is depicted. Microglial phagocytosis of neurons (neurophagy), myelin (myelinophagy), synapses (synaptophagy) and bacteria is regulated by a range of receptor-mediated signalling mechanisms between the microglia and the target. These are either pro-phagocytic or anti-phagocytic, represented by a green tick or red cross, respectively. Only established signals and receptors are shown, and where the receptor, opsonin, or 'eat-me' signal in a pathway is unknown, that component is represented by a '?' symbol. All depicted signalling mechanisms are further described within section 2.3. The arrow from C1q to C3 represents the fact that C3-mediated opsonisation of targets can be facilitated by C1q[122]. PtdSer: phosphatidylserine. CRT: calreticulin. LPS: lipopolysaccharide.

CR3 signals via the microglial adaptor DNAX-activation protein 12 (DAP12)[326]. CR3 facilitates microglial phagocytosis in various physiological contexts, notably in the developmental phagocytosis of synapses (reviewed in section 2.1.1)[32,221,355], and is highly expressed in brain regions undergoing synaptic pruning. CR3 also regulates the phagocytic elimination of non-apoptotic neurons by microglia in the embryonic mouse retina[461]. Thus, microglial CR3 enables the developmental elimination of neurons as well as neuronal substructures.

CR3 is upregulated in inflammatory-activated microglia[403], and is implicated in phagocytosis of complement-opsonised pathogens, for example bacterial *E. coli* injected intracerebrally into the corpus callosum of postnatal rats[462]. During brain injury or disease-associated demyelination, CR3 mediates phagocytic clearance of degenerated myelin by microglia[463]. However, phagocytosis via CR3 is also linked to detrimental neuron loss in neuroinflammatory and neurodegenerative contexts[326], as well as pathological synapse loss that occurs in Alzheimer's disease[464]. Furthermore, several groups have observed upregulation of CR3 in the aged brain, leading to suggestions that CR3-mediated microglial phagocytosis of neurons and/or myelin may contribute to age-associated brain atrophy[465].

2.3.1.3. Fragment-crystallisable-gamma receptors (FcγRs)

The FcγR family comprise a range of specialised receptors that bind the Fc domain of extracellular IgG antibodies to stimulate intracellular signalling cascades[466]. Two general classes of Fcγ receptors have been described, based on their intracellular signalling motifs

and downstream immunomodulatory activities[467]. 'Activatory' Fcγ receptors, including FcγRI, FcγRIIa, FcγRIIc and FcγRIIIa, signal intracellularly via immunoreceptor tyrosine activation motifs (ITAMs). Such signalling induces pro-inflammatory signalling pathways via activation of Src- and Syk-family kinases[61]. Downstream effects include antibody-dependent cellular cytotoxicity (ADCC) or phagocytosis (ADCP), as well as cytokine and chemokine secretion and lymphocyte activation[467,468]. On the other hand, the 'inhibitory' Fcγ receptor FcγRIIb signals via its immunoreceptor tyrosine inhibition motif (ITIM), which counteracts activatory FcγR signalling by activating intracellular phosphatases and inhibiting Src kinase[467].

Interestingly, both activatory and inhibitory Fcγ receptors have been found to mediate phagocytosis of IgG-opsonised targets[466], including bacteria[469] but also mammalian cells[470]. Microglia express both activatory and inhibitory Fcγ receptors including FcγRI, FcγRIIa, FcγRIIb and FcγRIIIa[471], implying a role in phagocytosis of IgG opsonised targets within the brain. IgG has been demonstrated to opsonise gram-positive *Staphylococcus aureus* for phagocytosis by microglia, and this opsonisation is enhanced by pre-treatment of the microglia with IFN-γ[467]. This is consistent with separate findings that inflammatory activation of microglia by IFN-γ upregulates FcγRIII and FcγRIV receptors[431]. Furthermore, the phagocytosis of red blood cells by human microglia is enhanced by opsonisation with IgG, which occurs through FcγR signalling[468]. Phagocytosis of the IgG-coated cells also induced ADCC and release of T-cell-stimulating factors[468]. Thus, microglial Fcγ receptors mediate phagocytosis of both foreign and host IgG-opsonised targets.

2.3.1.4. Low-density lipoprotein receptor-related protein 1 (LRP1)

LRP1 is a large (~600 kDa) transmembrane protein described as a major receptor for apolipoprotein E, calreticulin and β-amyloid[472]. When expressed in macrophages, LRP1 acts as a scavenger receptor for phagocytosis of apoptotic cells through recognition of surface-exposed calreticulin[64,473,474,475]. Although calreticulin can be exposed on viable cells, phagocytic induction is typically prevented through a dominant-inhibitory effect of 'don't eat-me' signalling pathways such as CD47-SIRPα[476], and calreticulin exposure is increased during apoptosis[473].

LRP1 is expressed ubiquitously in the CNS[472], including by microglia[477]. Microglial LRP1 has been shown to regulate phagocytosis of neurons by binding surface-exposed calreticulin[478], and also regulates phagocytosis of myelin[479]. Thus, microglial LRP1 facilitates the elimination of both cells and sub-cellular structures within the brain. Additionally, LRP1 activation has been shown to suppress polarisation of microglia to a classically-activated M1 phenotype. Genetic knockdown of LRP1 in cultured microglia resulted in increased protein expression of transcriptional activators associated with the M1 phenotype such as NF-κB, as well as increased expression of the inflammatory cytokines IL-1β and TNF-α[472]. Furthermore, microglia LRP1 is downregulated in response to LPS, indicating that its immunosuppressive capacity is actively prohibited during inflammation[472]. Moreover, LPS can stimulate shedding of surface-bound LRP1 by microglia, and the secreted soluble form of LRP1 is pro-inflammatory[480] - indicating opposing immunomodulatory properties of LRP1 depending on its form.

2.3.1.5. Mer receptor tyrosine kinase (MerTK)

One of three members of the TAM (Tyro3, Axl & Mer) family of receptor tyrosine kinases, MerTK is an integral membrane protein expressed by professional phagocytes including monocytes, macrophages, and dendritic cells[481]. MerTK is known to regulate phagocytosis of apoptotic cells by macrophages[482], and such phagocytosis is mediated by the extracellular opsonin Gas6 (reviewed in section 1.4.1.3.7) and also protein S. MerTK (as well as Axl) is expressed in the microglial cell line BV-2 and in primary mouse microglia[210]. Microglial MerTK levels increase after focal brain ischaemia *in vivo*[483], and bacterial LPS has been shown to upregulate MerTK expression in microglial BV-2 cells[212]. However, expression of MerTK is downregulated in human cultured microglia after treatment with LPS and IFN-γ to induce M1 polarisation[484]. MerTK has been demonstrated to regulate microglial phagocytosis of glutamate-stressed neurons *in vitro*, and MerTK deficiency reduces microglial phagocytosis of neurons and brain atrophy after focal brain ischaemia in mice[483]. The MerTK ligand Gas6 induces phagocytosis of fluorescent microspheres and also apoptotic Jurkat cells by microglia[210], implicating MerTK in this microglial phagocytosis. Galectin-3, another MerTK ligand[216], has been shown to induce microglial phagocytosis of neuron-like PC12 cells as well as neuronal debris, and this induction can be inhibited by blocking MerTK.

Furthermore, microglial phagocytosis of myelin is also inhibitable by blocking MerTK[484]. Together, these findings suggest that MerTK regulates microglial phagocytosis of a diverse range of cellular and sub-cellular targets.

2.3.1.6. Pyriminidergic receptor P2Y$_6$ (P2Y$_6$R)

P2Y$_6$R is a metabotropic G$_q$-coupled protein of the nucleotide-sensing P2 receptor family, and is highly sensitive to uridine 5'-diphosphate (UDP), which is considered its primary agonist[485] (though activation of P2Y$_6$R by UTP and ADP has also been reported[486]). P2Y$_6$R activation initiates an intracellular signalling pathway involving phospholipase C (PLC)-β, which triggers mobilisation of intracellular calcium stores and calcium release into the cytosol[486,487]. In the CNS, P2Y$_6$R expression has been reported in microglia[485] and specific neurons, including motor neurons in the ventral horn[488] and agouti-related peptide (AgRP) neurons in the hypothalamus[489]. Microglial P2Y$_6$R is minimally expressed in the healthy brain, but is upregulated during inflammation[490], for example after exposure to bacterial LPS[430]. P2Y$_6$R levels in the rat brain also increase after intraperitoneal injection with the neuroexcitatory stimulant kainic acid[485]. UDP triggers microglial phagocytosis of zymosan microparticles, which is inhibited by pharmacologically blocking P2Y$_6$R[485]. UDP also promotes microglial phagocytosis of microspheres modified with carboxylate, negatively-charged groups designed to mimic phosphatidylserine exposed on the surface of apoptotic cells[491]. Furthermore, activation of microglial P2Y$_6$R following release of UDP from damaged neurons triggers microglial phagocytosis of the neurons[485], indicating that microglial P2Y$_6$R may mediate phagocytic clearance of dying cells within the brain.

In addition to directly regulating microglial phagocytosis of targets, P2Y$_6$R has been suggested to mediate polarisation of microglia to the classically-activated M1 phenotype in response to LPS[430]. Microglia exposed to LPS upregulated various cytokines and inflammatory molecules including TNF-α, iNOS, IL-6 and COX-2, and this upregulation was inhibited by blockade or knock-down of P2Y$_6$R[430]. P2Y$_6$R has been implicated in the phagoptosis (death via phagocytosis) of stressed-but-viable neurons by microglia in multiple inflammatory contexts, such as those induced by LPS, LTA, amyloid-β or peroxynitrate[491]. Furthermore, unpublished work from our lab demonstrates a central role for P2Y$_6$R in microglial-mediated neuronal loss in models of Alzheimer's and Parkinson's disease, both *in*

vitro and *in vivo*. Such findings implicate microglial $P2Y_6R$ as a promising therapeutic target in neurodegenerative pathology.

2.3.1.7. T-cell membrane protein 4 (TIM-4)

T-cell membrane proteins are cell-surface receptors that can bind PtdSer[492], and while most are expressed exclusively by T cells, TIM-4 is also expressed by lymphocytes including macrophages and dendritic cells[493]. In zebrafish, TIM-4 is expressed by microglia, and knockdown of TIM-4 inhibits microglial phagocytosis of apoptotic neurons, thus causing apoptotic cells to accumulate within the brain[452]. Whilst TIM-4 has been well documented in regulating macrophage phagocytosis of apoptotic cells in mammalian systems[494,495,496], it is not clear to what extent TIM-4 regulates phagocytosis by microglia in the mammalian brain.

2.3.1.8. Triggering receptor expressed on myeloid cells 2 (TREM2)

A single-pass transmembrane protein in the immunoglobulin receptor superfamily[497], TREM2 is expressed by a wide range of myeloid-lineage cells, including macrophages, dendritic cells and osteoclasts[498]. TREM2 binds a diverse array of polyanionic extracellular ligands, including bacterial *E. coli* and *S. aureus* and bacterial-derived LPS and LTA[499], phosphatidylserine and other phospholipids[500], DNA[501] and β-amyloid oligomers[502], but also galectin-3[503] and apoE[504]. Ligand binding to TREM2 initiates an intracellular signalling cascade via the adaptor protein DAP12, and reported downstream effects of TREM2-signalling include increased cell motility, proliferation and enhanced survival[497,505].

In the CNS, TREM2 is highly expressed in microglia in the absence of inflammation[506,507]. TREM2 has been ascribed to a variety of roles in microglia specifically, with particular emphasis on its regulation of microglial activation and phagocytic capacity[505]. Knockdown of microglial TREM2 inhibits phagocytosis of apoptotic neurons[506] or neurons deprived of oxygen and glucose in a model of ischaemia[501], indicating that TREM2 regulates microglial clearance of apoptotic or damaged cells in the brain. In the ischaemia model, microglial expression of TREM2 was increased in microglia proximal (but not distal) to the infarct zones, and microglia deficient in TREM2 exhibited morphological indicators of a less

activated phenotype compared to microglia expressing TREM2 normally[501], suggesting that TREM2 is associated with activated microglia in experimental stroke. TREM2 has also been implicated in regulating microglial phagocytosis of myelin[360]. TREM2 can directly interact with lipid components of myelin[508], and mice lacking TREM2 exhibit defective clearance of myelin debris and reduced myelin phagocytosis by microglia in a model of demyelinating disease[509]. As in the ischaemia model, microglia lacking TREM2 displayed a more 'resting' morphology and lower expression of MHCII and iNOS[509], markers of the classically activated M1 phenotype, indicating that TREM2 is associated with the microglial activatory response to brain injury. In developing brain regions undergoing extensive synaptic pruning, microglia display various markers of an activated phenotype including enhanced synaptophagy (see section 2.1.1), and microglia lacking TREM2 are defective in synaptic pruning *in vitro* and *in vivo*[356]. Again, TREM2 deficiency was associated with a less activated phenotype, based on reduced protein expression of CD11b, MHCII, CD86 and reduced expression of inflammatory-associated genes *TNF* and *Il1b*, but increased expression of the homeostasis-associated gene *P2yr12*[356]. Thus, TREM2 is implicated in regulating microglial phagocytosis of diverse cellular and sub-cellular targets in development, homeostasis and pathology, and is of high therapeutic interest, particularly in neurodegenerative pathologies like Alzheimer's disease[497].

2.3.1.9. Vitronectin receptor (VNR)

VNR is a heterodimeric $\alpha_v\beta$ integrin, part of the superfamily of adhesion proteins[510] expressed by all cell types to mediate cell adhesion to the extracellular matrix (ECM), or to other cells[511]. VNR is composed of two major subunits - the αv and β5 chains - which each span the cell membrane and together form a large N-terminal ligand binding domain[510]. This binding domain recognises the peptide motif RGD, present in a wide range of adhesive proteins within the ECM and on the surface of cells[512,513]. Thus, VNR binds several known ligands, including vitronectin but also fibronectin, osteopontin, and lactadherin (MFG-E8)[512,514]. In leukocytes, VNR mediates a variety of biological functions, including adhesion, migration, extravasation across the vascular endothelium, and phagocytosis[513,514,515].

Microglia express multiple integrins including the vitronectin receptor[513], and microglial VNR has been shown to regulate activation and/or phagocytosis in various contexts. In a

model of demyelinating disease, increased presence of the VNR ligand vitronectin was associated with an activated microglial phenotype and upregulation of markers of an activated phenotype including macrophage-1 antigen (Mac-1) and matrix metalloprotease 9 (MMP-9), which was inhibited by blocking VNR[516]. Levels of fibronectin (a VNR ligand[512]) are increased in the injured rat brain, and this increase is associated with glial activation at both central and peripheral regions relative to the lesion[517]. MFG-E8 is a well-established phagocytic opsonin that mediates phagocytosis of target cells through binding VNR on the phagocyte surface and PtdSer on the target cell surface[514] (see section 1.4.1.3.6). Moreover, both MFG-E8 and VNR are expressed by microglia *in vivo*[478], implicating VNR-signalling in microglial phagocytosis of apoptotic cells. Inflammatory neuronal loss via microglial phagoptosis has also been shown to depend on VNR signalling (via microglial-induced neuronal exposure of PtdSer and MFG-E8 binding) when induced by LPS[518,519,520], TNF-α [521] or β-amyloid[522,197]. Furthermore, microglial phagocytosis of photoreceptor rods in the context of retinal photoreceptor degeneration is inhibited by blocking VNR[523]. Thus, microglial VNR is of great therapeutic interest in various CNS pathologies.

2.3.2. Anti-phagocytic receptors

As described in section 1.4.1.4, negative regulation of phagocytosis is crucial for retention and maintenance of physiologically indispensable host cells during periods of dynamic phagocytic activity, and dysfunction in anti-phagocytic signalling in the CNS is implicated in various neurodegenerative diseases and brain tumours[524]. Microglia express a range of anti-phagocytic receptors, including the sialic-acid binding immunoglobulin-type lectins (SIGLECs) and SIRPα, whose biological functions (in both normal physiology and pathology) are here reviewed.

2.3.2.1. Sialic acid-binding immunoglobulin-type lectins (SIGLECs)

SIGLECs are a family of type 1 lectins (carbohydrate-binding proteins), capable of binding sialic acid residues on glycan chains, as well as various immunoglobulin domains[525]. SIGLECs are expressed by several hematopoietic cells of the immune system, and also by Schwann cells and oligodendrocytes[526]. They are cell-surface receptors that bind the self-

associated molecular pattern (SAMP) sialic acid (see section 1.4.1.4.7), and so recognise sialylated glycoconjugates expressed on all mammalian cells (and also on some prokaryotes)[526]. In immune cells, SIGLECs mediate either activatory or inhibitory immune signalling cascades via intracellular ITAM or ITIM motifs, respectively (with the exception of Siglec-1 and Siglec-4 in humans, which do not contain either motif)[526]. Several immune roles have been ascribed to SIGLECs - including antibody production[527,528], neutrophil activation[529] and apoptotic induction[530].

Expression of various SIGLECs in microglia has been documented, including (in humans) Siglec-3/CD33[531], Siglec-11[532,533] and possibly Siglec-16[534], and (in mice) CD33[531], Siglec-E[535,536] and Siglec-H[537]. SIGLECs have been described to negatively regulate microglial activation and phagocytosis in several contexts. Ectopic expression of the human Siglec-11 in mouse microglia has been shown to suppress LPS-induced IL-1β and NOS-2 upregulation, and reduce their phagocytosis of apoptotic neuronal material[533]. Furthermore, neuronal loss induced by co-culturing neurons with microglia was alleviated through microglial Siglec-11 expression, implicating Siglec-11 in neuroprotection[533]. Knockdown of Siglec-E in mouse microglia increased, but overexpression of Siglec-E reduced, microglial phagocytosis of neuronal debris[536]. The induction of inflammatory cytokine expression and superoxide production through debris exposure was enhanced with Siglec-E knockdown, and Siglec-E inhibited microglial-mediated reduction of neurite length when in co-culture with neurons[536]. In contrast, enzymatic removal of sialic acid residues in neuronal cultures through sialidase application has been shown to enhance microglial-dependent reduction of neurite length[221], further implicating SIGLECs in regulating microglial phagocytosis of neuronal processes, as well as of whole neurons.

2.3.2.2. Signal regulatory protein α (SIRPα)

Otherwise known as SHPS1, PTPNS1 and CD172A, SIRPα is one of three SIRP proteins within the immunoglobulin receptor superfamily[326,538]. SIRPα is a membrane-bound protein predominantly expressed by myeloid cells[538], and like some SIGLECs, contains an inhibitory signalling motif (ITIM) that can initiate intracellular signalling cascades[539]. The best

characterised ligand for SIRPα is CD47 (reviewed in section 1.4.1.4.1), although other suggested ligands include the collectins SP-A and SP-D[245]. SIRPα-signalling negatively regulates a variety of functions in mammals: it inhibits phagocytosis of red blood cells[540,541] and apoptotic cells[473] by macrophages, represses inflammatory cytokine production by monocytes[542] and impedes transmigration of neutrophils *in vitro*[543].

In the brain, SIRPα is expressed by microglia[544] and also neurons[541]. Microglial SIRPα has been implicated in downregulating phagocytosis of myelin and myelin-producing oligodendrocytes during normal homeostasis[544]. Myelin has been shown to express CD47, which signals to microglial SIRPα to prevent phagocytosis of the myelin. More recently, CD47 has also been identified on synapses during periods of developmental pruning in the dorsal lateral geniculate nucleus (dLGN) of the mouse brain, and has been shown to preferentially colocalise on more active synapses, thus restricting engulfment of these synapses by microglia via SIRPα[357].

2.4. Microglia in CNS pathology

2.4.1. Microglial phagocytosis: ameliorating pathology

The protective capacity of microglial phagocytosis in myriad pathological conditions has been widely documented[361]. In brain cancer, microglia can phagocytically eliminate tumour cells exposing PtdSer[545] or damaged through UV exposure[546]; however, non-apoptotic glioma cells typically protect themselves against microglial phagocytosis[547], thus facilitating their perpetuation. In Alzheimer's disease, neurotoxic amyloid plaques accumulate in the extracellular space[548]. Microglia have been shown to surround amyloid plaques *in vivo*[549], and phagocytose fibrillary β-amyloid *in vitro*[550,551,552]. However, whether such phagocytic plaque elimination occurs *in vivo*, and the extent to which it might ameliorate Alzheimer's pathology, are not clear[361]. In multiple sclerosis (MS) and spinal cord injury, myelin degeneration results in the accumulation of extracellular myelin debris, which may be damaging[553]. Microglia have been widely documented as capable of phagocytosing myelin through various phagocytic receptors, including CR3[463], LRP1[479], MerTK[484] and TREM2[509],

and microglial phagocytosis of myelin has been observed in mouse models of MS[554]. Myelin phagocytosis by microglia can suppress downstream immune responses such as T cell proliferation[555], and in a mouse model of demyelination, myelin-phagocytosing microglia facilitate myelin regeneration through activation of oligodendrocyte precursor cells (OPCs)[556]. Thus, microglial phagocytosis in pathological demyelination may both clear degenerated myelin and promote regeneration of myelin on affected axons.

Of particular interest to this thesis is the capacity for microglial phagocytosis to limit pathogenic infection within the brain, specifically bacterial infection. Microglia can protect the brain against the causative agents of serious infections including bacterial meningitis[393] and meningoencephalitis[392], and brain abscess[557]. Such protective mechanisms are reviewed here (see also sections 2.1.3 and 2.2.2).

2.4.1.1. Bacterial meningitis/meningoencephalitis

Bacterial meningitis is a disease with high incidences in neonates, infants, the elderly and immunocompromised individuals, and can result in neurological damage, motor and cognitive impairment, or death[393]. Bacterial meningitis results when bacteria from the blood infiltrate the meninge tissue, which induces a severe and damaging neuroinflammatory response leading to host-cell death[557,558]. Moreover, such bacteria can also directly kill host cells. Causative agents of bacterial meningitis include *Streptococcus pneumoniae*, *Escherichia coli* and *Neisseria meningitidis*[393]. If the infection extends into the brain parenchyma, the result is meningoencephalitis[392]. Whilst bacterial encephalitis (infection of the brain parenchyma itself) is distinct from bacterial meningitis (infection of the meninge tissue surrounding the brain), bacterial infiltration to the brain parenchyma typically involves infection through the meninge tissue, meaning encephalitis often occurs in the broader context of meningoencephalitis. Moreover, meningitis commonly leads to encephalitis, and so the terms encephalitis and meningoencephalitis are sometimes used interchangeably[392]. Accordingly, the causative agents of meningitis (including *S. pnuemoniae, E. coli* and *N. meningitidis*) can also cause encephalitis[392], and studies on microglial responses to such bacteria are thus relevant in both cases.

In meningitis and encephalitis, activation of microglia by the invading bacteria occurs either directly (through recognition of PAMPs) or indirectly (through DAMPs derived from damaged host cells), as reviewed in section 2.1.3. In models of experimental meningitis, enhanced microglial phagocytosis has been associated with increased uptake and intracellular killing of the bacteria and more rapid resolution of neuroinflammation, which otherwise causes substantial damage to host tissue. Mouse microglial cultures stimulated with Pam3CSK4, LPS or CpG oligodeoxynucleotide (agonists for TLRs 1/2, 4 and 9 respectively) exhibited increased uptake of *E. coli* strains DH5α and K1, and also enhanced the efficiency of bacterial killing after engulfment[396]. Such treatments also enhanced phagocytic elimination of either encapsulated (D39 serotype:2) or unencapsulated (R6) strains of *S. pneumoniae*[397]. However, despite increasing phagocytic elimination of these bacteria, such treatments may be of limited therapeutic use due to the associated tissue damage that results from induced glial activation[393,557]. In light of this, more recent studies have demonstrated enhanced microglial phagocytosis of *E. coli* K1 without associated proinflammatory cytokine or NO release after dual treatment with TLR agonist and activin A, a neuroprotective protein of the TFG-β family[559]. Microglia treated with the endocannabinoid palmitoylethanolamide (PEA) exhibit increased capacity for phagocytosis of *S. pneumoniae* R6 and *E. coli* K1 *in vitro*[560], and in a mouse model of experimental meningoencephalitis, PEA enhanced survival of mice injected intracerebrally with *E. coli* K1[561]. Increased survival of the mice was associated with fewer detectable bacterial in the blood and importantly, lower levels of the inflammatory molecules IL-1β and IL-6 in brain homogenates[561]. Such therapeutic approaches that enhance microglial phagocytosis of the bacteria whilst simultaneously suppressing excessive neuroinflammation may prove clinically beneficial, and merit further study.

2.4.1.2. Brain abscess

Like encephalitis, brain abscesses are bacterial infections of the brain parenchyma[557]. However, they are distinct from the general neuroinflammation associated with encephalitis, as abscesses are characterised by focal infections in the brain that develop into pus-containing lesions contained within a vascularised, fibrotic capsule[557,562]. Brain abscesses originate either from local infections, such as ear infections and dental abscess, or distant infections, such as in the lungs[557]. Causative agents of bacterial abscess include a range of pyogenic (pus-generating) gram-positive and gram-negative bacteria. Abscesses have been found to most

commonly result from infection with gram-positive *Streptococcal* species or *Staphylococcus aureus*[563], although abscesses from gram-negative species of the genera *Bacteroides* and *Prevotella* have also been reported[564].

As expected given their exclusive residence within the brain parenchyma, microglia are considered key players in fighting the infectious agents of brain abscess[385,557]. Immediately following infection and throughout the lifespan of the abscess, microglial activation has been documented, and models of experimental abscess where microglia were treated with *S. aureus* or their cell-wall derived peptidoglycan (PGN) revealed increased microglial expression of several cytokines including TNF-α, IL-1β, IL-6, MIP-3 and MCP-1[565]. The same bacterial stimuli can also promote upregulation of the phagocytic receptors LOX-1 and PTX-3 in microglia[566], implicating microglial phagocytosis in response to brain abscess. Microglia can phagocytose *S. aureus*[403,567] and also *Streptococcal* species[397,568]. Furthermore, mice lacking Myd88 (an adaptor protein required for TLR-signalling, described in section 1.2.3) exhibit increased mortality after intracerebral injection with *S. aureus*, which was associated with reduced microglial cytokine generation and impaired neutrophil recruitment[385]. However, whether susceptibility to infection in Myd88-knockout mice is linked to negative regulation of microglial phagocytosis of the bacteria is not clear, as bacterial burdens between knockouts and wild-types were not found to be different (at least at the time-points analysed[385]). Thus, the importance of phagocytosis *per se* in the anti-bacterial activities of microglia in response to brain abscess is unconfirmed (although likely), and requires further study.

2.4.2. Microglial phagocytosis: exacerbating pathology and age-associated dysfunction

Despite the myriad physiological benefits and neuroprotective functions ascribed to microglia, their dysfunction has been implicated in exacerbating (or even causing) a wide range of neurological diseases - including brain cancers, neurodegeneration, psychiatric disorders, and brain trauma. In brain cancer, microglia have been described to actively promote and support tumour growth, either by directly inducing tumour proliferation, or releasing anti-inflammatory factors to suppress immune responses against the tumour[569,570,571]. Neurodegenerative diseases including Alzheimer's disease (AD), Parkinson's disease (PD), amyotrophic lateral sclerosis (ALS) and frontotemporal dementia (FTD) are all

characterised by chronic microglial activation, and such activation has been implicated in tissue damage and neuronal loss through sustained release of neuroinflammatory molecules and direct killing of live neurons via phagoptosis[7,569]. Ageing is the primary risk factor for most forms of neurodegeneration[572]. Although not a pathology *per se*, ageing is associated with increased activation of microglia across the brain, which may be linked with age-associated cognitive deficits[573]. Chronic microglial activation, and the associated phagocytosis and release of neuroinflammatory molecules, is also implicated in acute brain injury, stroke and multiple sclerosis[569], as well as autism and schizophrenia[574,569].

Of special relevance to this thesis is the pathological phagocytosis of synapses by microglia, or pathological synaptophagy[122]. Synapses are key for the transfer of information in the neural network of the CNS, and synaptic loss is a hallmark of multiple neuropathologies[549,575]. Importantly, microglial synaptophagy has been implicated in the synaptic loss that occurs in Alzheimer's disease, Parkinson's disease, frontotemporal dementia (FTD), glaucoma, schizophrenia, and viral infection[122], as well as in normal ageing. Putative roles for microglial synaptophagy in neuropathology - and the evidence behind them - are here reviewed.

2.4.2.1. Alzheimer's disease (AD)

AD is the most common form of dementia, affecting over 50 million individuals globally according to Alzheimer's Disease International[576]. Synaptic loss occurs early in AD pathology[575] and is attributed to multiple factors, with particular emphasis on i) the synaptotoxic properties of β-amyloid, and ii) re-initiation of developmental synaptophagy via complement signalling - and such factors may be interlinked. These two factors will be discussed sequentially.

One of the hallmarks of AD is accumulation of extracellular β-amyloid aggregates, and such aggregates can induce synaptic loss, as well as microgliosis and microglial activation[577,578,579]. In a mouse model of Alzheimer's disease, oligomeric β-amyloid has been shown to associate with synapses, and this association is correlated with synaptic loss[580]. β-amyloid can bind glutamatergic receptors present on the synaptic surface[581], and high resolution imaging has identified fibrillar β-amyloid that pierces through the synaptic

membrane[582]. β-amyloid plaques promote accumulation of glial cells including microglia[549], and it has been suggested that synapse-localised β-amyloid may promote microglial phagocytosis of the synapses via this recruitment[577]. This is supported by findings that soluble β-amyloid can impair long-term potentiation (induced by increased neuronal activity and associated with spine generation) but facilitate LTD (induced by decreased neuronal activity and associated with spine reduction) - consistent with findings that neuronal activity modulates microglial phagocytosis of synapses[32]. However, the ability for β-amyloid to directly tag synapses for phagocytic removal by microglia remains to be confirmed.

A role for complement-mediated synaptic loss in AD is strongly supported by several lines of evidence. Both C1q and C3, known regulators of microglial phagocytosis of synapses[32,222,583], are upregulated in mouse models of AD[584]. AD mice lacking C1q[585] or C3[586], or injected with a function-blocking anti-C1q antibody[587], reveal less disease-associated synaptic loss and reduced cognitive decline. Intrahippocampal injections of β-amyloid oligomers in mice can induce C1q deposition at synapses, which was associated with increased microglial phagocytosis and synaptic loss[586]. Furthermore, this induced synaptic loss was prevented by knocking-out C1q, or through application of anti-C1q antibodies[586]. Thus, β-amyloid may induce synaptic loss indirectly - by promoting synaptic tagging with complement, which subsequently promotes microglial phagocytosis of the synapse. It is of interest that levels of C1q within the CNS dramatically increase during normal (non-pathological) ageing[588], where synaptic loss is established[589] - and that ageing is the biggest risk factor for Alzheimer's disease (as well as other neurodegenerative diseases)[590]. Moreover, mice lacking C3 have been shown to be protected from age-associated synaptic loss within the hippocampus[591], thus also implicating microglial synaptophagy in age-associated synaptic loss in the absence of neurodegeneration.

2.4.2.2. Parkinson's disease (PD)

PD is a common neurodegenerative disease characterised by severe motor impairment and loss of nigrostriatal dopaminergic neurons, but also loss of synapses[592]. At the molecular level, PD is characterised by the intracellular accumulation of Lewy bodies - fibrillar aggregates of the protein α-synuclein[592]. As with β-amyloid in AD, the α-synuclein aggregates present in PD brains have been shown to localise at synapses, and such

localisation is associated with pathological synaptic loss[593]. Regarding microglia, α-synuclein aggregates can induce microglial activation and enhance microglial phagocytic capacity[594], thus implicating microglial phagocytosis in synaptic loss in PD as well as AD. Moreover, accumulation of complement proteins (such as iC3b) has been observed in Lewy bodies and neurons within the substantia nigra in PD, which may promote microglial phagocytosis of synapses[32]. However, evidence of any role for microglial synaptophagy in contributing to synaptic loss in PD is at present incidental, and requires further investigation.

2.4.2.3. Frontotemporal dementia (FTD)

FTD is characterised by neuronal and synaptic loss within the frontal and temporal lobes[595]. Familial FTD is commonly associated with an autosomal dominant loss-of-function mutation in the gene encoding progranulin[596], the protein-precursor to granulin, a glycoprotein involved in normal lysosome function[597]. However, it is unclear if or how this mutation relates to synaptic loss. Using a progranulin-deficient genetic mouse model of FTD, Lui *et al*[598] showed that: in addition to FTD-associated neurodegeneration and behavioural dysfunction, the FTD mice also exhibited enhanced complement activation and increased synaptic pruning. Microglia lacking progranulin produced more complement proteins than wild-type microglia, and also engulfed more synapses in a neuronal-glial culture model, which was prevented by knocking out C1qa. *In vivo*, Liu *et* al detected an accumulation of C1q on synapses in the ventral thalamus, which was accompanied by increased microglial density and reduced synaptic density in the same region - both of which were prevented in C1qa-knockout mice. C1qa knockout also ameliorated circuit dysfunction and behavioural deficits in the FTD mice, together providing strong evidence that microglial synaptophagy contributes to the pathological progression of familial FTD by promoting synaptic loss. However, mutations in progranulin do not account for all cases of familial FTD, and indeed, most known cases of FTD are not familial but sporadic[599]. Any role for microglial synaptophagy in the pathological progression of these forms of FTD remains to be elucidated.

2.4.2.4. Schizophrenia

An inheritable and neurodevelopmental disorder with an incidence of 15 per 100,000 people[600], schizophrenia is characterised by impaired cognition and perception at the

behavioural level[601], and by loss of grey matter[602] and synapses in the cerebral and prefrontal cortex[603,604] at the anatomical level. Whilst synaptic impairment in schizophrenia has long been established, it has been unclear how reduced synaptic densities are brought about during neurodevelopment. In 2016, Sekar *et al*[605] identified variations in the genes encoding complement component C4 as a primary factor of the genetic basis for schizophrenia. Alleles of these genes were associated with substantial variation in expression levels of C4 components C4a and C4b within the brain, and C4 expression levels were found to be increased in several regions of schizophrenic brains. In these schizophrenic brains, C4 accumulation was detected in both grey and white matter, and was particularly prominent in the hippocampus. Interestingly, C4 strongly colocalised with synaptic puncta in such regions, suggesting synaptic deposition of C4 in schizophrenic brains. C4 can promote activation of C3, and C3 proteins can tag synapses for developmental pruning via microglial phagocytosis[32]. In mice lacking C4, both C3 deposition at synapses and synaptic pruning within the dorsal lateral geniculate nucleus were reduced – importantly, at timepoints where developmental synaptic pruning via C3-mediated microglial synaptophagy have been previously established[32]. Such findings are consistent with a role for microglial synaptophagy as a pathological contributor to schizophrenia during CNS development, by promoting excessive synaptic pruning that results in net synaptic loss.

2.4.2.5. Glaucoma

One of the most common neurodegenerative diseases, glaucoma is an optic disease that results from the progressive and selective loss of retinal ganglion cells (RGCs)[606]. One of the earliest molecular hallmarks of glaucoma is the upregulation of complement proteins, particularly by microglia[607]. In a mouse model of glaucoma, Howell *et al*[607] detected loss of neuronal somas (cell bodies) and axons in RGCs, and such losses were ameliorated by a loss-of-function mutation in the gene encoding C1qa, which also protected against glaucoma-induced damage to the retina and optic nerve. Moreover, in the same disease model, Williams *et al*[608] detected early synaptic and dendritic loss in RGCs, which occurred before detectable loss of axons or somas in the RGCs. Importantly, loss of synapses and dendrites were both prevented by knocking out C1qa. Given the known role of complement in regulating microglial synaptophagy – and that microglial phagocytosis of RGC inputs in the context of developmental pruning is well-documented[32] – synaptic loss in glaucoma could in principle

result from complement-induced microglial synaptophagy. However, this requires confirmation.

2.4.2.6. West Nile Viral infection

First isolated in Uganda in 1937, West Nile Virus (WNV) is an enveloped virus of the genus *Flavivirus*[609]. WNV manifests as a neuroinvasive infection, and is commonly associated with neuroinflammation, microglial activation and neuronal loss in infected brain regions[610], with accompanying deficits in memory and visuospatial processing[611]. However, it has long been unclear as to the pathological mechanism underlying synaptic loss in WNV-infected brains. Using a mouse disease model of WNV, Vasek *et al*[610] reported a loss of synapses within the CA3 region of the mouse hippocampus. Similar synaptic loss was reported in the same region in WNV-infected human brain tissue, as was synaptic loss in the CA1 region and the entorhinal cortex. In WNV-infected mice, the authors detected increased microglial engulfment of synapses within the CA3 region compared to healthy mice, indicating that microglial synaptophagy was driving this synaptic loss. Moreover, C1qa was found to be upregulated in the hippocampus of infected mice, and C1q colocalised with both microglial processes and synapses in this region to a greater extent in infected mice. C3d (a cleavage product of C3) was also found to colocalise with hippocampal synapses to a greater extent in infected mice compared to controls. Furthermore, knocking out C3 in the mice reduced microglial phagocytosis of synaptic terminals that had been induced by WNV infection - as determined by co-staining for synaptophysin (a synaptic marker) and CD86, a microglial lysosome marker[610] – and also prevented virus-induced reductions in synaptic density. Together, this study provides strong evidence that WNV infection induces synaptic loss via microglial synaptophagy, and has implications for other viral infections where synaptic loss is known to occur, such as those caused by the human-immunodeficiency virus (HIV)[612].

Aims

In this work, I aimed to identify novel regulatory mechanisms in the microglial phagocytosis of two diverse targets, bacteria and synapses. This was to be achieved using two microglial cell models: the microglial cell-line BV-2 from mouse, and primary cortical microglia from rat. Having established early on that microglia inflammatory-activated by LPS secreted extracellular calreticulin (and later, galectin-3), I aimed to assess whether these proteins could opsonise bacterial targets for phagocytic clearance by microglia, and if so, what receptors/ligands where involved in mediating this opsonisation. To this end, a bacterial-microglial phagocytosis assay was developed, which was subsequently used to explore opsonisation capacities for other unexplored extracellular proteins, such as apolipoprotein E and β-amyloid.

Additionally, given interest in our lab into the role of the microglial receptor $P2Y_6R$ in phagocytosis of viable neurons during neurodegeneration, I further aimed to characterise cellular release of $P2Y_6R$ agonist using a $P2Y_6R$ reporter cell-system. Cells to be tested for secretion of $P2Y_6R$ agonist included a variety of brain cells – including microglia, astrocytes, and neuron-like PC12 cells exposed to different stimuli - and also bacterial cells. After these studies confirmed that extracellular $P2Y_6R$ agonist is generated by both bacteria and mammalian brain cells in a variety of contexts, a role for $P2Y_6R$ in mediating phagocytic clearance of bacteria by microglia was explored. Given the possible relevance of $P2Y_{12}R$ to immune responses of macrophages to bacterial presence[613], a role for $P2Y_{12}R$ in facilitating phagocytic clearance of bacteria by microglia was also explored.

Finally, given the increasing interest in microglial synaptophagy as a key contributor to developmental and pathological synaptic removal – and that known regulators of microglial synaptophagy also feature in innate immune responses of microglia to bacteria[325,351] – I further aimed to explore whether proteins that regulate microglial phagocytosis of bacteria could also regulate microglial phagocytosis of synapses. Originally, this was to be achieved using isolated synapses, or ‘synaptosomes’ - a commonly used model to study synaptophagy. Later, this expanded to include a novel neuronal culture-model of inflammatory-induced

synaptic removal by microglia, which was established by me and used to support findings obtained via the synaptosome model.

CHAPTER III

MATERIALS AND METHODS

3.1. Materials

3.1.1. Reagents

3.1.1.1. Cell lines

Cell line	Description	Species	Source
BV-2	A murine microglial cell line immortalised by infection with a v-raf/v-myc oncogene-carrying retrovirus[614]	Mouse	A gift from Dr Jennifer Pocock (Department of Neuroinflammation, University College London)
1321N1	A human astrocytoma cell line derived originally from malignant glioma tissue[615]	Human	A gift from the Department of Physiology, Development and Neuroscience, University of Cambridge
U937	A human monocyte cell line derived from malignant cells from diffuse histiocytic lymphoma[616]	Human	A gift from Dr Jane Goodall, Department of Medicine, University of Cambridge
PC12	A rat pheochromocytoma cell line derived from transplantable rat adrenal pheochromocytoma[617]	Rat	A gift from Dr Tony Jackson (Department of Biochemistry, University of Cambridge)

3.1.1.2. Cell-culture reagents

Reagent	**Abbreviation**	**Source**
4-(2-hydroxyethyl)piperazine-1-ethanesulfonic acid	HEPES	Sigma
B-27 Supplement	B-27	ThermoFisher
Collagen Type IV		Sigma
D-glucose		Sigma
Dulbecco's Modified Eagle's Medium	DMEM	ThermoFisher
Dulbecco's Modified Eagle's Medium: Nutrient Mixture F-12, no phenol red	DMEM/F12	ThermoFisher
Foetal Bovine Serum	FBS	ThermoFisher
Geneticin disulfate salt solution	G418	ThermoFisher
Gentamicin	Gent	ThermoFisher
Hank's Buffered Salt Solution	HBSS	ThermoFisher
Horse Serum	HS	ThermoFisher
L-Glutamine		ThermoFisher
GlutaMAX		ThermoFisher
Macrophage-Colony Stimulating Factor	M-CSF	BioLegend
Neurobasal Medium		ThermoFisher
Penicillin-Streptomycin	Pen/Strep	Sigma
Phorbol 12-myristate 13-acetate	PMA	Sigma
Phosphate-Buffered Saline	PBS	ThermoFisher
Polymyxin B sulphate salt	PMB	Sigma
Potassium chloride	KCl	Sigma
Poly-L-lysine	PLL	Sigma

Roswell Park Memorial Institute 1640 Medium	RPMI 1640	ThermoFisher
Trypan blue		Sigma
Trypsin-EDTA		Sigma
Versene dissociation reagent		ThermoFisher

3.1.1.3. Chemicals

Chemical	**Abbreviation**	**Alternative name(s)**	**Source**
1-Amino-9,10-dihydro-9,10-dioxo-4-[[4-(phenylamino)-3-sulfophenyl]amino]-2-anthracenesulfonic acid sodium salt	PSB0739		Bio-techne
1-((*trans*-4-Aminocyclohexyl)methyl)-N-butyl-3-(4-fluorophenyl)-1H-pyrazolo[3,4-d]pyrimidin-6-amine	UNC569		Calbiochem
2-(Butylamino)-4-[(trans-4-hydroxycyclohexyl)amino]-N-[[4-(1H-imidazol-1-yl)phenyl]methyl]-5-pyrimidinecarboxamide	UNC2881		Selleck Chemicals
Adenosine 5'-triphosphate disodium salt	ATP		Sigma
Adenosine 5'-disphophate sodium salt	ADP		Sigma
Agar			Formedium
Apolipoprotein E2	ApoE2		Sigma
Apolipoprotein E4	ApoE4		Sigma
Apyrase			Sigma

β-amyloid peptide 1-42	Aβ	Amyloid beta, Abeta	AnaSpec
Bovine serum albumin	BSA	Fraction V	Sigma
Calcium chloride	$CaCl_2$		Sigma
Calreticulin	CRT	Calregulin, CRP55, CaBP3, ERp60	Abcam
Carbenoxelone disodium salt	CBX		Sigma
Complement component C1q	C1q		Abcam
Cytochalasin D	Cyt D		Sigma
Dithiothreitol	DTT		Sigma
Ethanol	C_2H_5OH		Sigma
Ethylenediaminetetraacetic acid	EDTA		Sigma
Flufenamic acid	FFA		Sigma
Galectin-3	Gal-3	Mac-2, LGALS3	A gift from Dr Tomas Deierborg (Lund University)
Glycine	Gly		Sigma
Hydrochloric acid	HCl		Sigma
Lactose			Sigma
Lipopolysaccharide from *S. enterica* (serotype: typhimurium)	LPS		Sigma
Lipopolysaccharide from *E. coli*	LPS		Sigma
Magnesium chloride	$MgCl_2$		Sigma
Magnesium sulfate	$MgSO_4$		ThermoFisher

Manganese chloride	$MnCl_2$		Sigma
Methanol	CH_3OH		ThermoFisher
N,N''-1,4-Butanediylbis[N'-(3-isothiocyanatophenyl)thiourea	MRS2578		Sigma
Neuraminidase from *C. perfringens*	NEU	Sialidase	Sigma
Pluronic F-127			Sigma
Low density lipoprotein receptor-related protein-associated protein 1	RAP	LRPAP1	Bio-techne
Paraformaldehyde	PFA		Sigma
Percoll			GE Life Sciences
Potassium chloride	KCl		Sigma
Potassium dihydrogen phosphate	KH_2PO_4		ThermoFisher
Probenecid	PBD		Sigma
Saponin			Fluka Chemicals
Sodium azide	NaN_3		Sigma
Sodium chloride	NaCl		ThermoFisher
Sodium hydroxide	NaOH		Sigma
Staurosporine	STS		Sigma
Sucrose			ThermoFisher
Tau		MAPT	A gift from Professor Vilmante Borutaite (University of Vilnius)
Tris(hydroxymethyl)aminomethane	TRIS		Melford Laboratories
Tryptone			Melford Laboratories

Tumour necrosis factor-alpha	TNF-α	Cachexin, cachectin	Sigma
Uridine			Sigma
Uridine 5'-diphosphate disodium salt hydrate	UDP		Sigma
Uridine 5'-monophosphate disodium salt	UMP		Sigma
Yeast extract			Melford Laboratories

3.1.1.4. RNA primers

Target	**Species**	**Forward sequence**	**Reverse sequence**	**Source**
CALR	Mouse	CGCAGACCCTGCCATCTATT	GACAGTGCGTAAAATCGGGC	Sigma
LGALS3	Mouse	TTGAAGCTGACCACTTCAAGGTT	AGGTTCTTCATCCGATGGTTGT	Sigma
IL6	Mouse	TTCCATCCAGTTGCCTTCTTGG	TTCTCATTTCCACGATTTCCCAG	Sigma
ACTB	Mouse	CCACACCCGCCACCAGTTCG	CCCATTCCCACCATCACACC	Sigma

3.1.1.5. Primary antibodies

Antibody	**Cat. #**	**Host**	**Final concentration/ dilution**	**Application**	**Source**
Calreticulin	ADI-SPA-602-D	Rabbit	2 µg/ml	Function blocking	Enzo Life Sciences
Rabbit IgG	4041-01	Rabbit	2 µg/ml	Function blocking	Southern Biotech
PSD-95	MA1-046	Mouse	3.3 µg/ml (1:300)*	Immunofluorescence	ThermoFisher
Synaptophysin	32127	Rabbit	3.3 µg/ml (1:300)*	Immunofluorescence	Abcam

*unless otherwise stated in the text.

3.1.1.6. Secondary antibodies

Antibody	**Host**	**Final concentration/ dilution**	**Source**
Affinipure Fab anti-rabbit IgG	Goat	10 µg/ml	Jackson ImmunoResearch
AlexaFluor 488 anti-rabbit IgG	Goat	1:200 (10 µg/ml)	ThermoFisher
Cy3 anti-mouse	Goat	1:200 (10 µg/ml)	Jackson ImmunoResearch

3.1.1.7. Fluorescent dyes

Fluorescent dye	**Excitation (nm)**	**Emission (nm)**	**Final concentration/ dilution**	**Source**
Annexin-V FITC	495	519	4 µg/ml	Immunotools
Anti-MHC class II FITC	495	519	1 µg/ml	ThermoFisher
Calcein-AM	495	515	2 µM	Sigma
Fura 2-AM	340,380	510	0.5 µM	ThermoFisher
Hoechst 33342	346	460	4 µg/ml	Sigma
Isolectin-B_4-AlexaFluor 488 from *Griffonia simplicifolia* (IB_4)	495	519	2 µg/ml	ThermoFisher
Lectin from Arachis hypogaea (peanut) FITC	495	519	5 µg/ml	Sigma
pHrodo Red succinimidyl-ester (pHrodo-SE)	560	585	10 µM	ThermoFisher
Propidium iodide	535	617	1 µg/ml	Sigma
SYBR Green qPCR SuperMix-UDG (Platinum)	497	520	1:2	ThermoFisher
5-(and 6)-carboxytetramethylrhodamine succinimidly ester (TAMRA-SE)	546	579	50 µM	ThermoFisher

3.1.1.8. Commercially available kits

Product	**Application**	**Source**	**Catalogue #**
Corning Transwell polycarbonate membrane cell culture inserts	Migration assay	Sigma	CLS3422
FluoSpheres Polystyrene Microspheres, 1.0 µm, red fluorescent (580 nm/605 nn)	Phagocytosis assay	ThermoFisher	F13083
Mouse Calreticulin (CALR) ELISA	Protein detection	Abbexa	abx153760
Mouse Galectin-3 DuoSet ELISA	Protein detection	R&D Systems	DY1197
Mouse IL-6 ELISA MAX	Protein detection	BioLegend	431304
Monarch Total RNA Miniprep Kit	RNA isolation	New England Biolabs	T2010S
SuperScript II Reverse Transcriptase	cDNA generation	ThermoFisher	18064014
pHrodo Red *E. coli* BioParticles	Phagocytosis assay	ThermoFisher	P35361

3.1.2. Equipment

3.1.2.1. Flow cytometer

Accuri C6, BD Biosciences

Laser & filter details:

Channel	Excitation (nm)	Emission (nm)	Fluorophores
FL1	488	530	FITC, Alex Fluor 488, Calcein-AM
FL3	488	670	pHrodo Red, propidium iodide, TAMRA-SE, FluoSpheres Polystyrene Microspheres, Cy3

3.1.2.2. Microscope

Leica DMI6000 CS

HCX PL Fluotar 20x/0.40 dry objective

Laser & filter details

	Excitation (nm)	Emission (nm)	Dichroic mirror (nm)	Fluorophores
1	BP 360/40	BP 470/40	400	Hoechst 33342
2	BP 480/40	BP 527/30	505	AlexaFluor 488
3	BP 545/40	BP 610/75	565	pHrodo Red, TAMRA-SE propidium iodide

3.1.2.3. Confocal microscope

Leica TCS SP8

20x/0.75 (dry), 63x/1.4 (oil) objectives

Laser & filter details

	Excitation (nm)	Emission (nm)	Beam splitter	Fluorophores
1	405	461	LP 620	DAPI
2	488	519	LP 620	AlexaFluor 488
3	552	568	LP 560	Cy3

3.1.2.4. Plate readers

FLUOstar OPTIMA Microplate Reader, BMG Labtech

FlexStation 3 Multi-Mode Microplate Reader, Molecular Devices

3.1.2.5. RT-qPCR cycler

Rotor-Gene Q, QIAGEN

3.1.2.6. Spectrophotometers

Nanodrop ND 1000, ThermoFisher

BioPhotometer D30, Eppendorf

3.1.3. Software

Prism8, GraphPad Software Inc., USA

BD Accuri C6 Software v1.0.264.21, BD Biosciences, USA

ImageJ v.1.49, National Institutes of Health, USA

LAS AF v.2.21, Leica Microsystems GmbH, Germany

LAS X v3.52.18963, Leica Microsystems GmbH, Germany

Office 365, Microsoft Corporation, USA

3.2. Methods

All experiments were performed in accordance with the UK Animals (Scientific Procedures) Act (1986) and approved by the Cambridge University Local Research Ethics Committee.

3.2.1. Cell culture

All culture media was supplemented with either Pen/Strep (10 U/ml) or gentamicin (50 µg/ml), with antibiotic changed approximately every 6 months.

3.2.1.1. BV-2

BV-2 murine microglial cells were thawed from cryogenically frozen stocks and maintained in DMEM supplemented with 10% FBS ('BV-2 culture medium') in untreated 75 cm^2 flasks (37°C, 5% CO_2). Flasks were passaged upon reaching >60% confluence via either enzymatic detachment with 0.05% trypsin in PBS or via mechanical detachment with a serological pipette, followed by centrifugation (150g RCF, 5 minutes) and resuspension of the pellet in fresh BV-2 culture medium as required.

For experimentation, BV-2 pellets were resuspended in DMEM with 0.5% FBS ('low-serum culture medium'), unless otherwise stated, and counted using a haemocytometer. Trypan blue was used to identify dead cells, which were discounted. After diluting as appropriate in low-serum culture medium, cells were plated in untreated 96 well-plates at densities of 5 x 10^4/ 200µl/ well and incubated overnight at 37°C (5% CO_2) unless otherwise stated.

3.2.1.2. 1321N1

132N1 human astrocytoma cells were used to generate two stably transfected cell lines, obtained by Dr Stefan Milde: one expressing murine $P2Y_6R$ N-terminally linked to mCherry, the other expressing mCherry alone. 132N1s were thawed from cryogenically frozen stocks and maintained in DMEM supplemented with 10% FBS ('1321N1 culture medium') in untreated 75 cm^2 flasks (37°C, 5% CO_2). Flasks were passaged upon reaching >60%

confluence via enzymatic detachment with 0.05% trypsin in PBS, followed by centrifugation (150g RCF, 5 minutes) and resuspension of the pellet in fresh 1321N1 culture medium as required.

For experimentation, 1321N1s were counted using a haemocytometer. Trypan blue was used to identify dead cells, which were discounted. After diluting as appropriate, cells were plated in untreated black-wall/clear-bottom 96 well-plates at densities of 8 x 10^3/ 100 µl/ well and incubated overnight at 37°C (5% CO_2), unless otherwise stated.

3.2.1.3. U937

U937 human monocyte cells were thawed from cryogenically frozen stocks and maintained in suspension in RPMI supplemented with 10% FBS ('U937 culture medium') in untreated 75 cm^2 flasks (37°C, 5% CO_2). Flasks were passaged by diluting in fresh U937 culture medium as required. To induce differentiation into monocyte-derived macrophages, U937s were treated with PMA (1 µg/ml) and M-CSF (100 ng/ml) for 96-hours in 75 cm^2 flasks pretreated with PBS containing 0.1% poly-L-lysine. Differentiation was confirmed when U937s became capable of adhering to the base of the well.

For experimentation, U937s were counted using a haemocytometer. Trypan blue was used to identify dead cells, which were discounted. After diluting as appropriate, undifferentiated cells were plated in untreated 24 well-plates at densities of 5.0 x 10^4/ 500 µl/ well and incubated at 37°C (5% CO_2); PMA-differentiated cells were enzymatically detached using 0.05% trypsin in PBS and plated in 96 well-plates pretreated with PBS containing 0.1% poly-L-lysine at densities of 5.0 x 10^4/ 200 µl/ well and incubated overnight (37°C, 5% CO).

3.2.1.4. PC12

PC12 rat pheochromocytoma cells were thawed from cryogenically frozen stocks and maintained in suspension in RPMI supplemented with 10% HS and 5% FBS ('PC12 culture medium') in untreated 75 cm^2 flasks (37°C, 5% CO_2). Flasks were passaged by diluting in fresh PC12 culture medium as required.

For experimentation, PC12s were counted using a haemocytometer. Trypan blue was used to identify dead cells, which were discounted. After diluting as appropriate, cells were plated in 24 well-plates treated with PBS containing 0.5 mg/ml collagen type IV at densities of 1.5 x 10^5/ 500 µl/ well and incubated overnight at 37°C (5% CO_2) unless otherwise stated.

3.2.2. Primary Cell Culture

3.2.2.1. Cortical mixed glial cultures

Cultures were prepared from the cortices of post-natal day 3-6 mice or rats as described[518,618]. Pups were culled via the schedule-1 methods of cervical dislocation or decapitation, and heads retained in 70% ethanol (4°C). Brains were quickly extracted and retained in HBSS (4°C) while meninges were removed, and cortical slices generated. Cortical slices were pooled, immersed in HBSS containing 0.03% trypsin, shredded using scissors and incubated for 15 minutes at 37°C. Then, supernatant was aspirated and replaced with DMEM containing 10% Performance Plus FBS ('glial culture medium') before the tissue was subjected to several trituration steps using a 100-1000 µl pipette tip. Between each step, suspension material was saved and replaced with glial culture medium, until little/no pellet remained. Any pellet remaining after 6 trituration steps was discarded. Suspension material was spun down via centrifugation (150g RCF, 7 minutes, slow start/stop). After spinning, the supernatant was discarded and the pellet resuspended in fresh glial culture medium, before straining using 100 µm and then 40 µm cell-strainers (Falcon). Final suspension material was seeded into 75 cm^2 flasks pre-treated with PBS containing 0.02% poly-L-lysine and incubated at 37°C (5% CO_2). 24 hours later, debris was detached via gentle shaking and media was changed. Cultures were left incubating for 7-14 days *in vitro* (DIV) prior to isolation of primary microglia.

3.2.2.2. Isolated primary microglial cultures

Primary microglia were isolated from cortical mixed-glial cultures between DIV 7-14 via the shaking-off method[518,618], in which weakly adherent cells (i.e. microglia) are dislodged by bashing and gently vortexing the flasks for 1-2 minutes. Medium containing dislodged microglia was spun down via centrifugation (150g RCF, 7 minutes, slow start/stop). After spinning, the supernatant was saved and diluted in 2-parts fresh glial culture medium to generate 'conditioned' culture medium. Pellets were resuspended in conditioned culture medium and counted using a haemocytometer. After diluting in conditioned culture medium as required, cells were seeded in 96 well-plates pre-treated with PBS containing 0.02% poly-L-lysine at a density of 5 x 10^4 cells/ 200 µl/ well and incubated at 37°C (5% CO_2) overnight, unless otherwise stated.

3.2.2.3. Cerebellar neuronal cultures

Cultures were prepared from the cerebella of post-natal day 3-6 mice as described[619]. Pups were culled via the schedule-1 methods of cervical dislocation or decapitation, and heads retained in 70% ethanol (4°C). Brains were quickly extracted and retained in HBSS (4°C) while cerebellar slices were generated, and meninges removed. Cerebella were pooled, immersed in 0.48 mM Versene dissociation reagent (Gibco), shredded using scissors and incubated for 5 minutes at 37°C. Then, tissue was subjected to several trituration steps using a 100-1000 µl pipette tip. Between each step, suspension material was diluted into DMEM containing 5% HS, 5% FBS, 20 mM KCl, 13 mM glucose, 5 mM HEPES and 2 mM L-glutamine ('CGC culture medium') and replaced with Versene, until little or no pellet remained. Any pellet remaining after 6 trituration steps was discarded. Suspension material was spun down via centrifugation (150g RCF, 7 minutes, slow start/stop). After spinning, the supernatant was discarded and the pellet resuspended in CGC culture medium, before straining using 40 µm cell-strainers (Falcon). Final resuspension was counted using a haemocytometer, seeded into 24 well-plates pre-treated with PBS containing 0.01% poly-L-lysine at a density of 5 x 10^5 cells/ 500 µl/ well, and incubated at 37°C (5% CO_2). 24 hours later, media was changed. Cultures were left incubating for 14 DIV, with 50% media swaps typically performed on DIV 7 and 10.

3.2.3. Synaptosome isolation and maintenance

3.2.3.1. Preparation of Percoll gradients

Percoll gradients were prepared as described by Dunkley *et al*[620]. Percoll was prepared from slurry stock by sterile-filtering (0.2 μm) and pH adjusting to 7.4 with hydrochloric acid. Homogenising buffers (0.32 M sucrose, 1 mM EDTA, 5 mM Tris, 250 μM DTT, pH 7.4) containing 3%, 10%, 15% or 23% Percoll were prepared. 2 ml of 23% Percoll buffer was added to each of 6 centrifuge tubes; to this, 2 ml of 15% Percoll buffer was gently added by hand using a serological pipette, careful not to mix the two solutions. Successful separation of the gradient was determined by checking for a clear Schlieren line by eye[620]. 10% and 3% Percoll buffer solutions were added successively via the same method. Gradients were retained on ice until use.

3.2.3.2. Cortex homogenisation, synaptosome isolation and storage

Synaptosomes were isolated from rat cortex via the Percoll gradient procedure described by Dunkley *et al*[620]. Male rats weighing between 125-150 grams were culled via the schedule-1 method of cervical dislocation, followed by decapitation to confirm death. Brains were quickly extracted and retained in homogenizing buffer (0.32 M sucrose, 1 mM EDTA, 5 mM Tris, 250 μM DTT, pH 7.4) on ice while cortical slices were generated. Slices were homogenized via 10 firm up-down motions with a mechanical homogenizer, or until solution had cleared of visible remnants. Homogenate was stored on ice before spinning down via centrifugation (1000g RCF, 10 minutes, 4°C). The supernatant ('S1') fraction was saved and loaded onto prepared Percoll gradients at 2 ml per tube; the pellet was discarded. After loading S1, tubes were spun down using a JA 25.50 rotor (Beckman) at 20,000 RPM (4°C, slow start/stop). Spins were timed such that tubes were subjected to precisely 12 minutes at maximum speed, to ensure proper separation of fractions down the gradient. The synaptosome fraction was then extracted using a glass pipette, with care taken to avoid extracting undesired fractions, and diluted in ~40 ml of ice-cold homogenizing buffer. To eliminate any contaminating silica aggregates from the Percoll, this synaptosome-containing solution was spun again using a JA 25.50 rotor (Beckman) at 15,500 RPM (4°C, slow-stop). Supernatant was aspirated, with care taken not to dislodge the synaptosome pellet. The pellet

was then resuspended in ice-cold homogenizing buffer to 1.5 ml and spun using a benchtop centrifuge (Eppendorf) for 10 minutes (20,000 RCF, 4°C). The synaptosome pellet was finally resuspended to 1 ml with homogenizing buffer containing 5% DMSO, aliquoted and cryogenically frozen until use. A few microliters were retained and used to measure synaptosome concentration, which was approximated by quantifying protein density at 280 nm using a nanodrop (ThermoFisher).

3.2.3.3. Synaptosome maintenance post-cryofreezing

When required, synaptosome aliquots were brought rapidly to 37°C in a water bath. Quickly, the synaptosome solution was diluted in Hepes-buffered Krebs-like buffer (HBK; 143 mM NaCl, 4.7 mM KCl, 1.3 mM $MgSO_4$, 1.2 mM $CaCl_2$, 0.1 mM NaH_2PO_4, 20 mM HEPES and 10 mM D-glucose[621]), which was pH-adjusted to 7.4 with 1 M HCl, warmed and CO_2-infused in preparation. Synaptosomes were then ready for experimentation.

3.2.4. Cell treatments

3.2.4.1. Chronic (≥18 hour) treatments

Chronic treatments describe treatments made to cell cultures for at least 18 hours and usually 24 hours, to induce changes at the transcriptomic level. Chronic treatments for BV-2 include treatment with LPS from *S. enterica* (100 ng/ml), LPS from *E. coli* (100 ng/ml), recombinant human calreticulin (10 μg/ml), monomeric β-amyloid (250 nM), fibrillar β-amyloid (2.5 μM) or TNF-α (50 ng/ml), for 24 hours unless otherwise stated. Chronic treatments for primary rat microglia include treatment with LPS from *S. enterica* (100 ng/ml), LPS from *E. coli* (100 ng/ml or 1 ng/ml), recombinant human calreticulin (1 μg/ml) or MRS2578 (1 μM) for 24 hours, and UDP (100 μM) for 18 hours. Chronic treatments for cerebellar granule cell cultures include LPS from *E. coli* (10 ng/ml, unless otherwise stated) for 72 hours, MRS2578 (1 μM), PSB0739 (1 μM), UNC569 (500 nM), anti-calreticulin antibody (2 μg/ml), IgG serotype control (2 μg/ml) and recombinant human calreticulin (1 μg/ml) for 72.5 hours.

3.2.4.2. Short-term (<18 hour) treatments

Short-term treatments describe treatments made to ensure sufficient exposure time for target-blocking, epitope binding etc., but not intended to induce substantial changes at the transcriptomic level. Short-term treatments for BV-2 microglia include treatment with LPS from *S. enterica* (100 ng/ml), monomeric β-amyloid (250 nM), TNF-α (50 ng/ml), anti-calreticulin antibody (2 μg/ml) or IgG serotype control (2 μg/ml) for 3 hours; MRS2578 (500 nM or 1 μM), PSB0739 (10 μM), lactose (50 mM), sucrose (50 mM), UNC2881 (200 nM), UNC569 (500 nM), UDP (1 mM), ADP (1 mM), flufenamic acid (200 μM) or probenecid (200 μM) for 60 minutes; and apyrase (1 U/ml) for 30 minutes, unless otherwise stated. Short-term treatments for primary rat microglia include treatment with anti-calreticulin antibody (2 μg/ml) and IgG serotype control (2 μg/ml) for 3 hours; MRS2578 (500 nM or 1 μM), PSB0739 (10 μM), lactose (50 mM), sucrose (50 mM), UNC2881 (200 nM or 2 μM), UNC569 (500 nM or 5 μM), RAP (250 nM or 500 nM), UDP (1 mM), ADP (1 mM) and cytochalasin D (10 μM) for 60 minutes; and apyrase (1 U/ml) for 30 minutes.

3.2.4.3. Acute treatments

Acute treatments describe treatments made to induce an immediate response from cells. Acute treatments of 1321N1 cells include treatment with carbachol (10 μM), UDP, UMP, uridine (each applied at a range of concentrations), *E.* coli-conditioned flex buffer, CGC-conditioned buffer, BV-2 conditioned buffer, PC12-conditioned buffer, and 1321N1-conditioned buffer (further details provided in '3.2.5.2' of methods). BV-2 cells and primary rat microglia were acutely treated with UDP (1 mM).

3.2.5. General methods

3.2.5.1. β-amyloid preparation

β-amyloid was dissolved in hexafluoro-2-propanol (HFIP) to 2.5 mg/ml and immediately vortexed. Solution was aliquoted into 0.5 ml PCR tubes (ThermoFisher) and sealed for 60 minutes. Then, tubes were uncapped and left for 60 minutes for evaporation of HFIP to occur; any traces remaining were removed via aspiration.

For immediate use, Aβ was dissolved in aliquots using DMSO (5 mM), which was then added to ice-cold PBS or DMEM/F-12 to 100 μM. For monomeric Aβ, this solution was used immediately. For oligomeric Aβ, this solution was left at 4°C for 24 hours. For fibrillar Aβ, this solution was left at 37°C for 24 hours.

3.2.5.2. Buffer-conditioning assay

BV-2 cells were plated at 1.5 x 10^5/ 500 μl/ well in untreated 24 well-plates. PC12 cells were plated as described (see section 3.2.1.4). 1321N1 cells were plated at 1.5 x 10^5/ 500 μl/ well in untreated 24 well-plates. Cells were washed with Flex buffer (115 mM NaCl, 1 mM CaCl, 1 mM $MgCl_2$, 1 mM KCl, 10 mM HEPES, 10 mM glucose, pH 7.2) before adding 500 μl Flex buffer per well, unless otherwise stated. Buffer was conditioned with cells for varying durations at room temperature (R/T), except for durations ≥60 minutes, which were kept at 37°C. After the appropriate duration, buffer was removed from cells and retained on ice until application to Fura-2 AM-stained 1321N1 cells stably transfected with $P2Y_6R$-mCherry or mCherry for calcium detection (see 3.2.5.3).

3.2.5.3. Calcium detection assay

132N1 cells plated at 8 x 10^3/ 100 μL/ well in black-walled, clear-bottomed 96 well-plates were washed with Flex buffer (see 3.2.5.2) before staining with Flex buffer containing 0.5 μM Fura 2-AM and 0.5 mg/ml Pluronic F-127 for 60 minutes in darkness (R/T). Then, cells were washed twice with Flex buffer to remove extracellular Fura-2 AM. After 20 minutes, buffer was replaced with 100 μl/ well fresh Flex buffer and immediately transferred to the FlexStation 3 Multi-Mode Microplate Reader (Molecular Devices) for automated treatments and fluorescence detection. Fluorescence measurements (excitation 340nm & 380 nm, emission 510 nm) were made every 5 seconds for 90 seconds, unless otherwise stated. Treatments were added at 30 seconds.

For analyses (see Figure 3.1) fluorescence ratios at 340 nm and 380 nm (measured in relative fluorescence units, or RFUs) were calculated for each time point. Background fluorescence -

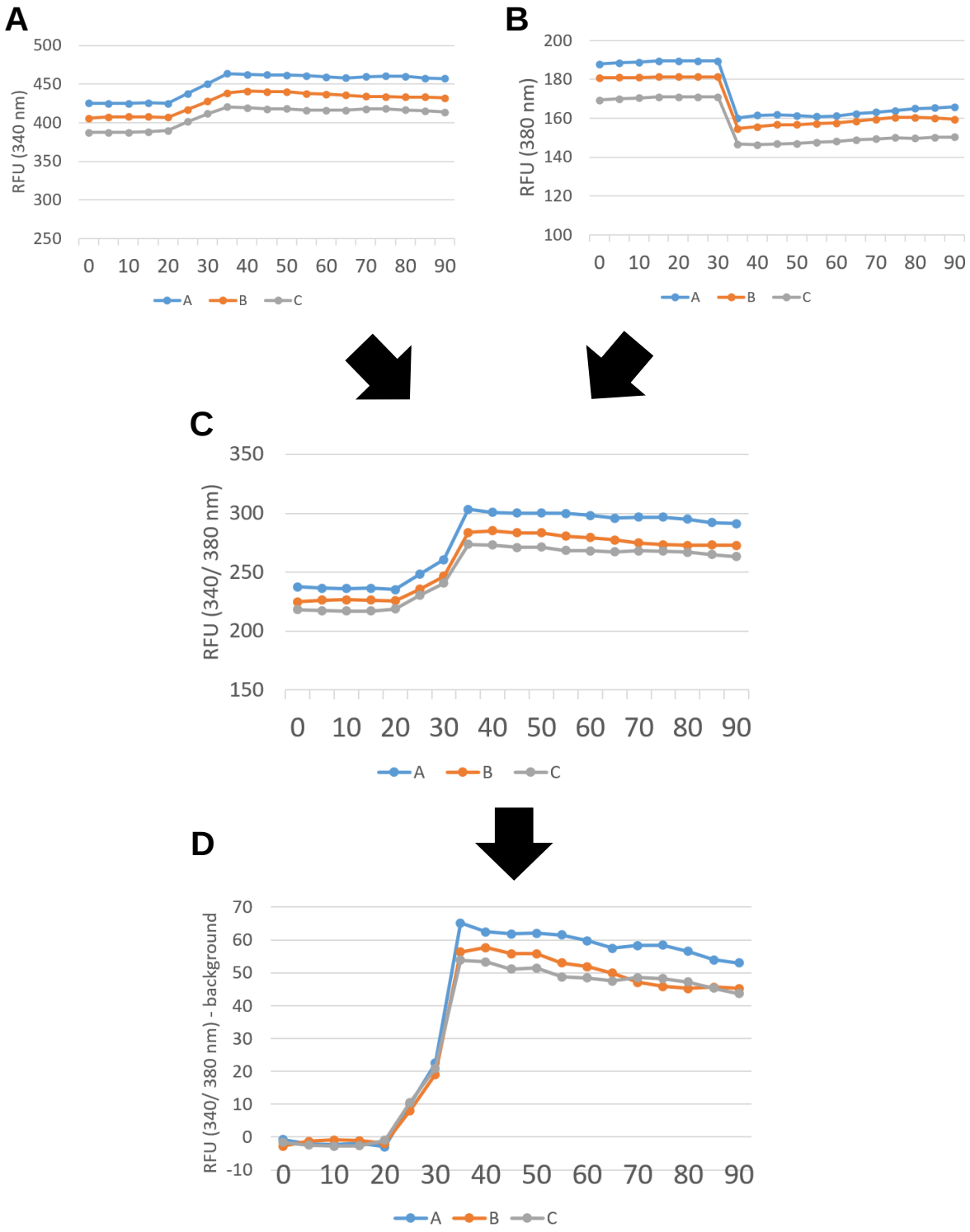

Figure 3.1. Analysis of fluorescence data obtained from Fura-2 AM-labelled 1321N1 cells stably transfected with P2Y$_6$R – and treated with 100 µM after 30 seconds – using a FlexStation 3 Multi-Mode Microplate Reader. Replicate fluorescence readings at 340 nm (**A**) and 380 nm (**B**) were taken every 5 seconds for at least 90 seconds. 340/ 380 nm RFU ratios were then generated for each timepoint (**C**). To deduct background fluorescence, the average fluorescence (340/ 380 nm) from the first 30 seconds (prior to treatment) was calculated and deducted from the fluorescence of each timepoint (**D**). Maximum fluorescence values from each replicate were then used as the representative fluorescence response for that replicate.

calculated as the mean of the first 6 fluorescence ratios in any given well prior to treatment - was deducted from each time-point to provide fluorescence changes in response to treatment. Peak values from each condition were used to represent the fluorescence response from that condition, and so used for comparative analysis between conditions. values from each replicate were then used as the representative fluorescence response for that replicate.

3.2.5.4. Confocal microscopy & image analysis

Glass slides containing mounted coverslips were obtained as described in section 3.2.5.7 and imaged using a TCS SP8 confocal microscope (Leica). Coverslips were imaged at 63x magnification (image size: 184.52 μm^2; pixel size: 180.38 nm^2; pixel dwell time: 862 ns; frame rate: 0.19/s), with 4 images taken per coverslip and z-stacks of 2 µm with 6 steps (0.4 µm/ step) per image. All images were analysed using ImageJ software; all puncta quantification was done using Trackmate v5.0.1[622]. For each image, a z-project was made (projection type: max intensity) and a gaussian blur was applied (sigma radius: 1). On Trackmate, a DoG detector was used (estimated blob diameter: 0.72 µm) and 'mean intensity' and 'quality' parameters were chosen based on qualitative assessment of puncta assignment from random example images taken from each experimental condition. Once chosen, the same parameters were used for all images within the same experiment, to ensure no bias between conditions. Data was represented as average synaptophysin puncta #/ field from all images of the same condition. DAPI-stained nuclei were counted manually, and this data was represented as average nuclei #/ field from all images of the same condition.

3.2.5.5. ELISA (enzyme-linked immunosorbent assay)

BV-2 microglia were plated at densities of 5.0 x 10^4/ 500 µl/ well (24 well-plate format) in low-serum culture medium. Primary mouse microglia were plated at densities of 1.0 x 10^4/ 100 µl/ well (96 well-plate format) in conditioned culture medium to measure calreticulin, or 2.0 x 10^4/ 100 µl/ well to measure galectin-3 and IL-6. Following treatments, cell media was removed and protein detection achieved via a calreticulin ELISA (Abbexa), galectin-3 ELISA (R&D Systems) or IL-6 ELISA (BioLegend) as per manufacturer instructions. For calreticulin, BV-2 and primary microglial samples were diluted 1/2 in assay diluent. For galectin-3, primary microglial samples were diluted 1/10. For IL-6, primary microglial

samples were diluted 1/10 in assay diluent; BV-2 samples were not diluted. Absorbances (450 nm) were measured using a FLUOstar Optima plate reader (BMG Labtech) and used to calculate final protein concentrations against a standard curve. Treatments were applied as follows: LPS from *S. enterica* (100 ng/ml), LPS from *E. coli* (100 ng/ml or 1 ng/ml), recombinant human calreticulin (10 or 1 μg/ml), monomeric β-amyloid (250 nM) or TNF-α (50 ng/ml), for 3 or 24 hours. Where used, polymyxin B was applied to cells at 10 U/ml 60 minutes prior to treatments.

3.2.5.6. Flow cytometry

Biological samples were analysed via flow cytometry using an Accuri C6 flow cytometer (BD Biosciences). Biological samples were retained in PBS on ice (unless otherwise stated) and run through the cytometer at 1 μl/second. Gating was performed to limit analysis to the target of interest; no samples containing similarly sized cells mixed together were subjected to flow cytometry in order to avoid ambiguity over event-cloud assignment. Where possible, 10,000 events per sample (of the target-of-interest) were analysed for forward-scatter (proportional to event size), side-scatter (proportional to event granularity), and fluorescence. Data analysis was performed using BD Accuri C6 software (BD Biosciences).

3.2.5.7. Immunocytochemistry

Cerebellar neuronal cultures were plated as described in 3.2.2.3 and treated as described in 3.2.4 or outlined in the results section. After 14 DIV, cells were washed with PBS and fixated with PBS containing 4% PFA for 10 minutes (R/T). Cells were washed 3 times and blocked using PBS containing 0.1 M glycine for 10 minutes. Cells were then washed as before and permeabilised using PBS containing 0.1% saponin for 10 minutes. Cells were then washed and blocked using PBS containing 15% BSA for 30 minutes. Cells were then washed and incubated with PBS containing 5% BSA, and the primary antibodies anti-synaptophysin (3.3 μg/ml) and anti-PSD-95 (3.3 μg/ml), overnight at 4°C (unless otherwise stated). The next day, cells were washed and incubated with PBS containing 5% BSA, and the secondary antibodies AlexaFluor-488 anti-rabbit IgG (10 μg/ml) and Cy3 anti-mouse (10 μg/ml) for 2 hours at room temperature (unless otherwise stated). Cells were then washed and mounted on

glass slides using mounting medium with DAPI. Slides were stored at 4°C until analysis via confocal microscopy.

3.2.5.8. Light microscopy & image analysis

Cell cultures were treated with the nuclear marker Hoechst 33342 (4 μg/ml), the necrotic marker propidium iodide (1 μg/ml) and/or the microglial-specific marker Isolectin-B_4-AlexaFluor 488 (2 μg/ml) (as stated) for 20 minutes in darkness (R/T), before exchanging with fresh media. Cells were then analysed using a DM16000 fluorescence microscope (Leica) at 20x magnification, with 4 images taken per well. All images were analysed using ImageJ software; cells were counted manually using the cell-counter plugin. For cerebellar neuronal cultures, viable neuronal counts were obtained by excluding IB_4-positive cells (microglia), obviously larger cells (astrocytes), chromatin-condensed cells (apoptotic cells, evident by Hoechst staining) and propidium-iodide positive cells (dead cells) from the total cell count, and data represented as average cell #/ field.

3.2.5.9. RNA isolation, cDNA generation and qPCR

RNA isolation from microglial BV-2 cells was achieved using a Monarch Total RNA Miniprep Kit (New England Biolabs). cDNA was subsequently generated from the RNA (1 μg) combined with random hexamer primers and the SuperScript II Reverse Transcriptase Kit (ThermoFisher). qPCR was performed using a Rotor-Gene Q cycler (Qiagen) in the presence of Platinum SYBR Green qPCR SuperMix (ThermoFisher). Primers for mouse *IL6*, *LGALS3*, *CALR* and *ACTB* were used. To determine relative mRNA levels of target genes, fold-changes in the delta-delta threshold cycle were taken and normalised to the internal (actin) control for each condition. Treatments were applied as follows: LPS from *S. enterica* (100 ng/ml) or fibrillar β-amyloid (250 nM) for 3, 24 or 48 hours as indicated.

3.2.5.10. Synaptosome immunostaining

Synaptosomes were thawed in warmed, CO_2-infused HBK buffer from cryogenically frozen stocks. Synaptosomes were spun down (20,000 RCF, 5 minutes) and resuspended in PBS containing 4% PFA for 15 minutes in darkness. Synaptosomes were spun again and

resuspended in PBS to wash away PFA; this step was repeated. Synaptosomes were spun again and resuspended in 90% methanol for 5 minutes in darkness. Samples were PBS-washed as before, spun down and resuspended in PBS containing 3% BSA. To this, primary antibodies anti-synaptophysin (5 µg/ml), anti-PSD-95 (20 µg/ml), rabbit IgG serotype control (5 µg/ml), or PBS (as vehicle) was added and samples were left gently shaking for 60 minutes (R/T). Samples were then washed twice as before, and finally resuspended in PBS containing 3% BSA. To this, secondary antibodies AlexaFluor-488 anti-rabbit (10 µg/ml) or Cy3 anti-mouse (10 µg/ml) were added and samples were left gently shaking for 30-minutes in darkness (R/T). Samples were spun down once more and resuspended in 60 µl PBS before analysing via flow cytometry.

3.2.5.11. TAMRA-based protein binding assay

Calreticulin (500 nM), galectin-3 (100 nM), monomeric β-amyloid (10 µM), oligomeric β-amyloid (10 µM), apoE2 (1 µM), apoE4 (1 µM) and tau (1 µM) were each incubated with 5-(and-6)-carboxytetramethylrhodamine-succinimidyl ester (TAMRA-SE, 50 µM) for 20 minutes at 37°C before diluting in 15 ml PBS (for *E. coli*) or HBK (for synaptosomes). Proteins were centrifuged using an Amicon Ultracentrifuge filter (Millipore) (10,000 Dalton cut-off) to remove unbound TAMRA. Targets (*E. coli* or synaptosomes) were then resuspended in the protein-containing fraction, or the protein-free fraction as a negative control. For calreticulin, sucrose (50 mM) or PBS (as vehicle) was added alongside *E. coli* or synaptosomes. For galectin-3, lactose (50 mM) or PBS (as vehicle) was added alongside *E. coli* or synaptosomes. For calreticulin and galectin-3, synaptosomes were treated for 30-minutes with neuraminidase from *C. perfringens* (0.4 U/ml) before adding protein. Extent of protein binding was then measured in terms of fluorescence changes of the target via flow cytometry (see section 3.2.5.6).

3.2.5.12. Viability assays

To measure cell viability, cells were treated with the necrotic marker propidium iodide (1 µg/ml) for 20 minutes in darkness (R/T), before exchanging with fresh media. Levels of necrosis were measured either via light microscopy (section 3.2.5.8) followed by manual counting in ImageJ, or via flow cytometry (section 3.2.5.6) using the ‘fluorescence gate-shift’

method (section 3.2.6). To measure synaptosome viability, synaptosomes (either fresh or thawed from cryogenic-freezing, described in section 3.2.5.10) were treated with the viability marker calcein-AM (2 μM) for 20 minutes in darkness (R/T), and fluorescence was measured via flow cytometry, again using the 'fluorescence gate-shift' method.

3.2.6. Phagocytosis experiments

All phagocytosis experiments were analysed via flow cytometry in terms of fluorescence-change of cellular events (Figure 3.2). During data analysis, phagocytic cells were gated (Figure 3.2A) and phagocytosis was measured in terms of either i) 'fluorescence gate-shift'; or ii) 'mean fluorescence shift' in the FL3 channel (488/ 670 nm). For the 'fluorescence gate-shift' method (Figure 3.2B), the 'fluorescence-positive' gate was generated (in FSC-A/ FL3-A) around the event population of untreated microglia, such that 1% of events in this population were located within the gate. For the 'mean fluorescence shift' method (Figure 3.2C), auto-fluorescence of cells (measured in RFU) was quantified from untreated microglia (Figure 3.2D) and deducted from mean fluorescence readings from treated microglia, thus providing the mean fluorescence change (RFU) due to phagocytosis (Figure 3.2E). All phagocytic targets - i.e. *E. coli*¸ synaptosomes, *E. coli* bioparticles and beads – were substantially smaller than all phagocytic cells tested, meaning no ambiguity in event-cloud assignment in FSC-A/SSC-A.

3.2.6.1. *Phagocytosis of* E. coli

Phagocytosis of *E. coli* by BV-2 microglia, primary mouse microglia, primary rat microglia and U937 monocyte cells were measured. BV-2 microglia were plated as described in 3.2.1.1, primary mouse microglia as described in 3.2.2.2, primary rat microglia as described in 3.2.2.2, and U937 monocytes as described in 3.2.1.3. *E. coli* were grown overnight in LB media as described[623], and then heat inactivated at 65°C for 15 minutes before spinning down (6,000 RCF, 5 minutes) on a benchtop centrifuge (Eppendorf). Pellets were resuspended in PBS and cell density was measured via absorbance at OD_{600} using a BioPhotometer D30 (Eppendorf). Bacteria were then diluted to OD_{600} ~1.3; depending on the experimental requirement, an appropriate volume was stained with pHrodo Red succinimidyl-ester (10 μM) for 15 minutes at 37°C in darkness. pHrodo-conjugated *E. coli* were then washed with 3

spin-resuspension cycles in PBS, before finally resuspending in PBS. PHrodo-conjugated *E. coli* were added directly to cells and co-cultures were incubated for 60 minutes (37°C, 5% CO_2), unless otherwise stated. After 60 minutes, microglia or PMA-differentiated U937 monocytes were washed with PBS and incubated with PBS containing 0.05% trypsin for 10 minutes at 37°C, before trypsin was quenched with 2 parts DMEM containing 10% FBS. Suspended samples were then spun down (150 RCF, 5 minutes), resuspended in PBS and retained on ice until analysis. For undifferentiated U937 monocytes, the suspension cells were washed in PBS via 3 spin-resuspension cycles (150 RCF, 5 minutes), before final resuspension in PBS. Cells were retained on ice until analysis via flow cytometry.

3.2.6.2. Phagocytosis of synaptosomes

Phagocytosis of synaptosomes by BV-2 microglia, primary mouse microglia and primary rat microglia were measured. BV-2 microglia were plated as described in 3.2.1.1, primary mouse microglia as described in 3.2.2.2, and primary rat microglia as described in 3.2.2.2. Synaptosomes were thawed in warmed, CO_2-infused HBK buffer from cryogenically frozen stocks. Synaptosomes were spun down (20,000 RCF, 5 minutes), resuspended in warmed HBK buffer and stained with pHrodo Red succinimidyl-ester (10 μM) for 15 minutes in darkness (37°C). pHrodo-conjugated *E. coli* were then washed with 3 spin-resuspension cycles before finally resuspending in HBK buffer. pHrodo-conjugated synaptosomes were added directly to cells and co-cultures were incubated for 60 minutes (37°C, 5% CO_2), unless otherwise stated. After 60 minutes, microglia were washed with PBS and incubated with PBS containing 0.05% trypsin for 10 minutes at 37°C, before trypsin was quenched with 2 parts DMEM containing 10% FBS. Suspended samples were then spun down (150 RCF, 5 minutes), resuspended in PBS and retained on ice until analysis via flow cytometry.

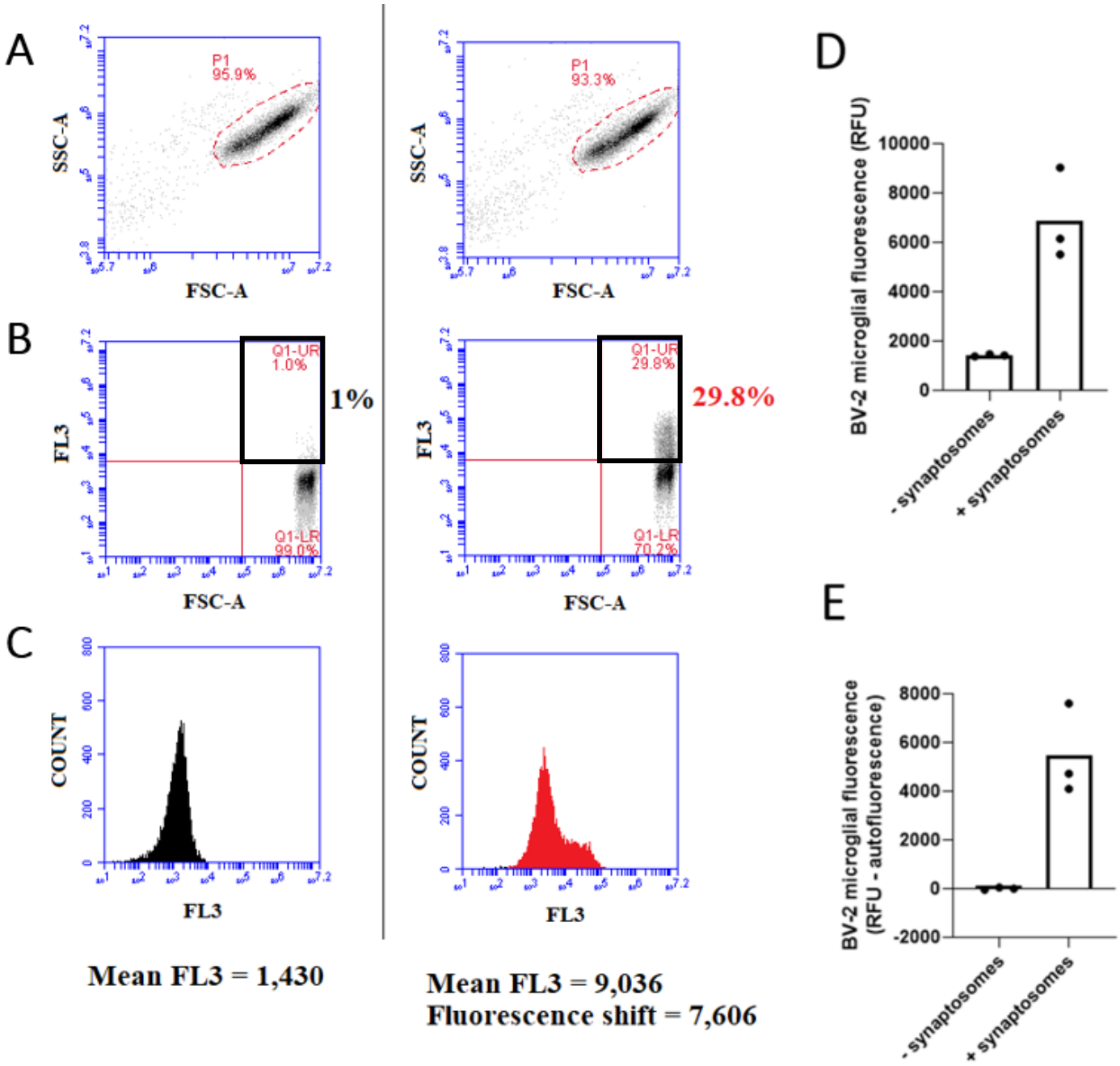

Figure 3.2. Example analysis of microglial phagocytosis data obtained via flow cytometry using Accuri C6 software. (A) The event cloud representing microglial events is identified via forward-scatter (FSC-A)/ side-scatter (SSC-A). Gated events are then analysed for changes in red fluorescence (FL3), in terms of either (B) 'fluorescence gate-shift' (i.e. the percentage of microglial events that migrate into a fluorescence-positive gate, generated manually based on the 'microglia alone' cloud which is arbitrarily set at 1%), or (C) 'mean fluorescence shift' (i.e. the change in mean fluorescence of the microglial population relative to the 'microglia alone' population). Fluorescence values (RFU) are combined with replicates to generate an average (D). To provide a fluorescence reading representative of the *change* in cell fluorescence due to phagocytosis, auto-fluorescence values (obtained from the 'microglia alone' population) are deducted from all fluorescence readings (E).

3.2.6.3. Phagocytosis of E. coli *bioparticles*

pHrodo Red *E. coli* Bioparticles (ThermoFisher) were prepared according to manufacturer instructions. Bioparticles were suspended in PBS and sonicated on ice for a cumulative 5 minutes (5 seconds on/off, with a 10 second gap after each minute to allow cooling of sample). Bioparticles were then spun down for 10 minutes (20,000 RCF, R/T) before final resuspension in PBS. Bioparticles were added directly to U937s plated at 2.0 x 10^4/ 200 µl/ well (96 well-plate format) unless otherwise stated. After 60 minutes incubation (37°C, 5% CO_2) cells were washed in PBS via 3 spin-resuspension cycles (150 RCF, 5 minutes), before final resuspension in PBS. Cells were retained on ice until analysis via flow cytometry.

3.2.6.4. Phagocytosis of beads

Phagocytosis of beads by U937 monocytes was measured. U937 monocytes were plated at 5.0 x 10^4/ 500 µl/ well (24 well-plate format), and 1 µm beads (ThermoFisher) were added at densities of 1.0 x 10^6 beads/ 500 µl and incubated for 60, 120 or 180 minutes (37°C, 5% CO_2). Cells were then washed in PBS via 3 spin-resuspension cycles (150 RCF, 5 minutes), before final resuspension in PBS. Cells were retained on ice until analysis via flow cytometry.

3.2.7. Statistical analyses

All statistical analyses described in this thesis were performed using GraphPad Prism version 8. All results described herein represent mean values averaged from at least 3 independent experiments. For experiments involving primary cell-culture, biological independence was ensured by performing experiments from different animals or groups of animals. In all cases, error bars indicate standard error of the mean (SEM). All data was analysed using one- or two-way ANOVA and post-hoc Tukey's or Sidak's multiple comparison tests, as appropriate, except for data comparing just two conditions, which was analysed by Student's t-test. P-values < 0.05 were considered statistically significant.

CHAPTER IV

OPSONISATION OF BACTERIA FOR MICROGLIAL PHAGOCYTOSIS

4.1. Introduction

As described in Chapter 2, bacteria can enter the brain in both healthy and immunocompromised individuals, and bacterial infections of the brain (including meningitis, meningoencephalitis, encephalitis and brain abscess) can be fatal. Microglia, the brain-resident macrophage, play a vital immune role in protecting the brain against pathogenic bacteria. Such protection is mediated by i) PRR recognition of PAMPs (and DAMPs) that circulate during infection, leading to inflammatory activation (M1 polarisation) of the microglia; ii) release of inflammatory cytokines and chemokines to stimulate and perpetuate the immune response; and iii) direct elimination of the invading bacteria, through release of bacteriolytic factors such as complement, or through phagocytosis[624]. A primary means by which microglial phagocytosis of bacteria is facilitated is via bacterial opsonisation (see section 1.4.1.3) - in which host-released opsonins such as antibodies and complement components tag the bacteria for receptor-mediated phagocytosis by the microglia[124]. However, little is known about how bacteria are opsonised for microglial phagocytosis within the unique environment of the brain parenchyma. In this chapter, novel roles for four proteins - calreticulin, galectin-3, apolipoprotein E and β-amyloid - in opsonising bacterial *E. coli* for microglial phagocytosis are described.

Calreticulin (see section 1.4.1.2.2) is a lectin (carbohydrate-binding protein) normally contained within the endoplasmic reticulum where it functions as a molecular chaperone, binding terminal glucose residues on developing glycan chains and thus facilitating protein glycosylation and folding[134]. However, calreticulin has been shown to translocate from the endoplasmic reticulum to the cell surface during apoptosis, or in conditions of endoplasmic reticulum stress. When exposed, calreticulin can act as an 'eat-me' signal to resident macrophages by binding the phagocytic receptor LRP1[473,136,137,476,139]. Calreticulin is a soluble protein; indeed, the calreticulin (CALR) gene can be alternatively spliced to generate the

isoform calnexin, which differs from calreticulin by the presence of a functional membrane-tethering domain[625]. Thus, calreticulin at the surface likely also circulates into the extracellular space. Furthermore, calreticulin is known to bind bacterial LPS[626], meaning extracellular calreticulin may tag bacteria and opsonise them for phagocytosis, but this has not been reported. Calreticulin exposed to the extracellular space may also act as a DAMP to activate immune cells[627], although contradictory findings[628] make this unclear, and it is not known whether released calreticulin can activate microglia.

Galectin-3 (see section 1.4.1.3.8) is also a lectin expressed and released by macrophages, including microglia[629,213,630,212]. Galectin-3 binds with high affinity to N-acetyl-lactosamine - a disaccharide of N-acetyl-glucosamine and galactose - present in glycan chains of proteins and also in gangliosides[213,214]. Binding to N-acetyl-lactosamine can induce oligomerisation of galectin-3 via its N-terminal domain, thus permitting cross-linking of glycoproteins and gangliosides[213,214]. Such cross-linking activity has been implicated in the opsonisation of targets for phagocytosis, such as phagocytosis of apoptotic neutrophils by monocyte-derived macrophages[215]. Galectin-3 is known to signal via the phagocytic receptor MerTK[216], and galectin-3 enhances microglial phagocytosis of neurons, which is inhibited by blocking MerTK[212]. Galectin-3 is upregulated in a variety of immune and non-immune cells after exposure to microbial stimuli and during bacterial infection, and has been described as a DAMP, as it can induce inflammatory activation of immune cells[211]. Like calreticulin, galectin-3 can bind bacterial LPS[631]. However, it is not clear whether such binding facilitates opsonisation of LPS-exposing bacteria by phagocytes.

ApoE is a lipoprotein known to be fundamental to lipid homeostasis, in the CNS and throughout the mammalian system. Extracellular apoE mediates lipid transport between cells, delivering lipids to cells via interactions with surface-exposed apoE receptors of the low-density lipoprotein (LDL) family[632]. However, apoE has also been implicated in immune responses. In the brain and during normal homeostasis, apoE is expressed and secreted by astrocytes[633] and microglia[634,635], but also in neurons during pathology[632,636]. In the mouse hippocampus, ApoE is upregulated by intracerebral injection with LPS[637], suggesting that apoE may also exist extracellularly during bacterial infection of the brain. ApoE can bind TREM2, a pro-phagocytic receptor expressed by microglia (see section 2.3.1.8)[638]. It is known that apoE

can also bind LPS[639], but it is unknown whether apoE binding to bacteria can opsonise the bacteria for phagocytosis by phagocytes such as microglia, or whether such effects are influenced by apoE isoform. 3 isoforms of apoE exist in humans – ε2, ε3 and ε4 – and apoE isoforms are heavily linked to familial Alzheimer's disease (AD): ε4 is associated with increased risk, whilst ε2 is associated with reduced risk[640].

β-amyloid is best known for its ability to oligomerise and aggregate into amyloid plaques, which are a defining hallmark of AD. However, the role of β-amyloid in normal physiology is not clear, although its importance is implied by high sequence conservation throughout vertebrate evolution[641]. Recently, it has been suggested that β-amyloid may have a role in innate immune defense against foreign pathogens[641,642]. β-amyloid is produced by immune cells - including astrocytes and microglia in the brain[643] - and LPS-induced inflammation of the mouse brain is associated with increased expression of the amyloid precursor protein (APP) and generation of β-amyloid[644]. Multiple lines of evidence have ascribed anti-microbial properties to β-amyloid, and postulated anti-microbial mechanisms of β-amyloid include i) involvement in nucleotide extracellular traps (NETs) to physically trap circulating pathogens and aid their removal by immune cells; and ii) penetration of the bacterial membrane to lyse the cell[642]. Like apoE, β-amyloid can bind the pro-phagocytic microglial receptor TREM2[498]. Soluble β-amyloid oligomers can also bind the gram-negative bacteria *Salmonella typhimurium* and the pathogenic fungus *Candida albicans*[645]. However, it is not known whether binding can opsonise these pathogens for phagocytosis by immune cells, and if so, whether such binding and/or opsonisation is influenced by the oligomerisation status of the protein.

In this chapter, I demonstrate novel roles for calreticulin, galectin-3, apoE (isoform ε2) and monomeric β-amyloid in the phagocytosis of *E. coli* by BV-2 and/or primary rat microglia. All proteins could bind bacteria, and such binding opsonised the bacteria for microglial phagocytosis *in vitro*. For calreticulin, bacterial opsonisation was inhibitable by adding sucrose or by blocking the calreticulin receptor LRP1 with RAP. For galectin-3, opsonisation was inhibitable by blocking the galectin-3 receptor MerTK with UNC2881 or UNC569. Inflammatory activation of the microglia with LPS induced upregulation and extracellular release of calreticulin and galectin-3, and also enhanced microglial phagocytosis of the bacteria. LPS-induced phagocytosis was inhibitable by sucrose, an anti-calreticulin antibody,

RAP, UNC2881, UNC569, or simply by removing factors released from the microglia through a media swap, directly implicating microglial-released calreticulin and galectin-3 in this LPS-induced phagocytosis. Furthermore, exogenous calreticulin induced microglial release of the inflammatory cytokine IL-6, and also enhanced microglial phagocytosis of bacteria after chronic exposure, indicating that extracellular calreticulin has immunomodulatory properties. Interestingly, calreticulin was not able to opsonise *E. coli* or *E. coli* bioparticles for phagocytosis by the human monocyte cell line U937, or by macrophages derived from the monocytes after differentiation by phorbol 12-myristate 13-acetate (PMA), suggesting that calreticulin opsonisation of bacteria may be a brain-specific phenomenon. Whilst the ε2 isoform of apoE could bind *E. coli* and opsonise them for microglial phagocytosis, no statistically significant binding or phagocytosis was observed with the ε4 isoform, indicating that such activities may be isoform-dependent. Similarly, monomeric (but not oligomeric) β-amyloid significantly bound *E. coli* and opsonised them for phagocytosis by BV-2 microglia. Together, these findings provide novel insights into how microglia phagocytose (and so eliminate) bacteria, and have implications for bacterial removal by peripheral macrophages generally.

4.2. Results

Please note that data presented in this chapter has been published by Cockram et al[124].

4.2.1. LPS-activated microglia upregulate and release calreticulin and galectin-3

At the start of this study, calreticulin was known to function as both an ‘eat-me’ signal and as a phagocytic co-receptor, but it was not clear whether it could also function as an opsonin, which would require that it could be secreted by cells (normally inflammatory-activated immune cells) into the extracellular space. To test whether microglia secrete calreticulin – and whether any secretion could be induced by inflammatory-activating the microglia - microglial BV-2 cells were treated with various inflammatory stimuli including LPS (100 ng/ml), β-amyloid (2.5 μM) and TNF-α (50 ng/ml), for 3 or 24 hours, before extracting the supernatants and measuring calreticulin levels via ELISA (Figure 4.1A). No significant levels of calreticulin

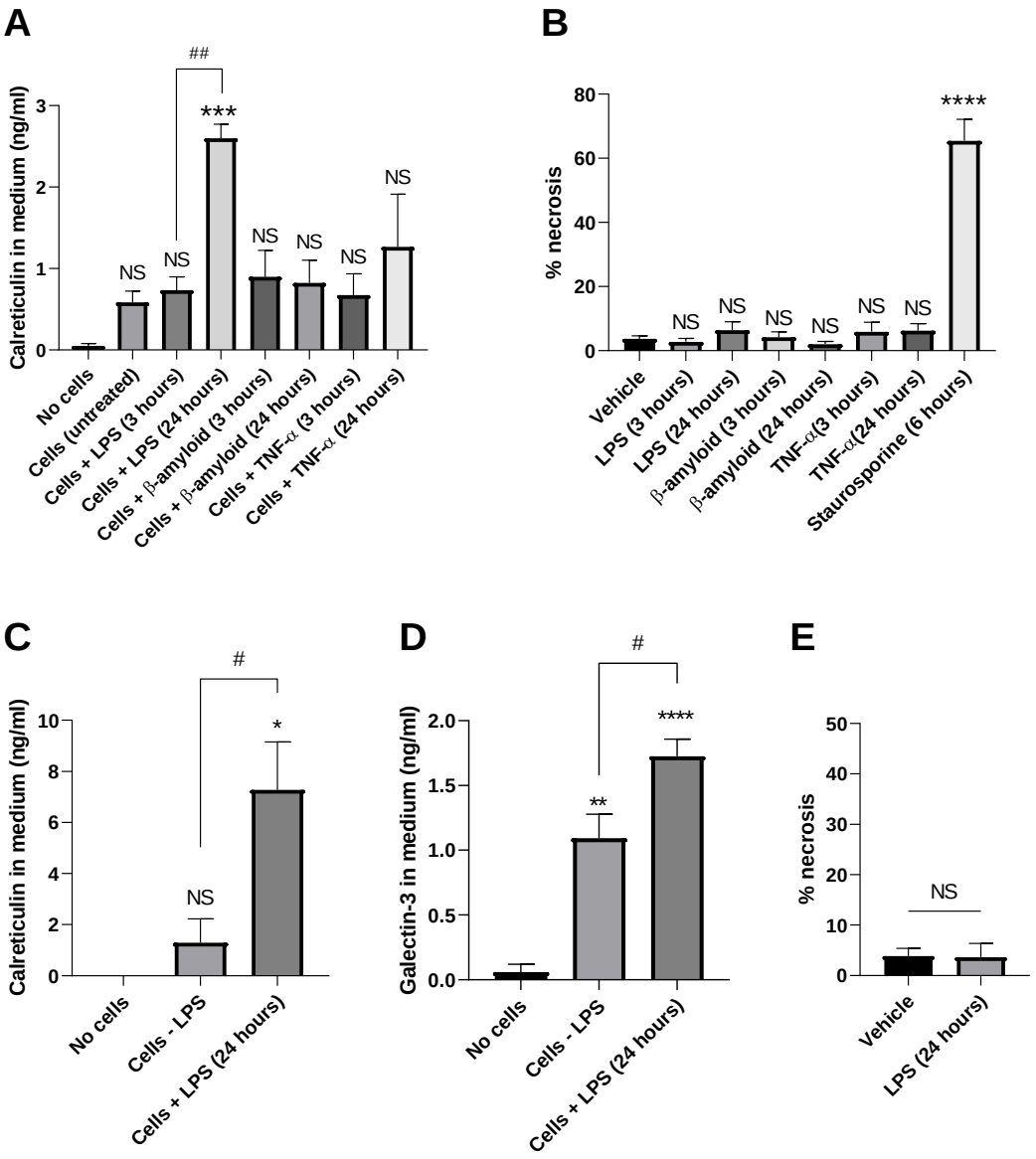

Figure 4.1. LPS-activated microglial release extracellular calreticulin and galectin-3. (A) BV-2 microglia were treated with vehicle or LPS (100 ng/ml), β-amyloid (2.5 μM) or TNF-α (50 ng/ml) for 3 or 24 hours. Cells-conditioned supernatant was tested for calreticulin protein presence via ELISA and compared with the 'no cells' control. (B) BV-2 viability was not affected by any treatements applied, as determined by the percentage of cells stained with propidium iodide and compared to the 'vehicle' control. Staurosporine (10 μM) was used as a positive control for cell death. (C & D) Primary microglia from mice were treated with vehicle or LPS (100 ng/ ml) for 24 hours. Cell-conditioned supernatant was tested for calreticulin protein (C) or galectin-3 (D) presence via ELISA and compared with the 'no cells' control. (E) Primary microglial viability was not affected by the same LPS treatment, as determined by propidium iodide staining. Statistical comparisons were made via one-way ANOVA except for E, which was via Student's t-test, with comparisons versus 'no cells' (A, C & D) or 'vehicle' controls (B & E). Values are means ± SEM of at least 3 independent experiments. NS p=0.05, *p<0.05, **p<0.01, ***p<0.001, ****p<0.0001 versus controls; #p<0.05, ##p<0.01.

were detected in culture medium conditioned with vehicle-treated BV-2 cells compared to medium with 'no cells' (p=0.946), indicating that calreticulin is not released by microglia without stimulation. 24 hours (but not 3 hours) of treatment with LPS was found to induce substantial calreticulin release into the media (2.60 ng/ml ± 0.17), which was significantly greater than from vehicle-treated cells (p=0.007). Neither β-amyloid nor TNF-α were found to

induce detectable calreticulin release after either 3 or 24 hours. To exclude the possibility that the cells might be leaking calreticulin due to treatment-induced necrosis, cells were stained with propidium iodide (a marker for necrotic cells) and quantified via flow cytometry. No significant increase in necrosis due to LPS (or any other) treatments were observed (Figure 4.1B), indicating that LPS-induced secretion of calreticulin is regulated.

To determine whether this result could be replicated using primary cells (considered more physiologically relevant), primary microglia were cultured from mice and treated ± LPS as before. As with BV-2s, no significant calreticulin was detected in medium from vehicle-treated microglia compared to the 'no cells' control ($p=0.741$, Figure 4.1C). LPS treatment for 24 hours induced a substantial release of calreticulin into the media (7.28 ± 1.87 ng/ml) which was significantly greater than that from vehicle-treated cells ($p=0.030$).

Galectin-3 has been reported to be released from blood-marrow macrophages, and also from BV-2 microglia inflammatory-activated by LPS[646,630,212]. To test whether this could be replicated using primary microglial cells, primary mouse microglia were treated ± LPS as before. Unlike with calreticulin, vehicle-treated microglia were found to release significant levels of galectin-3 into the medium (1.09 ± 0.185 ng/ml, $p=0.001$), which was further increased by 24 hours treatment with LPS (1.73 ± 0.13 ng/ml, $p=0.023$) (Figure 4.1D). Again, a viability assay was performed to determine whether necrotic leakage may have contributed to such release – no significant necrosis was observed after the LPS treatment (Figure 4.1E). Thus, inflammatory activation of microglia (both BV-2 and primary cells) by LPS triggers extracellular release of calreticulin and galectin-3.

To test whether LPS affected expression of either calreticulin or galectin-3, RNA was isolated from BV-2 cells treated with LPS (100 ng/ml) for 3, 24 or 48 hours (and also with fibrillar β-amyloid (250 nM)) for 24 hours, and RNA was measured by qPCR. An inflammatory-activated transcription profile was confirmed by measuring IL-6 mRNA, which increased substantially after 24-hours treatment with LPS compared to the 'vehicle' control ($p=0.001$; Figure 4.2A).

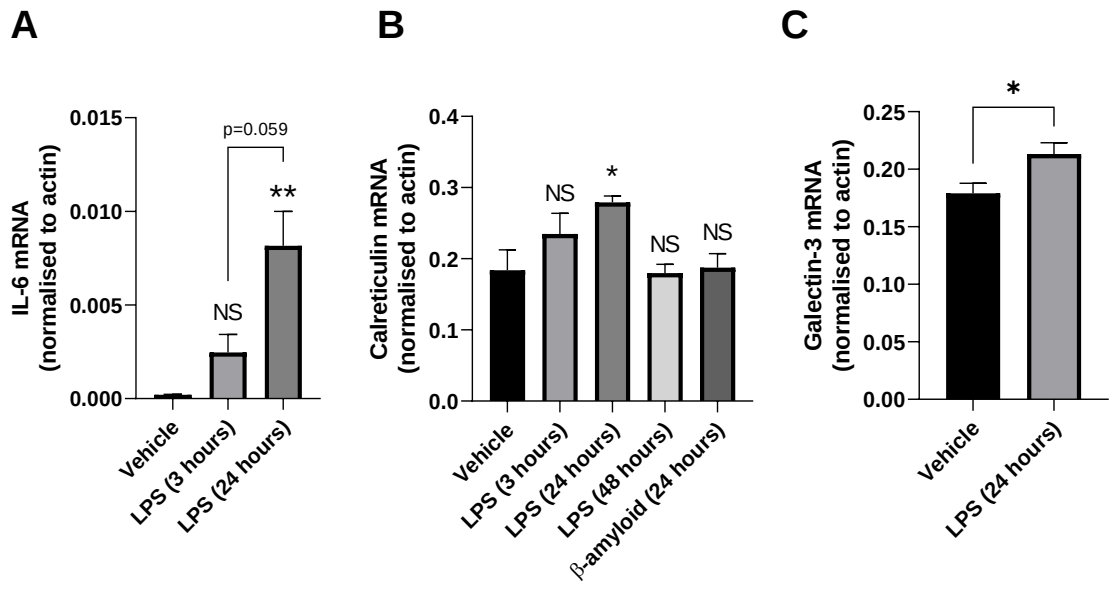

Figure 4.2. LPS-activated microglia upregulate calreticulin and galectin-3. (A) IL-6 mRNA was quantified in BV-2s treated with vehicle or LPS (100 ng/ml) for 3 or 24 hours. Expression was normalised to actin mRNA. (B) Calreticulin mRNA was quantified in BV-2 cells treated with vehicle, LPS (100 ng/ml) or fibrillar β-amyloid (250 nM). (C) Galectin-3 mRNA was quantified in BV-2s treated with vehicle or LPS (100 ng/ml). Statistical comparisons were made via one-way ANOVA except for C, which was by Student's t-test. Values are means ± SEM of at least 3 independent experiments. NS $p \geq 0.05$, *$p < 0.05$, **$p < 0.01$ versus 'vehicle' controls.

LPS increased calreticulin mRNA by 28% (± 16) after 3 hours (p=0.438 versus 'vehicle' control), reaching 52% (± 6) after 24-hours (p=0.021) before returning to control levels after 48 hours (p=0.999) (Figure 4.2B). No effect on calreticulin expression was detected after treatment with fibrillar β-amyloid (p>0.999). LPS also increased galectin-3 mRNA by 19% (± 5) compared to vehicle (p=0.032; Figure 4.2C). Taken together, these data demonstrate that microglia inflammatory activated with LPS upregulate and release calreticulin and galectin-3 into the extracellular space.

4.2.2. Calreticulin opsonises *E. coli* for phagocytosis by microglia

To investigate a potential opsonisation role for these proteins in terms of microglial phagocytosis of bacteria, a phagocytosis assay was developed by labelling *E. coli* with the fluorophore pHrodo-SE (10 μM) – a compound that fluoresces exclusively in acidic environments such as the phagolysosome, and is a commonly used marker for phagocytosis[647]. Labelled bacteria were incubated with BV-2 microglia for 60, 120 or 180 minutes in low-serum medium (DMEM + 0.5% FBS), and phagocytosis was measured by flow cytometry, depicted schematically in Figure 4.3A. Phagocytosis was quantified in terms

A

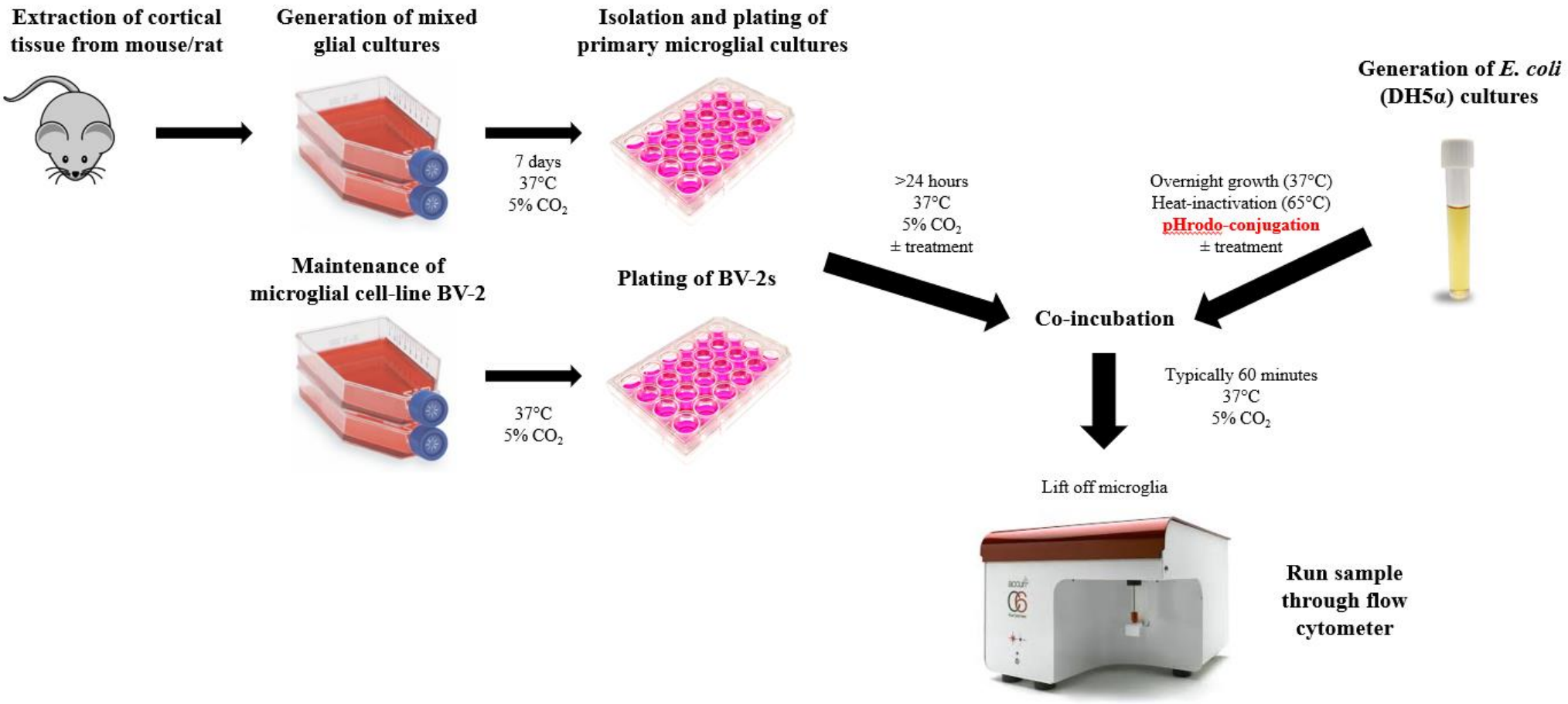
Extraction of cortical tissue from mouse/rat
Generation of mixed glial cultures
Isolation and plating of primary microglial cultures
7 days
37°C
5% CO2
Generation of E. coli (DH5α) cultures
Maintenance of microglial cell-line BV-2
Plating of BV-2s
37°C
5% CO2
>24 hours
37°C
5% CO2
± treatment
Overnight growth (37°C)
Heat-inactivation (65°C)
pHrodo-conjugation
± treatment
Co-incubation
Typically 60 minutes
37°C
5% CO2
Lift off microglia
Run sample through flow cytometer

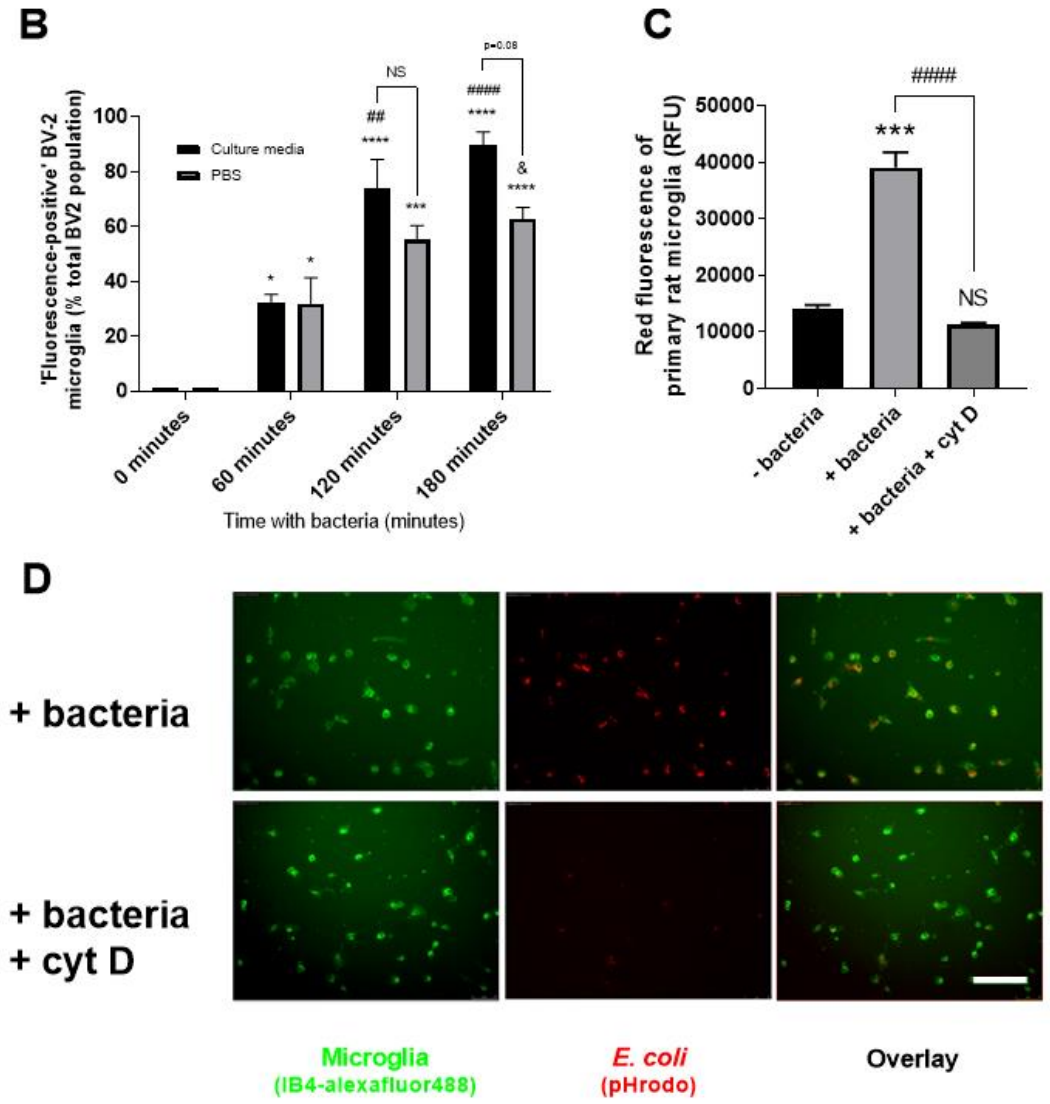

Figure 4.3. BV-2 and primary rat microglia rapidly phagocytose *E. coli in vitro*. (A) Schematic workflow for assaying microglial phagocytosis of bacteria. Primary microglia from mouse/rat or BV-2 microglia were cultured and co-incubated with pHrodo-labelled *E. coli*; phagocytosis was quantified via flow cytometry. (B) BV-2 microglia phagocytose pHrodo-conjugated *E. coli* to significant levels within 60 minutes in both PBS and culture media, compared to the '0 minutes' control. (C & D) Primary rat microglia also phagocytose pHrodo-conjugated *E. coli* over 60 minutes in culture as quantified by flow cytometry and measured by mean fluorescence (RFU) when compared to the '- bacteria' control, which was prevented by cytochalasin D (10 μM) (C); phagocytosis was also visualised by microscopy (D). Scale bar (100 μM). Values are means ± SEM of at least 3 independent experiments. Statistical comparisons were made via one-way ANOVA. NS $p \geq 0.05$, *$p<0.05$, ***$p<0.001$, ****$p<0.0001$ versus '0 minutes' (B) or '- bacteria' (C) controls ; ##$p<0.01$, ####$p<0.0001$ versus '60 minutes (culture media)' condition unless otherwise indicated; &$p<0.05$ versus '60 minutes (PBS)' condition.

of the percentage of microglial events that had shifted into the 'fluorescence-positive' gate (generated using microglia alone) as a percentage of total microglial events (i.e. the 'fluorescence gate-shift' method, as described in section 3.2.6). A linear increase in phagocytosis was observed over the first 120 minutes of incubation, with the percentage of

BV-2s fluorescing red approaching 100% by 180 minutes (Figure 4.3B). Considering future experiments would investigate potential opsonisation roles of calreticulin and galectin-3 – and that components of the serum may have unpredictable effects on any such opsonisation – phagocytosis was also measured with PBS replacing medium. PBS did not affect phagocytosis levels by 60 minutes compared to low-serum ($p>0.999$), but reductions in phagocytosis were observed at 120 minutes ($p=0.392$) and at 180 minutes ($p=0.078$), although these did not reach statistical significance.

Having optimised the assay with BV-2 cells, phagocytosis of pHrodo-conjugated *E. coli* by primary microglia from rat was measured (as primary rat microglia can be obtained in substantially higher yields than primary mouse microglia). Labelled bacteria were incubated with primary rat microglia for 60 minutes as shown (Figure 4.3A) and phagocytosis was quantified by flow cytometry (Figure 4.3C) or visualised by microscopy (Figure 4.3D). Significant levels of phagocytosis were observed after the 60-minute co-incubation, measured here by mean fluorescence changes of the microglial events (see section 3.2.6) and compared to microglia without bacteria ($p<0.001$). Cytochalasin D (10 μM), which inhibits the cytoskeletal remodeling required for phagocytosis[648], completely abolished this fluorescence increase ($p<0.001$; $p=0.528$ versus the '- bacteria' control) - confirming that phagocytosis *per se* was responsible for the fluorescence increase detected.

Calreticulin is a carbohydrate-binding protein that is known to bind lipopolysaccharide (LPS) from gram-negative bacteria[626]. Given that LPS constitutes much of the surface of gram-negative bacteria, it was hypothesised that calreticulin could bind *E. coli* directly. To test this, recombinant calreticulin was labelled with the fluorophore TAMRA-SE (50 μM) and incubated with *E. coli* for 90 minutes, and protein-binding to the bacteria was measured via flow cytometry. In the presence of TAMRA-conjugated calreticulin, bacterial fluorescence was significantly increased ($p=0.047$ versus the '- calreticulin' control; Figure 4.4A). To test whether the carbohydrate-recognition domain of calreticulin may mediate this interaction, sucrose (50 mM) was added and fluorescence was measured: binding by calreticulin was inhibited in the presence of sucrose to levels not significantly different to the '- calreticulin' control ($p=0.302$).

To determine whether calreticulin could opsonise bacteria for phagocytosis by microglia, pHrodo-conjugated *E. coli* were incubated with calreticulin (500 nM) for 90 minutes, washed several times to remove unbound calreticulin (which could interfere with a potential opsonisation effect), and applied to either BV-2 or primary rat microglia. In these cases, data

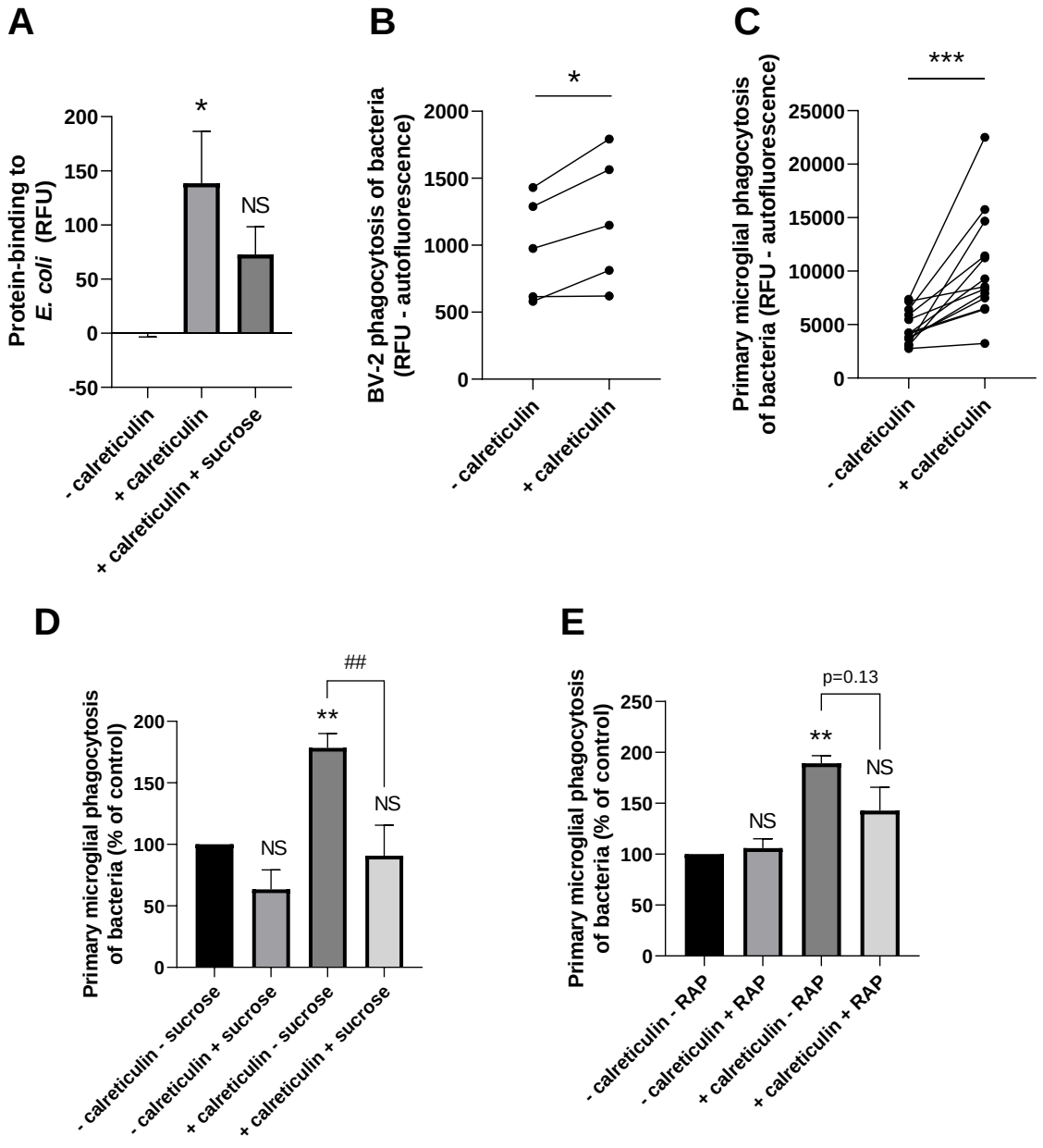

Figure 4.4. Calreticulin binds and opsonises *E. coli* for microglial phagocytosis. (A) TAMRA-conjugated calreticulin (500 nM) binds *E. coli* after 90 minutes co-incubation, measured in terms of relative fluorescence unit increase versus the '- calreticulin' (protein-free) control; no significant binding is observed in the presence of sucrose (50 mM). (B & C) Recombinant calreticulin (500 nM) opsonises *E. coli* for phagocytosis by BV-2 (B) and primary rat microglia (C) when pre-incubated for 90 minutes (and subsequently washed to remove unbound protein). (D & E) Opsonisation of *E. coli* for microglial phagocytosis by recombinant calreticulin is inhibitable by 50 mM sucrose when compared to '- calreticulin – sucrose' control (D) or 500 nM RAP when compared to '– calreticulin – RAP' control (E). Data is normalised to the '- calreticulin - sucrose' and '- calreticulin - RAP' conditions for (D) and (E), respectively. Values are means ± SEM of at least 3 independent experiments. Statistical comparisons were made via one- or two-way ANOVA as appropriate except for B & C, which were by Student's t-test. NS $p \geq 0.05$, **$p<0.01$, ***$p<0.001$ versus controls; ##$p<0.01$ as indicated.

was analysed using the 'mean fluorescence shift method', so fluorescence values shown represent the change in cellular fluorescence due to phagocytosis of fluorescent targets (described in section 3.2.6). Calreticulin opsonised the bacteria for phagocytosis by BV-2 cells by 21 ± 6% compared to the '- calreticulin' control ($p=0.024$; Figure 4.4B), and for phagocytosis by primary rat microglia by 124 ± 29% ($p<0.001$; Figure 4.4C). This opsonisation effect was prevented by 50 mM sucrose ($p=0.004$; Figure 4.4D) - consistent with findings that sucrose inhibited the binding of calreticulin to the bacteria (Figure 4.4A), and indicating that the carbohydrate-recognition domain of calreticulin is required for opsonisation. Sucrose was not found to significantly affect microglial phagocytosis of bacteria in the absence of applied calreticulin ($p=0.323$), which is consistent with no significant release of calreticulin by non-activated microglia shown previously (Figures 4.1A & 4.1C), and suggests that calreticulin can enhance (but is not required for) phagocytosis of bacteria by non-activated microglia. Note that, given high variability between independent experiments, data was normalised internally to the control in each experiment - hence the control with zero variance (this analytical method of normalisation to the untreated control condition is commonly used throughout this thesis, and in all cases is readily apparent by the lack of error bars around the control mean).

Our lab has previously demonstrated that calreticulin on the surface of PC12 cells can promote microglial phagocytosis via the phagocytic receptor LRP1, which is inhibitable with the LRP1-specific ligand RAP[478]. To determine whether applied calreticulin was promoting microglial phagocytosis of bacteria by binding LRP1, RAP was applied to microglia shortly prior to co-incubation with the bacteria. RAP did not inhibit phagocytosis in the absence of exogenous calreticulin, but it inhibited the calreticulin-induced phagocytosis, to levels not significantly greater than the '- calreticulin – RAP' control ($p=0.164$; Figure 4.4E). Taken together, these data suggest that calreticulin opsonises bacteria for microglial phagocytosis, which is achieved by i) binding to bacteria via its carbohydrate-recognition domain, and ii) binding to microglia via LRP1.

4.2.3. Galectin-3 opsonises *E. coli* for phagocytosis by microglia

Given calreticulin can bind and opsonise bacteria for microglial phagocytosis - and both calreticulin and galectin-3 secretion was induced by bacterial LPS - a similar investigation was performed using galectin-3. Galectin-3 is a lectin also known to have binding affinity for bacterial LPS[631], which may be mediated by its carbohydrate-recognition domain(s). Galectin-3 was conjugated with TAMRA-SE as for calreticulin and incubated with heat-inactivated *E. coli* for 90 minutes, with protein-binding measured via flow cytometry as before. The fluorescence of bacteria pre-incubated with TAMRA-galectin-3 was significantly greater than the '- galectin-3' control ($p=0.002$; Figure 4.5A). Galectin-3 binds lactose via a carbohydrate-recognition domain, and lactose can inhibit the ability of galectin-3 to promote phagocytosis of mammalian cells[212]. To test whether the lactose-inhibitable carbohydrate-recognition domain of galectin-3 mediates binding to bacteria, lactose (50 mM) was added alongside TAMRA-galectin-3 and fluorescence of the bacteria was measured. Lactose did not interfere with protein-binding to the bacteria compared to galectin-3 alone ($p=0.759$), and this binding was significantly greater than the '- galectin-3' control ($p=0.001$), indicating that galectin-3 binding to bacteria is mediated via a different mechanism than for binding to mammalian cells.

To test whether galectin-3 can opsonise bacteria for microglial phagocytosis, pHrodo-conjugated *E. coli* were incubated with galectin-3 (20 nM) for 90 minutes and incubated with either BV-2 or primary rat microglia as before. Bacterial phagocytosis by BV-2 cells after galectin-3 preincubation was enhanced by 77 ± 7% compared to the '- galectin-3' control, ($p=0.077$; Figure 4.5B); similarly, bacterial phagocytosis by primary rat microglia was enhanced by 73 ± 15% compared to the control ($p=0.008$; Figure 4.5C). Even though lactose did not interfere with protein-binding to the bacteria, it is known to interfere with the interaction between galectin-3 and microglia[212], and so could still influence galectin-3 opsonisation of the bacteria. Lactose significantly inhibited microglial phagocytosis of bacteria in the absence of exogenous galectin-3 when compared to the '- galectin-3 – lactose' control ($p<0.001$; Figure 4.5D), and also inhibited phagocytosis in the presence of galectin-3 ($p=0.009$); however, significantly more phagocytosis was observed in the '+ galectin-3 + lactose' condition compared to '- galectin-3 + lactose', suggesting that galectin-3 opsonisation of the bacteria may not be affected by lactose.

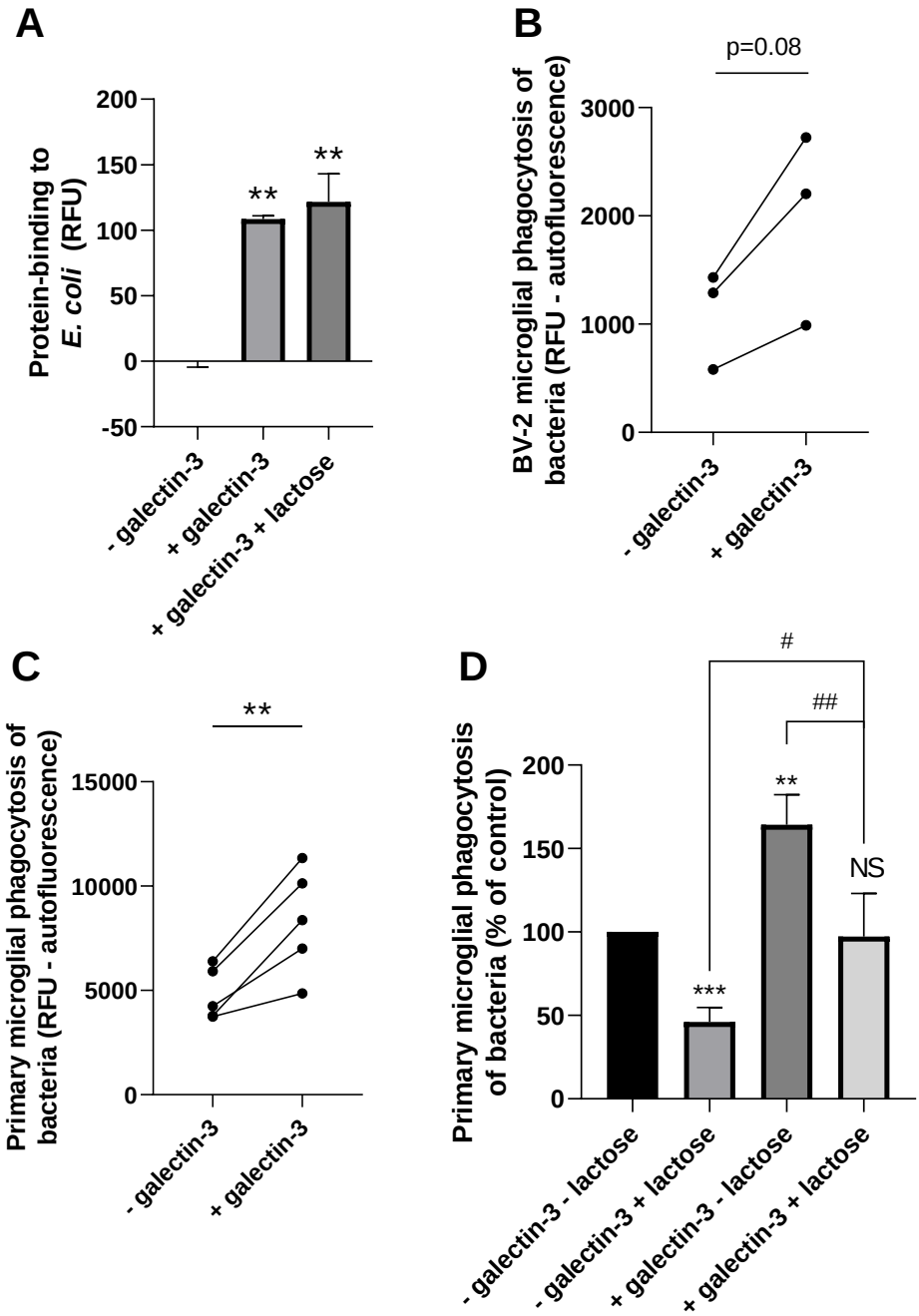

Figure 4.5. Galectin-3 binds and opsonises *E. coli* for microglial phagocytosis. (A) TAMRA-conjugated galectin-3 (20 nM) binds *E. coli* after 90 minutes co-incubation, measured in terms of relative fluorescence unit increase versus the '- galectin-3' (protein-free) control; no reduction in binding was observed in the presence of lactose (50 mM). (B & C) Recombinant galectin-3 (20 nM) opsonises *E. coli* for phagocytosis by BV-2 (B) and primary rat microglia (C) when pre-incubated for 90 minutes (and subsequently washed to remove unbound protein). (D) Microglial phagocytosis of *E. coli* is inhibitable by lactose (50 mM) when compared to '- gal-3 – lactose' control; however, galectin-3 increased phagocytosis even in the presence of lactose. Values are means ± SEM of at least 3 independent experiments. Statistical comparisons were made via one- or two-way ANOVA except for B & C, which were by Student's t-test. NS $p \geq 0.05$, **$p<0.01$, ***$p<0.001$ versus controls; #$p<0.05$, ##$p<0.01$ as indicated.

Galectin-3 has been suggested to opsonise mammalian cells for microglial phagocytosis by bridging between sugars (on the target cell) and the phagocytic receptor MerTK (on the microglia)[212,216]. To determine whether the opsonisation of bacteria by galectin-3 was mediated via microglial MerTK, phagocytosis was measured in the presence or absence of UNC2881, a MerTK-specific inhibitor. In the presence of UNC2881, galectin-3 opsonisation was inhibited to levels not significantly greater than the '- galectin-3 – UNC2881' control (p=0.272; Figure 4.6A), although high variability in the data made it difficult to draw a firm conclusion. To address this, an alternative MerTK inhibitor, UNC569, was used at a higher concentration (5 μM): UNC569 substantially inhibited microglial phagocytosis of bacteria in the absence of applied galectin-3, and also significantly reduced galectin-3-induced

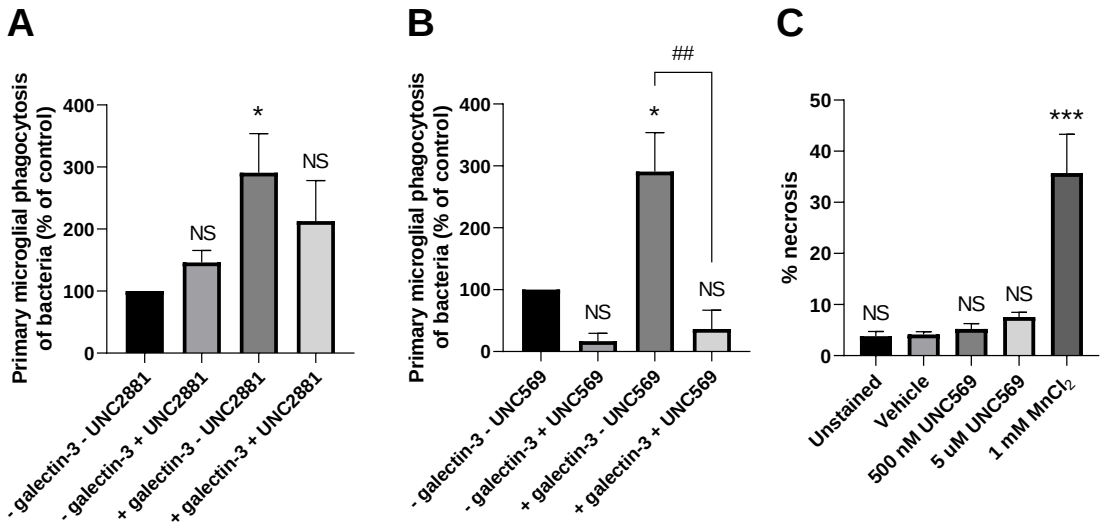

Figure 4.6. Galectin-3 opsonisation of *E. coli* for microglial phagocytosis is inhibited by blocking microglial MerTK. (A & B) Opsonisation of *E. coli* for microglial phagocytosis by recombinant galectin-3 is inhibitable by 200 nM UNC2881 when compared to '- gal-3 – UNC2881' control (A), or 5 μM UNC569 when compared to '– gal-3 – UNC569' control (B). (C) UNC569 was not found to induce necrosis of the microglia, as determined by the percentage of cells stained with propidium iodide and compared to the 'vehicle' control. $MnCl_2$ (1 mM) was used as a positive control for cell death. Values are means ± SEM of at least 3 independent experiments. Statistical comparisons were made via one- or two-way ANOVA. NS $p \geq 0.05$, *$p<0.05$, ***$p<0.001$ versus controls; ##$p<0.01$ as indicated.

phagocytosis to levels not significantly different from the '- galectin-3 + UNC569' control (Figure 4.6B). Moreover, this treatment was not found to kill the cells (Figure 4.6C), indicating that reduced phagocytosis did not simply result from death of the microglia. These findings indicate that i) MerTK is a major phagocytic receptor of microglial phagocytosis of bacteria, and ii) that phagocytosis induced by applied galectin-3 is mediated via microglial MerTK.

4.2.4. LPS-induced microglial phagocytosis of *E. coli* requires extracellular calreticulin and galectin-3

Inflammatory-activation of microglia by LPS is known to enhance their capacity to phagocytose bacteria[396,397]. Since LPS induced the extracellular release of calreticulin and galectin-3 by microglia – and that both proteins could opsonise *E. coli* for microglial phagocytosis – it was hypothesised that these opsonins may be responsible for the enhanced phagocytic capacity of microglia after treatment with LPS. To investigate this, microglia were treated with LPS (100 ng/ml) for 24 hours before co-incubation with *E. coli* for 60 minutes, and phagocytosis was measured via flow cytometry (as before). LPS treatment increased the phagocytosis of bacteria by both BV-2s (479% ± 152; Figure 4.7A) and primary rat microglia (56% ± 22; Figure 4.7B), and both to significant levels ($p=0.005$ each). To test whether this LPS-induced phagocytosis is mediated by components secreted by the microglia into the extracellular space (i.e. opsonins), a media swap was performed immediately prior to bacterial addition, and the effect on phagocytosis was measured (Figure 4.7C). This media swap did not significantly affect phagocytosis of bacteria by untreated microglia, but it significantly reduced phagocytosis by LPS-stimulated microglia ($p=0.015$), to levels not significantly different from the control ($p=0.944$). This indicates that the LPS-induced increase in phagocytosis depends entirely on secreted factors, and is consistent with extracellular opsonins being required for the LPS-induction of phagocytosis.

To test directly whether extracellular calreticulin was mediating the increase in phagocytosis of bacteria induced by LPS, microglia were treated with a function-blocking anti-calreticulin antibody or a serotype control IgG (2 μg/ml each) prior to co-incubation with bacteria, and the effect on LPS-induced phagocytosis was measured. When applied to microglia 3 hours prior to addition of bacteria, the anti-calreticulin antibody significantly inhibited the LPS-induced

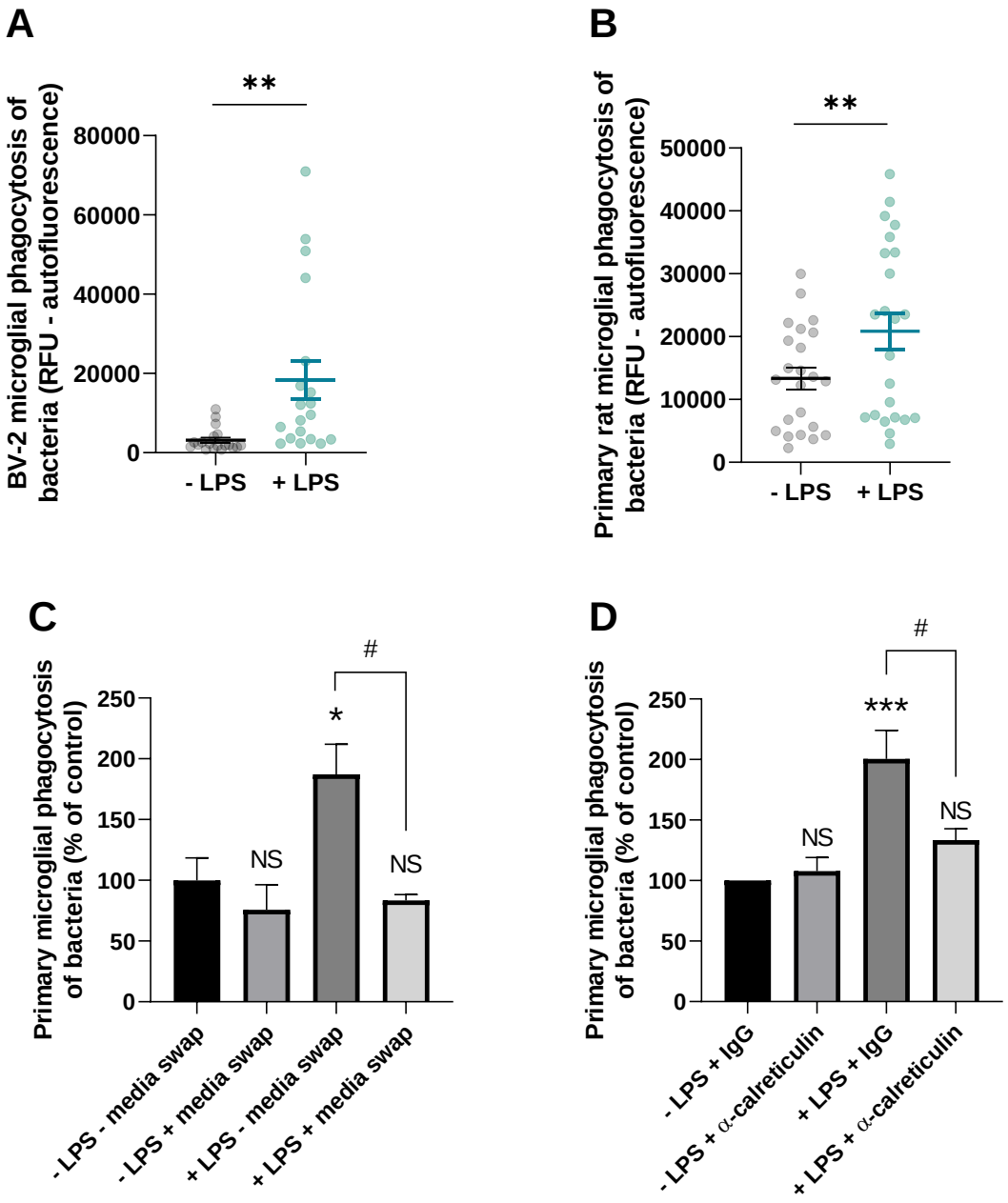

Figure 4.7. LPS-treament of microglia increases their phagocytosis of *E. coli*, and this requires extracellular calreticulin. (A & B) Treatment with LPS (100 ng/ml) for 24 hours increases phagocytosis of *E. coli* by BV-2 (A) and primary rat microglia (B). (C) LPS-induced phagocytosis of *E. coli* by primary microglia is abolished through a simple media swap immediately prior to bacterial addition, when compared to the '- LPS - media swap' control. (D) LPS-induced phagocytosis of *E. coli* by primary microglia is inhibited in the presence of a function-blocking anti-calreticulin antibody, when compared to the '- LPS + IgG' control. Values are means ± SEM of at least 3 independent experiments. Statistical comparisons were made via one- or two-way ANOVA as appropriate except for A & B, which were by Student's t-test. NS $p \geq 0.05$, *$p<0.05$, **$p<0.01$, ***$p<0.001$ versus controls; #$p<0.05$ as indicated.

increase in phagocytosis compared to the serotype control (p=0.029, Figure 4.7D), to levels that were not significantly greater than the '- LPS + IgG' control. No reduction in baseline phagocytosis was observed with the antibody, consistent with the idea that extracellular

calreticulin is not required for phagocytosis by non-activated microglia. Similar experiments using BV-2 microglia identified a similar, although less substantial, reduction in LPS-induced phagocytosis with the same anti-calreticulin antibody (data not shown). Together, these data indicate that the LPS-induced phagocytosis of bacteria requires extracellular calreticulin.

Calreticulin opsonisation of bacteria for microglial phagocytosis was inhibitable by sucrose (Figure 4.4D); whilst lactose inhibited phagocytosis in the presence and absence of exogenous galectin-3 (Figure 4.5D). So, lactose and sucrose were tested for inhibition of LPS induction of phagocytosis. Phagocytosis by BV-2s pretreated ± LPS for 24 hours was significantly inhibited by adding lactose (50 mM) 60 minutes or 25 hours prior to co-incubation with the bacteria ($p<0.001$ each; Figure 4.8A), or by adding sucrose (50 mM) 25 hours prior to the bacteria ($p<0.001$), but not 60 minutes prior ($p=0.649$; $p<0.001$ versus '- LPS – sugar' control). Phagocytosis by primary rat microglia pretreated ± LPS for 24 hours was significantly inhibited

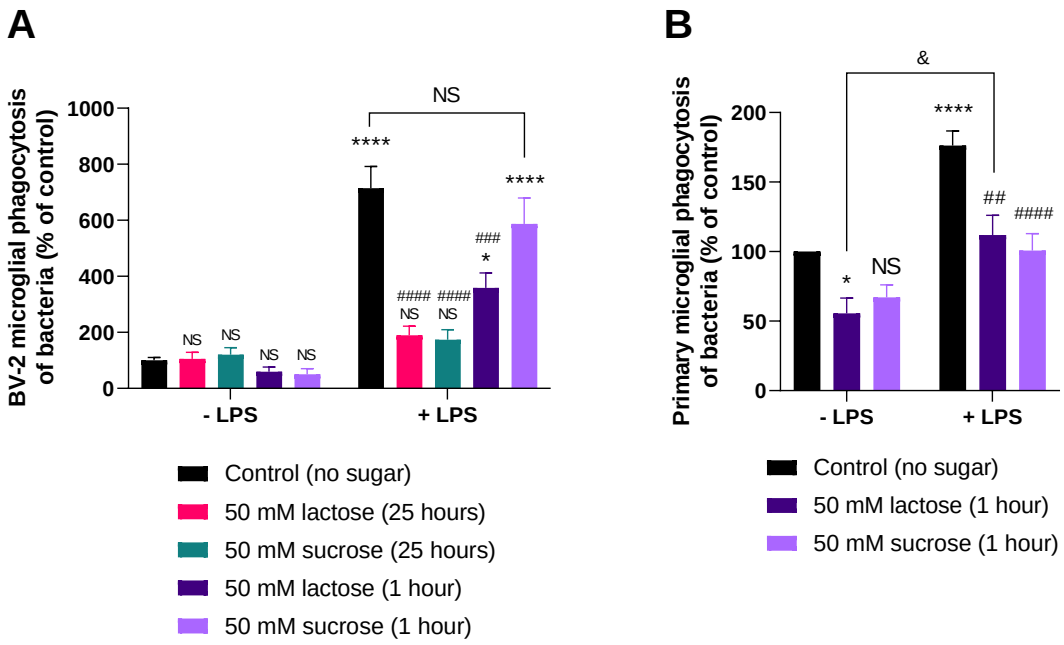

Figure 4.8. LPS-induced microglial phagocytosis of *E. coli* is inhibitable by lactose or sucrose. (A) Treatment with LPS (100 ng/ml) for 24 hours increases phagocytosis of *E. coli* by BV-2 microglia; this induction is inhibitable by application of lactose (50 mM) for 25 or 1 hours, or by application of sucrose (50 mM) for 25 hours prior to bacterial addition, compared to '- LPS control (no sugar)' . (B) Treatment with LPS (100 ng/ml) for 24 hours increases phagocytosis of *E. coli* by primary rat microglia; this induction is inhibitable by application of lactose (50 mM) or sucrose (50 mM) 1 hour prior to bacterial addition, compared to '- LPS control (no sugar)'. Values are means ± SEM of at least 3 independent experiments. Statistical comparisons were made via two-way ANOVA. NS $p\geq0.05$, *$p<0.05$, ****$p<0.0001$ versus controls; ##$p<0.01$, ###$p<0.001$, ####$p<0.0001$ versus '+ LPS control (no sugar)' conditions; &$p<0.05$ as indicated.

by adding lactose (50 mM) 60 minutes prior to the bacteria ($p=0.001$; Figure 4.8B), but also by adding sucrose (50 mM) for the same duration ($p<0.001$).

Given that the LRP1 inhibitor RAP could inhibit calreticulin-induced opsonisation of the *E. coli*, the ability of RAP to inhibit the LPS-induced microglial phagocytosis of bacteria was tested. RAP was observed to significantly inhibit the LPS-induced phagocytosis by primary rat microglia ($p=0.021$; Figure 4.9A). The MerTK inhibitors UNC2881 and UNC569 were also tested for inhibition of LPS-induced bacterial phagocytosis by both BV-2 and primary rat microglia. UNC2881 (200 nM) caused no drop in the LPS-induced phagocytosis by BV-2 microglia when applied to the microglia 60 minutes prior to addition of bacteria ($p=0.903$; $p<0.006$ versus '- LPS – UNC2881' control; Figure 4.9B), but the same treatment significantly inhibited LPS-induced phagocytosis by primary rat microglia ($p=0.027$) to levels not significantly greater than the control ($p=0.363$; Figure 4.9C). UNC569 (500 nM) inhibited LPS-induced phagocytosis by both BV-2s (Figure 4.9D) and primary rat microglia (Figure 4.9E) when applied to the microglia 60 minutes prior to addition of bacteria.

Taken together, these data demonstrate that calreticulin and galectin-3 both opsonise bacteria for phagocytosis by microglia, and indicate that they are required for the LPS-induction of microglial phagocytosis of bacteria, which is mediated by their carbohydrate-recognition domains and the microglial phagocytic receptors LRP1 and MerTK.

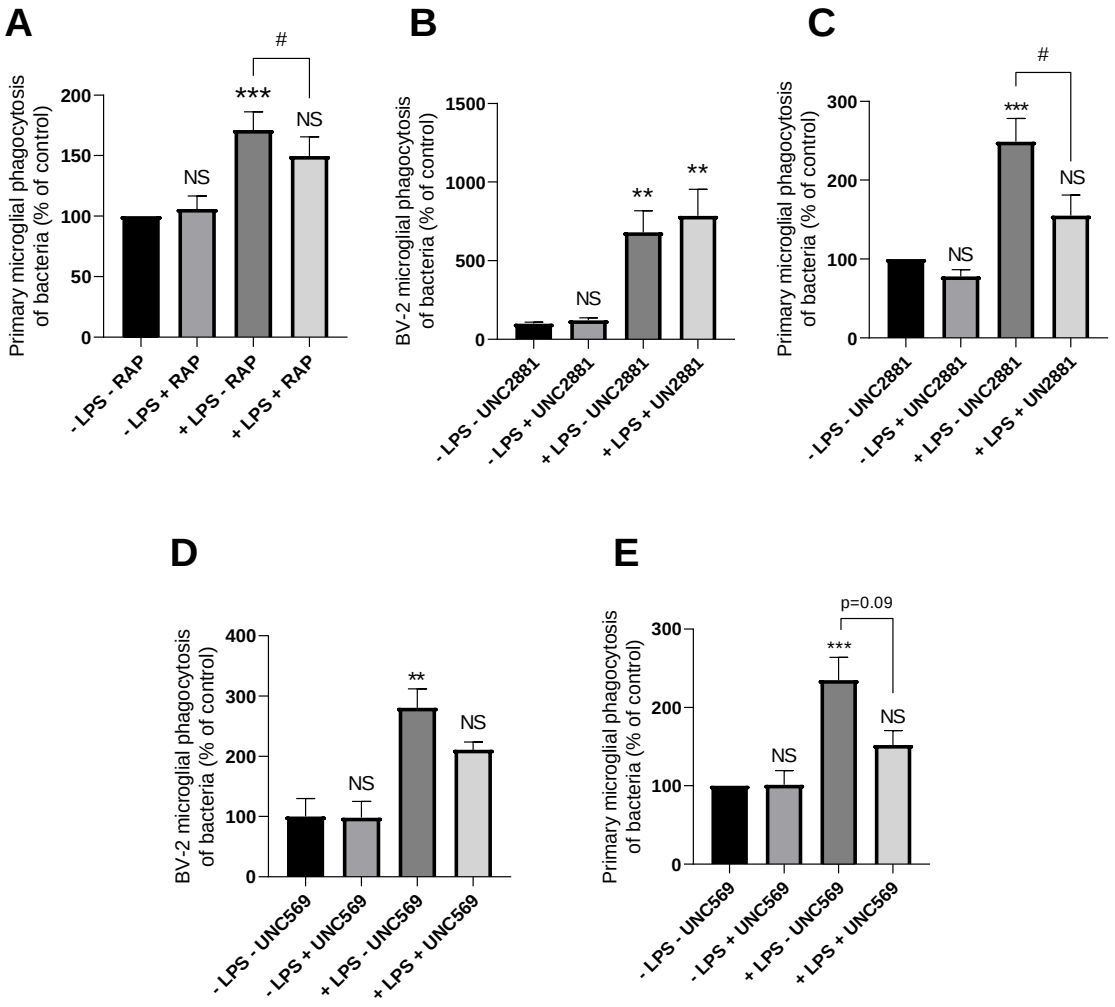

Figure 4.9. LPS-induced microglial phagocytosis of *E. coli* is inhibitable by blocking microglial LRP1 and MerTK . (A) Treatment with LPS (100 ng/ml) for 24 hours increases phagocytosis of *E. coli* by rimary rat microglia; this induction is inhibitable by application of the LRP1 blocker RAP (500 nM) 1 hour prior to bacterial addition, compared to the '- LPS - RAP' control. (B) LPS-induced phagocytosis of *E. coli* by BV-2 microglia is unaffected by application of the MerTK blocker UNC2881 (200 nM) 1 hour prior to bacterial addition, compared to the '- LPS - UNC2881 control'. (C) LPS-induced phagocytosis of *E. coli* by primary rat microglia is inhibited by the same treatment of UNC2881 (200 nM), compared to the '- LPS - UNC2881' control. (D & E) LPS-induced phagocytosis of *E. coli* by BV-2 (D) or primary rat microglia (E) is inhibited by application of the MerTK blocker UNC569 (500 nM) 1 hour prior to bacterial addition, compared to the '- LPS - UNC569' control. Values are means ± SEM of at least 3 independent experiments. Statistical comparisons were made via one- or two-way ANOVA as appropriate. NS p=0.05, **p<0.01, ***p<0.001 versus controls; #p<0.05 as indicated.

4.2.5. Calreticulin does not opsonise bacteria for phagocytosis by U937 cells

Microglia are exclusively brain-resident macrophages. To investigate whether inflammatory-activated immune cells outside the brain may release calreticulin to opsonise bacteria peripherally, the human monocyte cell-line U937 was used. Phagocytosis by U937s was

initially assayed using 1 μm beads, approximately the size of an *E. coli* bacterium (see Figure 6.1): significant levels of bead uptake were detected after 60 minutes ($p<0.001$) compared to the '0 minutes' control (Figure 4.10A). These levels were not enhanced at 120 or 180 minutes, suggesting phagocytic saturation within 60 minutes.

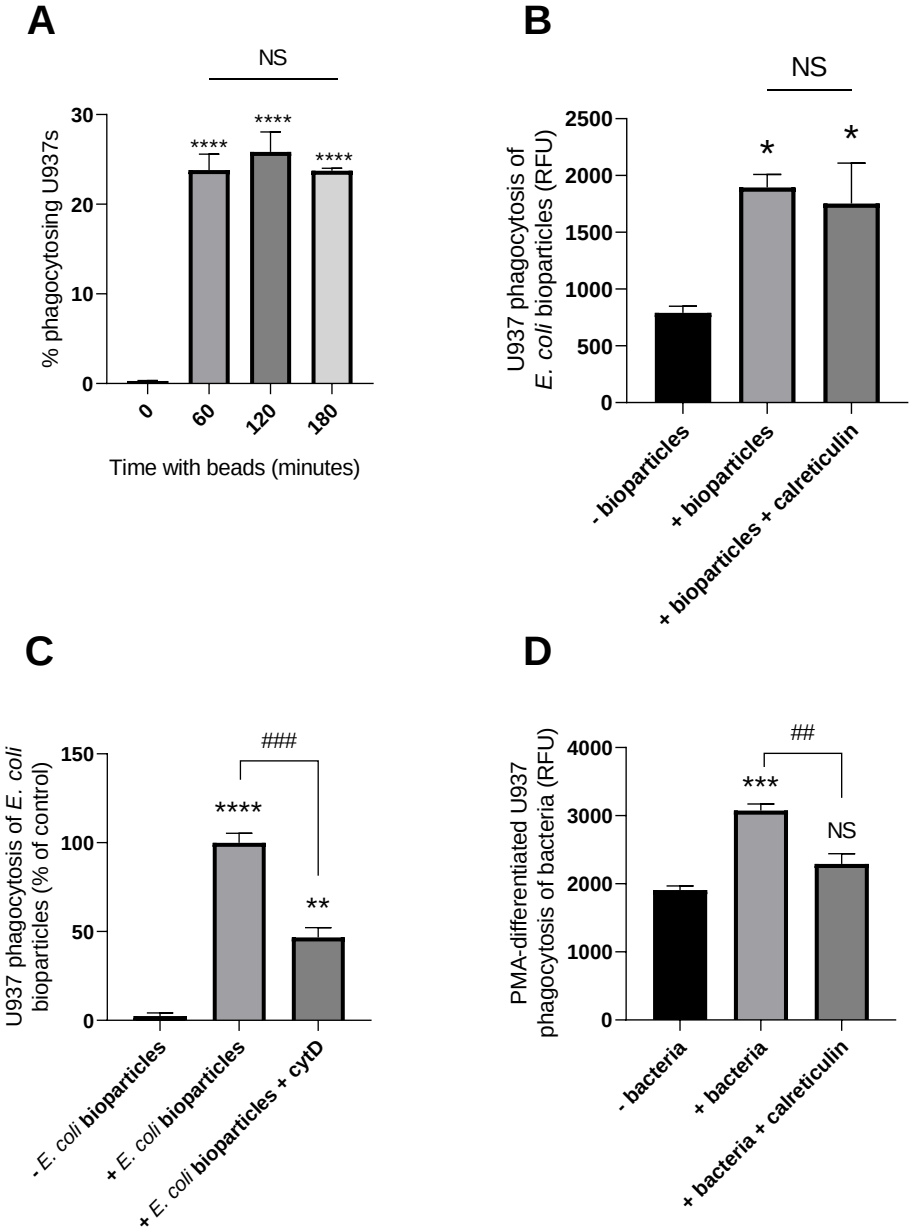

Figure 4.10. U937 phagocytosis of *E. coli* is not enhanced by calreticulin. (A) U937 monocytes detectably phagocytose 1 μm beads within 60 minutes compared to the 0 minutes control, with no further phagocytosis by 180 minutes. (B) U937 monocytes phagocytose *E. coli* bioparticles within 60 minutes compared to the '- bioparticles' control; this is not enhanced by preincubating the bioparticles with calreticulin (500 nM) for 90 minutes. (C) U937 monocyte uptake of *E. coli* bioparticles is only partly inhibited by cytochalasin D (10 μM). (D) PMA-differentiated U937s phagocytose pHrodo-conjugated *E. coli* within 60 minutes, compared to the '- bacteria' control; this is inhibited by preincubating the bioparticles with calreticulin (500 nM) for 90 minutes. Values are means ± SEM of at least 3 independent experiments. Statistical comparisons were made via one-way ANOVA. NS $p\geq0.05$, *$p<0.05$, ***$p<0.001$, ****$p<0.0001$ versus controls; ##$p<0.01$, ###$p<0.001$ as indicated.

To determine whether calreticulin can opsonise bacteria for phagocytosis by U937 cells, pHrodo-conjugated *E. coli* bioparticles were initially used as phagocytic targets and treated with calreticulin as for heat-inactivated *E. coli*. Significant uptake of the bioparticles by U937s was observed by flow cytometry compared to the '- bioparticles' control ($p=0.027$; Figure 4.10B). However, no effect on uptake by preincubation with calreticulin was observed ($p=0.895$, $p=0.047$ versus control). Next, U937 cells were differentiated into monocyte-derived macrophages by dual treatment with PMA and macrophage colony stimulating factor (M-CSF), and bacterial phagocytosis was tested. Cytochalasin D (the phagocytic inhibitor) was unable to completely abolish the fluorescence increase of U937s cultured with *E. coli* bioparticles (Figure 4.10C), so heat-inactivated *E. coli* (as used with the microglia) were used instead. Differentiated U937s phagocytosed significant levels of pHrodo-conjugated *E. coli* over 60 minutes compared to the '- bacteria' control ($p<0.001$; Figure 4.10D). Unexpectedly, preincubation with calreticulin (under the same conditions as those used to opsonise bacteria for microglial phagocytosis) significantly inhibited phagocytosis of the bacteria by differentiated U937s ($p=0.005$, $p=0.105$ versus control). Thus, calreticulin opsonisation of bacteria may be a microglial-specific phenomenon, although this would have to be investigated more extensively. It should also be noted that attempts were made to test whether LPS treatment could trigger extracellular release of calreticulin by undifferentiated U937s – no release was identified, although a lack of response by media from physically-ruptured cells, used as a positive control, made the results impossible to interpret conclusively (data not shown).

4.2.6. Calreticulin induces an 'activated' phenotype in microglia

Given calreticulin was released in conditions of inflammation (i.e. induced by LPS), it may play other important roles extracellularly, for example by provoking an immune response by host immune cells such as microglia. To investigate this, calreticulin was first tested for its ability to induce microglial release of the cytokine IL-6, a marker of an inflammatory-activated phenotype, when applied chronically (i.e. for 24 hours). BV-2 microglia were treated ± LPS (100 ng/ml) or calreticulin (10 µg/ml; Figure 4.11A). Since the recombinant calreticulin used was generated in *E. coli*, polymyxin B (10 U/ml) was added to sequester any contaminating endotoxin which could induce a false-positive response. LPS (100 ng/ml) induced significant IL-6 release from the BV-2s compared to the 'PBS' control ($p<0.001$),

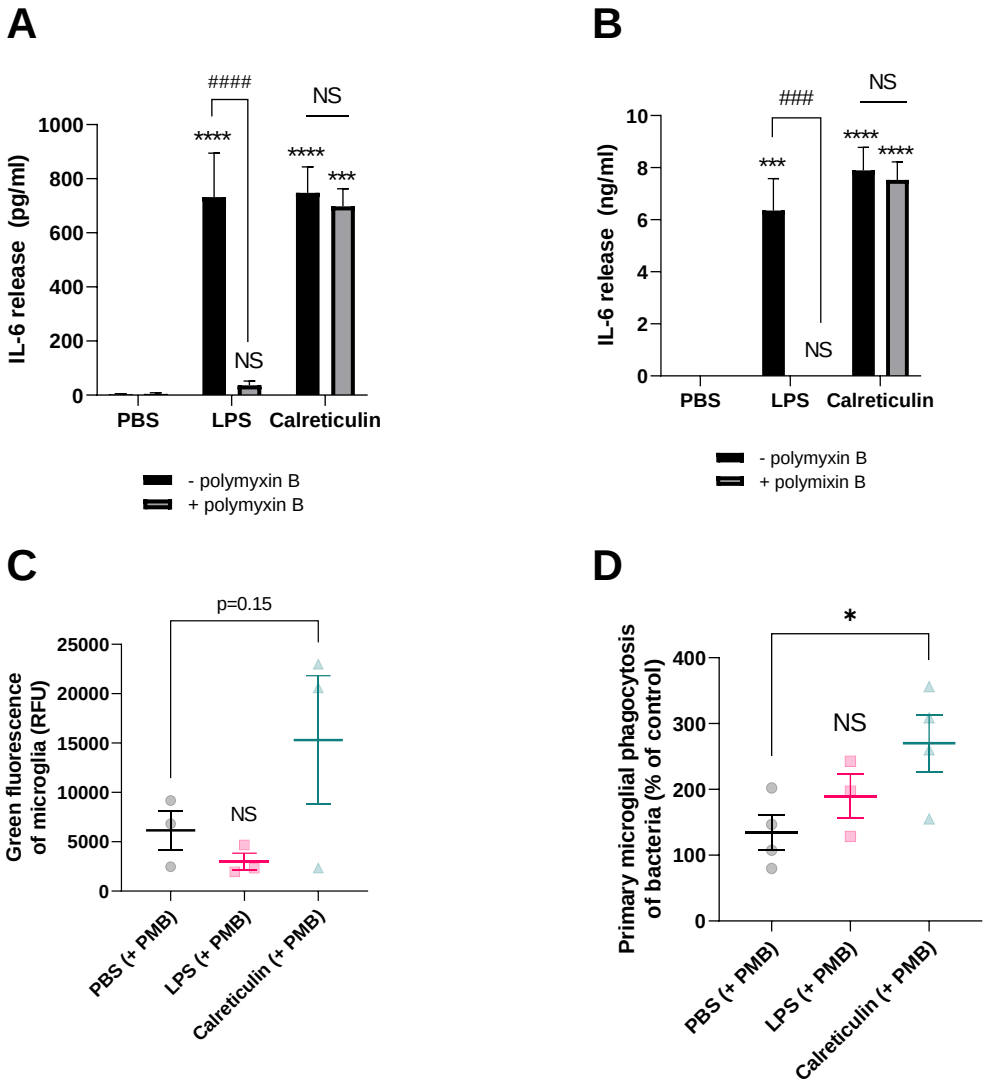

Figure 4.11. Calreticulin induces an 'activated' microglial phenotype. (A) Treatment with calreticulin (10 μg/ml) for 24 hours induced IL-6 release from BV-2 microglia with or without polymyxin B (10 U/ml); polymyxin B abolished IL-6 release induced by LPS from *E. coli* (100 ng/ml), when compared to the 'PBS - polymyxin B' control. (B) Treatment with calreticulin (1 μg/ml) for 24 hours induced IL-6 release from primary mouse microglia with or without polymyxin B (10 U/ml); polymyxin B abolished IL-6 release induced by LPS from *E. coli* (1 ng/ml), when compared to the 'PBS - polymyxin B' control. (C) Treatment with calreticulin (1 μg/ml) for 24 hours may increase MHC-II exposure of primary mouse microglia even with polymyxin B present (10 U/ml); LPS from *E. coli* (1 ng/ml) + polymyxin B did not increase MHC-II exposure when compared to the 'PBS (+ PMB)' control. (D) Treatment with calreticulin (1 μg/ml), but not LPS from *S. enterica* (100 ng/ml), for 24 hours enhances primary rat microglial phagocytosis of *E. coli* with polymyxin B present (10 U/ml) and with a media swap applied immediately prior to bacterial addition, compared to the 'vehicle (+ PMB)' control. Values are means ± SEM of at least 3 independent experiments. Statistical comparisons were made via one- or two-way ANOVA as appropriate. NS $p \geq 0.05$, *$p<0.05$, ***$p<0.001$, ****$p<0.0001$ versus controls; ###$p<0.001$, ####$p<0.0001$ as indicated.

which was abolished with polymyxin B ($p<0.001$, $p>0.999$ versus control). Calreticulin (10 μg/ml) also induced significant IL-6 release ($p<0.001$) compared with that induced by LPS ($p>0.999$) which was unaffected by polymyxin B ($p=0.998$). Similar results were obtained

using primary mouse microglia (Figure 4.11B): LPS (1 ng/ml) induced a significant IL-6 release compared to the control ($p<0.001$) which was abolished with polymyxin B ($p>0.999$). Calreticulin (1 µg/ml) induced a similar IL-6 release with or without polymyxin B ($p<0.001$ each). Of note, separate experiments confirmed that 1 µg/ml calreticulin was the minimum concentration to induce IL-6 release from the primary microglia (data not shown).

To further study the phenotype of microglia chronically exposed to calreticulin, microglial surface-exposure of MHCII (major histocompatibility complex II) - an antigen-presenting receptor expressed by a variety of immune cells – was assayed via immunostaining and measured by flow cytometry (Figure 4.11C). LPS (1 ng/ml) in the presence of polymyxin B did not enhance surface-exposure of MHCII compared to the 'PBS (+ PMB)' control; however, calreticulin (1 µg/ml) induced an apparent increase in green fluorescence of the microglia, indicating increased MHCII surface-exposure. However, given high variability of the results this increase was not found to be statistically significant ($p=0.15$), meaning no firm conclusion could be drawn.

Finally, the capacity for microglia to phagocytose bacteria after chronic exposure to calreticulin was measured using primary rat microglia. To separate any potential effect of such chronic exposure on phagocytosis from the opsonisation effect already reported, cells were subjected to a media swap immediately prior to co-incubation with the bacteria, as performed previously with LPS (Figure 4.7C). As before, LPS (100 ng/ml) did not induce phagocytosis of bacteria by microglia after the media swap (and in the presence of polymyxin B) ($p=0.497$ versus 'vehicle (+ PMB)' control; Figure 4.11D). Calreticulin (1 µg/ml) induced a significant increase in bacterial phagocytosis, even after the media swap and in the presence of polymyxin B ($p=0.041$). This indicates that i) chronic exposure to calreticulin induces a pro-phagocytic phenotype by the microglia, and ii) this phenotype is distinct from that induced by LPS, since phagocytic induction by calreticulin, but not LPS, was retained after swapping the media.

4.2.7. ApoE binds and opsonises *E. coli* for microglial phagocytosis in an isoform-specific manner

Having established roles for soluble extracellular calreticulin and galectin-3 in regulating microglial phagocytosis of bacteria, possible opsonisation capacities of other proteins known to circulate extracellularly in the brain (and in contexts of inflammation) were explored. Apolipoprotein E (apoE) is expressed by and released from microglia in the brain[635] and can bind bacterial LPS[639]. Moreover, apoE levels in the brain increase following LPS insult[637], indicating that circulating apoE may play an active role against bacterial infection. However, it is not known whether apoE can bind bacteria to promote their recognition or phagocytosis

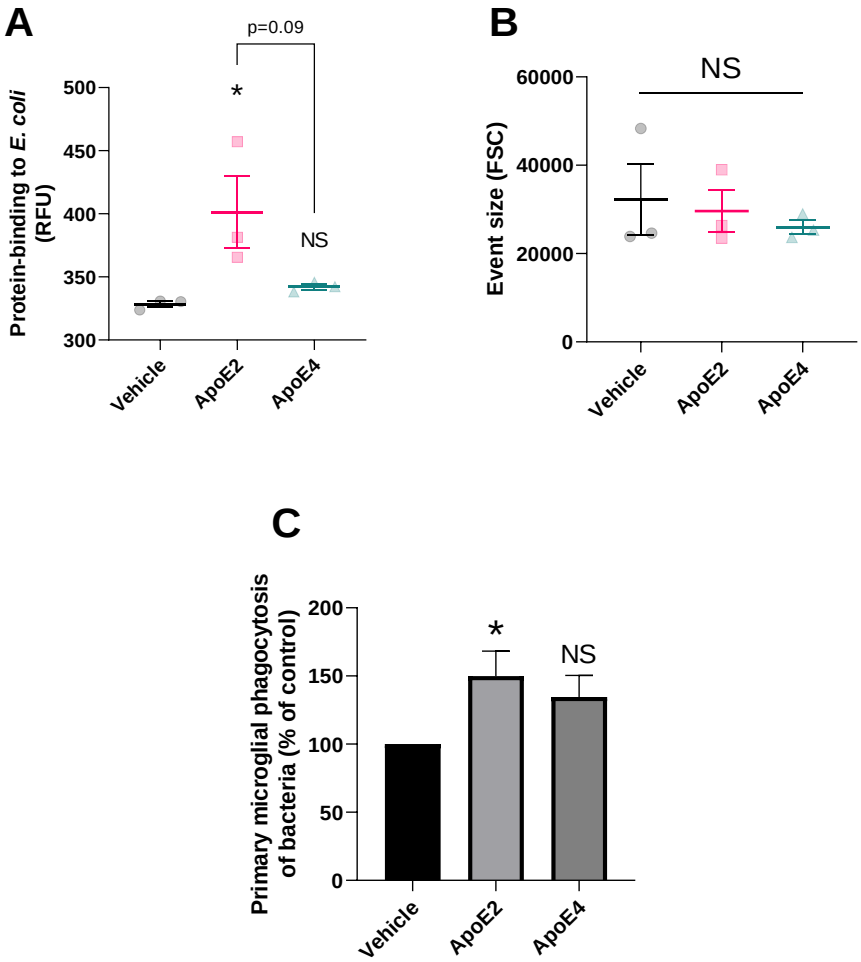

Figure 4.12. ApoE2 can bind and opsonise *E. coli* for microglial phagocytosis. (A) TAMRA-conjugated apoE2 (1 μM) binds *E. coli* after 90 minutes co-incubation, measured in terms of relative fluorescence unit increase versus the 'vehicle' (protein-free) control; no significant binding is observed from the same concentration of apoE4. (B) Neither apoE2 nor apoE4 affect the size of bacterial events when compared to the 'vehicle' control, as determined by mean forward scatter (FSC). (C) ApoE2 significantly opsonises *E. coli* for phagocytosis by primary rat microglia compared to the 'vehicle' control, when precincubated for 90 minutes at 1 μM (and subsequently washed to remove unbound protein). Values are means ± SEM of at least 3 independent experiments. Statistical comparisons were made via one-way ANOVA. NS $p \geq 0.05$, *$p < 0.05$ versus controls.

by brain immune cells such as microglia. To test this, two isoforms of recombinant human apoE – ε2 and ε4 (1 μM each) – were labelled with TAMRA-SE (50 μM) and incubated with heat-inactivated *E. coli* for 90 minutes to measure protein binding to the bacteria, which was achieved via flow cytometry. Compared to the 'vehicle' control (Figure 4.12A), bacterial fluorescence was significantly increased in the presence of ε2 ($p=0.046$), but not ε4 ($p=0.832$), indicating isoform-specific bacterial binding, possibly through differing affinities for bacterial LPS. Incubation with apoE did not affect the forward-scatter of bacteria (Figure 4.12B), indicating no promotion of bacterial aggregation by apoE. Note that final protein concentrations were quantified by spectroscopy (A_{280}): no significant difference in concentration between the two proteins was observed (data not shown).

To test whether apoE can opsonise bacteria for microglial phagocytosis – and whether such opsonisation is isoform-dependent - pHrodo-conjugated *E. coli* were incubated with ε2 or ε4 (1 μM each) for 90 minutes, washed, and then incubated with primary rat microglia as before. Bacterial phagocytosis was significantly enhanced by 50 ± 18% in the presence of the ε2 isoform compared to the 'vehicle' control ($p=0.049$; Figure 4.12C). However, in the presence of ε4, no statistically significant effect on phagocytosis was observed when compared to the control ($p=0.226$), suggesting a differential capacity for opsonisation between the two isoforms.

4.2.8. Monomeric β-amyloid opsonises bacteria for microglial phagocytosis

β-amyloid precursor protein (APP) production and β-amyloid aggregates are increased in the brain during infection by various bacterial strains[642], and β-amyloid has been suggested to bind bacterial cell walls[645]. However, it is unknown whether such binding can opsonise bacteria for phagocytosis by resident phagocytes such as microglia, or whether this is affected by oligomerisation status of the protein. To test this, both monomeric and oligomeric preparations of β-amyloid were generated, labelled with TAMRA-SE (50 μM) and incubated with heat-inactivated *E. coli* for 90 minutes to measure protein binding to the bacteria, achieved via flow cytometry. Compared to the 'vehicle' control (Figure 4.13A), bacterial fluorescence was significantly increased in the presence of monomeric β-amyloid ($p=0.026$) but not oligomeric

β-amyloid (p=0.251), suggesting a binding capacity of the peptide for bacteria that is dependent on oligomerisation status. Incubation with β-amyloid (monomeric or oligomeric) did not affect the forward-scatter of bacterial events (Figure 4.13B), indicating no promotion of bacterial aggregation by β-amyloid.

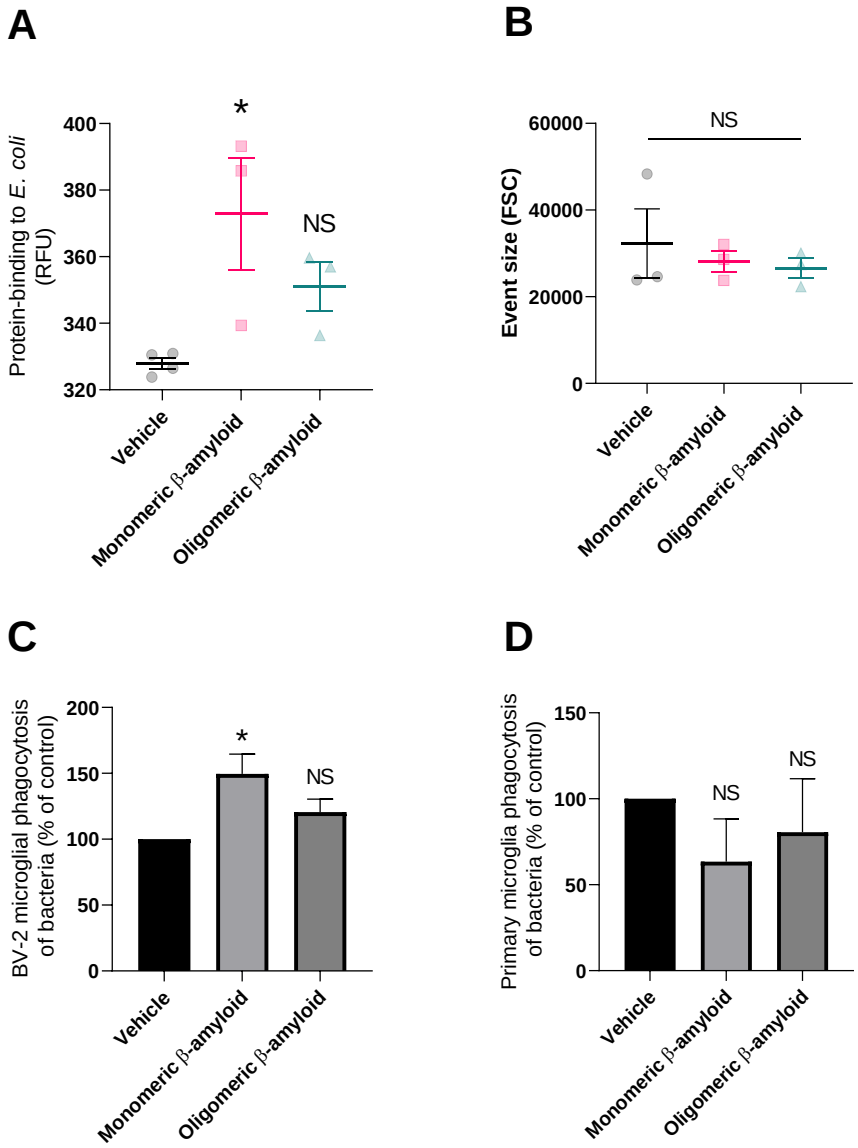

Figure 4.13. Monomeric β-amyloid can bind and opsonise *E. coli* for microglial phagocytosis. (A) TAMRA-conjugated monomeric β-amyloid (50 μM) binds *E. coli* after 90 minutes co-incubation, measured in terms of relative fluorescence unit increase versus the 'vehicle' (protein-free) control; no significant binding is observed from the same concentration of oligomeric β-amyloid. (B) Neither monomeric nor oligomeric β-amyloid affect the size of bacterial events when compared to the 'vehicle' control, as determined by mean forward scatter (FSC). (C) Monomeric, but not oligomeric, β-amyloid (2.5 μM) opsonises *E. coli* for phagocytosis by BV-2 microglia compared to the 'vehicle' control, when precincubated for 60 minutes (and subsequently washed to remove unbound protein). (D) Neither monomeric nor oligomeric β-amyloid were able to opsonise *E. coli* for phagocytosis by primary rat microglia under the same pre-treatment conditions, when compared to the 'vehicle' control. Values are means ± SEM of at least 3 independent experiments. Statistical comparisons were made via one-way ANOVA. NS $p \geq 0.05$, *$p < 0.05$ versus controls.

To test whether β-amyloid can opsonise bacteria for microglial phagocytosis – and whether such opsonisation is dependent on oligomerisation status of the peptide - pHrodo-conjugated *E. coli* were incubated with β-amyloid (monomeric or oligomeric, 2.5 μM each) for 90 minutes and incubated with BV-2 or primary rat microglia as before. Bacterial phagocytosis by BV-2 cells was significantly enhanced in the presence of monomeric, but not oligomeric, β-amyloid compared to the 'vehicle' control ($p=0.035$ & 0.402 respectively; Figure 4.13C). However, neither monomeric nor oligomeric β-amyloid enhanced bacterial phagocytosis by primary rat microglia under the same pretreatment conditions (Figure 4.13D).

4.3. Discussion

In this chapter, the ability of four proteins – calreticulin, galectin-3, apoE and β-amyloid – to bind and opsonise the gram-negative bacteria *E. coli* for phagocytosis by microglia has been demonstrated, and is presented schematically (Figure 4.14, page 157). Such findings will be discussed sequentially.

4.3.1. Calreticulin

Cell-surface exposure of typically endoplasmic reticulum-resident calreticulin was first documented over 20 years ago[649], and has been found on the surface of several cell types to mediate various extracellular functions[650], including mitogenesis[651], migration[652] and regulation of the complement cascade through C1q binding[142,653]. More recently, it has been shown that calreticulin present on the apoptotic cell surface acts as an 'eat-me' signal to professional phagocytes[473]. Although surface-exposed calreticulin was also identified on viable (non-apoptotic) cells, phagocytic clearance of these cells was prevented through dominant inhibitory signaling via the target-exposed CD47 and phagocyte-exposed SIRPα[473]. Furthermore, calreticulin exposure on the cell surface is increased in cells undergoing apoptosis[473], and can be induced via oxidative stress[654], anthracyclins[655], γ-irradiation[656], UV-exposure[656], and possibly nutrient deprivation[657]. Thus, calreticulin has been described as a DAMP[658,659]. The ability for cells to actively secrete (rather than simply expose) calreticulin has received less attention[658]. However, recent work by Feng *et al*[143] demonstrates that

peritoneal macrophages can secrete calreticulin following LPS exposure, and that extracellular calreticulin can bind and opsonise neutrophils for phagocytosis, thus facilitating neutrophil turnover in a phenomenon called 'programmed cell-removal'. In this chapter, I show that microglia (the brain-resident macrophage) upregulate and secrete calreticulin in response to LPS stimulation. Similar to Feng *et al*[143], calreticulin release was minimal or non-existent in the absence of LPS stimulation, consistent with extracellular calreticulin being a DAMP. Calreticulin has been detected in human serum at approximately 5 ng/ml, although levels significantly increase during inflammatory disease[660], again supporting the idea that extracellular calreticulin is a DAMP.

Calreticulin has been shown to bind LPS, the most prevalent lipid moiety on the surface of gram-negative bacteria[626]. Since calreticulin binding to *E. coli* was identified by me, it has been shown to bind multiple other bacterial species including gram-negative *Acinetobactor baumannii, Klebseilla pneumonia* and *Psuedomonas aeruginosa*, as well as the gram-positive bacteria *Staphylococcus aureus*[626]. In addition to binding *E. coli*¸ I found that calreticulin opsonised the bacteria for microglial phagocytosis in culture, which was inhibitable by the disaccharide sucrose, or by the LRP1 ligand RAP. Moreover, calreticulin was shown to be required for LPS-induced phagocytosis of the bacteria by microglia, as this LPS-induced phagocytosis was inhibited by an anti-calreticulin antibody (but not a serotype control antibody). As an endoplasmic reticulum-resident lectin, calreticulin typically binds monoglucosylated N-glycan chains on developing glycoproteins – specifically the glucan $Glc_1Man_{2\text{-}7}GlcNAc_2$ – and this binding can be strongly inhibited in the presence of synthetic oligosaccharides that mimic truncated versions of the natural N-glycan ligand[661]. Sucrose is composed of a single glucose molecule linked to a single fructose molecule, and so in principle could interact with the lectin domain of calreticulin. Sucrose was found to inhibit i) the binding of calreticulin to bacteria; ii) calreticulin-induced opsonisation of *E. coli* for microglial phagocytosis; and iii) LPS-induced microglial phagocytosis of *E. coli*. These data directly implicate the sugar-binding domain of calreticulin in mediating its bacterial binding and opsonisation effects. No significant change in baseline phagocytosis of the bacteria by microglia (i.e. without exogenous calreticulin or LPS) was observed when sucrose was added. However, a small reduction was observed, which may prove significant if tested further. Given no significant release of calreticulin was observed by BV-2 or primary rat microglia in the

absence of LPS stimulation, it cannot be ruled out that sucrose may interfere with phagocytosis through a calreticulin-independent mechanism, although this would have to be investigated.

Phagocytosis induced by pre-treating the bacteria with calreticulin or inflammatory activating the microglia with LPS was also inhibited by RAP, a competitive ligand for LRP1. LRP1 is known to interact with calreticulin[662], and calreticulin on apoptotic cells promotes phagocytosis of such cells by binding LRP1 on the phagocyte[473]. Thus, my findings are consistent with LRP1 being the main phagocytic receptor for calreticulin in the context of microglial phagocytosis of bacteria. LRP1 is expressed by phagocytes other than microglia, such as peritoneal macrophages[474] and bone-marrow derived monocytes[663], and calreticulin is ubiquitously expressed by all nucleated cells[133]. Thus, in principle, inflammatory activation of phagocytic cells other than microglia (and outside the brain) may induce them to secrete calreticulin extracellularly, and such released calreticulin may opsonise bacteria for phagocytic removal. Indeed, to explore this idea, the human monocyte cell line U937 was tested for i) LPS-induced calreticulin release and ii) calreticulin opsonisation of *E. coli* for phagocytosis. No conclusive findings were obtained regarding calreticulin release (i), and no opsonisation effect with calreticulin was demonstrated (ii), even after differentiation into macrophages was induced by PMA/ M-CSF treatment. However, it has been shown that calreticulin is released by peritoneal macrophages from mice after LPS stimulation[143], opening the possibility that extracellular calreticulin may indeed tag and opsonise bacteria peripherally, and this merits further investigation.

In addition to opsonising bacteria for phagocytosis, exogenous calreticulin was found to stimulate release of IL-6 – a classical inflammatory cytokine – from both BV-2 and primary mouse microglia. Such release occurred even in the presence of polymyxin B, which sequesters endotoxin and abolished IL-6 release induced by LPS directly, indicating that calreticulin itself (rather than any contaminating endotoxin potentially present) stimulated IL-6 release from the cells. Furthermore, there was an indication that calreticulin could increase surface exposure of MHCII by microglia, and chronic (24 hours) exposure to calreticulin was found to enhance microglial phagocytosis of bacteria. Such phagocytic enhancement did not occur due to opsonisation of the bacteria by the exogenous calreticulin, as the cells were washed prior to adding bacteria, implying that calreticulin induced a phenotypic change in the microglia that

increased their phagocytic ability. Together, these findings indicate that extracellular calreticulin may act as an alarmin (i.e. an endogenous immune-activating protein released by damaged or infected cells[664]). The fact that calreticulin induced IL-6 release from the microglia indicates a polarisation to the classically-activated M1 phenotype (see section 2.2.2); however, the increase in bacterial phagocytosis that was induced by chronic calreticulin (followed by a media swap) was not induced by LPS (followed by a media swap), and LPS is a classical M1 stimulant[328]. This indicates that calreticulin may induce a different activation phenotype to that induced by LPS and supports the notion that classification of microglial (and macrophage) activation states into M1/M2 phenotypes is an oversimplification (see section 2.2.4). The fact that calreticulin can facilitate microglial phagocytosis of bacteria opens the possibility that applying (or inducing) calreticulin may be therapeutically beneficial to bacterial infections of the brain (and if this phenomenon occurs outside the brain, to peripheral infections generally). However, it is first essential to more completely characterise the extent to which calreticulin induces inflammation via immune cell activation, as such inflammation can cause detrimental tissue damage which may limit its therapeutic value. Indeed, there is clinical interest in antibacterial treatments that eliminate bacteria with minimal associated inflammation and tissue damage, as many antibiotics – particularly those targeting bacterial meningitis – are bacteriolytic and cause bacterial release of PAMPs that trigger dramatic and damaging immune responses[378].

As a final note, calreticulin exposure has been shown to induce phagocytic removal of cancer cells that is followed by downstream adaptive immune responses against the same cancer cell, including presentation of antigen by the phagocyte and T cell priming[656,665]. Importantly, calreticulin was found to be essential for the immunogenicity of this cell death[656]. Indeed, calreticulin has been used as an immunologic adjuvant to promote adaptive immune responses to tumour-associated antigen[666]. Calreticulin opsonised bacteria for microglial phagocytosis, and preliminary findings indicate that it also enhances surface expression of MHCII, though this requires confirmation. Thus, calreticulin-mediated phagocytosis of bacteria may elicit adaptive immune responses against the bacteria through presentation of bacterial antigen and priming of T cells, although this would require testing. If this is found to be the case, calreticulin may present a particularly promising anti-bacterial therapeutic that not only induced phagocytic removal of the bacteria, but also enhanced adaptive immune responses against the bacteria to perpetuate immune protection against the bacteria.

4.3.2. Galectin-3

Galectin-3 is an evolutionarily conserved protein distributed throughout the mammalian system, having been identified in the digestive tract, lungs, heart, blood and kidneys, as well as in the brain[211]. A wide and varied list of roles has been ascribed to galectin-3, with particular emphasis in recent years on its participation in immune responses against pathogens[211]. Galectin-3 can be released from diverse cell types including epithelial and myeloid cells exposed to various microbial (and non-microbial) stimuli[211]. I show here that non-activated primary mouse microglia express and release significant levels of galectin-3, and such expression and release is enhanced following LPS stimulation of the microglia.

Galectin-3 is known to bind LPS from bacterial species including *Klebsiella pneumoniae*[631], *Salmonella minnesota*[631], *E. coli*[667] and *Pseudomonas aeruginosa*[668]. Galectin-3 is a structurally unique member of the galectin protein family, which can crosslink with other galectin-3 monomers to form oligomers[211]. LPS binding to galectin-3 has been shown to promote galectin-3 oligomerisation and enhance immune recognition of LPS by neutrophils, thus inducing their activation[667]. Moreover, binding of galectin-3 to LPS has been reported to occur at two independent sites: a C-terminal carbohydrate binding site (e.g. for LPS from *K. pneumoniae*), and an N-terminal site (e.g. for LPS from *S. minnesota*)[631]. Importantly, binding to the C-terminal site is inhibitable by lactose, whilst binding to the N-terminal site is not. I found that galectin-3 could bind *E. coli* (likely via LPS[667]), but such binding was not inhibitable by lactose, suggesting that *E. coli* binding occurs at the N-terminal site of galectin-3. Furthermore, galectin-3 opsonised *E. coli* for phagocytosis by microglia, and while lactose significantly inhibited baseline phagocytosis, such levels were significantly increased in the presence of exogenous galectin-3. The inhibition of phagocytosis by lactose was also lifted after inflammatory activating the microglia with LPS. Galectin-3 binding to BV-2 microglia has been shown to be abolished by lactose[212], and impaired binding of galectin-3 to microglia in the presence of lactose may be a sufficient explanation for the lactose-induced reduction in baseline phagocytosis observed here (note that galectin-3 was released at significant levels by microglia in untreated conditions). However, this is brought into question given that both applied galectin-3 and LPS could partially rescue lactose-inhibited phagocytosis. As an alternative explanation, lactose may interfere with phagocytosis through a galectin-3-independent mechanism, and this requires investigation.

The increased phagocytosis observed due to both exogenous galectin-3 and LPS was inhibited in the presence of the small molecules UNC2881 and UNC5569, which block MerTK[669,670]. MerTK is a phagocytic receptor expressed by myriad myeloid cells including macrophages, monocytes, dendritic cells and natural killer cells[671,672], and is known to bind galectin-3[216]. Furthermore, phagocytosis of apoptotic cells and cellular debris induced by galectin-3 is prevented by inhibiting MerTK[216]. Our lab has also shown that galectin-3 promotes microglial phagocytosis of neuron-like PC12 cells and neuronal debris, which can be inhibited by blocking MerTK[212]. Thus, my data are consistent with galectin-3 mediating phagocytosis of targets via MerTK signaling, albeit in the novel context of bacterial opsonisation in the brain. At nanomolar concentrations, UNC inhibitors of MerTK were found to inhibit galectin-3 or LPS induced phagocytosis without affecting phagocytosis in control conditions. However, at micromolar concentrations, the same inhibitors dramatically reduced bacterial phagocytosis by control microglia (i.e. microglia not exposed to galectin-3-coated bacteria or LPS). It is possible that such concentrations are necessary to inhibit MerTK-dependent bacterial phagocytosis by control microglia. However, studies by Williams *et al* have demonstrated that macrophages completely lacking MerTK through genetic deletion are not impaired in their phagocytosis of *E. coli*[673], indicating that micromolar UNC may be exerting an off-target effect. Thus, my findings would benefit from experiments involving genetic knockdown or deletion of MerTK in the microglia.

Galectin-3 has been identified in plasma and also in CSF, and levels increase during pathology[674] - for example in traumatic brain injury, where galectin-3 acts as an alarmin to activate immune cells (including microglia) and promotes neuroinflammation[675]. Thus, galectin-3 circulates in the brain, and may be physiologically relevant in limiting brain infection by bacteria. Expression of galectin-3 (and MerTK) by other immune cells outside the brain further implicates galectin-3-mediated bacterial elimination in peripheral infections generally. Indeed, galectin-3 has been shown to play important roles in limiting bacterial infection of the gastric tract by the gram-negative bacterium *Helicobacter pylori*[676], and also protecting against infection by *S. pneumoniae* (the primary cause of community-acquired pneumonia[677]), supporting a role for galectin-3-mediated opsonisation in innate defense against bacterial infection outside the brain.

4.3.3. ApoE

Several lines of evidence suggest functional roles for apoE during bacterial infection. ApoE levels in serum are substantially increased after intravenous injection of LPS in mice[678]. In the brain, apoE is upregulated in the mouse hippocampus following intracerebroventricular injection of LPS[637], and levels also increase following traumatic brain injury[679]. ApoE possesses intrinsic anti-microbial properties: recombinant and synthetically produced apoE peptides reduce survival rates of multiple bacterial strains, including *S. aureus*, *E. coli* and *P. aeruginosa*[680]. Furthermore, apoE can bind LPS[639], and such binding has been implicated in the apoE-mediated protection of LPS-induced cytokine production and septic-related death observed in rodents[678]. Additionally, apoE peptides have been shown to inhibit LPS-induced production of the inflammatory cytokines IL-8 and COX-2 in macrophages, and also inhibit LPS-induced secretion of TNF-α from peripheral blood mononuclear cells[680]. Thus, binding to LPS by extracellular apoE may function to sequester circulating endotoxin, limiting undesirable immune activation in the absence of true infection and/or shielding against harmful levels of endotoxin during infection. Indeed, recent work in our lab has demonstrated that the ε2 isoform of apoE (but not the ε4 isoform) can protect against LPS-induced neuronal phagoptosis in cerebellar neuronal cultures (unpublished). Although it is not clear how such protection is mediated, it is possible that LPS-sequestration via direct binding of apoE to LPS is isoform-dependent. In this work, I demonstrate that apoE binding to bacterial *E. coli* is heavily influenced by the isoform: ε4 binding was minimal, whilst ε2 binding was dramatically higher, despite no difference in concentration of the proteins at the point of application. Whilst it is not demonstrated here that such binding is mediated by LPS, the surface of *E. coli* (as a gram-negative bacterial strain) is predominantly LPS[626], making it seem likely. Furthermore, the ε2 isoform significantly opsonised bacteria for phagocytosis by the microglia in culture. The ε4 isoform increased phagocytosis less than ε2 and not to statistically significant levels, consistent with lower binding of ε4 to *E. coli*. The ability for apoE (regardless of isoform) to bind and opsonise bacteria for microglial phagocytosis is a novel finding *per se*, and this activity may play an important role in preventing and/or responding to bacterial infection in the brain. It is unclear how apoE might signal *in trans* from the bacterial surface to induce phagocytosis. ApoE is a known ligand for TREM2[638], and TREM2 activation promotes microglial phagocytosis of multiple targets in different physiological and pathological contexts (see section 2.3.1.8). Thus, apoE may signal via microglial TREM2, but this would need testing. ApoE is also a known ligand for LRP1[477],

and so might promote phagocytosis of bacteria via this microglial receptor, but again this would need testing.

ApoE is the major genetic risk factor for AD, with the ε2 isoform being associated with decreased risk, ε4 with increased risk, and ε3 with a neutral effect on risk[640]. If apoE association with LPS is indeed isoform-dependent, this may also be of relevance to AD pathology. LPS levels in the blood and brain are elevated in AD brains, and this increase has been implicated in AD-associated immune activation, β-amyloid aggregation, neuronal loss, synaptic loss and memory deficits[681]. An increased capacity for the ε2 isoform of apoE to bind LPS (relative to ε3 or ε4) may correspond to an increased ability for ε2 to sequester the circulating endotoxin that might otherwise contribute to chronic neuroinflammation. However, such a hypothesis requires further investigation. It is known that bacterial density and species diversity are increased in AD brains[682,683,684], and it has been suggested that such an increase in bacterial presence contributes to the increased endotoxin levels detected in the brain (that are associated with AD pathology)[681]. Thus, the differential capacity for apoE isoforms to bind and opsonise bacteria for phagocytic elimination by microglia may contribute to AD indirectly by affecting bacterial load in the brain.

4.3.4. β-amyloid

β-amyloid accumulation and aggregation is one of the major hallmarks of AD pathology[685], but anti-β-amyloid therapies designed to treat AD have been unsuccessful. Interestingly, many instances of increased bacterial and viral infection have been reported in treatment groups[642], leading to speculation that β-amyloid possesses anti-microbial properties and/or innate immune functions. Multiple bacterial species have been shown to increase APP expression and/or β-amyloid deposition, including *Chlamydia pneumoniae, Treponema palladium, Borrelia burgdorferi* and *Porphyromonas gingivalis*[642]. Correspondingly, various immune cells have been shown to upregulate β-amyloid production and/or secretion following inflammatory activation, including microglia[686] but also monocytes[687,688]. β-amyloid has been shown to bind bacterial and fungal cells directly via its heparin binding domain[645]. Furthermore, β-amyloid has been identified within NETs generated by neutrophils, where the positive charge of β-amyloid aggregates has been suggested to bind (and trap) the polyanionic surface of bacteria whilst ignoring the host cell surface[689]. β-

amyloid can also interact with immune cells including microglia, through direct binding to the phagocytic receptor TREM2[498]. However, to my knowledge, it has not been shown that β-amyloid association with bacteria can induce their phagocytosis by immune cells, or whether this might depend on β-amyloid oligomerisation status.

I show here that monomeric β-amyloid can bind *E. coli*, and this binding opsonises the bacteria for phagocytosis by BV-2 (but not primary rat) microglia. The ability for monomeric β-amyloid to opsonise bacteria for microglial phagocytosis may represent an additional antimicrobial mechanism for β-amyloid in the brain. However, given that monomeric β-amyloid was only able to opsonise the bacteria for phagocytosis by BV-2 but not primary microglia, this requires confirmation. Such a difference may relate to differential gene expression between the two cell systems[690], or be simply due to increased serum in the culture media for primary microglia, which could interact with β-amyloid during experimentation. Strikingly, oligomeric β-amyloid binding to *E. coli* was substantially lower and not significant compared to the control. Oligomeric β-amyloid was also unable to opsonise the bacteria for phagocytosis by BV-2 or primary rat microglia. This is of particular interest to AD pathology, as i) β-amyloid aggregates are increased in AD, and ii) bacterial load and species diversity are increased in the brains of AD patients[682,683,684] which may result in AD-associated neuroinflammation and neuronal loss. Thus, oligomerisation of β-amyloid may indirectly exert neurotoxic effects by inhibiting β-amyloid-mediated bacterial phagocytosis, allowing accumulation of bacteria and bacteria-associated endotoxin within the brain.

Figure 4.14. Model for microglial phagocytosis of bacteria via opsonisation with extracellular calreticulin, galectin-3, apoE and β-amyloid

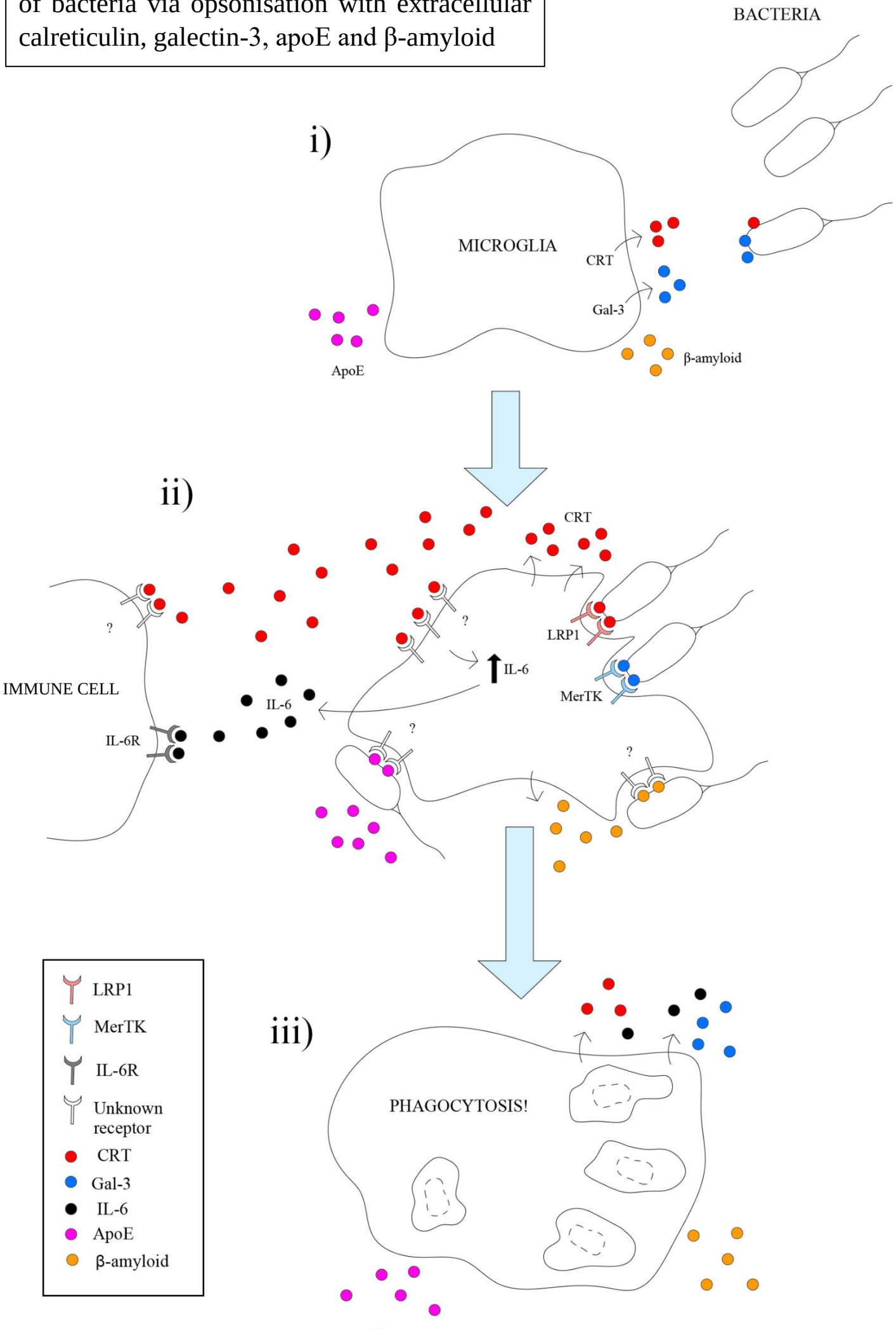

Figure 4.14. Model for microglial phagocytosis of bacteria via opsonisation with extracellular calreticulin, galectin-3, apoE and β-amyloid. i) Microglia activated by bacterial endotoxin upregulate and extracellularly secrete both calreticulin and galectin-3. ii) Calreticulin and galectin-3 bind to bacteria and opsonise them for microglial phagocytosis, mediated by the microglial receptors LRP1 and MerTK respectively. Calreticulin also induces the release of extracellular IL-6 by microglia, which can further stimulate the immune system by binding IL-6R expressed on the surface of immune cells[691]. ApoE and β-amyloid also bind and opsonise bacteria for microglial phagocytosis, through unknown receptors. iii) Microglia phagocytose and so eliminate the bacteria, whilst continuing to release calreticulin, galectin-3 and IL-6 into the extracellular space.

CHAPTER V

NUCLEOTIDE REGULATION IN MICROGLIAL PHAGOCYTOSIS OF BACTERIA

5.1. Introduction

The P2Y receptors are a family of GPCRs expressed by almost all human cell types, and homologues are conserved across a large subset of animal species, suggesting importance to basic cellular function[692]. P2Y receptors are activated by nucleotide binding, and so the receptors have been categorised as purinoreceptors (responding to adenosine or guanosine) or pyrimidinoreceptors (responding to cytidine, thymidine or uridine). However, many can be activated by both purines and pyrimidines, albeit with differing affinities[692]. There are eight known P2Y receptors in humans: $P2Y_1$, $P2Y_2$, $P2Y_4$, $P2Y_6$, $P2Y_{11}$, $P2Y_{12}$, $P2Y_{13}$ and $P2Y_{14}$[693]. Of particular relevance to this thesis are the $P2Y_6$ and $P2Y_{12}$ receptors, both of which are expressed by microglia in the brain[118,485].

As described in Chapter 2, $P2Y_6R$ is a phagocytic receptor expressed by microglia that is primarily activated by uridine-5'-diphosphate[694] (UDP) and is directly implicated in mediating microglial phagocytosis of dead and dying neurons in the brain through binding UDP released from the dead or dying cell[485]. Unpublished data in our lab has further established $P2Y_6R$ as fundamental to the microglial phagoptosis of viable neurons in multiple inflammatory contexts, including LPS-induced neuroinflammation. $P2Y_6R$ is upregulated in inflammatory-activated microglia[695], including microglia exposed to bacterial LPS[430]. Furthermore, $P2Y_6R$ signalling has been implicated in protecting mice against peripheral bacterial infection through macrophage recruitment in a model of peritonitis[696]. However, it is unclear if $P2Y_6R$ plays a role in the context of bacterial infection of the brain. In microglia, $P2Y_6R$ signalling aids process extension towards bacteria[697], but whether such signalling via $P2Y_6R$ facilitates phagocytic clearance of the bacteria is not known.

$P2Y_{12}R$ is a purinoreceptor expressed constitutively (and exclusively) by microglia during normal brain homeostasis[118,698], but is downregulated after LPS-induced inflammation[118]. $P2Y_{12}R$ is activated primarily by ATP/ADP[692], and $P2Y_{12}R$ activation has been linked to chemotactic migration by the microglia. Activation of $P2Y_{12}R$ by ADP induces morphological changes in microglia associated with a migratory phenotype[699], and $P2Y_{12}R$ has been demonstrated as required for ADP-dependent migration by rat microglia[700]. Furthermore, $P2Y_{12}R$ activation regulates microglial process extension toward injured neurons[118] or hyperactive neurons[367], and so is heavily implicated in mediating microglial migration towards tissue damage. However, any role for $P2Y_{12}R$ in microglial clearance of bacteria in the brain is unknown. Bacteria can release ATP and/or ADP[701], which in principle can act as chemoattractants to promote microglial migration toward the bacteria via $P2Y_{12}R$ signalling and facilitate their phagocytic clearance, but this has not been reported.

In this chapter, I present novel data implicating both $P2Y_6R$ and $P2Y_{12}R$ signalling in microglial phagocytosis of bacteria. Using a $P2Y_6R$ cell-reporter system, I show that agonist for $P2Y_6R$ is released by bacterial *E. coli*, and also from LPS-activated microglia. Interestingly, this reporter system identified $P2Y_6R$ agonist release from unstimulated BV-2 microglia, 1321N1 astrocytes, and PC12 pheochromocytoma (neuron-like) cells under specific experimental conditions, which has implications for utility of the reporter system for measuring secreted $P2Y_6R$ agonist, and may be physiologically relevant. UDP (as the primary agonist for $P2Y_6R$[694]) substantially increased phagocytosis of bacteria by microglia in culture, which was significantly inhibited by blocking $P2Y_6R$ with MRS2578. Moreover, LPS-induced phagocytosis of bacteria by the microglia was inhibited by MRS2578 or apyrase (a nucleotidase that degrades UDP[702]), consistent with UDP-$P2Y_6R$ signalling in mediating the LPS-induced phagocytosis. Additionally, blocking $P2Y_{12}R$ with PSB0739 significantly inhibited phagocytosis of bacteria by the microglia, as did an excess of ADP, implicating ADP-$P2Y_{12}R$ signalling in facilitating phagocytosis. However, unlike with $P2Y_6R$, blocking $P2Y_{12}R$ with PSB0739 did not prevent LPS-induced microglial phagocytosis of the bacteria. Together, these findings implicate $P2Y_6R$ and $P2Y_{12}R$ signalling in microglial phagocytosis of bacteria, which may be important in the immune response to brain infections.

5.2. Results

5.2.1. BV-2 microglia burst-release nucleotide agonist of the microglial receptor $P2Y_6R$

Extracellular nucleotides mediate a variety of intracellular functions, and UDP signalling via $P2Y_6R$ has been implicated in inducing microglial process extension during bacterial infection[697]. At the start of this study, it was unclear where extracellular UDP (or any $P2Y_6R$ agonist) may originate in the context of bacteria in the brain. We hypothesised that $P2Y_6R$ agonist may be released by cells, for example inflammatory-activated immune cells or bacterial cells. To investigate cellular release of $P2Y_6R$ agonist, a $P2Y_6R$ reporter cell line expressing $P2Y_6R$ N-terminally linked to mCherry was generated using human astrocytoma 1321N1 cells by Dr Stefan Milde. As a negative control, the same cell line transfected with mCherry alone was also generated. Both cell-lines were observed via microscopy to fluoresce red (Figure 5.1A). Interestingly, red fluorescence was homogenous within cells transfected with mCherry alone, whilst fluorescence appeared more granular in cells transfected with $P2Y_6R$-mCherry - presumably due to a specific localisation of $P2Y_6R$, possibly within the nucleus or on the extracellular membrane. $P2Y_6R$ activation induces a rise in intracellular calcium[486,487], and so $P2Y_6R$ activation was measured via a Fura-2 AM-based calcium assay. To identify a suitable control (i.e. a compound capable of inducing a calcium response from 1321N1 cells independent of P2Y6R), the ability for carbachol – a cholinergic agonist which triggers an increase in intracellular calcium through activation of ryanodine receptors[703] – to promote calcium responses in the cell lines was tested. Calcium responses were measured for at least 60 seconds at 5 second intervals following treatment (Figure 5.1B), and peak responses were quantified (Figure 5.1C) as described in the Materials and Methods (section 3.2.5.3). Calcium responses to carbachol were substantial and not significantly different between the $P2Y_6R$-mCherry and mCherry-only cell lines. Thus, carbachol was considered an appropriate positive control for the cells in future experiments.

To confirm this system was suitable to measure $P2Y_6R$ activation, dose-responses to UDP from each line were measured. Significant calcium responses from $P2Y_6R$-expressing cells were

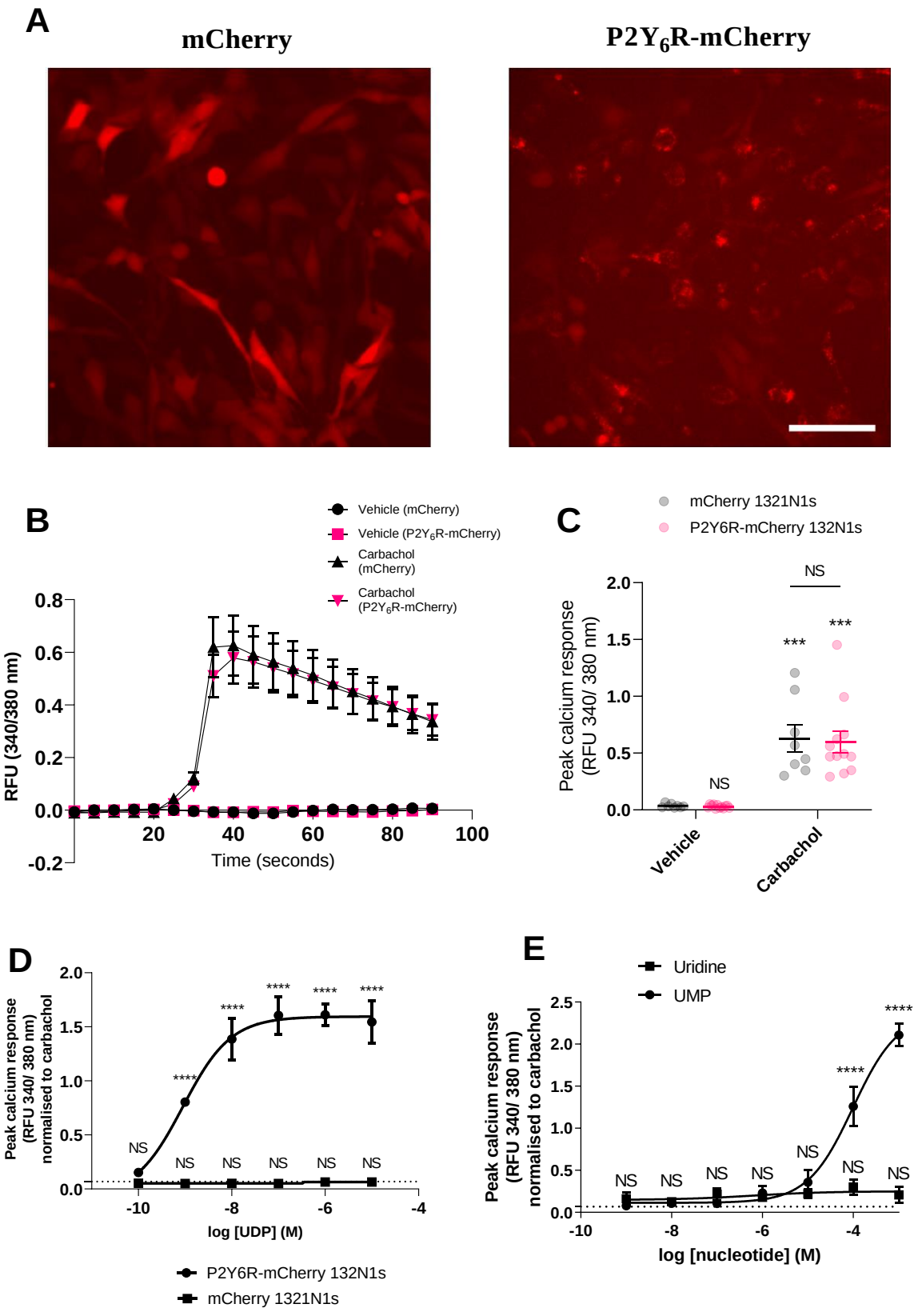

Figure 5.1. UDP induces a calcium response from 1321N1 astrocyte cells stably-transfected with $P2Y_6R$-mCherry, but not with mCherry alone . (A) Images of human 1321N1 astrocytoma cells stably transfected with mCherry or $P2Y_6R$-mCherry. Scale bar (100 μm). (B & C) Treatment with carbachol (10 μM) induces a rapid calcium response in 1321N1s stably transfected with $P2Y_6R$ -mCherry or mCherry alone, measured by fluorescence (340/380 nm) after staining with the calcium probe Fura 2-AM. Fluorescence data is represented over time (B), and also in terms of maximal fluorescence responses (C). Peak responses to carbachol are not affected by $P2Y_6R$. (D) Dose-response to UDP from 1321N1s stably transfected with $P2Y_6R$-mCherry or mCherry only. $P2Y_6R$-expressing cells respond to UDP down to 1 nM, with saturation reached between 10 and 100 nM. No responses were observed from cells lacking $P2Y_6R$ at any concentration of UDP compared to vehicle (dotted line). (E) $P2Y_6R$-reporter cells respond to UMP at 100 μM, but not to uridine, when compared to vehicle controls (dotted line). Values are means ± SEM of at least 3 independent experiments. Statistical comparisons were made via two-way ANOVA. NS $p \geq 0.05$, ***$p<0.001$, ****$p<0.0001$ versus 'vehicle' controls (B) or dose-matched responses from mCherry 1321N1 cells (D & E). Further statistical information for D & E are contained within the Appendix.

detected from 1 nM UDP ($p<0.001$ versus 'vehicle' control), with response saturation reached between 10 and 100 nM (Figure 5.1D). No significant responses to UDP from $P2Y_6R$-lacking cells were observed at any concentration tested. To confirm specificity of $P2Y_6R$ to UDP, dose-responses to the related compounds uridine-5'-monophosphate (UMP) and uridine were also tested. Neither molecule elicited a response from $P2Y_6R$ over the same concentration range (Figure 5.1E). Significant responses to UMP were observed from 100 μM, although such concentrations were considered unlikely to be physiologically relevant.

To test directly whether microglia release $P2Y_6R$ agonist, 'flex' buffer (section 3.2.5.2) was conditioned with BV-2 cells for 60 minutes before applying directly to the $P2Y_6R$ reporter cells, and peak calcium responses were recorded. Significant $P2Y_6R$ agonist was detected in this buffer compared to the 'no BV-2s (vehicle)' control ($p<0.001$, Figure 5.2A), and the same buffer did not induce responses from cells lacking $P2Y_6R$ ($p>0.999$ versus control). To determine whether such agonist release could be enhanced by activating the microglia via different stressors, BV-2s were pre-treated with LPS (100 ng/ml) or β-amyloid (250 nM) for 24 hours and conditioned with flex buffer as before. Again, $P2Y_6R$ agonist release was detected from these cells, but levels were not significantly different compared to those released from untreated cells ($p>0.999$ for each). To test whether the $P2Y_6R$ agonist being released was nucleotide, buffers were treated ± apyrase (1 U/ml) before applying to the reporter cells, and responses were measured (Figure 5.2B). Apyrase was able to completely abolish responses elicited by $P2Y_6R$-expressing 1321N1s from all buffers, consistent with the detected $P2Y_6R$ agonist being UDP. Nucleotide release from cells can occur through a variety of mechanisms,

for example via connexin- or pannexin-based channels, which are located in the cell membrane and expressed by microglia[704,705]. To test whether $P2Y_6R$ agonist release from BV-2s occurs through such channels, BV-2s were treated with either probenecid. a pannexin-specific channel blocker[706] or flufenamic acid, a non-specific blocker of connexin- and pannexin-based channels[704], and conditioned with flex buffer. Agonist release was measured as before. Neither

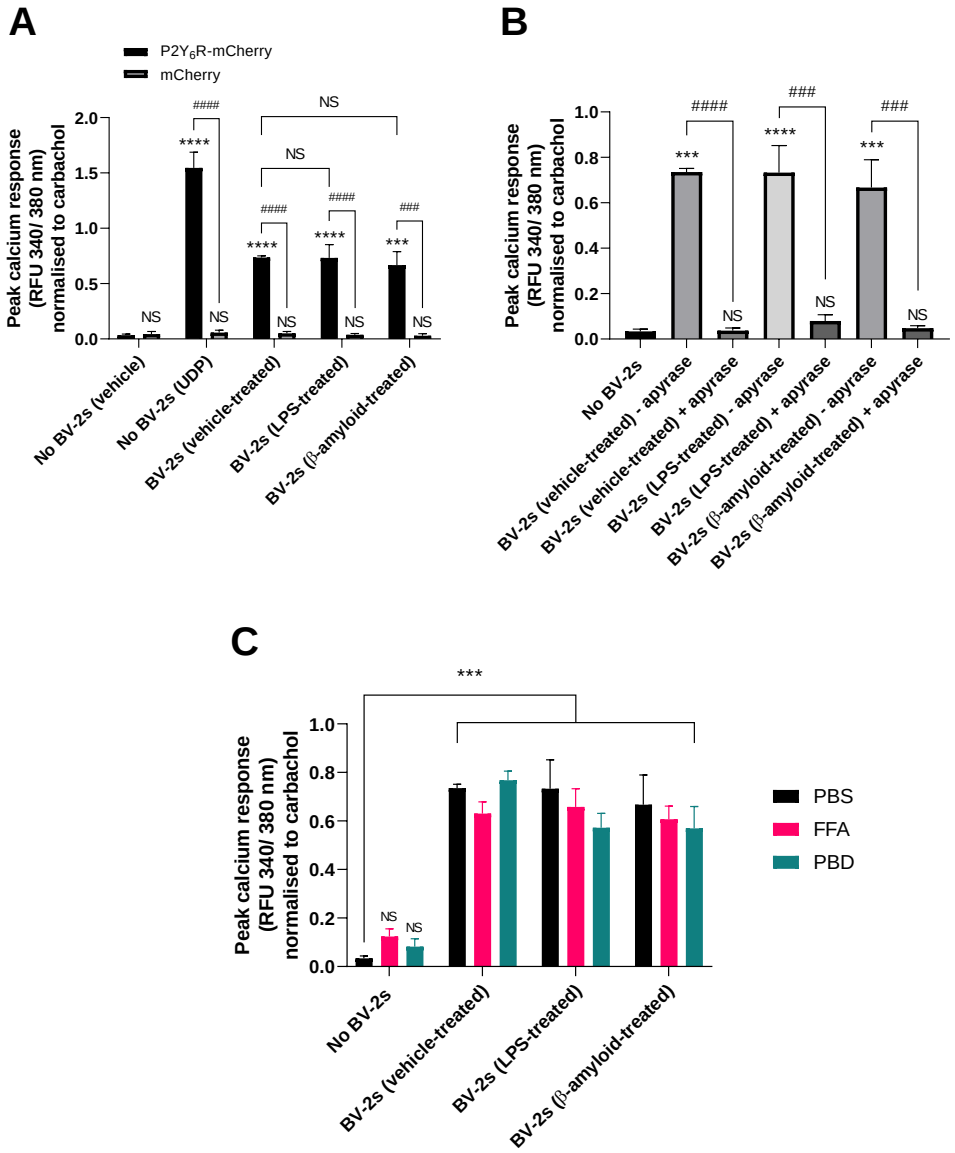

Figure 5.2. BV-2 microglia release nucleotide $P2Y_6R$ agonist into the extracellular space. (A) Flex buffer conditioned with BV-2 cells for 60 minutes contained significant levels of $P2Y_6R$ agonist compared to the 'no BV-2s (vehicle)' control, or compared to responses from 1321N1s lacking $P2Y_6R$ (as indicated). This was not enhanced by pretreatment of the microglia with LPS (100 ng/ml) or monomeric β-amyloid (250 nM). (B) $P2Y_6R$ agonist released by microglia is eliminated by treating the conditioned buffer with apyrase (1 U/ml, 10 minutes), indicating nucleotide agonist and consistent with UDP. (C) $P2Y_6R$ agonist released by the microglia is unaffected by pretreatment of the microglia with probenecid (PBD, 200 µM) or flufenamic acid (FFA, 200 µM) compared to phosphate-buffered saline (PBS). Values are means ± SEM of at least 3 independent experiments. Statistical comparisons were made via one- or two-way ANOVA; all statistical comparisons made versus 'no BV-2s' controls unless otherwise indicated. NS$p \geq 0.05$, ***$p<0.001$, ****$p<0.0001$ versus controls; ###$p<0.001$, ####$p<0.0001$ as indicated.

flufenamic acid (200 µM) nor probenecid (200 µM) inhibited the release of $P2Y_6R$ agonist from BV-2s subjected to any treatment (Figure 5.2C), suggesting that the nucleotide release may occur through a channel-independent mechanism.

Given the fact that media conditioned by BV-2 cells gave a partial calcium response when added to the $P2Y_6R$-reporter cells, we questioned whether such release might result from the specific culture conditions of the BV-2 cells, which could mask any stimulus-induced $P2Y_6R$ agonist release from these cells. To explore whether the system could be optimised to test this, BV-2 cells were conditioned with flex buffer for various durations, with the aim of identifying a duration which gave minimal $P2Y_6R$ agonist release from untreated cells. Thus, flex buffer was conditioned with BV-2s for 1, 5, 10 or 180 minutes, and $P2Y_6R$ agonist levels were measured as before (Figure 5.3A). Surprisingly, $P2Y_6R$ agonist was detected in buffer that had seen cells for just 1 minute compared to the 'no BV-2s' control ($p<0.001$), with similar levels being detected after 5 or 10 minutes in buffer. Buffer conditioned with cells for 180 minutes still contained $P2Y_6R$ agonist at significant levels versus the control ($p<0.001$), although this was significantly lower than levels in buffer conditioned with cells for 5 minutes (p-0.014), suggesting the agonist is released rapidly and diminishes over time.

At this point in the study, this rapid release of $P2Y_6R$ agonist from BV-2 cells was considered sufficiently interesting to merit further investigation. Agonist levels released from cells after 1 minute in buffer were not significantly different to those at 10 minutes, so it was considered possible that the cells actively maintain a dynamic steady state of extracellular $P2Y_6R$ agonist, for example by balancing release with extracellular nucleotidase activity. To test this, BV2-conditioned flex buffer was supplemented with 5 nM UDP, and responses from reporter cells were measured, either immediately or after a further 10 minutes with cells (Figure 5.3B). A significant rise in detectable $P2Y_6R$ agonist was observed immediately after the addition of UDP compared to the 'BV-2s (5 minutes) – UDP' condition ($p=0.023$), which did not diminish after 10 minutes - suggesting that an extracellular equilibrium of agonist is not actively maintained by the cells, but rather, a specific level of agonist is rapidly released by the cells after exposure to fresh buffer.

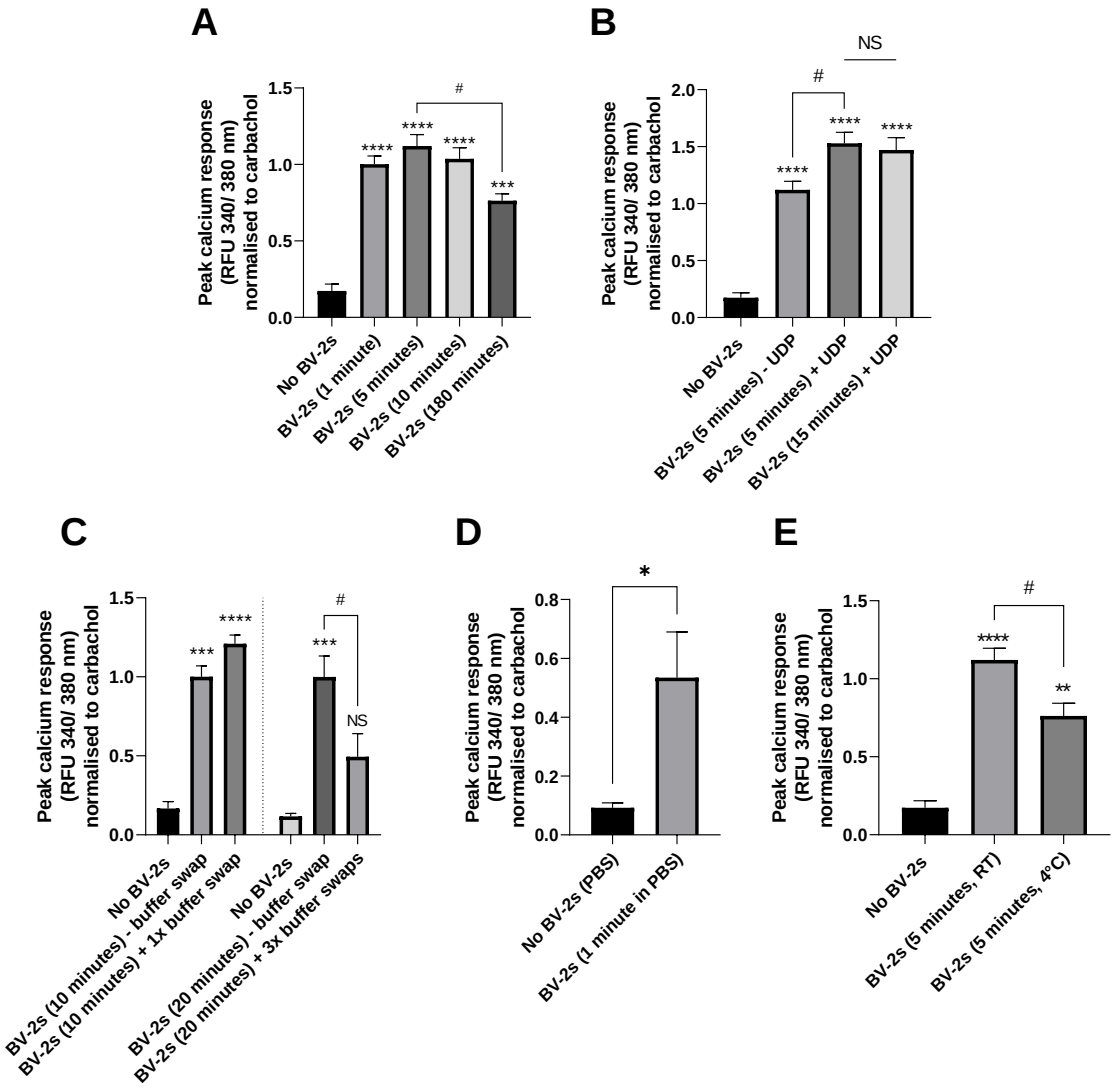

Figure 5.3. BV-2 microglia burst-release $P2Y_6R$ agonist into the extracellular space. (A) Flex buffer conditioned with BV-2 cells for just 1 minute contained significant levels of $P2Y_6R$ agonist compared to the 'no BV-2s' control, which was still present after 180 minutes (although at a significantly reduced level). (B) UDP (5 nM) added to buffer after 5 minutes with cells significantly increased $P2Y_6R$ agonist levels at 5 minutes, and this was not reduced after a further 10 minutes, suggesting extracellular $P2Y_6R$ agonist is not maintained at a steady-state by the cells. (C) Levels of $P2Y_6R$ agonist in buffer conditioned with cells for 10 minutes is not reduced by applying a single buffer swap after 5 minutes; levels in buffer conditioned with cells for 20 minutes is significantly reduced by applying 3 buffer swaps at 5, 10 and 15 minutes with cells, indicating a finite capacity for extracellular $P2Y_6R$ agonist release by the cells. (D) BV-2 release of $P2Y_6R$ agonist is retained using PBS instead of flex buffer (note that responses to carbachol were unchanged in PBS versus flex buffer; data not shown). (E) BV-2 release of $P2Y_6R$ agonist is significantly inhibited at 4°C compared to room temperature. Values are means ± SEM of at least 3 independent experiments. Statistical comparisons were made via one-way ANOVA except for (D), which was by Student's t-test. All statistical comparisons were versus 'no BV-2s' contros unless otherwise indicated by a line. NS $p \geq 0.05$, *$p<0.05$, **$p<0.01$, ***$p<0.001$, ****$p<0.0001$ versus controls; #$p<0.05$ as indicated.

To explore whether this release might result from an osmotic shift from culture medium to flex buffer, $P2Y_6R$ agonist release from BV-2s subjected to multiple buffer replacements (i.e. from buffer to buffer) was tested (Figure 5.3C). BV-2 cells conditioned with flex buffer for 10 minutes (with no interim buffer replacement) released similar levels of $P2Y_6R$ agonist as cells conditioned with buffer for 10 minutes but with an interim buffer replacement at 5 minutes

(p=0.527). This was particularly interesting as it suggested that i) $P2Y_6R$ agonist release does not occur due to the osmotic shift from culture medium to flex buffer, and that ii) BV-2s release a specific amount of $P2Y_6R$ agonist into the flex buffer, but this amount does not reflect their full capacity for release. To determine the number of buffer swaps required to deplete $P2Y_6R$ agonist stores from the cells, swaps were performed successively, and agonist levels measured as before. After 2 buffer swaps, there was an indication of a drop in agonist release compared to the time-matched control without swaps, although high variability in the data made it difficult to draw a conclusion (data not shown). After 3 buffer swaps, there was a significant drop in agonist levels compared to the time-matched 'BV-2s (20 minutes) + 3x buffer swaps' control (p=0.017), to levels that were not significantly different from the 'no BV-2s' control (p=0.093; Figure 5.3C).

Despite being a basic buffer solution, flex buffer contains a variety of salts that could potentially induce nucleotide release from cells i.e. $P2Y_6R$ agonist release from the BV-2s. To test whether salts dispensable for maintaining short-term cell viability could be responsible for the agonist release, BV-2s were conditioned with PBS instead of flex buffer, and agonist presence was measured as before (Figure 5.3D). Significant levels of $P2Y_6R$ agonist were detected in PBS conditioned with cells for 1 minute, compared to the 'no BV2s (PBS)' control (p=0.022).

Finally, to test whether release of $P2Y_6R$ agonist by BV-2s was temperature-sensitive (indicating whether release of the agonist occurs passively or via a controlled cellular process), BV-2 release of agonist into buffer at either room temperature or 4°C was measured as before. Whilst agonist was detected in the 4°C buffer compared to the 'no BV-2s' control (p=0.003; Figure 5.3E), levels were significantly lower than from the time-matched condition at room temperature (p=0.022), indicating that this process is temperature-sensitive.

5.2.2. PC12 pheochromocytomas and 1321N1 astrocytes burst-release extracellular $P2Y_6R$ agonist

All major cell-types in the brain can generate intracellular UDP, opening the possibility that cell-types other than microglia may be capable of releasing $P2Y_6R$ agonist extracellularly. To test this, neuron-like PC12 cells were conditioned with flex buffer as for the BV-2s, and presence of $P2Y_6R$ agonist was measured as before. Significant responses were observed from $P2Y_6R$-reporter cells after applying flex buffer conditioned with PC12s for 60 minutes, compared to the 'no PC12s' control ($p<0.001$), and such responses were absent in $P2Y_6R$-lacking control cells (Figure 5.4A). As for the BV-2s, this agonist was eliminated after treatment with apyrase (Figure 5.4B), indicating nucleotide agonist and consistent with UDP. Given the rapid release of agonist from BV-2 cells, flex buffer was conditioned with PC12s for a similar range of durations. Buffer conditioned with PC12s for 1 minute contained significant levels of $P2Y_6R$ agonist compared to the 'no PC12s' control (Figure 5.4C), which was not significantly lower than those found in buffer conditioned for 60 minutes ($p=0.170$) (note that a 180 minute condition was not tested here). Together, these data demonstrate that PC12s can burst-release nucleotide agonist of $P2Y_6R$, and demonstrate that this phenomenon is not specific to microglial BV-2s.

To test whether $P2Y_6R$ agonist can be released from astrocytes in a similar manner, 1321N1 cells were conditioned with flex buffer as for the BV-2s and PC12s, and presence of $P2Y_6R$ agonist was measured as before. Interestingly, no detectable responses from $P2Y_6R$-expressing reporter cells were observed after applying buffer conditioned with 132N1s for 1 or 10 minutes compared to the 'no 1321N1' controls ($p=0.329$ & 0.988 respectively; Figure 5.4D). Microglia[485] and neuron-like PC12s[707], but not 1321N1 astrocytes[708], express $P2Y_6R$. Data obtained thus far were consistent with a model in which pools of $P2Y_6R$ agonist are retained at, or close to, the surface of BV-2s and PC12s, opening the possibility that such pools may be attached to exposed $P2Y_6R$ by BV-2s and PC12s (but not 1321N1s). To further explore this, 1321N1s stably-transfected with $P2Y_6R$ were subjected to the same buffer-conditioning experiment, and presence of $P2Y_6R$ agonist was measured as before. However, expression of $P2Y_6R$ was not found to promote any release of $P2Y_6R$ agonist from the 1321N1s compared to the same cells lacking $P2Y_6R$ at either 1 minute or 10 minutes in buffer ($p=0.823$ & 0.998 respectively; Figure 5.4D). It should be noted that presence of agonist in buffer conditioned by

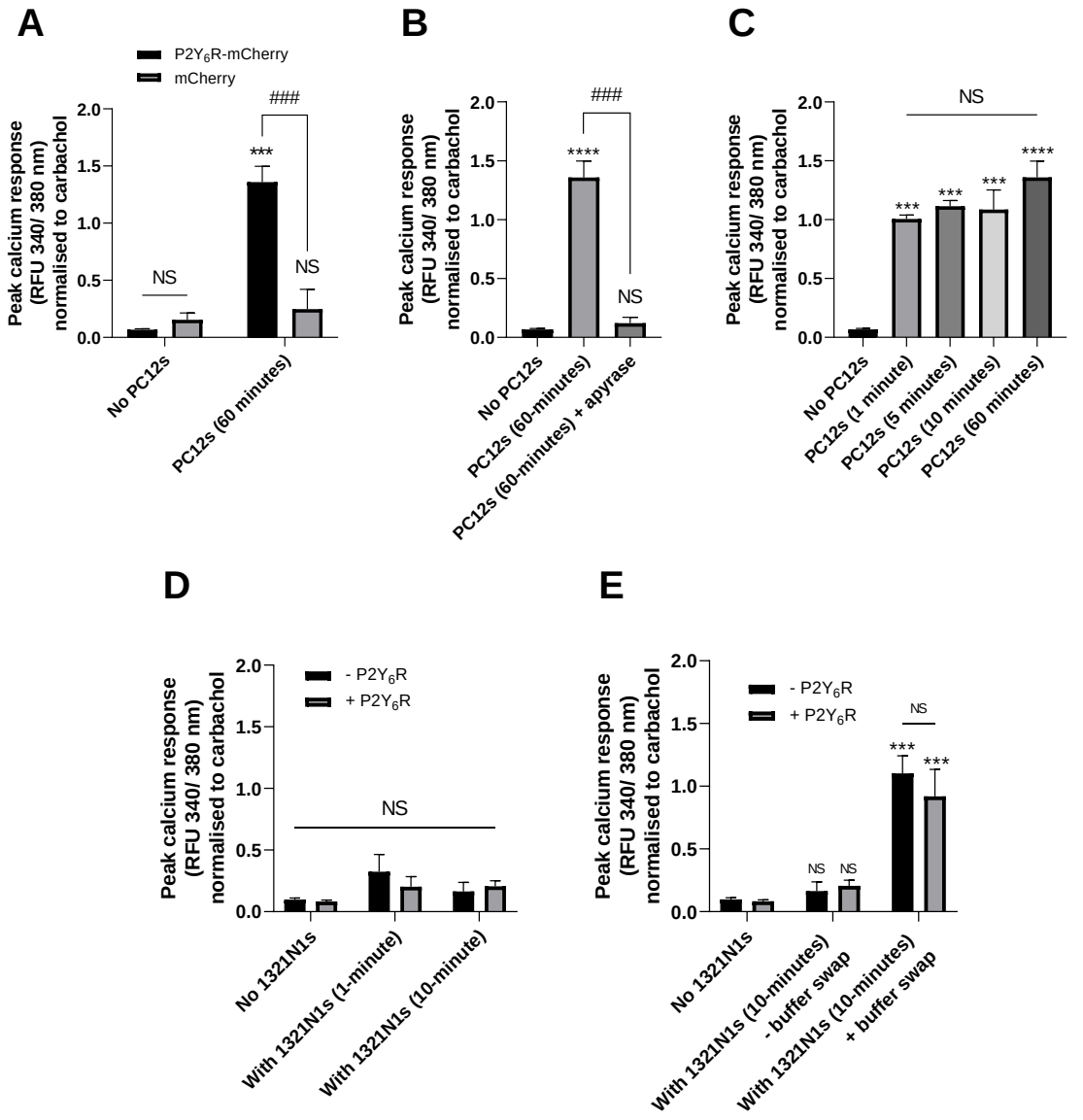

Figure 5.4. PC12 pheochromocytomas and 1321N1 astrocytes burst-release $P2Y_6R$ agonist into the extracellular space. (A) Flex buffer conditioned with PC12 cells for 60 minutes contained significant levels of $P2Y_6R$ agonist compared to the 'no PC12s' control, or compared to responses from 1321N1s lacking $P2Y_6R$ (as indicated). (B) $P2Y_6R$ agonist released by PC12s is eliminated by treating the conditioned buffer with apyrase (1 U/ml, 10 minutes). (C) PC12s released significant levels of $P2Y_6R$ agonist into flex buffer within 1 minute, which was not significantly different from that detected after 60 minutes. (D) Flex buffer conditioned with 1321N1 cells (either expressing or lacking $P2Y_6R$) for 1 or 10 minutes contained no detectable levels of $P2Y_6R$ agonist compared to the 'no 1321N1s' controls. (E) $P2Y_6R$ agonist release from 1321N1 cells was induced by applying an interim buffer swap after 5 minutes compared to the 'no 1321N1 control', or compared to the same conditioning time without a buffer swap. Values are means ± SEM of at least 3 independent experiments. Statistical comparisons were made via one- or two-way ANOVA; all statistical comparisons versus 'no PC12s' or 'no 132N1s' controls unless otherwise indicated by a line. NS $p \geq 0.05$, ***$p<0.001$, ****$p<0.0001$ versus controls; ###$p<0.001$.

either $P2Y_6R$-expressing or $P2Y_6R$-lacking 1321N1 cells for 60 minutes was also tested, with an indication that both lines release agonist over this extended time range, although this was not confirmed with 3 independent experiments (data not shown). Unexpectedly, significant levels of $P2Y_6R$ agonist were detected in buffer conditioned with 1321N1s (either expressing

or lacking $P2Y_6R$) for 10 minutes that had been subjected to an interim buffer swap at 5 minutes, compared to respective time-matched conditions (p=0.001 & 0.004 respectively; Figure 5.4E).

Taken together, these data demonstrate that a variety of cells – including microglia, astrocytes, and neuron-like PC12s - release $P2Y_6R$ agonist into the extracellular space under specific culture conditions. This has implications for $P2Y_6R$-agonist reporter systems, as well as for neurophysiology more broadly.

5.2.3. Inflammatory activated BV-2s release extracellular $P2Y_6R$ agonist

An original aim was to identify whether microglial release of $P2Y_6R$ agonist can be induced by inflammatory activation (i.e. with LPS), but performing a media swap to the cells induced a burst release of the agonist which may have hidden any LPS-induced release. Since extracellular agonist diminished slightly over time (Figure 5.3A), incubation of BV-2s in flex

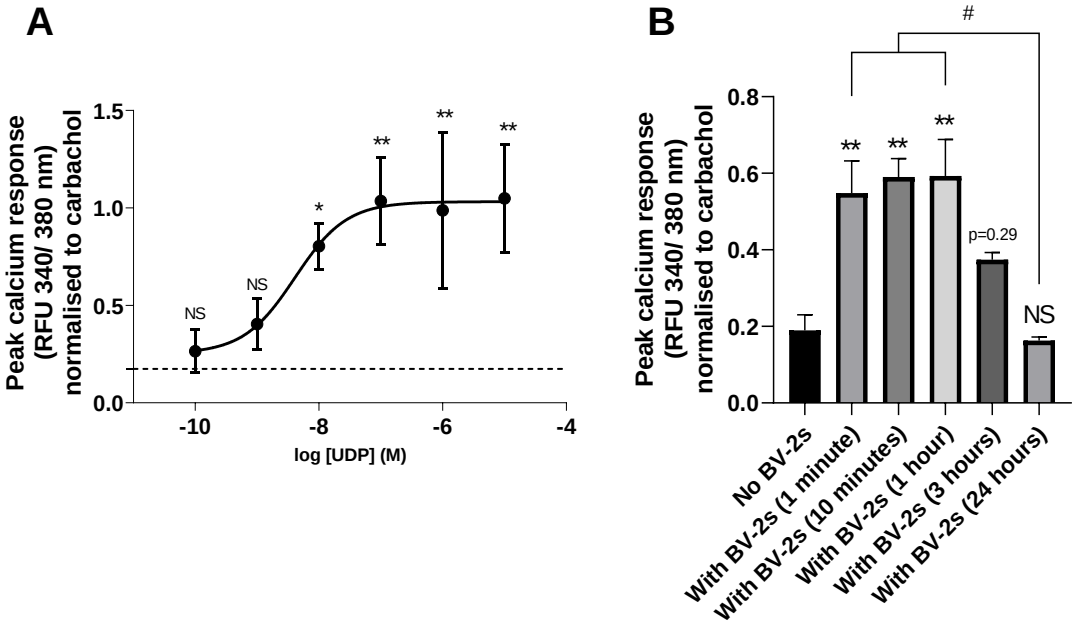

Figure 5.5. BV-2 release of $P2Y_6R$ agonist into extracellular media diminishes after 24 hours. (A) $P2Y_6R$ dose-response to UDP in DMEM-F12 + 0.5% FBS (flex media) as vehicle. $P2Y_6R$-expressing cells respond to UDP down to at least 10 nM compared to the vehicle control (dotted lne). (B) BV-2 cells burst release $P2Y_6R$ agonist into flex media within 1 minute, but levels diminish by 24 hours compared to the 'no BV-2s' control. Values are means ± SEM of at least 3 independent experiments. Statistical comparisons were made via one-way ANOVA. NS $p \geq 0.05$, *$p<0.05$, **$p<0.01$ versus controls; #$p<0.05$.

buffer for 24 hours was attempted; however, viability was severely reduced (data not shown) and so this was not considered suitable for such an investigation. To circumvent this, DMEM-F12 + 0.5% serum ('flex media') - which is an appropriate culture medium for BV-2 maintenance - was tested for suitability as a vehicle for UDP in the $P2Y_6R$ reporter system (Figure 5.5A). UDP was found to induce calcium responses from the reporter cells when flex media was used as vehicle, with detectable responses observed down to 10 nM compared to

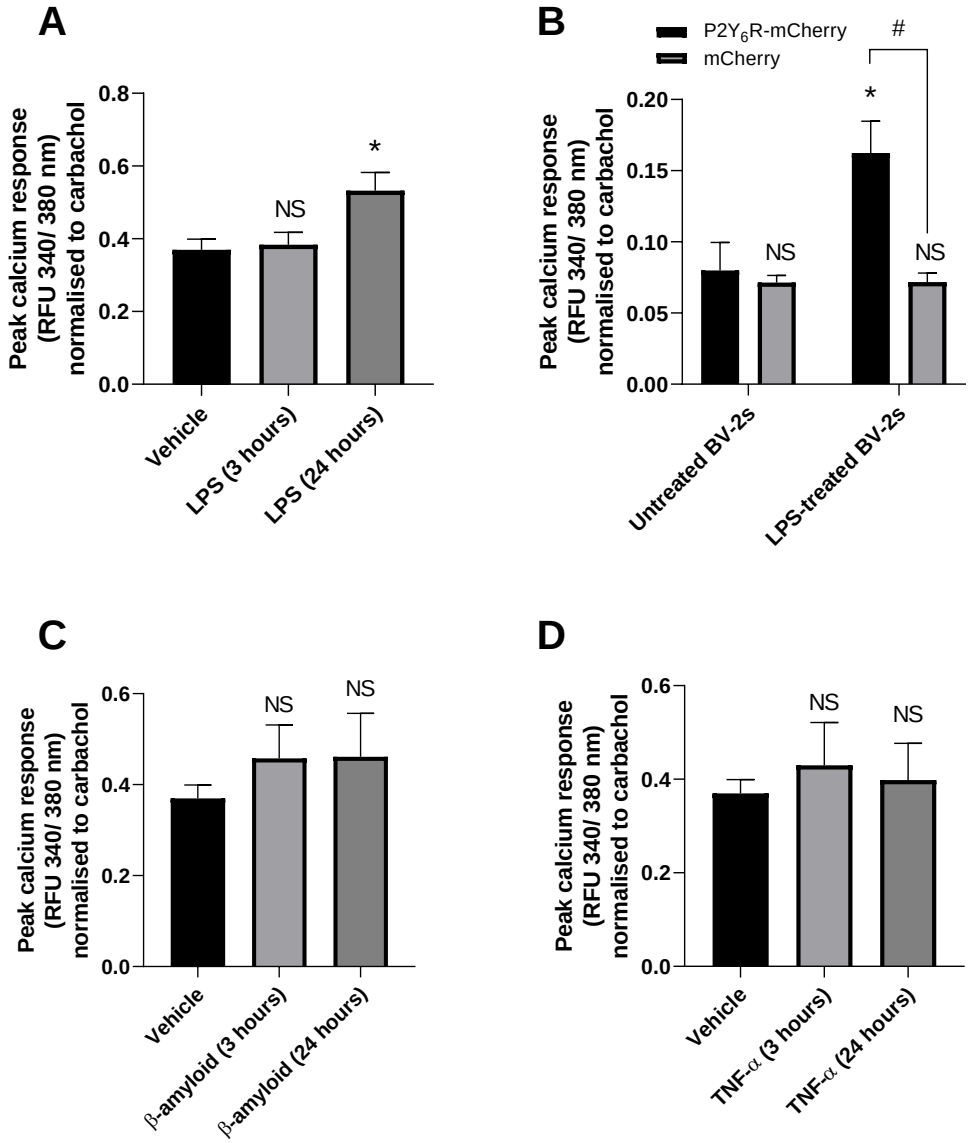

Figure 5.6. LPS-activated BV-2 microglia release $P2Y_6R$ agonist into the extracellular media. (A & B) BV-2 microglia treated with LPS (100 ng/ml) for 24 (but not 3) hours release significant levels of $P2Y_6R$ agonist into the extracellular media (A); this induced calcium responses from $P2Y_6R$-expressing, but not $P2Y_6R$-lacking, 1321N1 reporter cells, when compared to the 'untreated BV-2s' control (B). (C) BV-2 microglia treated with β-amyloid (250 nM) for 3 or 24 hours do not release extracellular $P2Y_6R$ agonist compared to the 'vehicle' control. (D) BV-2 microglia treated with TNF-α (50 ng/ml) for 3 or 24 hours do not release extracellular $P2Y_6R$ agonist compared to the 'vehicle' control. Note that, due to variable interference at the 380 nm wavelength, RFU values shown in (A), (C) and (D) are not ratiometric, but are simply the RFUs at 340 nm. Values are means ± SEM of at least 3 independent experiments. Statistical comparisons were made via one- or two-way ANOVA. NS $p \geqslant 0.05$, *$p<0.05$ versus controls; #$p<0.05$.

the vehicle control (p=0.041), and so was considered suitable for conditioning with BV-2s for longer time periods. BV-2s were conditioned with flex media for 1 minute, 10 minutes, 1, 3 or 24 hours, and presence of $P2Y_6R$ agonist was measured as before (Figure 5.5B). As expected, significant levels of $P2Y_6R$ agonist were detected in media conditioned with cells for 1 minute (p=0.010), 10 minutes (p=0.004) and 1 hour (p=0.004) compared to the 'no BV2s' control. Levels were reduced after 3 hours (as found before), and completely abolished after 24 hours (p=0.999 compared to control), indicating that a conditioning period of at least 24 hours would be suitable for further tests. BV-2s cultured in flex media were treated with vehicle or LPS for 3 or 24 hours, and $P2Y_6R$ agonist presence was measured as before. Compared to the vehicle, a small but significant increase in detectable $P2Y_6R$ agonist was observed after 24 hours LPS treatment (p=0.041), but not after 3 hours LPS treatment (p=0.971; Figure 5.6A). Importantly, $P2Y_6R$ agonist released after 24 hours LPS did not induce calcium responses from reporter cells lacking $P2Y_6R$ (Figure 5.6B). No such induction of agonist release was observed after treatments with β-amyloid (Figure 5.6C) or TNF-α (Figure 5.6D). Together, these data suggest that microglia inflammatory-activated by LPS, but not by β-amyloid or TNF-α, release extracellular agonist of $P2Y_6R$.

5.2.4. *E. coli* release $P2Y_6R$ agonist into the extracellular space

To test whether bacteria release $P2Y_6R$ agonist, live *E. coli* were resuspended in flex buffer and added directly to $P2Y_6R$ reporter cells. A dramatic calcium response was observed from $P2Y_6R$-expressing 1321N1 cells, which was substantially greater than the response from cells lacking $P2Y_6R$ (Figure 5.7A). Comparing peak response values between conditions (as before), a significant calcium response was observed from $P2Y_6R$ -expressing cells treated with *E. coli* compared to vehicle (p<0.0001; Figure 5.7B) which was significantly higher than responses from $P2Y_6R$-lacking cells subjected to the same treatment (p=0.003). These data indicate that foreign bacteria (*E. coli*) as well as host cells (microglia, astrocytes and neurons) can release $P2Y_6R$ agonist extracellularly.

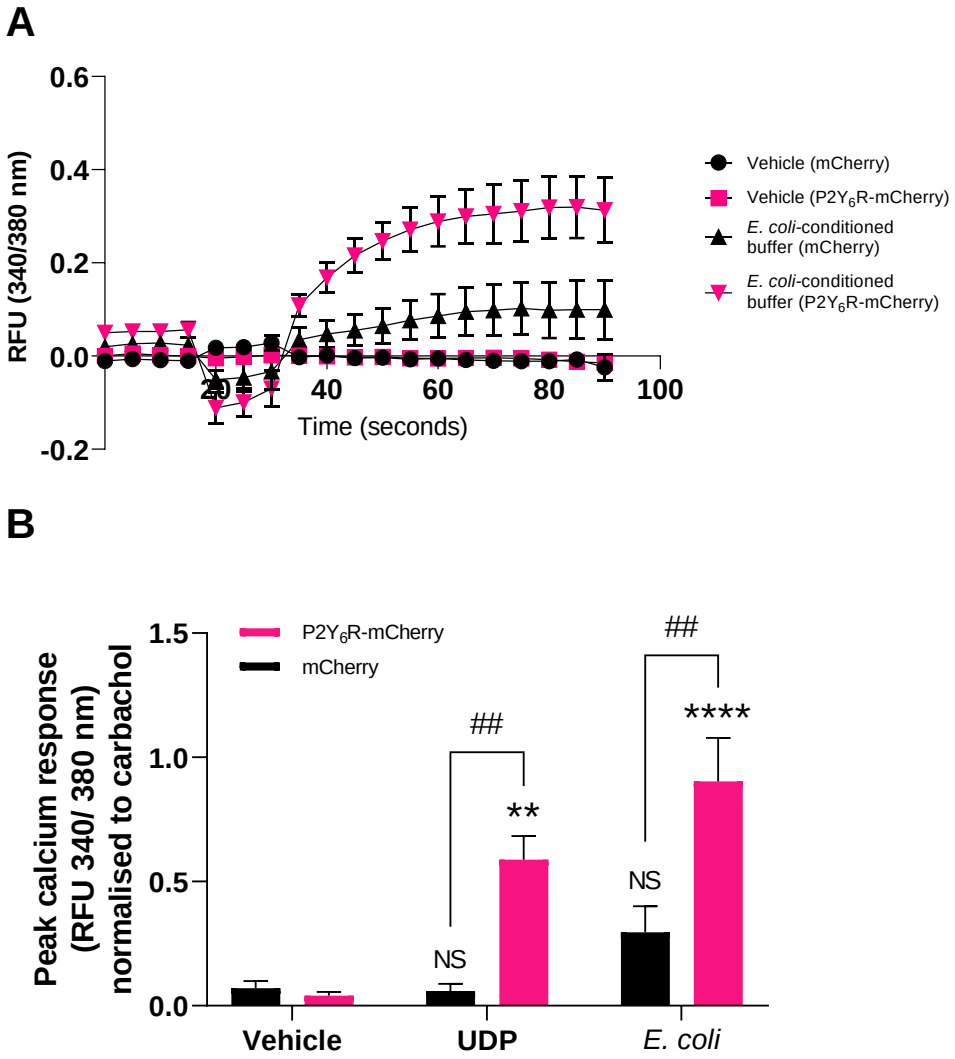

Figure 5.7. *E. coli* release P2Y$_6$R agonist into the extracellular space. (A) *E. coli*-containing flex buffer induces a rapid calcium response from P2Y$_6$R-reporter cells, which is substantially greater than that from P2Y$_6$R-lacking cells. No calcium response in either cell line was observed from buffer alone. (B) Quantification of peak calcium responses observed in each condition after normalisation to the carbachol control. UDP (100 μM) and *E. coli*-containing buffer both induced a significant calcium response from P2Y$_6$R-expressing, but not P2Y$_6$R-lacking, cells, compared to their respective 'vehicle' controls. Values are means ± SEM of at least 3 independent experiments. Statistical comparisons were made via two-way ANOVA. NS $p \geq 0.05$, **$p<0.01$, ****$p<0.0001$ versus controls; ##$p<0.01$ as indicated.

5.2.5. UDP induces microglial phagocytosis of *E. coli*, which is inhibited by MRS2578

To test whether extracellular P2Y$_6$R agonist can induce microglial phagocytosis of bacteria, primary rat microglia were treated with UDP and incubated with pHrodo-conjugated *E. coli*, and phagocytosis was measured via flow cytometry. Due to high variation in absolute

measurements, logarithmic comparisons were considered more appropriate. UDP applied to microglia immediately after addition of bacteria significantly increased their phagocytosis by primary rat microglia by 109 ± 37% when co-incubated for 30 minutes (p=0.012, Figure 5.8A). To test whether UDP-induced phagocytosis occurs through microglial $P2Y_6R$, the $P2Y_6R$-

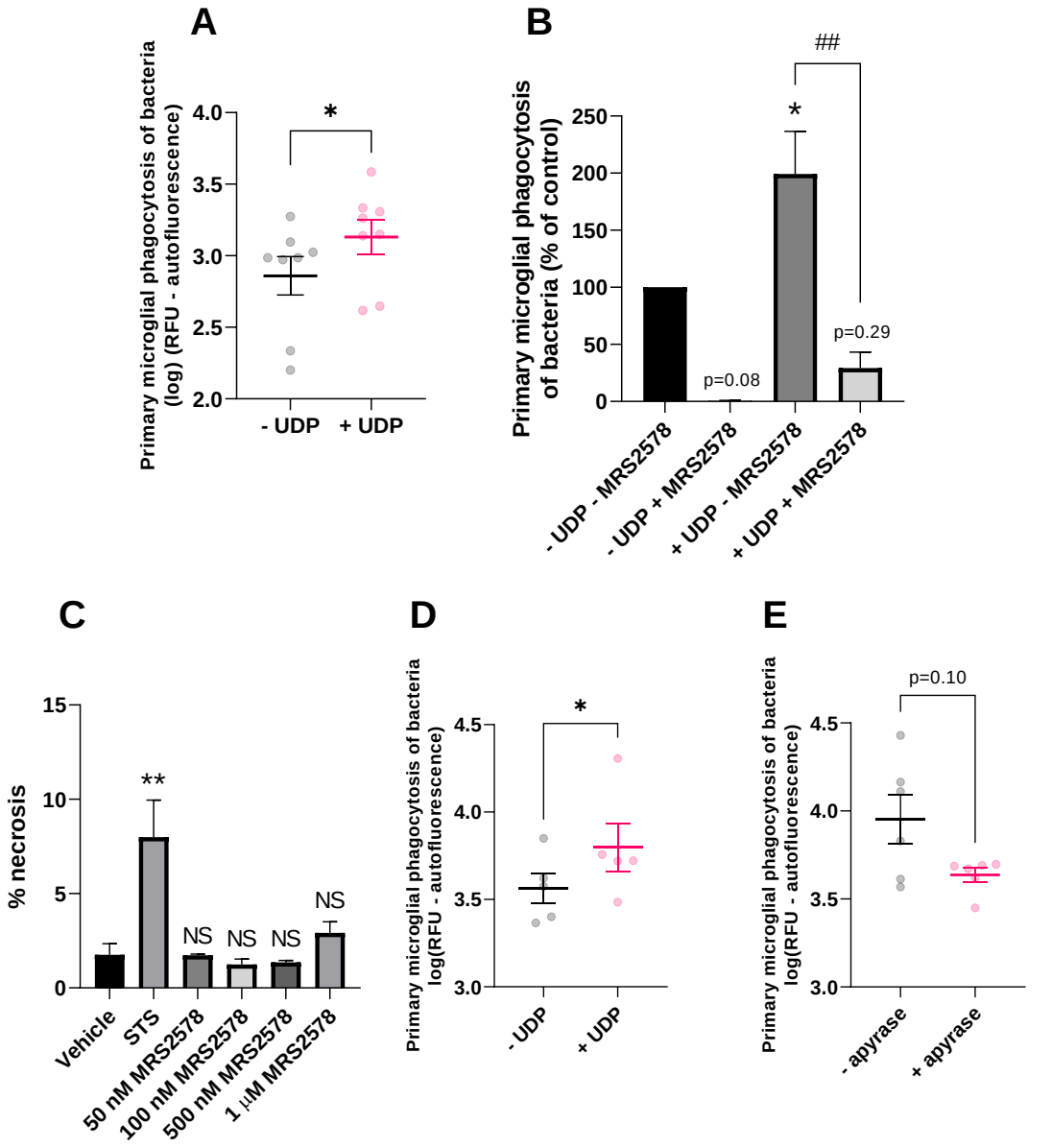

Figure 5.8. UDP induces microglial phagocytosis of *E. coli*, which is blocked by MRS2578. (A) Acute UDP (1 mM) increases phagocytosis of *E. coli* by primary rat microglia. (B) MRS2578 (1 μM) - a $P2Y_6R$ blocker - inhibited phagocytosis of *E. coli* by primary rat microglia when compared to the '- UDP - MRS2578' control, and also inhibited UDP-induced phagocytosis. (C) MRS2578 does not cause necrosis of primary rat microglia over 2 hours, as determined by the percentage of cells stained with propidium iodide and compared to the 'vehicle' control. Staurosporine (20 μM) was used as a positive control for cell death. (D) Acute UDP (1 mM) increased phagocytosis of *E. coli* by primary mouse microglia. (E) Apyrase (2 U/ml) reduced phagocytosis of *E. coli* by primary rat microglia when applied 30 minutes prior to coincubation, although this did not reach statistical significance. Values are means ± SEM of at least 3 independent experiments. Statistical comparisons were made via Student's t-test (A, D & E) or one- or two-way ANOVA as appropriate (B & C) . *p<0.05, **p<0.01 versus controls; ##p<0.01 as indicated.

specific blocker MRS2578 (24) was used. MRS2578 abolished phagocytosis in the presence and absence of exogenous UDP (Figure 5.8B), and this treatment did not induce detectable necrosis of the microglia (Figure 5.8C), indicating that i) UDP activates $P2Y_6R$ to induce phagocytosis, and ii) phagocytosis in control conditions requires $P2Y_6R$, possibly mediated by $P2Y_6R$ agonist release by the *E. coli* (Figure 5.7B). To support the notion that UDP-induced phagocytosis occurs through $P2Y_6R$, primary microglia from mouse (of which wild-type and $P2Y_6R$ knockout strains are available in our lab) were subjected to a similar test. UDP was also found to significantly enhance phagocytosis of *E. coli* by wild-type primary mouse microglia by 84 ± 34% (p=0.040, Figure 5.8D). However, due to problems with litter availabilities, no conclusive result has yet been obtained for the $P2Y_6R$ KO microglia.

To further support the idea that extracellular $P2Y_6R$ agonist (i.e. UDP) promotes bacterial phagocytosis, the ability of apyrase (which degrades UDP to UMP/uridine, compounds shown as incapable of activating $P2Y_6R$ at physiological concentrations; Figure 5.1E) to inhibit phagocytosis was tested. Application of apyrase (2 U/ml) to the microglia for 30 minutes prior to coincubation with *E. coli* inhibited phagocytosis of the bacteria by 35.0% on average (± 20; Figure 5.8E), although this effect did not reach statistical significance (p=0.10).

Data shown in Figure 5.8 represents a UDP induction effect optimised empirically - prior to this, UDP pre-treatment and co-incubation times were varied. Interestingly, application of UDP to microglia 15 minutes prior to addition of bacteria to microglia did not induce any phagocytosis of *E. coli* by BV-2 (Figure 5.9A) or primary rat microglia (Figure 5.9B) after 60 minutes co-incubation. Changing the pre-treatment time to 60 minutes also had no inductive effect on phagocytosis (Figure 5.9C), suggesting that UDP may induce an acute increase in phagocytic capacity of the microglia, but cannot induce phagocytosis if UDP pre-treatment time and/or co-incubation time is extended. UDP has been suggested to be involved in the LPS-induced activation phenotype of BV-2 microglia[430], and LPS-activation of microglia enhances their phagocytosis of bacteria (Chapter 4). Thus, the ability for UDP to induce microglial phagocytosis of *E. coli* after chronic exposure was tested. UDP (100 μM) applied 18 hours prior to addition of bacteria increased phagocytosis of *E. coli* by primary rat microglia by 102% ± 55 (p=0.08; Figure 5.9D) after 30 minutes co-incubation, although this increase did not reach statistical significance. To test whether this increase was mediated via $P2Y_6R$, UDP induction

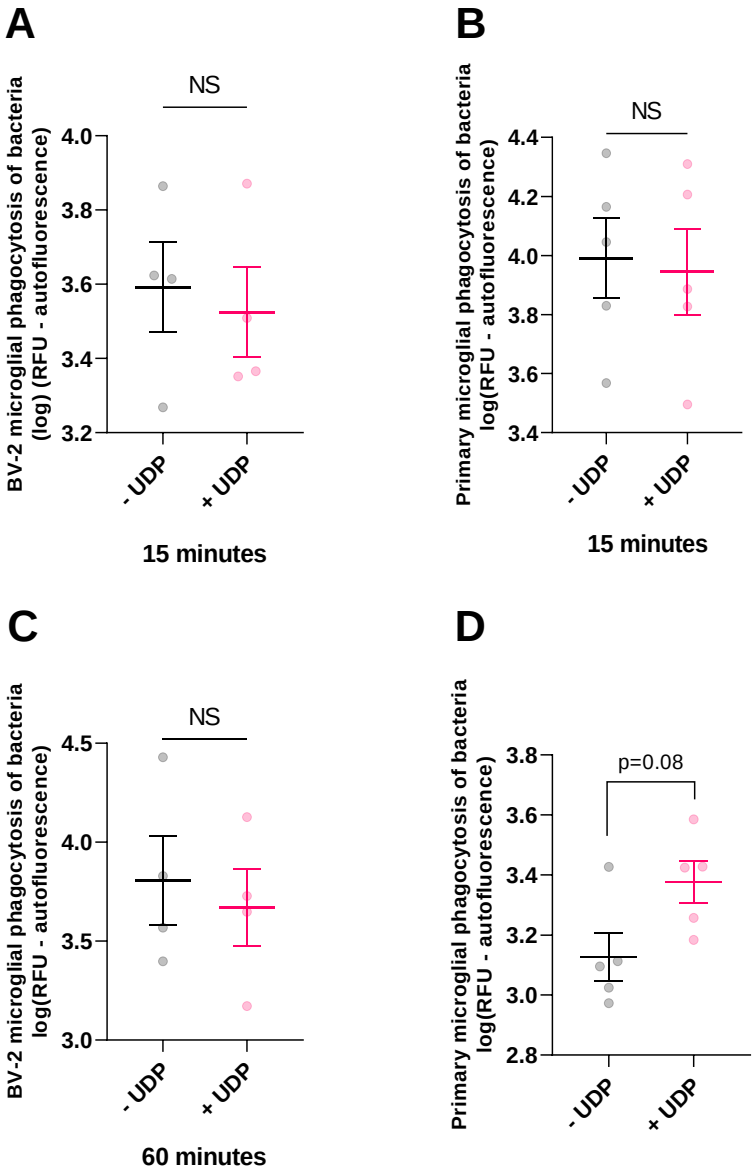

Figure 5.9. UDP induction of microglial phagocytosis of *E. coli* is time-sensitive. (A & B) UDP (1 mM) did not increase phagocytosis of *E. coli* by primary rat microglia (A) or BV-2s (B) when applied 15 minutes prior to co-incubation, compared to the '- UDP' controls. (C) UDP (1 mM) did not increase phagocytosis of *E. coli* by primary rat microglia when applied 60 minutes prior to co-incubation. (D) UDP (100 μM) increased phagocytosis of *E. coli* by primary rat microglia after 18 hours. Values are means ± SEM of at least 3 independent experiments. Statistical comparisons were made Student's t-test. NS $p \geq 0.05$ as indicated.

of *E. coli* phagocytosis by rat microglia was tested ± MRS2578 as before; however, chronic MRS2578 treatment induced substantial necrotic death in the microglia (data not shown), so this could not be concluded.

5.2.6. LPS-induced microglial phagocytosis of *E. coli* is inhibited by apyrase and MRS2578

LPS treatment for 24 hours significantly increased microglial phagocytosis of *E. coli* (Chapter 4), and was also found to induce extracellular release of $P2Y_6R$ agonist by microglia (Figure 5.6). Thus, it is feasible that LPS-induced phagocytosis is facilitated through signalling between extracellular $P2Y_6R$ agonist (i.e. UDP) and microglial $P2Y_6R$. To investigate this, BV-2 or primary rat microglia were LPS-activated, and the ability of apyrase or MRS2578 to inhibit LPS-induced phagocytosis was measured. BV-2 microglial phagocytosis of *E. coli* was substantially enhanced by LPS pre-treatment (p=0.002 versus '- LPS – apyrase' control), and this induction was slightly reduced after 20 minutes pre-treatment with apyrase (2 U/ml), but not to any significant level (p=0.323) and such levels remained significantly greater than the control (p=0.014; Figure 5.10A). In contrast, LPS induced phagocytosis of *E. coli* by primary rat microglial phagocytosis was abolished by the same apyrase treatment to levels not significantly greater than the control (p=0.873; Figure 5.10B) - suggesting that this LPS-

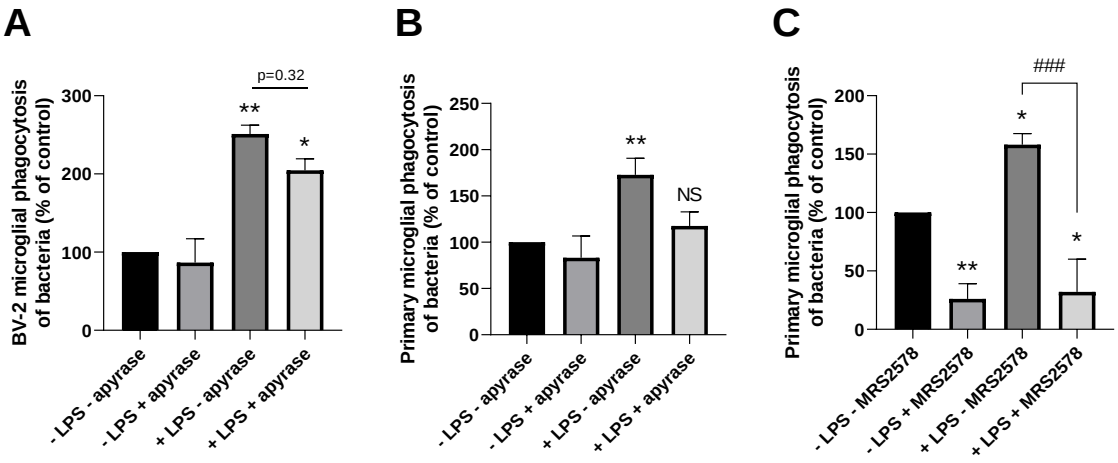

Figure 5.10. LPS-induced microglial phagocytosis of *E. coli* is inhibited by apyrase and MRS2578. (A) BV-2 microglial phagocytosis of *E. coli* induced by LPS (100 ng/ml) may be partially inhibited by apyrase (2 U/ml, 20 minutes). (B) Primary microglial phagocytosis of *E. coli* induced by LPS is inhibited by apyrase (2 U/ml, 20 minutes). (C) MRS2578 (1 μM) inhibited phagocytosis of *E. coli* by primary microglia when compared to the '- LPS - MRS2578' control, and also inhibited LPS-induced phagocytosis. In all cases, microglia were co-incubated with bacteria for 60 minutes. Values are means ± SEM of at least 3 independent experiments. Statistical comparisons were made via two-way ANOVA. NS $p \geq 0.05$, *$p<0.05$, **$p<0.01$ versus controls; ###$p<0.001$ as indicated.

induction effect is mediated by extracellular nucleotides, and consistent with involvement of nucleotide $P2Y_6R$ agonist (i.e. UDP). To test this further, the ability for MRS2578 to inhibit LPS-induced phagocytosis of *E. coli* by primary rat microglia was tested: again, MRS2578 significantly inhibited baseline phagocytosis (p=0.002), but also abolished the LPS-induction

effect ($p<0.001$; Figure 5.10C). Taken together, these data suggest that UDP-$P2Y_6R$ signalling is involved in phagocytosis of *E. coli* by both unactivated and LPS-activated microglia in culture.

5.2.7. ADP and $P2Y_{12}R$ may be involved in microglial phagocytosis of *E. coli*

In addition to $P2Y_6R$, $P2Y_{12}R$ is a well characterised microglial purinoreceptor demonstrated to promote microglial chemotaxis in response to ATP/ADP[709,368,710]. Given release of extracellular ATP from various bacterial strains has been reported[701], it is possible that ATP and/or ADP may promote chemoattraction of microglia toward bacteria via $P2Y_{12}R$, which could then promote microglial phagocytosis of the bacteria, but this has not been reported. So, the ability for either exogenous ADP or PSB0739 (a $P2Y_{12}R$ blocker) to inhibit microglial phagocytosis of *E. coli* was tested. ADP was found to inhibit BV-2 phagocytosis of *E. coli* by 53 ± 6% ($p=0.031$; Figure 5.11A), and to also inhibit primary rat microglial phagocytosis of *E. coli* by 62 ± 8% ($p=0.048$; Figure 5.11B), consistent with its role as a microglial chemoattractant toward bacteria (as exogenously applied ADP would mask any concentration gradient through which microglia could locate and migrate or extend processes toward bacteria). Furthermore, PSB0739 was found to inhibit BV-2 phagocytosis of *E. coli* by 97% ± 3 ($p=0.025$; Figure 5.11C) and also primary rat microglial phagocytosis of *E. coli* by 35% ± 10 ($p=0.009$; Figure 5.11D). Importantly, this same PSB0739 treatment was not shown to induce necrosis of the primary rat microglia (Figure 5.11E). Together, these data are consistent with a role for $P2Y_{12}R$ in mediating the migratory response of microglia toward the bacteria, thus facilitating phagocytosis.

To test whether ADP-$P2Y_{12}R$ signalling may also mediate LPS-induced phagocytosis of *E. coli* by microglia, the ability of ADP or PSB0739 to inhibit phagocytosis by LPS-activated microglia was investigated. ADP did not significantly inhibit the LPS-induced phagocytosis by BV-2s ($p=0.563$; Figure 5.12A) and such levels were significantly greater than the '- LPS + ADP' control ($p=0.010$). In contrast, ADP inhibited LPS-induced phagocytosis by primary rat microglia ($p<0.001$; Figure 5.12B) to levels that were not significantly different to either the '- LPS – ADP' control ($p=0.736$) or the condition with ADP alone ($p=0.934$), indicating that ADP can inhibit LPS-induced phagocytosis of *E. coli* by primary microglia. The abolition of *E. coli*

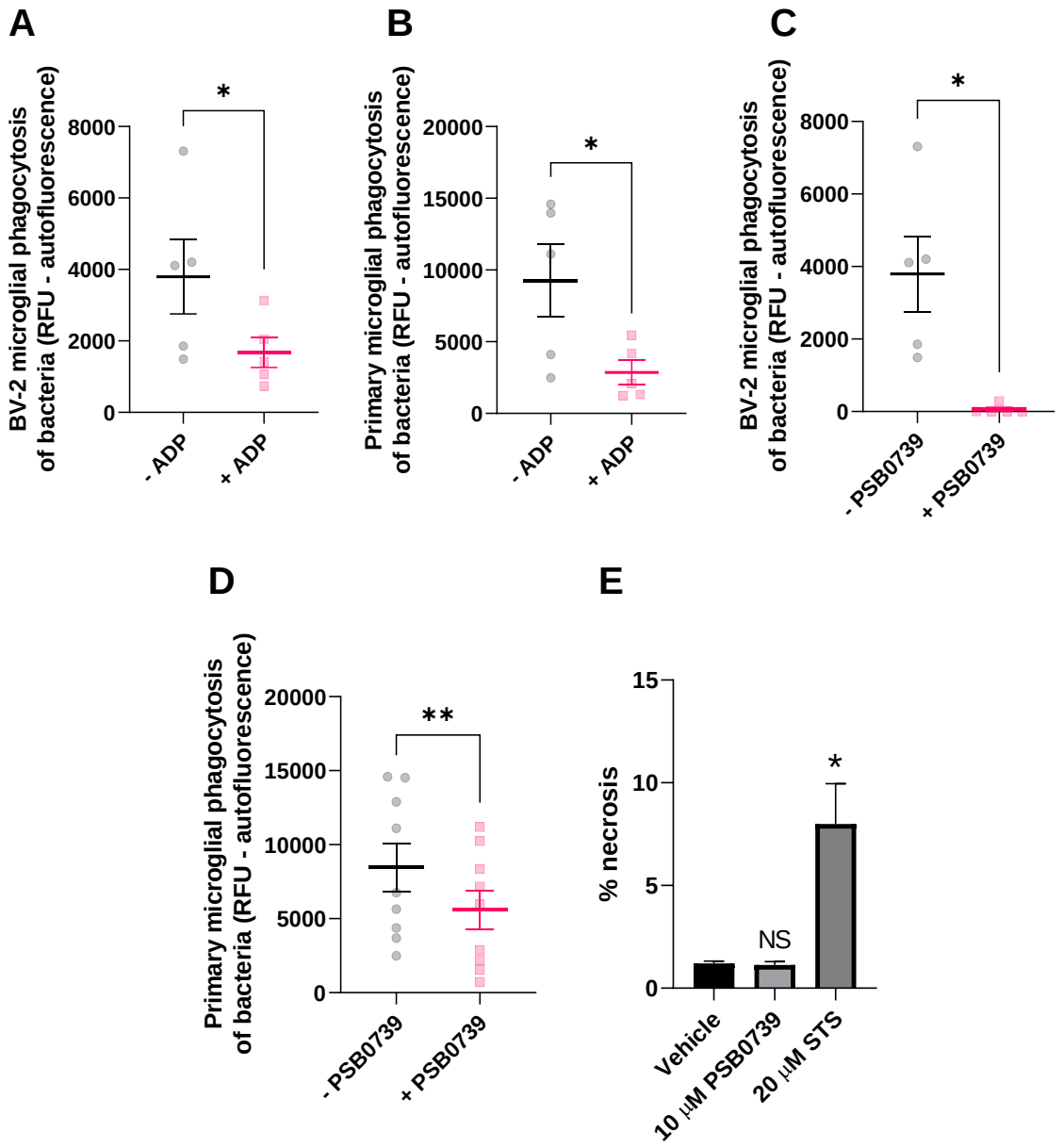

Figure 5.11. ADP and PSB0739 inhibit microglial phagocytosis of *E. coli*. (A & B) ADP (1 mM) inhibits phagocytosis of *E. coli* by BV-2 microglia (A) and also primary rat microglia (B), when applied 15 minutes prior to co-incubation. (C & D) The $P2Y_{12}R$ blocker PSB0739 (10 μM) inhibits phagocytosis of *E. coli* by BV-2 microglia (C) and also primary rat microglia (D) when applied 60 minutes prior to co-incubation. (E) PSB0739 does not induce necrosis in primary rat microglia, as determined by the percentage of cells stained with propidium iodide and compared to the 'vehicle' control. Staurosporine (20 μM) was used as a positive control for necrosis. Values are means ± SEM of at least 3 independent experiments. Statistical comparisons were made via Student's t-test, except for (E), which was via one-way ANOVA. NS $p \geq 0.05$, *$p<0.05$, **$p<0.01$ versus 'vehicle' controls, or as indicated.

phagocytosis by BV-2s that was induced by PSB0739 was lifted after LPS-activation of the microglia (Figure 5.12C). Similarly, in primary rat microglia, microglial phagocytosis of *E. coli* in the presence of PSB0739 was significantly increased by LPS (Figure 5.12D). Together, these data indicate a role for $P2Y_{12}R$ in microglial phagocytosis of bacteria by unactivated (but

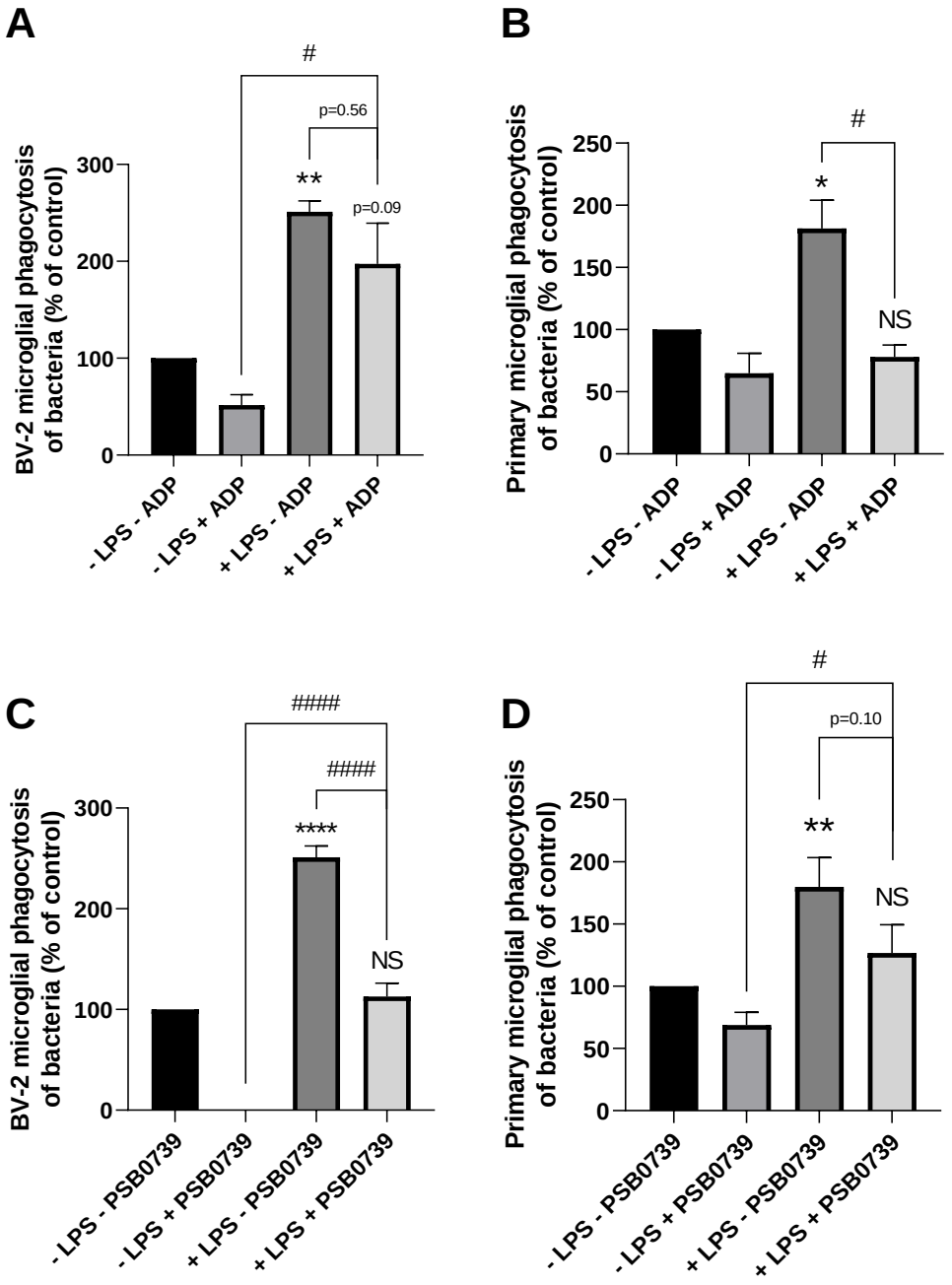

Figure 5.12. LPS-induced microglial phagocytosis of *E. coli* is inhibitable by ADP but not PSB0739. (A) LPS-induced phagocytosis of *E. coli* by BV-2 microglia was not inhibited by ADP (1 mM). (B) LPS-induced phagocytosis of *E. coli* by primary rat microglia is significantly inhibited by ADP (1 mM). (C) PSB0739 (10 μM) abolished phagocytosis of *E. coli* by BV-2s, but did not inhibit the LPS-induction of phagocytosis. (D) Similarly, PSB0739 (10 μM) did not inhibit the LPS-induction of phagocytosis by primary rat microglia. Values are means ± SEM of at least 3 independent experiments. Statistical comparisons were made via two-way ANOVA. NS $p \geq 0.05$, *$p<0.05$, **$p<0.01$, ****$p<0.0001$ versus controls (black bars); #$p<0.05$, ####$p<0.0001$ as indicated.

not LPS-activated) microglia, consistent with previous findings that LPS activation of microglia downregulates $P2Y_{12}R$[118].

5.3. Discussion

Much is known regarding the direct recognition of bacteria by macrophages via surface-expressed PRRs (see section 1.2.3), but less is known regarding immune responses to bacterial-released factors, such as nucleotides. In microglia, $P2Y_{12}R$ is expressed at high levels during normal homeostasis (i.e. in the M0 state), but is substantially downregulated following inflammation, such as LPS-induced inflammation[709]. *A priori*, this seems logical, as unactivated microglia (that have not been exposed to pathogens or tissue damage) require chemotactic receptors to mediate initial migratory responses to the infected or damaged site. After arrival at the site, such receptors are no longer necessary, and indeed may be counter-productive if they induce migratory responses away from the site before the issue is fully addressed. In contrast to $P2Y_{12}R$, $P2Y_6R$ is upregulated following inflammatory microglial activation[695,430], consistent with a role for $P2Y_6R$ in phagocytic elimination of dead or damaged cells at the point of inflammation. Koizumi *et al*[485] have shown that UDP is released from damaged neurons, and released UDP triggers removal of these cells by promoting microglial phagocytosis through $P2Y_6R$ activation.

Here, I show that live *E. coli* added to $P2Y_6R$ reporter cells significantly activated $P2Y_6R$, directly implicating $P2Y_6R$ in bacterial recognition, likely via bacterial release of UDP (although this was not confirmed). Moreover, exogenously applied UDP enhanced microglial phagocytosis of heat-inactivated *E. coli* when applied acutely, and the $P2Y_6R$ blocker MRS2578 abolished this phagocytosis in the presence or absence of UDP, consistent with a role for $P2Y_6R$ in phagocytic clearance of bacteria by microglia. UDP induction of phagocytosis was absent when cells were pre-treated (up to 60 minutes) with UDP, possibly due to desensitisation of $P2Y_6R$ following initial activation[694]. Inflammatory activation of BV-2 microglia by LPS triggered extracellular release of $P2Y_6R$ agonist. Since this was identified by me, Yang *et al*[430] have shown that BV-2s stimulated with LPS release UDP, and Qin *et al* observed similar effects in peripheral macrophages[711], consistent with my findings. LPS activation increased microglial phagocytosis of the *E. coli*, which was inhibited by i) apyrase and ii) MRS2578. Together, these data support a model (depicted schematically in Figure 5.13, page 187) whereby unactivated (M0) microglia recognise *E. coli*-released $P2Y_6R$ agonist, which directly induces the microglia to phagocytose the bacteria via $P2Y_6R$ signalling. As the microglia become inflammatory activated through PAMP recognition (and possibly by

extracellular nucleotides like UDP[430]), $P2Y_6R$ signalling is augmented through i) receptor upregulation[430] and ii) microglial release of $P2Y_6R$ agonist, which together enhance phagocytic clearance of the bacteria.

MRS2578 is widely used as a $P2Y_6R$ blocker[695,430,712,713,714], and is selective for $P2Y_6R$ over other P2Y-family receptors[715]. MRS2578 completely abolished phagocytosis of *E. coli* by primary rat microglia, and this was not due to any demonstrable necrotic death induced by the chemical, as tested by staining the microglia with propidium iodide. However, it cannot be ruled out that MRS2578 may be mediating off-target effects that contributed to such a large inhibition of phagocytosis. Findings here would certainly benefit from experiments using microglia genetically deficient in $P2Y_6R$. As mentioned, $P2Y_6R$ knockout animals are available in our lab, but poor litter availabilities precluded their use in a sufficient number of experiments to gather meaningful data. When available, microglia derived from these animals should be tested directly to assess effects of $P2Y_6R$ deletion on both UDP- and LPS-induced bacterial phagocytosis.

Outside the brain, UDP has been shown to promote host defences against *E. coli* in a mouse model of peritonitis[696]. In this model, intraperitoneal injection of UDP enhanced *E. coli* clearance and reduced mortality, and both effects were inhibited with MRS2578, directly implicating $P2Y_6R$ in this protection. In contrast, injected apyrase (which degrades UDP[702]) significantly impaired *E. coli* clearance, consistent with extracellular UDP (derived from bacteria and/or activated immune cells) facilitating bacterial clearance by the immune cells, possibly through phagocytosis. This idea is supported by the findings of Qin *et al*, who observed an increase in UDP levels in the peritoneal cavity of *E. coli*-infected mice[711]. They also showed that bacterial quantity in the peritoneal cavity was reduced in UDP-injected mice, and this reduction was prevented with MRS2578. Based on my data, such findings may be attributed to UDP-enhanced clearance of the bacteria through promotion of macrophage phagocytosis via $P2Y_6R$, although this would require testing. They also imply that UDP-$P2Y_6R$ signalling may be protective in the context of bacteria in the brain, but again, this would need testing.

$P2Y_6R$ in the brain may be a promising therapeutic target in the context of neurodegeneration-associated neuronal loss, as unpublished findings from our lab have implicated microglial $P2Y_6R$ signalling in the phagoptosis of viable neurons in both amyloidogenic and tauopathic models of AD, as well as in an LPS model of PD. Findings shown in this chapter have implications for use of $P2Y_6R$ as a therapeutic target. If $P2Y_6R$ signalling is indeed a fundamental means by which microglia (as the brain-resident macrophage) phagocytically clear pathogens like bacteria, inhibiting $P2Y_6R$ could have negative effects on immune responses against pathogens in the brain, particularly in immunocompromised patients. This is important, as immunodeficiency and progressive neurodegeneration are linked[716].

Despite extracellular UDP being reported in the aforementioned pathological contexts, UDP release from cells in the absence of inflammation or pathology has been poorly documented[489]. Using the $P2Y_6R$ cell-reporter system, I found that diverse cell-types – including microglia (BV-2), astrocytes (1321N1) and neuron-like pheochromocytoma (PC12) cells – rapidly released $P2Y_6R$ agonist extracellularly. At least in the cases of BV-2s and PC12s, this $P2Y_6R$ agonist was eliminated by apyrase, indicating a nucleotide agonist and consistent with UDP. $P2Y_6R$ agonist release from BV-2s was not inhibited by blocking pannexin- or connexin-based hemichannels (known to facilitate nucleotide release from cells[717]), and the release persisted even after multiple media swaps. Whilst it was originally considered possible that the BV-2s actively maintain a steady state of extracellular $P2Y_6R$ agonist, this was considered unlikely after finding exogenous UDP did not negate BV-2 generated $P2Y_6R$ agonist release, but rather supplemented such release, as shown by increased calcium responses from the $P2Y_6R$ reporter cells. Such findings are more consistent with a burst release of UDP at sub-saturating levels (with respect to $P2Y_6R$ activation). What was particularly striking was the fact that the same sub-saturating levels were released by BV-2s after multiple successive media swaps, with extracellular levels found to diminish only after several swaps. The fact that this effect was slightly (but significantly) inhibited in ice-cold temperatures indicate that this is a metabolic process. It remains unclear how such agonist is released by the cells, or what role this may play in normal cellular physiology. One possibility is that extracellular UDP is in rapid equilibrium with high affinity binding sites on the surface of the cells, so that when the medium is changed UDP is released from the surface of the cells into the medium. Note that if the agonist being released is UDP, as seems likely, then the concentration of UDP reached extracellularly is approximately 1 nM - equivalent to the release of less than 1 picomole of UDP by the cells.

Thus, very small amounts of UDP bound to the surface of the cells with a dissociation constant of approximately 1 nM could buffer extracellular UDP levels at this concentration.

What might trigger $P2Y_6R$ agonist release from these cells? Outside the brain, it has been shown that osteoblasts can release ATP after simple mechanical stimulation with a glass pipette[718]. This release was not due to vesicular exocytosis, but rather attributed to transient (10 - 100 millisecond) permeabilisation of the cell membrane. Released ATP stimulated calcium responses from neighbouring cells, and was suggested to play a mechano-adaptive role in skeletal development[718], although it is not obvious how such a phenomenon may be physiologically relevant in the context of the brain. However, it is possible that the release by BV-2 (and 1321N1 and PC12) cells was due to transient membrane permeabilisation induced by the physical stimulation of the media swap. An alternative explanation is provided by mechano-sensitive channels. Also known as stretch-activated channels[719], these are widely expressed in muscular, vascular, neurosensory and epithelial tissues. Importantly, microglia (as well as astrocytes) are highly mechanosensitive cells[720], and both can detect changes in stiffness of their surrounding tissue through stretch-activated channels expressed on their membrane[721,722], such as the astrocyte-expressed channel Piezo1[720]. Indeed, such channels have been implicated in the detection of (relatively stiff) amyloid plaques by glial cells in the context of AD[720]. Moreover, stretch-activated channels are known to regulate cellular mechano-transduction through release of ATP from expressing cells[723,724]. Thus, it is possible that the nucleotide release observed by BV-2s, 1321N1s and PC12s results from mechano-stimulation of the cells that would inevitably have occurred during the media swap. Whether the activation of $P2Y_6R$ that resulted from such release is physiologically relevant remains an open question, although it may promote microglial phagocytosis of proximal cells exerting physical pressure on the microglia to facilitate normal cell turnover, or to tackle tumour growth. Alternatively, the physical stresses that inevitably accompany phagosome formation during normal phagocytosis may release $P2Y_6R$ agonist to help complete the phagocytic process via $P2Y_6R$ signalling.

Regarding $P2Y_{12}R$: $P2Y_{12}R$ activation occurs after exposure to ATP or ADP[692], and these nucleotides can originate from multiple host- or pathogen-derived sources. Viable cells (and also dying cells[725]) can release ATP extracellularly through opening of pannexin- and/or

connexin-based hemichannels expressed on their surface[717]. ATP and ADP can also be released as the cell membrane permeabilises during necrotic death, and as such, has been described as a DAMP[726]. ATP is generated intracellularly by all bacteria and at high concentrations[701]. Importantly, extracellular release of ATP from a diverse range of gram-negative and gram-positive bacteria has been reported, including *E. coli*, *S. enterica*, *K. pneumoniae*, *S. aureus*, *Acinetobacter junii* and *Enterococcus gallinarum*[701,727]. Thus, bacterial-derived ADP may act as a chemoattractant to microglia via $P2Y_{12}R$ in the brain. Indeed, Zhang *et al*[613] have recently shown that ADP levels increase in *E. coli*-infected mice, and exogenous ADP protected mice from *E. coli*-induced peritonitis by promoting the recruitment of macrophages to the infected site. Importantly, $P2Y_{12}R$ deficiency inhibited the ADP-mediated immune response, and increased infectivity of the bacteria[613]. Here, I show that phagocytic clearance of bacteria by both BV-2 and primary rat microglia was inhibited by the $P2Y_{12}R$ blocker PSB0739, consistent with a role for $P2Y_{12}R$ in facilitating phagocytosis through microglial migration and/or process extension toward the bacteria. PSB0739 did not cause observable necrosis in BV-2s or the primary microglia, and has been shown to directly inhibit ADP signalling in BV-2s in our lab (unpublished), supporting a targeted effect of PSB0739 on $P2Y_{12}R$. However, like with MRS2578, an off-target effect cannot be ruled out. Furthermore, exogenously applied ADP substantially and significantly inhibited phagocytosis of the bacteria by both BV-2 and primary rat microglia. This is consistent with ADP-$P2Y_{12}R$ signalling acting chemotactically rather than phagocytically, as ADP gradients originating from the bacteria and recognised by microglial $P2Y_{12}R$ would be masked by excess levels of exogenously applied ADP. However, it cannot be ruled out that ADP may be exerting a direct anti-phagocytic effect on the microglia. $P2Y_{12}R$ is substantially downregulated in microglia following activation by bacterial LPS[709]. LPS-induced phagocytosis of *E. coli* was not inhibitable by PSB0739 in either BV-2 or primary rat microglia, consistent with a role for $P2Y_{12}R$ in facilitating microglial clearance in non-activated microglia only. In support of this, the ADP-inhibition effect on BV-2 phagocytosis of bacteria was lifted by inflammatory activating the microglia with LPS. However, ADP abolished the LPS-induced phagocytosis by primary rat microglia, opening the possibility that ADP interferes with bacterial phagocytosis via a $P2Y_{12}R$-independent mechanism, although this would require further investigation.

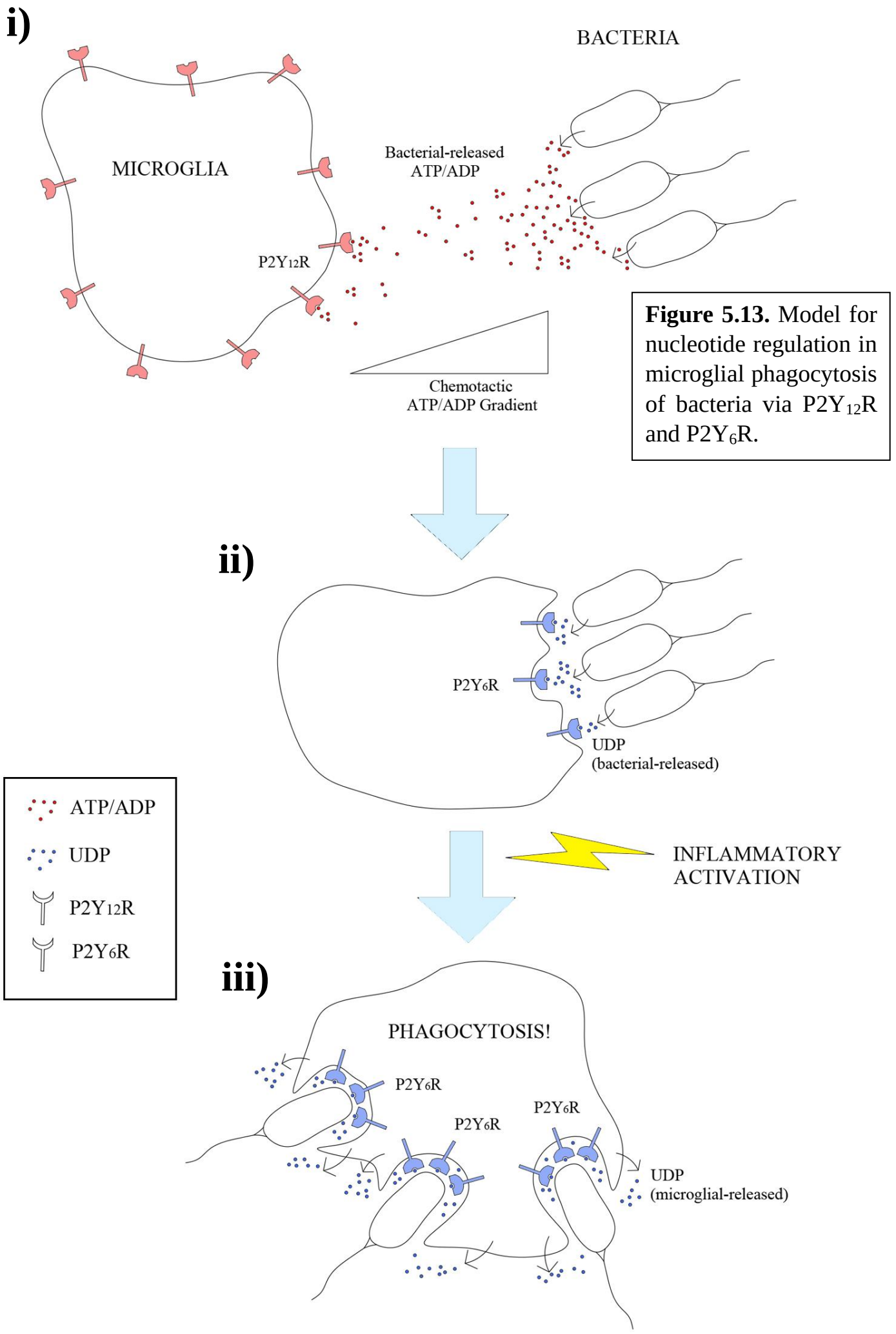

Figure 5.13. Model for nucleotide regulation in microglial phagocytosis of bacteria via $P2Y_{12}R$ and $P2Y_6R$.

Figure 5.13. Model for nucleotide regulation in microglial phagocytosis of bacteria via $P2Y_{12}R$ and $P2Y_6R$. i) Microglia detect bacterial-released ATP/ADP via surface-expressed $P2Y_{12}R$. $P2Y_{12}R$-signalling triggers migration of microglia toward the bacteria along the chemotactic ATP/ADP gradient. ii) Having reached the bacteria, microglial phagocytosis is promoted by activation of microglial $P2Y_6R$ by UDP released from the bacteria. iii) Microglia become inflammatory activated after exposure to bacteria/bacterial endotoxin, which upregulates $P2Y_6R$ and also promotes extracellular release of UDP by the microglia -both enhancing $P2Y_6R$-mediated phagocytosis of the bacteria.

CHAPTER VI

REGULATION OF MICROGLIAL PHAGOCYTOSIS OF SYNAPSES

6.1. Introduction

The literature regarding microglial function in the brain has historically focused on inflammation and pathology. Indeed, 'resting' microglia have long been considered 'passengers' during normal physiology, whose sole roles relate to initiation and maintenance of inflammation in response to brain injury or infection[325,351]. However, it is now well established that microglia play fundamental roles in the brain during development and normal homeostasis – particularly in the developmental pruning of synapses through phagocytosis, also known as synaptophagy (see section 2.1.1). Whilst various cell-signalling mechanisms have been identified in the regulation of microglial phagocytosis of neurons[326], less is known regarding synapse-specific phagocytosis by microglia. However, signalling via the microglial receptors CR3[32], TREM2[356] and SIRPα[357] have been established (see section 2.1.1), and further regulatory pathways will doubtless be elucidated. The ability for microglia to specifically phagocytose synapses - whilst leaving the remaining neuron intact and viable - is presumed to be fundamental for orthodox development of neural circuitry in the CNS[325,351]. Thus, further characterisation of synaptophagy regulation is necessary for us to better understand how synaptic turnover is controlled in normal development, and how its dysregulation can contribute to synaptic loss in pathological contexts, such as Alzheimer's disease[577].

The extensive literature regarding mechanisms that regulate microglial phagocytosis of whole cells (predominantly neurons) presents a number of candidate mechanisms for the specific regulation of microglial synaptophagy. Calreticulin and galectin-3 are both upregulated in, and secreted by, inflammatory-activated microglia[124], and microglia exhibit several markers of an activated phenotype during developmental synaptic pruning[32,356], suggesting that these proteins may circulate extracellularly during periods of such pruning. Both calreticulin and galectin-3 bound and opsonised bacterial targets for phagocytosis by microglia[124], and so in principle may also opsonise synapses, although this has not been reported. ApoE is also released by

microglia[634,635], and has been shown to regulate synaptic pruning by astrocytes in an isoform-dependent manner[728], which may be associated with the synaptic loss characteristic of AD. However, whether apoE influences synaptic pruning via microglial phagocytosis is not known. Extracellular tau is also implicated in AD pathology[729] and has been detected within the CNS[730,731]. Moreover, unpublished data from our lab demonstrates that extracellular tau promotes microglial phagoptosis of neurons in culture, but any regulation of microglial synaptophagy is again unknown. Finally, the P2Y receptors $P2Y_6R$ and $P2Y_{12}R$ present as promising candidates for regulating synaptophagy by microglia. $P2Y_{12}R$ is expressed exclusively by microglia within the brain[372], and has been implicated in microglial-mediated synaptic plasticity in the mouse visual cortex[372]. $P2Y_6R$ is a key microglial phagocytic receptor[485] and is upregulated in inflammatory-activated microglia[430]. Preliminary findings from our lab also indicate increased synaptic densities in cortical and hippocampal regions of mice lacking $P2Y_6R$, possibly due to impaired microglial phagocytosis of the synapses. Importantly, nucleotide transmission at synapses has been well documented[732], and both $P2Y_6R$ and $P2Y_{12}R$ are activated by binding nucleotide[692,694].

A particularly useful and widely-used model for studying synapse biology is through use of isolated synapses, also known as synaptosomes[733]. Synaptosomes have been well characterised as re-sealed synaptic terminals which maintain membrane potentials via functional ion channels, generate ATP, take up and release neurotransmitter, and contain a range of functional enzymes and proteins typically found in neuronal terminals[733,620,734,735,736,737]. Importantly, synaptosomes have been used to model phagocytosis of synapses in culture, by astrocytes[728,738,739] and also microglia[356,740,741], the two major phagocytic cells in the brain. Synaptosomes are particularly amenable to opsonisation studies: as with bacteria, synaptosomes can be pre-incubated with target proteins and then washed prior to co-incubation with microglia to assay phagocytosis. Thus, distinguishing between true opsonisation effects and phagocytic enhancement without opsonisation (for example, through microglial activation via PRR binding) is possible using the synaptosome model. Such distinctions are challenging to demonstrate directly *in vivo*, or with other *in vitro* methods such as neuronal cultures. However, the ability of neurons to generate functional synapses in culture[356] also suggests that neuronal-glial co-cultures may be a useful tool for studying general regulatory mechanisms for microglial phagocytosis of synapses. Indeed, neuronal culture systems have been used to support synaptophagy data obtained using synaptosomes and/or *in vivo* data obtained through

animal models[356,728,742,743]. In my work, both synaptosome-based and neuronal culture-based models were used to investigate microglial phagocytosis of synapses.

In this chapter, I demonstrate novel roles for several proteins – including calreticulin, galectin-3, apoE and tau – in opsonising synapses for microglial phagocytosis using the synaptosome model. Synaptosomes were first characterised in terms of size, synaptic-marker expression, viability and exposure of the classic 'eat-me' signal phosphatidylserine (see section 1.4.1.2.1), and a phagocytosis model, in which pHrodo-conjugated synaptosomes were co-incubated with BV-2 or primary rat microglia, was established. Calreticulin bound to and opsonised synaptosomes for microglial phagocytosis, and such opsonisation was inhibited by sucrose and the LRP1 blocker RAP. Galectin-3 also bound and opsonised synaptosomes for microglial phagocytosis, which was inhibited by lactose and the MerTK antagonists UNC2881 and UNC569. ApoE bound and opsonised synaptosomes for microglial phagocytosis, and the data indicate that binding and opsonisation may be isoform-specific: the ε2 isoform biding was greater than ε4, and this increased binding was associated with a significant opsonisation effect for ε2 but not ε4. Finally, tau bound synaptosomes at low nanomolar concentrations, and opsonised them for phagocytosis by microglia.

The synaptosome model was also used to explore the role of the P2Y receptors $P2Y_6R$ and $P2Y_{12}R$ in microglial synaptophagy. Blocking either $P2Y_6R$ or $P2Y_{12}R$ inhibited phagocytosis of synaptosomes by BV-2 and/or primary rat microglia, as did adding exogenous ADP - consistent with roles for $P2Y_6R$- and $P2Y_{12}R$-signalling in regulating microglial phagocytosis of synapses. To support these findings, a novel synaptophagy culture model was established in which mixed cerebellar cultures (containing neurons and glia) were treated with the microglial stimulant LPS to promote M1-polarisation of the microglia (a phenotype implicated in both developmental and pathological synaptophagy[32,356]). Synaptic densities were measured through immunostaining for synaptophysin and imaging via confocal microscopy. Synaptophysin puncta (but not neurons) were significantly less dense in cultures chronically exposed to 10 ng/ml LPS, and this reduction in puncta density was prevented by i) $P2Y_6R$ knockout, or ii) $P2Y_{12}R$ inhibition with PSB0739. These findings are consistent with synaptic loss resulting from microglial-mediated synaptic pruning, and implicate P2Y receptors as regulators of microglial synaptophagy in both developmental and pathological contexts.

6.2. Results

6.2.1. Characterising synaptosomes isolated from rat cortex

At the start of this study, synaptosomes were characterised in terms of size, synaptic marker presence, viability and exposure of phagocytic 'eat-me' signals like phosphatidylserine. Synaptosomes isolated as described by Dunkley *et al*[620] were of the expected size - between 1 and 5 µm[744] - and were of comparable size (although significantly larger) to *E. coli*, as measured by flow cytometry (p=0.008; Figure 6.1A). Synaptosomes were highly enriched for both the presynaptic marker synaptophysin (Figure 6.1B) and the post-synaptic marker PSD-95 (Figure 6.1C) when compared to their respective controls, confirming the isolation method generates an enriched population of synapses.

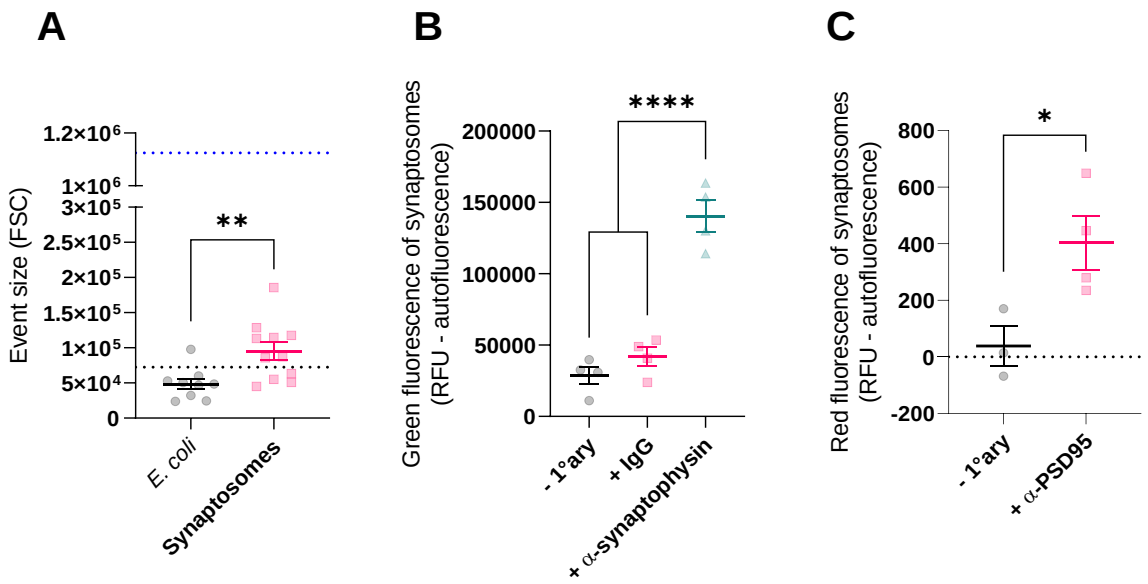

Figure 6.1. Synaptosomes isolated from rat cortex are enriched for synaptic markers synaptophysin and PSD-95. (A) Synaptosomes from rat cortex are in the range of 1-5 µm, based on FSC of 1 and 5µm beads (dotted black and blue lines, respectively), and comparable to (although significantly larger than) *E. coli*. (B) Synaptosomes stain positively for synaptophysin compared to the '- 1°ary' or '+IgG' controls (all synaptosomes were immunostained with AlexaFluor 488). Note that the '+ IgG' control data was obtained later. (C) Synaptosomes stain positively for PSD-95 compared to the '- 1°ary' control (all synaptosomes were immunostained with Cy3). Values are means ± SEM of at least 3 biologically independent experiments. Statistical comparisons were made via Student's t-test (A & C) or one-way ANOVA (B). NS $p \geq 0.05$, *$p<0.05$, ****$p<0.0001$.

To test for ‘viability’, the dye calcein-AM was used, which enters membrane-bound compartments (e.g. cells and synaptosomes) and is cleaved by esterases to a membrane-impermeable form, meaning it remains trapped inside the cell/synaptosome[744]. Thus, calcein-AM staining indicates both membrane integrity and functional cellular/synaptosomal esterase activity, and was considered an appropriate marker for synaptosome viability. 92 ± 3% of synaptosome events shifted into the ‘fluorescence-positive’ gate, as measured by flow cytometry (Figure 6.2A). Since the synaptosome isolation procedure was time-consuming, it was not considered feasible to perform experiments on fresh synaptosomes. So, synaptosomes were cryogenically frozen immediately after isolation and thawed as required[745]. The effect of the freeze-thaw process on viability was also tested. A small (but significant) drop in viability was observed ($p=0.001$). However, total viability of the freeze-thawed synaptosomes (70 ± 5%, $p<0.001$ versus ‘- calcein-AM’ control) was considered sufficiently high to justify continuation of freezing as a method of tissue storage. Moreover, these fluorescence measurements were performed on paraformaldehyde-fixed synaptosomes, and later, freeze-thawed synaptosomes that had not been fixed exhibited increased fluorescence after the same calcein-AM treatment (data not shown). Thus, viability levels shown here (Figure 6.2A) are likely an underestimate of true population viability. To determine whether synaptosome viability was negatively affected after time in HEPES-buffered Krebs-like (HBK) buffer (considering future opsonisation experiments), viability was measured after 15, 30 and 60 minutes in the HBK buffer (Figure 6.2B): no drop in viability was observed over this time range. To measure phosphatidylserine exposure, synaptosomes were incubated with annexin-V conjugated to the fluorophore FITC, and fluorescence-shift was measured via flow cytometry as for calcein-AM. Phosphatidylserine-exposure levels were found to vary between synaptosome batches to a greater degree than calcein-AM staining, with an average of 52 ± 13% of synaptosome events shifting into the fluorescence-positive gate (Figure 6.2C). Such levels were not significantly altered after the freeze-thaw process ($p=0.934$), or after 60 minutes in HBK buffer ($p=0.831$ versus ‘15 minutes’; Figure 6.2D).

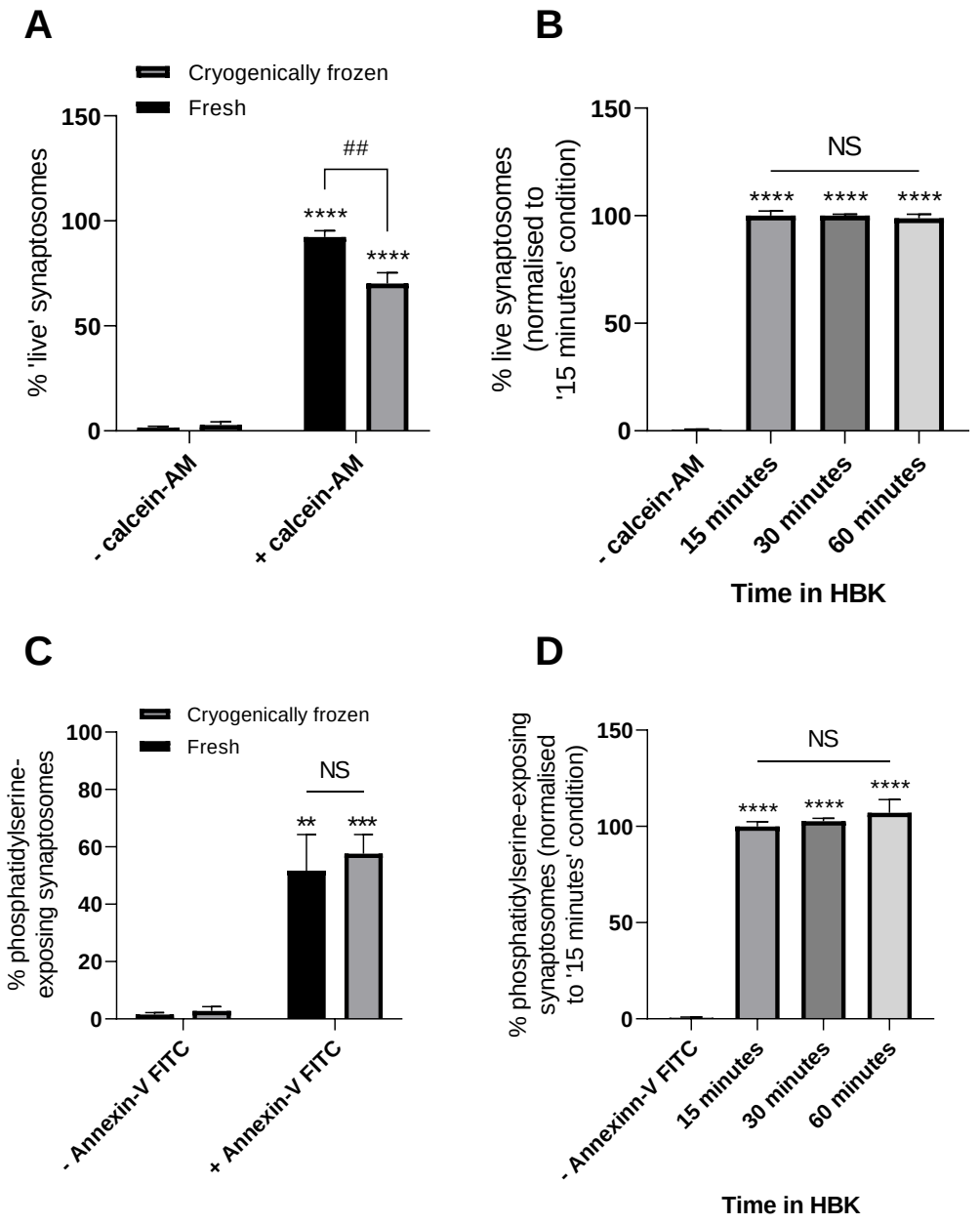

Figure 6.2. Isolated synaptosomes are viable and phosphatidylserine-exposing. (A) Synaptosomes stain strongly for the viability marker calcein-AM, whether fresh or cryogenically freeze-thawed, compared to the '- calein-AM' control (measured by flow cytometry in terms of fluorescence gate-shift). Cryogenic freeze-thawing promoted a small but significant drop in calcein-AM staining. (B) Synaptosomes remain viable for at least 60 minutes after thawing in HBK buffer, with no drop in calcein-AM staining observed. (C) Synapyotosomes stain positively for annexin-V FITC (which binds exposed phosphatidylserine residues) whether fresh or cryogenically freeze-thawed, compared to the '- annexin-V' control (measured by flow cytometry in terms of green fluorescence shift). Cryogenic freeze-thawing does not alter annexin-V FITC staining. (D) Synaptosomes do not alter their phosphatidylserine exposure over 60 minutes after thawing in HBK buffer. Values are means ± SEM of at least 3 biologically independent experiments. Statistical comparisons were made via one- or two-way ANOVA as appropriate. NS $p \geq 0.05$, **p<.01, ***p<0.001, ****p<0.0001; ##p<0.01 as indicated.

To investigate regulators of microglial synaptophagy, a phagocytosis assay was developed by labelling the synaptosomes with pHrodo-SE (10 μM) (see section 3.2.6.2), as was done with the bacteria (see Chapter 4). Labelled synaptosomes were incubated with primary rat microglia

for 60 minutes, and phagocytosis was visualised by microscopy (Figure 6.3A) or quantified by flow cytometry (Figure 6.3B). Significant phagocytosis was observed within 60 minutes compared to the '- synaptosomes' control ($p<0.001$), which was abolished by cytochalasin D

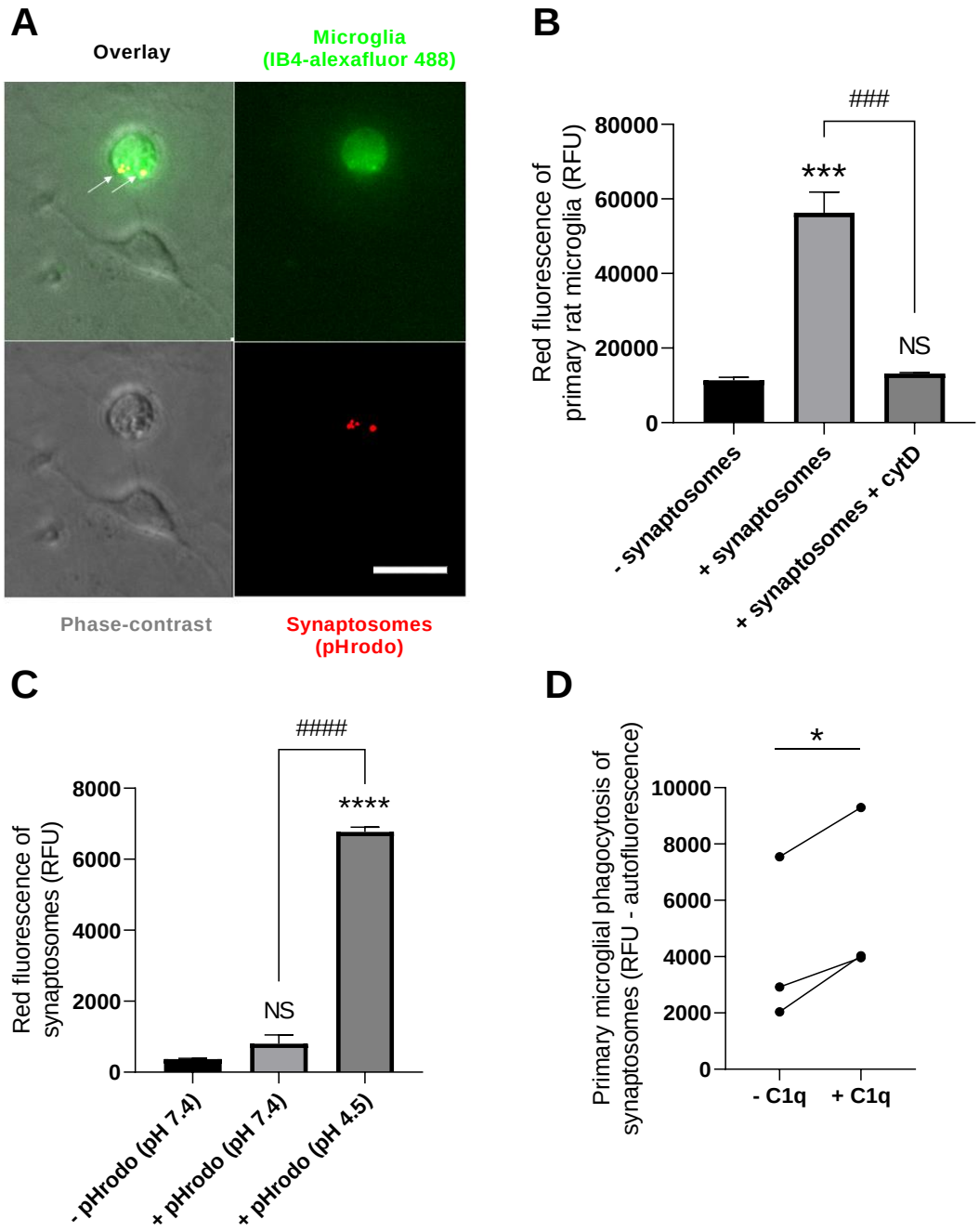

Figure 6.3. Isolated synaptosomes are rapidly phagocytosed by microglia and opsonised by C1q. (A & B) Primary rat microglia phagocytose pHrodo-conjugated synaptosomes over 60 minutes *in vitro*, visualised by microscopy (A) and quantified by flow cytometry (B) compared to the '- synaptosomes' control; this phagocytosis is abolished by cytochalasin D (10 μM). Scale bar (20 μm). (C) pHrodo-stained synaptosomes fluoresce red in citrate buffer (pH 4.5), but not HKB buffer (pH 7.4), compared to the '- pHrodo (pH 7.4)' control. (D) Recombinant human C1q (1 μM) opsonises synaptosomes for phagocytosis by primary microglia when precincubated for 60 minutes and subsequently washed to remove unbound protein. Values are means ± SEM of at least 3 biologically independent experiments. Statistical comparisons were made via one-way ANOVA (B & C) or Student's t-test (D). NS $p \geq 0.05$, *$p<0.05$, ***$p<0.001$, ****$p<0.0001$; ###$p<0.001$, ####$p<0.0001$ as indicated.

(10 μM) ($p<0.001$, $p=0.923$ versus control). The pH-dependence of pHrodo fluorescence was confirmed by measuring red fluorescence of pHrodo-conjugated synaptosomes in HKB (pH 7.4) compared to citrate buffer (pH 4.5), where fluorescence was significantly increased ($p<0.001$; Figure 6.3C). Importantly, no significant fluorescence shift was observed at pH 7.4 compared to the '- pHrodo (pH 7.4)' control ($p=0.215$). To further validate the use of synaptosomes as a model for studying microglial synaptic pruning via synapse opsonisation, the ability for C1q – a known opsonin for synaptic pruning[145,221,222,583] – was tested. Pre-incubating the synaptosomes with C1q (1 μM) for 60 minutes (followed by several washing steps to remove unbound C1q) caused a significant increase in their phagocytosis by microglia ($p=0.03$; Figure 6.3D).

6.2.2. Calreticulin and galectin-3 bind and opsonise synaptosomes for phagocytosis by microglia

Calreticulin and galectin-3 were found to be released by inflammatory activated microglia, and once released, bound and opsonised bacteria for phagocytic removal by the microglia (Chapter 4). During CNS development, and in peak stages of synaptic pruning, microglia can adopt a phenotype comparable to that induced by inflammatory activation in terms of morphology, cytokine expression (*Tnf, Tgfb1 & Il1b)*, and expression of receptors characteristic of an 'activated' profile including CD68, MHCII, CD11b, CD86 and CR3[32,356]. Thus, calreticulin and/or galectin-3 release by microglia may feature in the context of developmental synaptic pruning (as well as in pathological synaptic loss), where in principle they could bind and opsonise synapses for microglial synaptophagy. To investigate this, the binding of calreticulin and galectin-3 to synaptosomes was tested via the TAMRA-staining method used previously (Chapter 4). Synaptosomes incubated with TAMRA-conjugated calreticulin or galectin-3 significantly increased in red fluorescence compared to protein-free controls ($p<0.001$ each, Figure 6.4A), indicating a binding capacity of these proteins for synapses. Binding of TAMRA-conjugated calreticulin was significantly inhibited in the presence of sucrose by 17% ±2 ($p=0.038$, Figure 6.4B), consistent with findings regarding bacterial binding (Chapter 4) and indicating a role for the carbohydrate-recognition domain in calreticulin binding to synapses. In contrast to the bacteria, binding of TAMRA-conjugated galectin-3 was significantly inhibited with lactose by 28% ±2 ($p=0.025$, Figure 6.4C), highlighting the role of the lactose-inhibitable carbohydrate-recognition domain for galectin-3 in binding synapses.

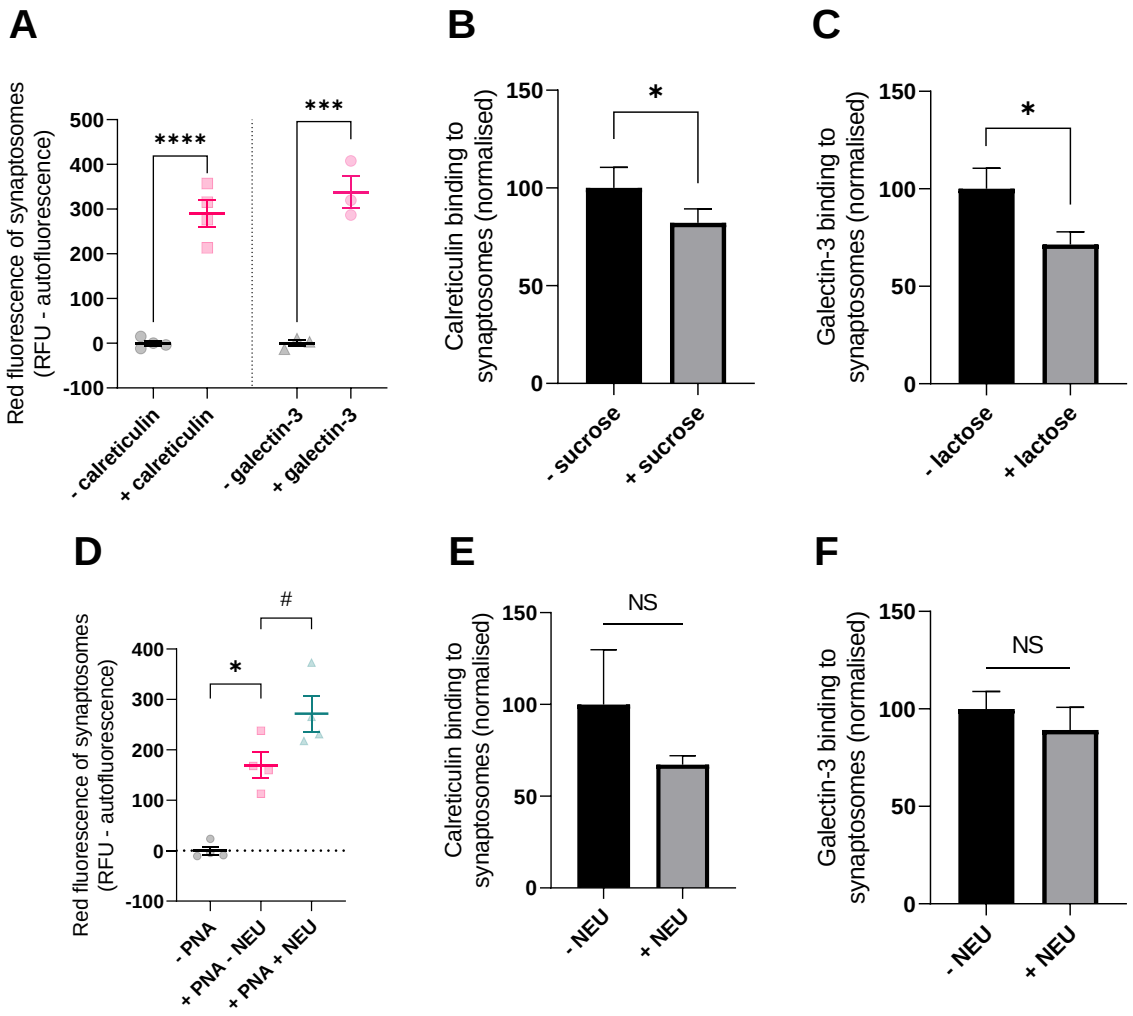

Figure 6.4. Calreticulin and galectin-3 bind synaptosomes. (A) TAMRA-conjugated calreticulin (500 nM) and galectin-3 (100 nM) bind synaptosomes after 60 minutes coincubation, measured in terms of relative fluorescence unit increase versus controls. (B) Binding of TAMRA-conjugated calreticulin is significantly inhbited by sucrose (50 mM). (C) Binding of TAMRA-conjugated galectin-3 is significantly inhibited by lactose (50 mM). (D) Peanut agglutinin (PNA) binds synaptosomes, and binding is enhanced after 30 minutes treatment with neuraminidase (NEU) (0.4 U/ml), indicating surface desialylation. (E & F) Treatment with neuraminidase did not enhance binding of calreticulin (E) or galectin-3 (F) to synaptosomes. Values are means ± SEM of at least 3 biologically independent experiments. Statistical comparisons were all made via Student's t-test except for D, which was via one-way ANOVA. NS $p \geq 0.05$, *$p<0.05$, ****$p<0.0001$; #$p<0.05$ as indicated.

Enzymatic desialylation of the synaptic surface promotes microglia phagocytosis of synapses, which is likely due (at least in part) to increased tagging of the synapse by complement factors (e.g. C1q) after desialylation[221]. To test whether desialylation of the synaptosomal surface might influence binding of calreticulin or galectin-3, synaptosomes were treated with exogenous neuraminidase (i.e. sialidase). Peanut agglutinin (PNA) – a lectin that binds terminal galactose residues exposed after sialic-acid removal[746] – bound synaptosomes to significant levels (p=0.027; Figure 6.4D) which was further enhanced by treatment with neuraminidase

(p=0.049), confirming desialylation. However, neither calreticulin nor galectin-3 binding to synaptosomes was enhanced by the same neuraminidase treatment in subsequent experiments, indicating desialylation-independent binding (Figures 6.4E & 6.4F respectively).

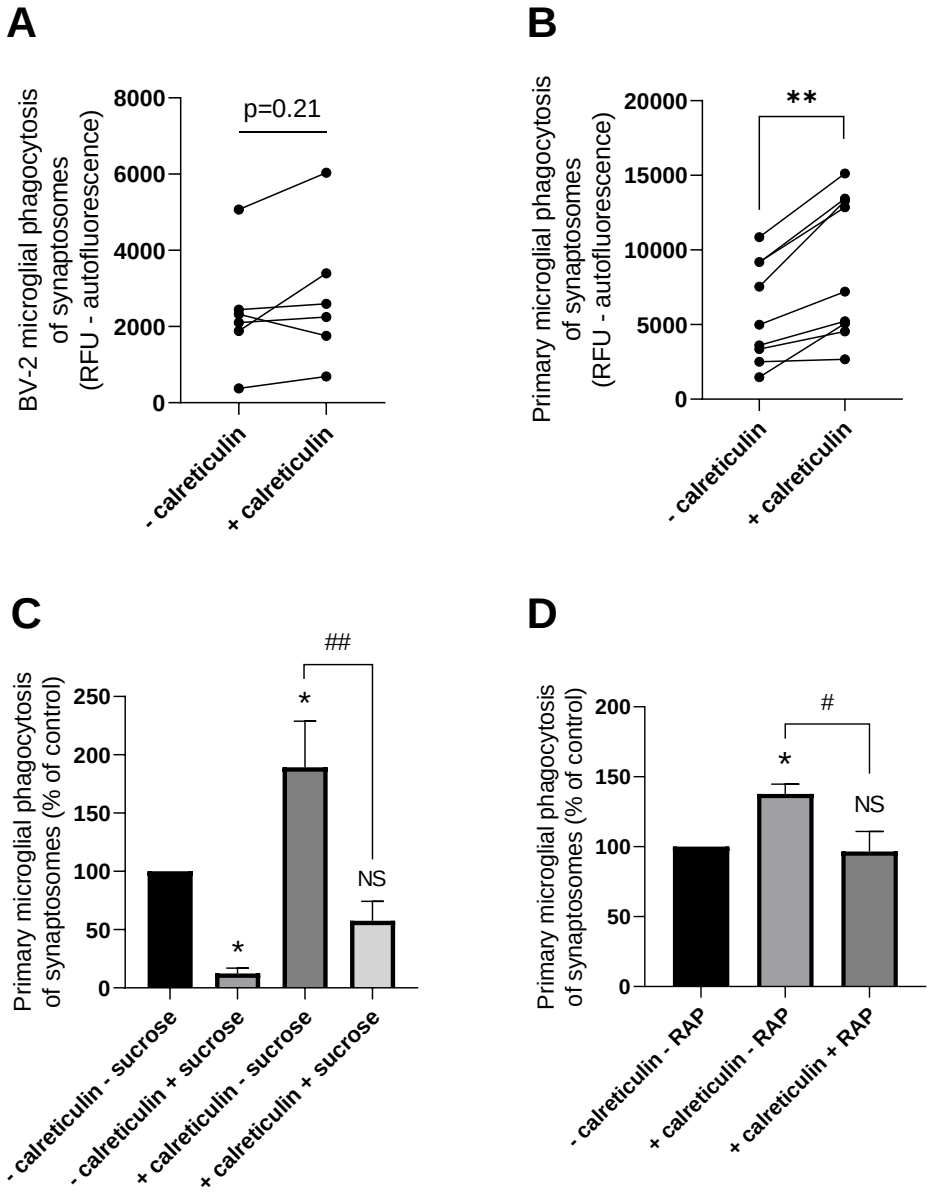

Figure 6.5. Calreticulin opsonises synaptosomes for microglial phagocytosis. (A & B) Recombinant calreticulin (500 nM) does not significantly opsonise synaptosomes for phagocytosis by BV-2 microglia (A), but does for phagocytosis by primary microglia (B). (C) Sucrose (50 mM) substantially inhibited microglial phagocytosis of synaptosomes compared to the '- calreticulin - sucrose' control, and also inhibited opsonisation by exogenous calreticulin. (D) Opsonisation by calreticulin was inhibited by the LRP1 blocker RAP (500 nM) compared to the '- calreticulin - RAP' control. Values are means ± SEM of at least 3 biologically independent experiments. Statistical comparisons were made via Student's t-test (A & B) or one- or two-way ANOVA (C & D) as appropriate. NS $p \geq 0.05$, *$p<0.05$, **$p<0.01$; #$p<0.05$, ##$p<0.01$.

To test whether calreticulin can opsonise synaptosomes for microglial phagocytosis, pHrodo-conjugated synaptosomes were incubated with calreticulin (500 nM) for 60 minutes (followed

by several washing steps to remove unbound protein) and incubated with either BV-2 or primary rat microglia. Calreticulin did not significantly increase BV-2 phagocytosis of synaptosomes ($p=0.211$; Figure 6.5A). However, calreticulin significantly increased phagocytosis of synaptosomes by primary rat microglia ($p=0.001$; Figure 6.5B), suggesting it can opsonise synapses for microglial phagocytosis. Given the effect of sucrose on calreticulin binding to synaptosomes (Figure 6.4B) - as well as on calreticulin opsonisation of bacteria (Chapter 4) - the effect on opsonisation of synaptosomes was tested (Figure 6.5C). Unlike with the bacteria, sucrose significantly inhibited microglial phagocytosis of synaptosomes in the absence of exogenous calreticulin ($p=0.019$ versus '- calreticulin – sucrose' control), suggesting that calreticulin originating from (or on) the synapse may facilitate microglial phagocytosis in control conditions (or that sucrose was inhibiting phagocytosis independent of calreticulin). Sucrose also inhibited phagocytosis induced by calreticulin opsonisation ($p=0.002$) to levels not significantly greater than the '- calreticulin + sucrose' condition ($p=0.438$), suggesting that calreticulin opsonisation depends on its carbohydrate-recognition domain. Furthermore, the microglial LRP1-inhibitor RAP also inhibited calreticulin opsonisation ($p=0.012$ versus '+ calreticulin – RAP'; Figure 6.5D), indicating that calreticulin opsonisation is mediated by microglial LRP1.

To test whether galectin-3 can opsonise synaptosomes for microglial phagocytosis, pHrodo-conjugated synaptosomes were incubated with galectin-3 (20 nM) for 60 minutes and incubated with either BV-2 or primary rat microglia. As with calreticulin, galectin-3 had no significant effect on BV-2 phagocytosis of synaptosomes ($p=0.256$; Figure 6.6A). However, galectin-3 significantly opsonised synaptosomes for phagocytosis by primary rat microglia ($p=0.017$ versus control; Figure 6.6B). Given the effect of lactose on microglial phagocytosis of bacteria in the presence and absence of exogenous galectin-3, the effect on synaptosomes was tested (Figure 6.6C). As with the bacteria, lactose significantly inhibited phagocytosis in the absence of applied galectin-3 ($p<0.001$ versus '- galectin-3 – lactose' control). Unlike with bacteria, lactose inhibited the galectin-3 opsonisation to levels not significantly different to the '- galectin-3 + lactose' condition ($p=0.452$), and such levels were significantly lower than the '+ galectin-3 – lactose' control ($p<0.001$). These data suggest that galectin-3 opsonisation does depend on its lactose-inhibitable carbohydrate-recognition domain, and are consistent with the finding that lactose inhibits binding of galectin-3 to synaptosomes (Figure 6.4C).

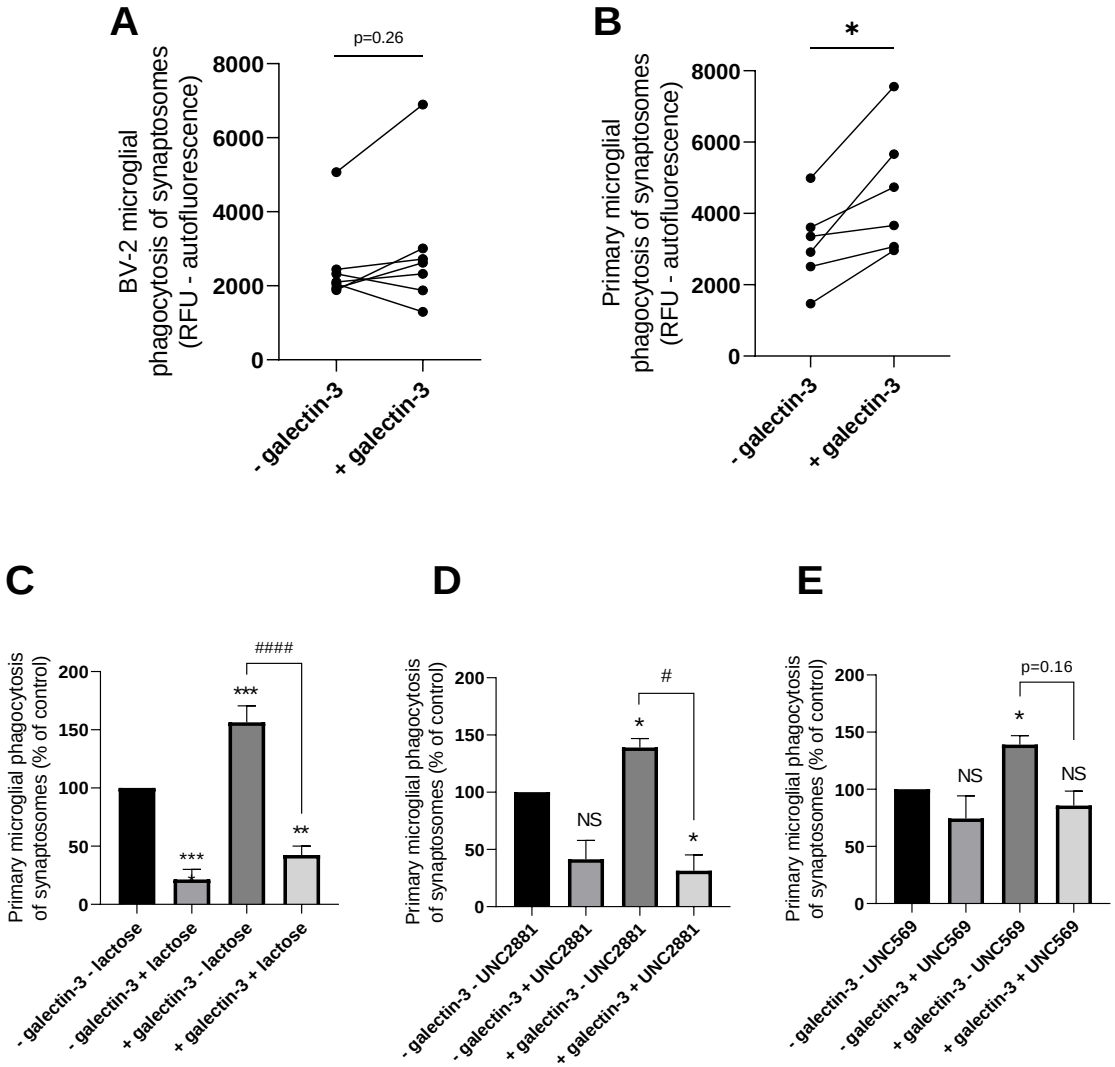

Figure 6.6. Galectin-3 opsonises synaptosomes for microglial phagocytosis. (A & B) Recombinant galectin-3 (20 nM) did not significantly opsonise synaptosomes for phagocytosis by BV-2 microglia (A), but did for phagocytosis by primary rat microglia (B). (C) Lactose (50 mM) substantially inhibited microglial phagocytosis of synaptosomes compared to the '- galectin-3 - sucrose' control, and also inhibited opsonisation by exogenous galectin-3. (D & E) Opsonisation of synaptosomes for microglial phagocytosis by galectin-3 is inhibitable by UNC2881 (2 μM) (D) or UNC569 (500 nM) (E). Values are means ± SEM of at least 3 independent experiments. Statistical comparisons were made via Student's t-test (A & B) or two-way ANOVA (C, D & E). NS $p \geq 0.05$, *$p<0.05$, **$p<0.01$, ***$p<0.001$, ****$p<0.0001$; #$p<0.05$, ####$p<0.0001$.

Given that galectin-3 is known to opsonise mammalian cells by activating the microglial receptor MerTK[216] – and that blocking MerTK inhibited galectin-3-induced phagocytosis of bacteria by microglia[124] (Chapter 4) – the effect of blocking MerTK on synaptosome phagocytosis was tested. UNC2881 (2 μM) inhibited baseline phagocytosis by 57% ± 17 (Figure 6.6D), indicating a role for MerTK in phagocytosis of synaptosomes in the absence of exogenous galectin-3. UNC2881 also significantly inhibited galectin-3-induced phagocytosis ($p=0.014$) to levels not significantly different from the '- galectin-3 + UNC2881' condition

(p=0.363). UNC569 (500 nM) did not inhibit baseline phagocytosis to any significant level (p=0.624 versus '- galectin-3 – UNC569' control), but it inhibited galectin-3-induced phagocytosis to control levels (Figure 6.6E).

Taken together, these data indicate that calreticulin and galectin-3 can opsonise synaptosomes for phagocytosis by microglia in culture, and that this is mediated by their carbohydrate-recognition domains and the microglial phagocytic receptors LRP1 (for calreticulin) and MerTK (for galectin-3).

6.2.3. ApoE binds and opsonises synaptosomes for phagocytosis by microglia in an isoform-specific manner

ApoE is released by immune cells in the brain[635], and has been shown to regulate synaptic pruning by astrocytes in an isoform-dependent manner[728]. However, it is unclear whether apoE directly opsonises the synapses for phagocytosis (by astrocytes or microglia), and if so, whether such opsonisation may be isoform-dependent, which may be relevant to AD. To test differential binding capacity of the ε2 and ε4 isoforms of apoE, recombinantly produced forms of the proteins were TAMRA-labelled and incubated with synaptosomes at a range of concentrations, and binding was measured via flow cytometry (using the 'fluorescence gate-shift' method described in section 3.2.6). No significant binding was detected from either isoform applied at 10 nM when compared to the protein-free control (Figure 6.7A). ε2, but not ε4, significantly bound synaptosomes at 100 nM. Both ε2 and ε4 significantly bound at 1 μM, but with significantly greater binding of the ε2 isoform (p=0.014). Thus, both the ε2 and ε4 isoforms can associate with synaptosomes, with a greater capacity for association with ε2 than ε4. Note that final protein concentrations were quantified by spectroscopy (A_{280}): no significant difference in concentration between the two proteins was observed (data not shown).

To test whether apoE can opsonise synaptosomes for microglial phagocytosis, pHrodo-conjugated synaptosomes were incubated with either ε2 or ε4 (1 μM each) for 60 minutes and then, after washing to remove unbound protein, incubated with BV-2 or primary rat microglia. Neither the ε2 nor the ε4 isoform significantly affected BV-2 phagocytosis of synaptosomes, when compared to the 'vehicle' control p=0.577 & p=0.409 respectively; Figure 6.7B).

However, a statistically significant difference was observed between the two isoforms (p=0.035), i.e. synaptosomes pre-incubated with ε2 are phagocytosed by BV-2 microglia

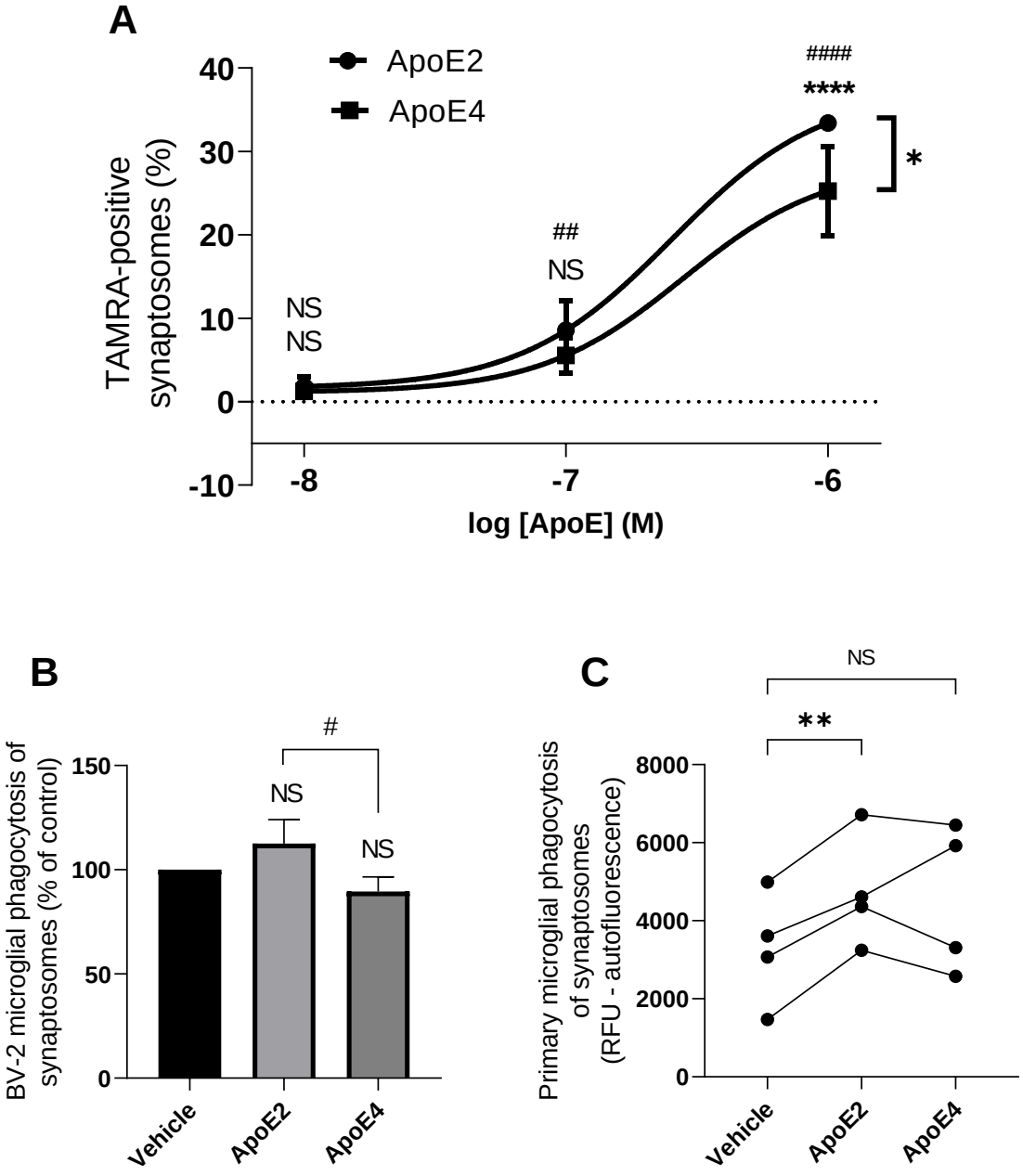

Figure 6.7. Apolipoprotein E binds synaptosomes and regulates their microglial phagocytosis in an isoform-dependent manner. (A) Binding of apoE2 and apoE4 to synaptosomes compared to vehicle control (indicated by a dotted line). ApoE2 (1 μM) binding to synaptosomes is greater than that of apoE4 at the same concentration. (B) BV-2 microglial phagocytosis of synaptosomes preincubated with apoE2 (1 μM) is significantly greater than apoE4 at the same concentration. (C) ApoE2 (1 μM) opsonises synaptosomes for phagocytosis by primary microglia, compared to the 'vehicle' control; no significant opsonisation was observed with apoE4 (1 μM). Values are means ± SEM of at least 3 biologically independent experiments. Statistical comparisons were made via one-way ANOVA. NS $p \geq 0.05$, **$p<0.01$, ****$p<0.0001$ comparing apoE4 binding to the control (A) or as indicated; #$p<0.05$, ##$p<0.01$, ####$p<0.0001$ comparing ApoE2 binding to the control (A) or as indicated. Further statistical information for A is contained within the Appendix.

significantly more than those incubated with ε4. ε2 significantly increased phagocytosis of synaptosomes by primary rat microglia by 56% ± 22 (p=0.009 compared to the control; Figure 6.7C). However, no significant increase in phagocytosis was observed with the ε2 isoform (p=0.115).

Taken together, these data demonstrate that apoE binds synaptosomes in an isoform-dependent manner, and that the ε2 isoform can significantly opsonise synaptosomes for microglial phagocytosis.

6.2.4. Extracellular tau binds and opsonises synaptosomes for phagocytosis by microglia

Tau has been detected circulating within the CNS[730,731], and recent work in our lab indicates that it can promote microglial phagocytosis of neurons by microglia, but it is not known whether it can bind or opsonise synapses for phagocytosis by microglia. To test this, recombinant tau was TAMRA-labelled and incubated with synaptosomes at a range of concentrations, and binding was measured via flow cytometry in terms of mean fluorescence shift (see section 3.2.6). Small but significant levels of association were observed at 10 nM, the lowest concentration tested, with increased levels at 100 nM and again at 1 µM (Figure 6.8A). To test whether tau can opsonise synaptosomes for microglial phagocytosis, pHrodo-conjugated synaptosomes were incubated with tau (1 µM) for 60 minutes and incubated with either BV-2 or primary rat microglia. No significant increase in BV-2 phagocytosis of synaptosomes was detected, compared to the '- tau' control (p=0.558; Figure 6.8B). However, tau significantly increased phagocytosis of synaptosomes by primary rat microglia (p=0.025; Figure 6.8C). Together, these data indicate that extracellular tau can bind synaptosomes and opsonise them for microglial phagocytosis.

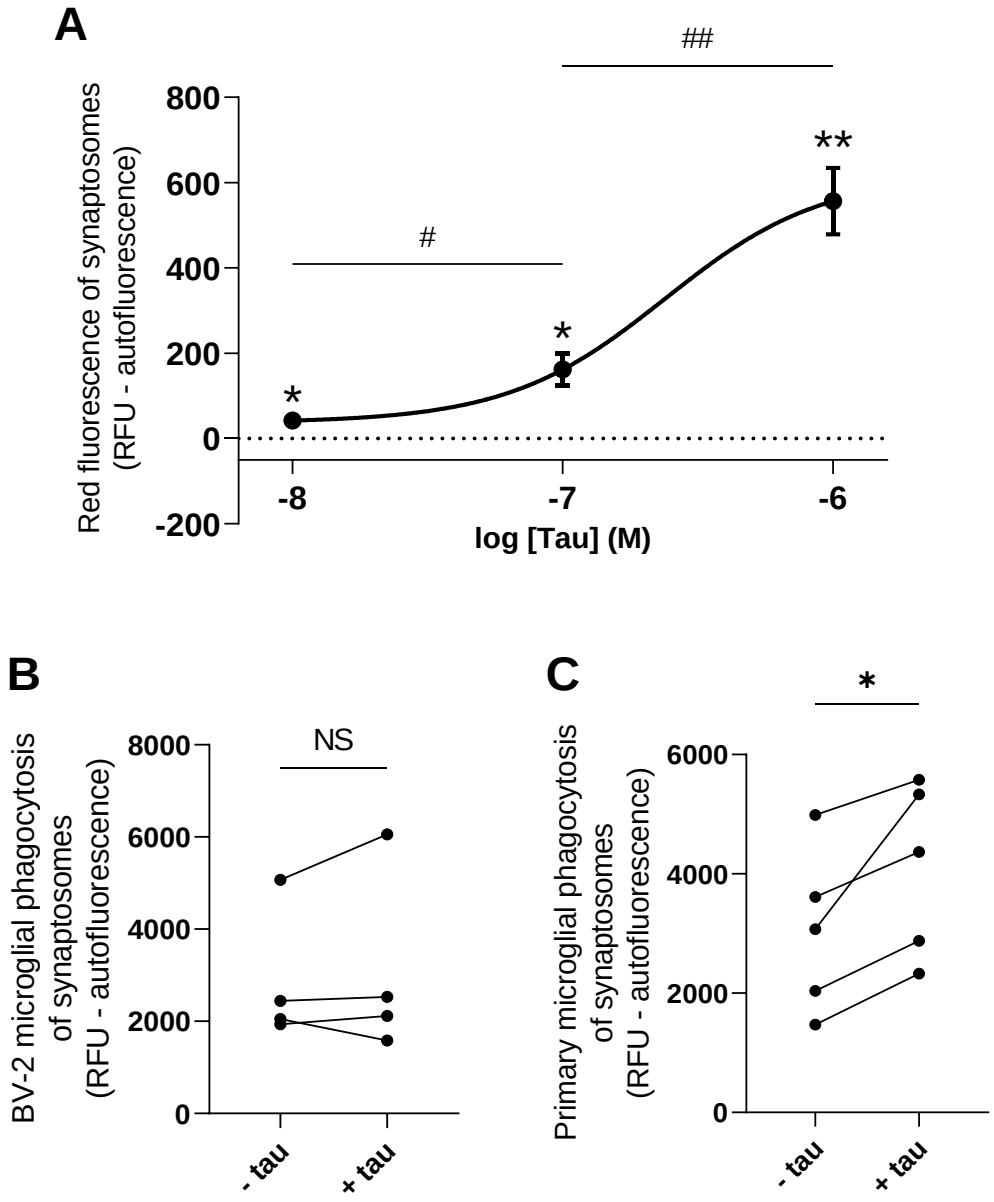

Figure 6.8. Tau binds and opsonises synaptosomes for microglial phagocytosis. (A) Binding of tau to synaptosomes (dose-range). Binding was detected down to 10 nM compared to the 'vehicle' control, indicated by a dotted line. (B) Extracellular tau (1 μM) did not significantly affect BV-2 phagocytosis of synaptosomes. (C) Extracellular tau (1 μM) significantly opsonised synaptosomes for phagocytosis by primary microglia. Values are means ± SEM of at least 3 biologically independent experiments. Statistical comparisons were made via one-way ANOVA (A) or Student's t-test (B & C). NS $p \geq 0.05$, *$p<0.05$, **$p<0.01$ versus the 'vehicle' control (A) or as indicated; #$p<0.05$, ##$p<0.01$ as indicated.

6.2.5. $P2Y_6R$ may be involved in microglial phagocytosis of synaptosomes

The microglial pyrimidinoreceptor $P2Y_6R$ has been shown by us and others as a key regulatory receptor of phagocytosis in a range of contexts[485,521,520], and expression in microglia is increased by inflammatory activation[430]. As mentioned, microglia can adopt an 'activated' profile during synaptic pruning, suggesting $P2Y_6R$ may play a role in this pruning. Furthermore, nucleotide transmission at synapses is well documented (reviewed by Pankratov *et al*[732]), and $P2Y_6R$ is activated by binding nucleotide, primarily UDP. Unpublished findings from our lab using $P2Y_6R$ KO mice indicate that $P2Y_6R$ is required for the neuronal loss that occurs via microglial phagocytosis of viable neurons in models of Alzheimer's and Parkinson's disease. However, whether $P2Y_6R$ expressed by microglia regulates their phagocytosis of synapses is not known.

To test whether UDP can induce microglial phagocytosis of synapses, exogenous UDP (100 µM) was applied to BV-2 or primary rat microglia for 30 minutes prior to co-incubation with pHrodo-conjugated synaptosomes (60 minutes), and phagocytosis was measured as before. No significant induction of phagocytosis was observed by either BV-2 ($p=0.829$; Figure 6.9A) or primary rat microglia ($p=0.677$; Figure 6.9B). However, it should be noted that UDP induction of bacterial phagocytosis by microglia was highly sensitive to duration of both pre-treatment and co-incubation (Chapter 5), meaning UDP may induce synaptosome phagocytosis under different experimental conditions. To test whether $P2Y_6R$ can regulate microglial phagocytosis of synapses, microglia were pre-treated with the $P2Y_6R$ blocker MRS2578 and phagocytosis of synaptosomes was measured as before. MRS2578 (500 nM) significantly inhibited synaptosome phagocytosis by BV-2 microglia by 43% ± 11 ($p=0.027$; Figure 6.9C). This MRS2578 treatment did not induce necrosis of the cells, as determined by propidium iodide staining (Figure 6.9D), indicating that such inhibition was not due to cell death. MRS2578 (500 nM) also inhibited synaptosome phagocytosis by primary rat microglia by 35% ± 11 ($p=0.042$; Figure 6.9E); again, conditions previously demonstrated to not induce microglia necrosis (Chapter 5), which could otherwise prevent phagocytosis.

To validate this data, phagocytosis of synaptosomes by microglia isolated from wild-type or $P2Y_6R$ knockout mice was measured and compared. Due to high variability in the data and a poor availability of $P2Y_6R$ knock-out microglia, no statistically significant difference in

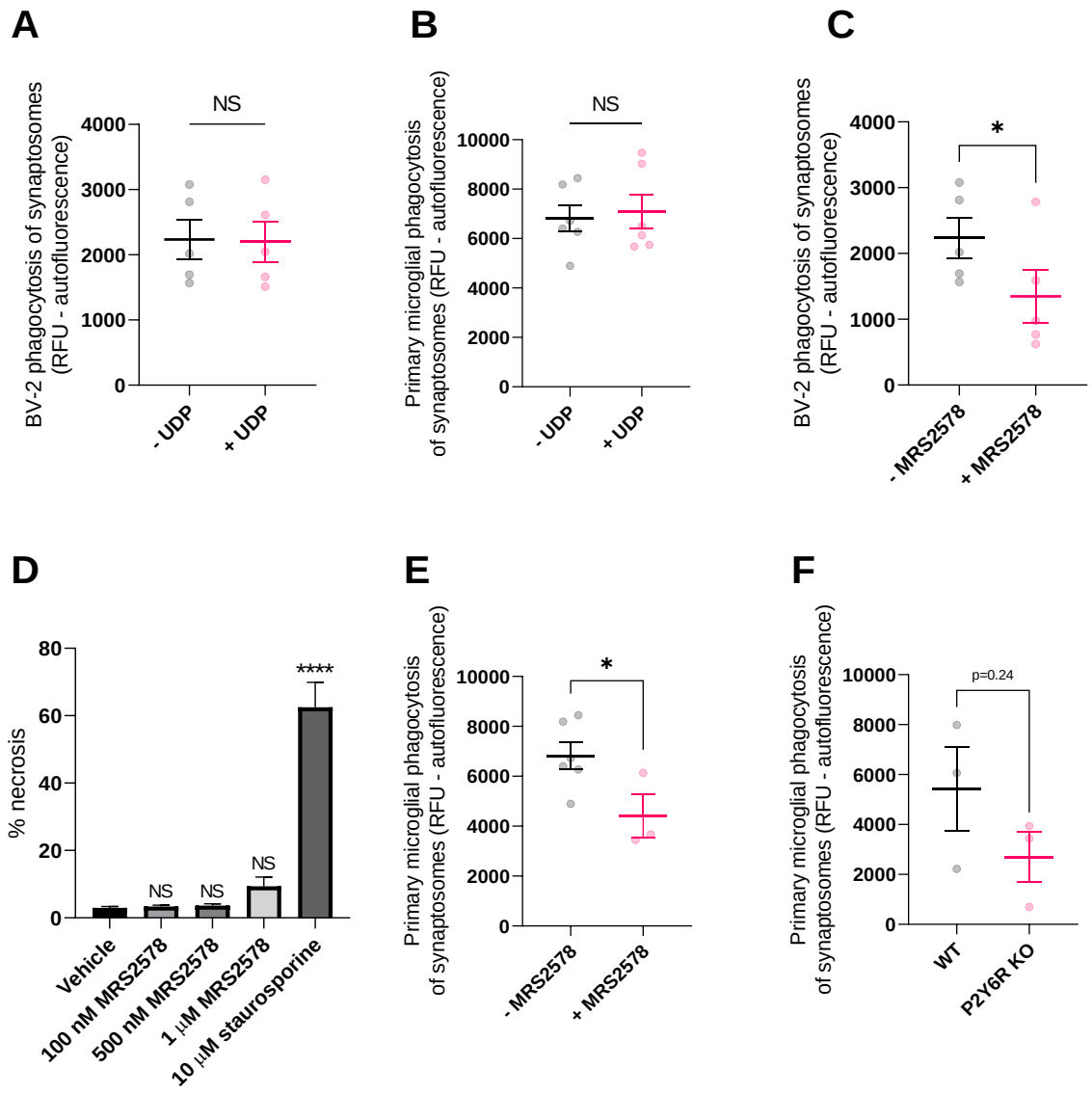

Figure 6.9. Microglial phagocytosis of synaptosomes is inhibited by blocking $P2Y_6R$. (A & B) UDP (100 μM) does not enhance phagocytosis of synaptosomes by BV-2 (A) or primary rat microglia (B). (C) MR2578 (500 nM) inhibits phagocytosis of synaptosomes by BV-2 microglia. (D) MRS2578 treatment did not induce necrosis of BV-2s, as determined by the percentage of cells stained with propidium iodide and compared to the 'vehicle' control. As a positive control for necrosis, cells were treated with staurosporine (10 μM) for 6 hours. (E) MRS2578 (500 nM) inhibited phagocytosis of synaptosomes by primary rat microglia. (F) Phagocytosis of synaptosomes may be reduced in $P2Y_6R$ KO microglia from mouse compared to WT. Values are means ± SEM of at least 3 independent experiments. Statistical comparisons were made via Student's t-test except for (D), which was via one-way ANOVA. NS $p \geq 0.05$, *$p<0.05$, ****$p<0.0001$.

phagocytosis of synaptosomes between wild-type and $P2Y_6R$-knockout microglia was obtained through my data alone ($p=0.238$; Figure 6.9F), although there was an indication that levels were reduced in the $P2Y_6R$ knockout. However, it should be noted that repeats

performed more recently by others in the lab have also identified a reduction in synaptosome phagocytosis with $P2Y_6R$ knockout compared to wild-types (unpublished), and combined with my data, identifies a statistically significant effect. Taken together, these data suggest that $P2Y_6R$ regulates microglial phagocytosis of synapses.

6.2.6. $P2Y_{12}R$ may be involved in microglial phagocytosis of synaptosomes

Microglial $P2Y_{12}R$ is a well characterised purinoreceptor that promotes microglial chemotaxis in response to ATP/ADP[709,747,710], which may be relevant in microglial phagocytosis of *E. coli* (Chapter 5). To explore whether $P2Y_{12}R$ can regulate microglial phagocytosis of synapses (which release ATP/ADP[732]) microglia were pre-treated with the $P2Y_{12}R$ blocker PSB0739 and phagocytosis of synaptosomes was measured as before. PSB0739 (10 µM) significantly inhibited synaptosome phagocytosis by BV-2 microglia by 84 ± 3% when applied 30 minutes prior to co-incubation ($p<0.001$; Figure 6.10A), and by 84 ± 2% when applied 10 minutes prior ($p<0.001$), suggesting this phagocytosis requires $P2Y_{12}R$. Treatment of the cells with PSB0739 did not induce necrosis of the cells, as determined by propidium iodide staining (Figure 6.10B), indicating that such inhibition was not due to cell death. PSB0739 (10 µM) also significantly inhibited phagocytosis of synaptosomes by primary rat microglia ($p=0.048$; Figure 6.10C). This PSB0739 treatment was previously demonstrated to not induce necrosis of the primary rat microglia (Chapter 5).

Given $P2Y_{12}R$ promotes microglial chemotaxis in response to ATP/ADP, and exogenous ADP inhibited microglial phagocytosis of bacteria in culture (possibly by interfering with endogenous ADP chemotactic gradients, as described in Chapter 5), the ability for exogenous ADP to inhibit microglial phagocytosis of synaptosomes was tested. ADP (1 mM) significantly inhibited synaptosome phagocytosis by primary rat microglia by 68% ± 7 ($p=0.026$; Figure 6.10D). Taken together, these data are consistent with a role for $P2Y_{12}R$ in mediating the migratory response of microglia toward synapses, thus facilitating phagocytosis.

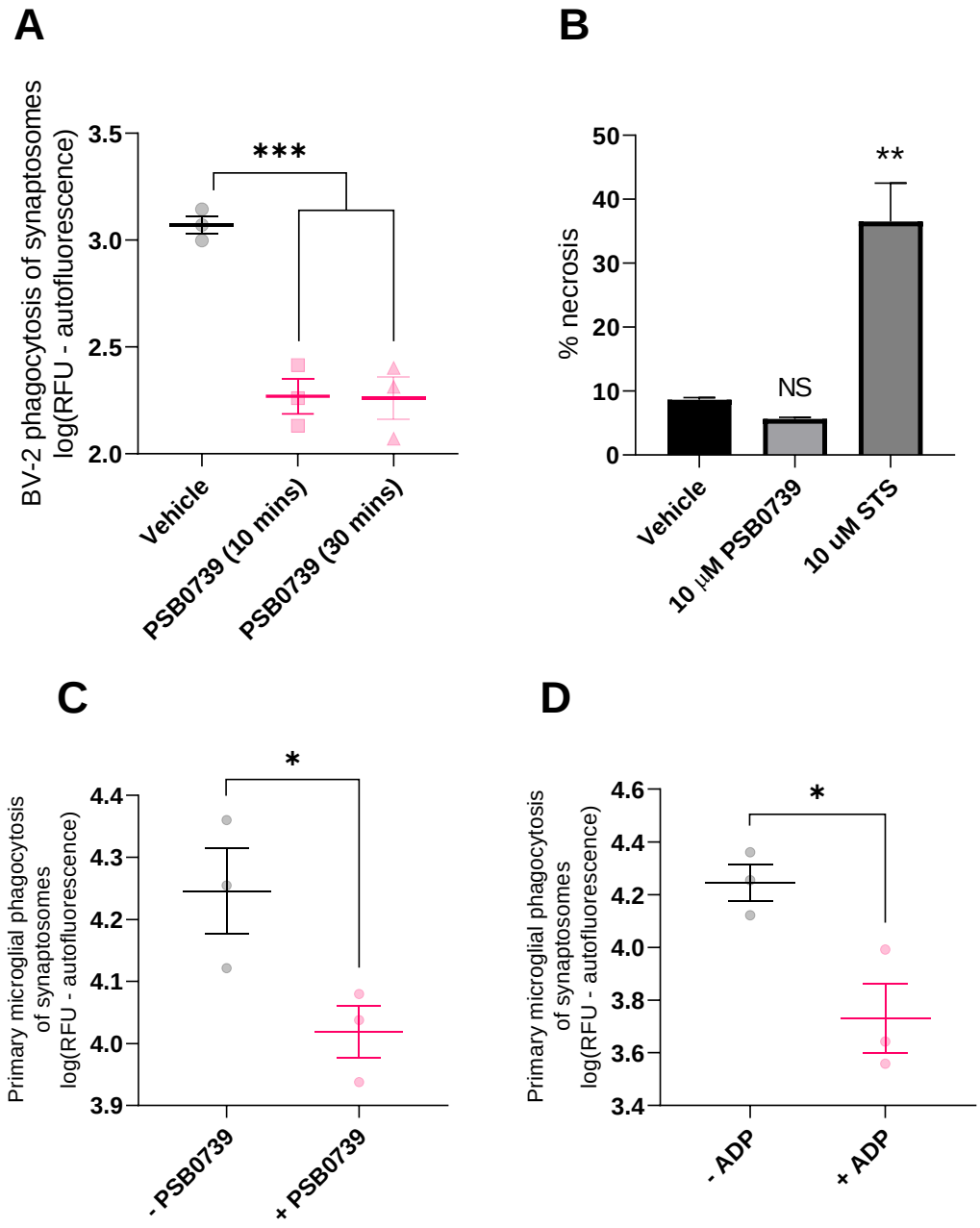

Figure 6.10. Microglial phagocytosis of synaptosomes is inhibited by blocking $P2Y_{12}R$. (A) PSB0739 (10 μM) inhibits phagocytosis of synaptosomes by BV-2 when applied 10 or 30 minutes prior to co-incubation. (B) PSB0739 treatment does not cause BV-2 necrosis after 70 minutes. (C) PSB0739 (10 μM) inhibits phagocytosis of synaptosomes by primary rat microglia. (D) ADP (1 mM) inhibits phagocytosis of synaptosomes by primary rat microglia. Values are means ± SEM of at least 3 independent experiments. Statistical comparisons were made via one-way ANOVA (A & B) or Student's t-test (C & D). NS $p \geq 0.05$, *$p<0.05$, **$p<0.01$, ***$p<0.001$.

6.2.7. LPS induces synaptophysin loss in wild-type cerebellar neuronal cultures, which is absent in P2Y$_6$R-knockout cultures, and inhibited by PSB0739

Inflammatory activation of microglia with LPS increased their phagocytosis of bacteria (Chapter 4), which was mediated by the extracellular opsonins calreticulin and galectin-3[124]. Given both calreticulin and galectin-3 opsonised synaptosomes for microglial phagocytosis (Figures 6.5 & 6.6 respectively), it was expected that inflammatory-activating the microglia with LPS would enhance their phagocytosis of synaptosomes. Surprisingly, the same treatment of LPS (100 ng/ml) that promoted phagocytosis of bacteria did not enhance phagocytosis of synaptosomes (p=0.17; Figure 6.11). In organotypic hippocampal slice cultures from mice, LPS can induce loss in detectable synaptophysin (without neuronal loss) that is mediated by microglia and consistent with LPS-induced microglial phagocytosis of synapses[748]. Whilst this model would clearly be useful for investigating the mechanisms regulating LPS-induced synaptic loss, organotypic culture generation is laborious compared to cell culture. Primary

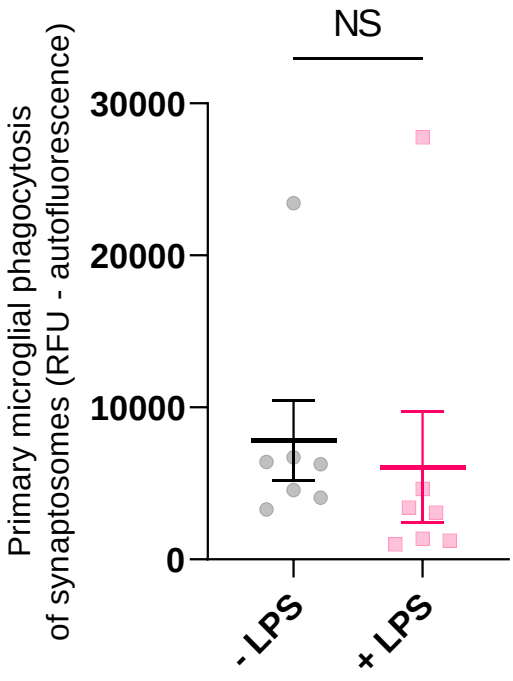

Figure 6.11. Chronic LPS treatment does not enhance microglial phagocytosis of synaptosomes. 24 hours treatment of primary rat microglia with LPS (100 ng/ml) does not enhance their phagocytosis of synaptosomes. Values are means ± SEM of at least 3 independent experiments. Statistical comparisons were made via Student's t-test. NS $p \geqslant 0.05$.

neuronal cultures are capable of generating functional synapses *in vitro*[749], and such cultures have been used to investigate microglial phagocytosis of synapses[356,598,750]. However, it is not known whether inflammatory activation of neuronal cultures can cause synaptic loss, or whether such loss occurs via microglial phagocytosis.

To investigate this, cerebellar neuronal cultures (also known as cerebellar granule cell cultures, or CGC cultures) were treated with LPS for 72 hours, and synaptic densities were measured by confocal microscopy. CGC cultures contain predominantly neurons, but also microglia and astrocytes[751], and LPS treatment of CGC cultures can induce neuronal loss via microglial phagocytosis of viable neurons[518]. Thus, it was essential to identify an LPS treatment condition

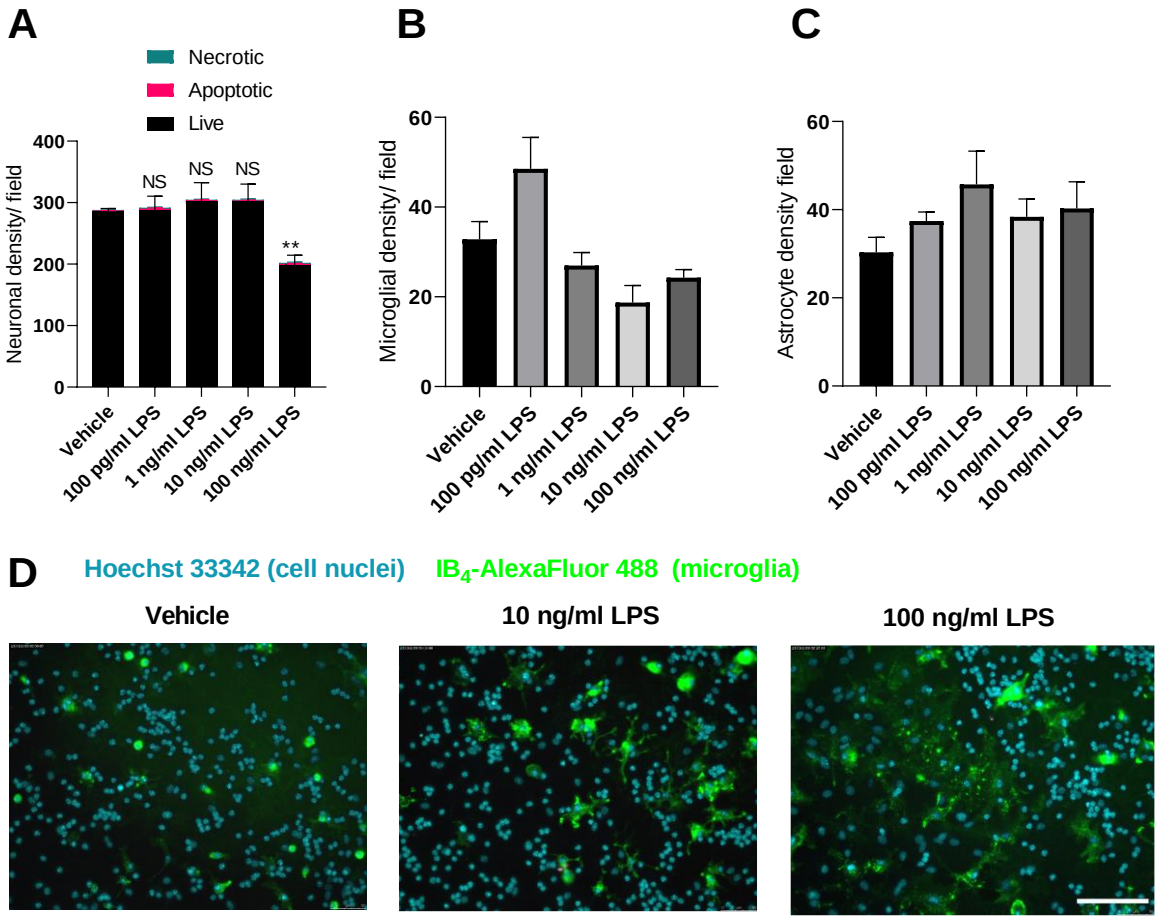

Figure 6.12. Chronic treatment of cerebellar granule cell cultures with up to 10 ng/ml LPS from *E. coli* does not cause neuronal loss. (A) Neuronal loss in CGC cultures is induced by 72 hours treatment with 100 ng/ml LPS from *E. coli*, but not 10 ng/ml or less. (B & C) LPS does not affect density of microglia (B) or astrocytes (C) in the cultures at any concentration tested. (D) Representative images of CGC cultures after 72 hours treatment with vehicle, 10 ng/ml or 100 ng/ml LPS, indicating a dose-dependent effect on microglial morphology. Scale bar (100 μm). Values are means ± SEM of at least 3 independent experiments. Statistical comparisons were made via one-way ANOVA. NS $p \geq 0.05$, ***$p<0.001$ versus 'vehicle' control.

that did not promote neuronal loss, from which inevitable synaptic loss could be falsely attributed to synapse-specific pruning. CGCs were treated with LPS from *E. coli* at a range of concentrations, and neuronal density was quantified by microscopy (Figure 6.12A). As expected, LPS induced a significant loss in neuronal density at 100 ng/ml ($p<0.001$ versus 'vehicle' control), which was not associated with an increase in detectable necrotic or apoptotic neurons, and consistent with neuronal loss by microglial phagoptosis[518]. However, no neuronal loss was observed after application of LPS at 10 ng/ml or lower. LPS was not found to induce any significant change in densities of microglia at any concentration tested (Figure 6.12B). However, it should be noted that quantification achieved by manual counting (as done here) is limited by dramatic morphological enlargement of the IB_4-AlexaFluor488-labelled microglia with LPS, which renders cell outlines difficult to demarcate. Quantification is further complicated by the fact that LPS has been described to induce microglial multinucleation[618]. No LPS treatment tested induced any significant change in astrocyte density either (Figure 6.12C). Interestingly, 10 ng/ml LPS did appear to cause a change in microglial morphology with increased process extension (Figure 6.12D-F), but this was not quantified.

The highest concentration of *E. coli* LPS that did not induce neuronal loss in CGC cultures over 72 hours was 10 ng/ml. To explore whether this treatment could induce synaptic loss, cultures were immunostained against synaptophysin - a well-established synaptic marker[752,753] - and imaged via confocal microscopy. Wild-type cultures stained positively for synaptophysin after treatment with vehicle or LPS (10 ng/ml) (Figure 6.13A). To assess whether $P2Y_6R$ influences synaptic densities, CGC cultures from $P2Y_6R$ knockout mice were cultured and imaged as for the wild-types. Again, staining against synaptophysin was observed in these cultures in the presence or absence of chronic LPS treatment, although such staining appeared qualitatively less dense than in the wild-types. To determine quantitatively whether or not this LPS treatment influences the number of synaptophysin-positive puncta (in both wild-type and $P2Y_6R$-knockout cultures), puncta were quantified using Trackmate[622] (Figure 6.13B). In wild-type CGC cultures, LPS was found to induce a significant reduction in detectable puncta (32 ± 6%; $p=0.005$). However, no significant change in puncta number was observed in the $P2Y_6R$ knockout cultures when LPS was present ($p=0.385$), implicating $P2Y_6R$ in this LPS-induced synaptic loss. Importantly, no statistically significant reductions in cell nuclei were observed after LPS treatment in the wild-type or $P2Y_6R$ knockout cultures (Figure 6.13C), consistent with previous findings that such treatment did not affect neuronal, microglial or astrocyte

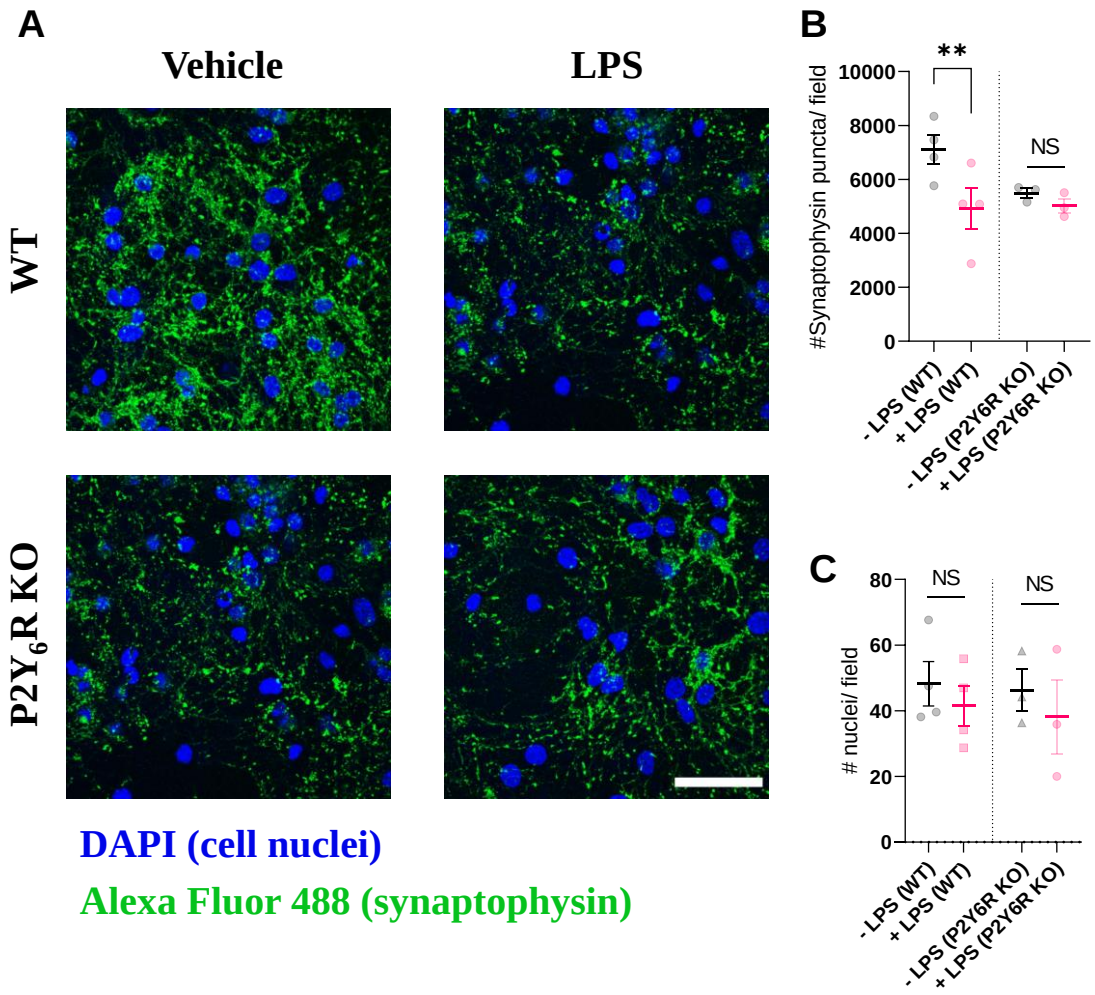

Figure 6.13. 10 ng/ml LPS causes synaptic loss in wild-type (but not $P2Y_6R$ knockout) CGC cultures. (A) CGC cultures (WT or $P2Y_6R$ KO) stain positively for synaptophysin (green) in the presence of vehicle or 10 ng/ml LPS (72 hours), as visualised by confocal microscopy. Nuclei (blue) are stained with DAPI. Scale bar (50 µm). (B) LPS (10 ng/ml, 72 hours) induces a reduction in synaptophysin-positive puncta in wild-type CGC cultures, but not in $P2Y_6R$-knockout CGC cultures. (C) This LPS treatment did not affect the number of DAPI-positive nuclei in the cultures, consistent with no neuronal loss induced by this LPS treatment, as demonstrated previously. Statistical comparisons were made via Student's t-test. NS $p \geq 0.05$, **$p<0.01$, as indicated.

densities in the CGC cultures (Figure 6.12). Together, these data demonstrate that LPS can induce significant synaptic loss in CGC cultures without causing significant neuronal loss, and that cultures lacking $P2Y_6R$ are protected against LPS-induced loss.

To further investigate how this LPS-induced synaptophysin loss is regulated, CGC cultures were treated with the $P2Y_{12}R$ blocker PSB0739, shown previously to inhibit microglial phagocytosis of synaptosomes (Figure 6.10), and effects on LPS-induced synaptophysin loss were assessed. PSB0739 (1 µM) applied for 72.5 hours (i.e. 30 minutes prior to LPS) did not

visibly affect staining against synaptophysin in the CGC cultures (Figure 6.14A), and did not significantly affect the number of synaptophysin puncta quantified (p=0.704; Figure 6.14B). However, PSB0739 completely prevented LPS-induced synaptophysin loss (p<0.001; p=0.997 versus '- LPS - PBS' control). No effect on cell nuclei densities were observed with the PSB0739 treatment (Figure 6.14C). Thus, this data indicates that $P2Y_{12}R$ is involved in LPS-induced synaptophysin loss. Since $P2Y_{12}R$ is exclusively expressed by microglia in the brain[372], this data also directly implicates microglia in this LPS-induced synaptophysin loss, and is consistent with LPS-induced microglial synaptophagy.

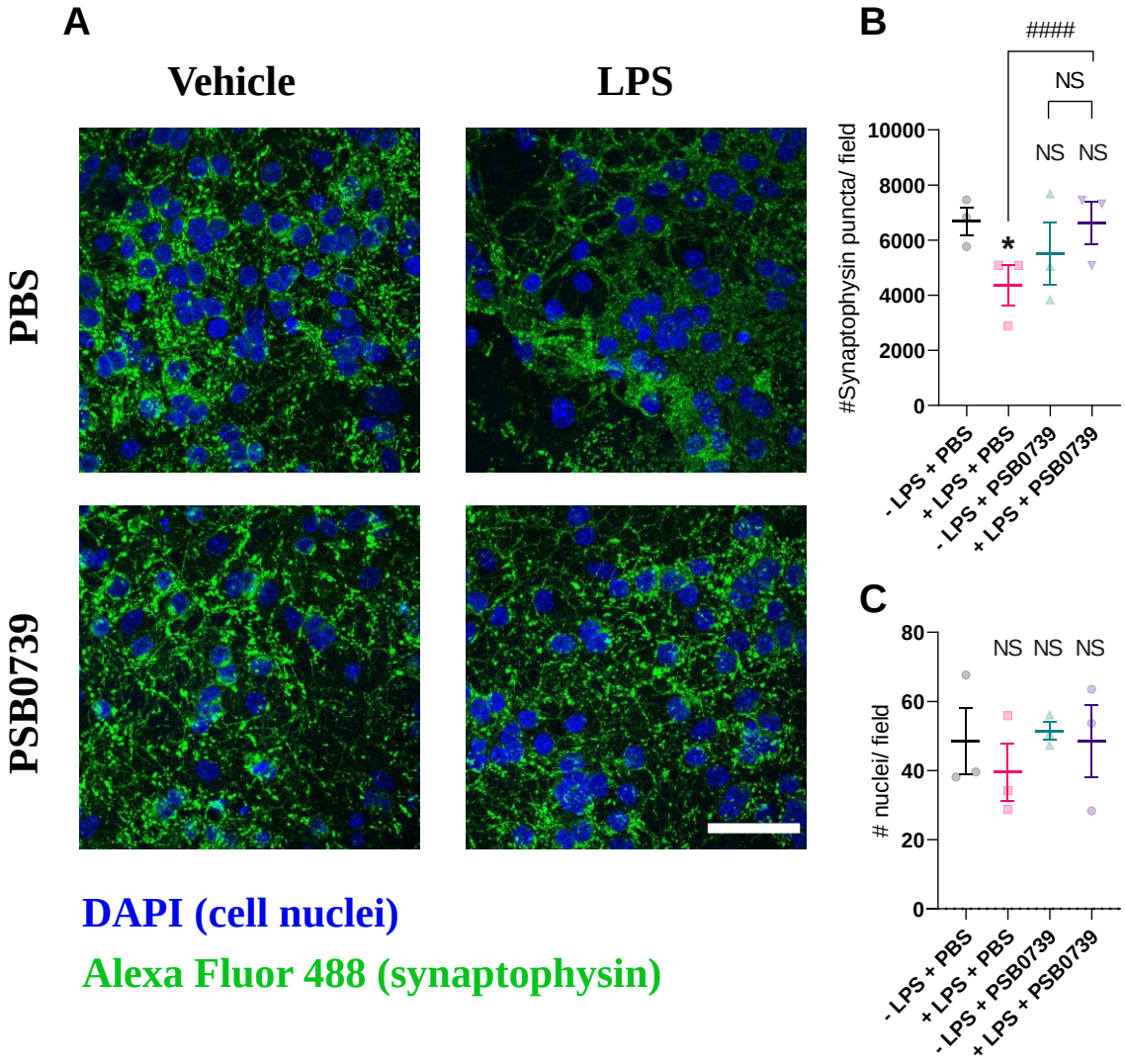

Figure 6.14. LPS-induced synaptic loss in CGC cultures is prevented by PSB0739. (A) CGC cultures stain positively for synaptophysin (green) in the presence of vehicle or LPS (10 ng/ml, 72 hours) and with or without PSB0739 (1 μM), as visualised by confocal microscopy. Nuclei (blue) are stained with DAPI. Scale bar (50 μm). (B) LPS (10 ng/ml, 72 hours) induces a reduction in synaptophysin-positive puncta in CGC cultures, which is prevented by PSB0739 (1 μM, 72.5 hours). (C) No effect on the number of DAPI-positive nuclei was observed under any conditions tested. Statistical comparisons were made via ANOVA. NS $p \geq 0.05$, *$p<0.05$ versus '-LPS + PBS' control; ####$p<0.0001$ as indicated.

6.3. Discussion

Microglial phagocytosis of synapses is well known to contribute to the development of neural circuitry in the CNS[325,372,351], but how this phagocytosis is regulated is not completely clear. The best characterised phagocytic receptors (with respect to microglial synaptophagy) are CR3[32,221,754] and TREM2[356]. Synapses tagged with the complement proteins C1q or C3 promote can microglial phagocytosis, for example via the microglial receptor CR3 (for C3), and such tagging is known to depend on neuronal activity and surface desialylation[32,221]. TREM2 can bind a variety of ligands (see section 2.3.1.8), and whilst the specific binding partner(s) involved in synaptophagy are unknown, TREM2 deficient mice exhibit reduced microglial synaptophagy and impaired synaptic elimination, as well as reduced long-range neural connectivity and behavioural deficits associated with autism[356]. Both CR3 and TREM2 are upregulated in microglia in contexts of neuroinflammation[403,501,509], as well as during developmental pruning of synapses[32,356]. The fact that microglia functionally express these phagocytic receptors during periods of synaptic pruning – and that developmental microglia also exhibit several other markers of an activated phenotype (see section 2.1.1) – thus implicates the myriad other receptors and signalling pathways known to regulate microglial phagocytosis in inflammation or pathology. Moreover, CR3 and TREM2 are implicated in regulating microglial phagocytosis of diverse targets other than synapses, including myelin[360,463], neurons[326,501,506], cellular debris[506], amyloid plaques[755] and bacteria[462]. The fact that these receptors can regulate phagocytosis of such diverse targets, but also specialise in synapse-specific phagocytosis (without associated phagocytosis of the attached neuron) highlights the idea that general phagocytic receptors can be modified to exert target-specificity in developmental contexts. However, how such specialisation of phagocytic function occurs is not known, and is a subject of intense research and debate.

In this chapter, I demonstrate novel roles for multiple opsonins and receptor-mediated signalling mechanisms in the regulation of microglial phagocytosis of synapses. These will be discussed sequentially. A renewed model of the signalling mechanisms that regulate microglial phagocytosis of synapses is also shown in Figure 6.15 (page 225).

6.3.1. Calreticulin/LRP1

As demonstrated previously, calreticulin is upregulated in and secreted by inflammatory activated microglia[124], and extracellular calreticulin can opsonise diverse targets, including bacterial and mammalian cells[143]. However, whether extracellular calreticulin can bind or opsonise synapses for phagocytosis by microglia has not previously been reported. I found that calreticulin associated with synaptosomes isolated from rat cortex, and this association was inhibitable by sucrose, indicating surface binding via calreticulin's carbohydrate-recognition domain. Furthermore, calreticulin opsonised the synapses for phagocytosis by primary rat microglia, which was inhibitable by sucrose but also by the LRP1 ligand RAP, consistent with LRP1 being the main phagocytic receptors for surface-exposed calreticulin[124,473]. Given the M1-like phenotype adopted by microglia during periods of synaptic pruning[32,356], it seems likely that calreticulin is secreted extracellularly by microglia (and possibly other immune cells) during such periods, although this has not been reported. My findings indicate that extracellular calreticulin can trigger microglial phagocytosis of synapses, and that such phagocytosis occurs through direct opsonisation of the synapses. If this is the case *in vivo*, it remains to be determined how calreticulin binds the synaptic surface, and how such binding can be synapse-specific. Linnartz *et al* showed that C1q tags (i.e. opsonises) neuronal dendrites for microglial phagocytosis, and this opsonisation is enhanced by enzymatically removing sialic acid residues from the dendritic surface[221]. Sialic acid residues are described as 'don't eat-me' signals (see section 1.4.1.4.7), and calreticulin opsonisation of neutrophils by peripheral macrophages has been shown to depend on calreticulin binding to desialylated glycan chains present on the neutrophil surface[143], suggesting that calreticulin opsonisation of synapses may also be desialylation-dependent. However, despite staining positively for the desialylation marker peanut agglutinin (which was enhanced after application of an exogenous sialidase), no increase in binding of calreticulin to synaptosomes was observed after enzymatic desialylation of the synaptic surface. This does not rule out the possibility that calreticulin binding to synaptosomes is mediated by pre-exposed desialylated glycan chains, although this would have to be tested: for example, by measuring calreticulin binding in the presence and absence of unlabelled peanut agglutinin. It is of interest to note that calreticulin also binds C1q[142,653], and so in principle could opsonise synapses for phagocytosis indirectly by binding any C1q present on the synapse, or alternatively, by binding the synapse independently of C1q and then presenting C1q to the phagocyte. Indeed, C1q is also known to bind directly to LRP1 and thereby modulate phagocytosis[756], consistent with the finding that blocking LRP1 with the

peptide RAP inhibited calreticulin opsonisation of the synaptosomes. However, any role for calreticulin in mediating C1q-dependent opsonisation of synapses would require testing, for example by measuring C1q binding to synapses in the presence of exogenous calreticulin/ an anti-calreticulin blocking antibody, or alternatively by measuring calreticulin binding to synapses in the presence of exogenous C1q/ an anti-C1q blocking antibody.

The extent to which extracellular calreticulin plays a role in developmental synaptophagy by microglia *in vivo* may be challenging to investigate, as this type of study has relied heavily on knockout animal models in the past[32,356,222,357], but homozygous calreticulin knockout is embryonically lethal in mice[757]. I have demonstrated previously that function-blocking antibodies against calreticulin can inhibit calreticulin-mediated opsonisation of bacteria for phagocytosis by microglia[124] (Chapter 4). In a tauopathic mouse model of AD, inhibiting C1q-induced synaptophagy via a blocking antibody prevented microglial engulfment of synapses and associated synaptic loss in the hippocampus[743]. In a separate AD model, Hong *et al* showed that the synaptic loss induced by ventricular injection of oligomeric β-amyloid (which was linked to CR3-dependent microglial phagocytosis) was inhibited by co-injection of a function-blocking antibody against C1q[586]. Importantly, this antibody-mediated rescue of synaptic loss was comparable to that achieved by genetically knocking out C1q. Thus, use of a function-blocking antibody against calreticulin may be sufficient to conclude a role in developmental (or indeed pathological) synaptic loss *in vivo*, and merits investigation. *In vivo* studies could also target LRP1, the microglial phagocytic receptor for calreticulin. However, since LRP1 knockout also causes embryonic lethality in mice[758], use of LRP1 compounds or antibodies may also be required for such studies.

6.3.2. Galectin-3/MerTK

Galectin-3 is released by both non-activated and inflammatory-activated microglia[124,212], and levels increase in the brain and CSF following tissue damage[675]. Galectin-3 can enhance microglial phagocytosis of neuron-like PC12 cells and neuronal debris by activating the microglial receptor MerTK[212], and I have shown that galectin-3 opsonises bacteria for microglial phagocytosis via MerTK[124]. However, any role for galectin-3 in opsonising synapses for removal (e.g. via microglial phagocytosis) has not been reported. In this chapter, I show that galectin-3 bound synapses, and this was inhibited by lactose, consistent with a role

for the carbohydrate-recognition domain in mediating synapse binding. Additionally, galectin-3 opsonised the synapses for microglial phagocytosis, which was inhibited by lactose or blocking MerTK - consistent with MerTK being the main microglial phagocytic receptor for galectin-3. Work in our lab has previously shown that galectin-3 binds neuron-like PC12 cells, and this binding was enhanced by enzymatic desialylation of the PC12 surface[212]. Moreover, this enzymatic desialylation also enhanced their galectin-3-induced phagocytosis by microglia, consistent with a sialylation-dependent opsonisation effect of galectin-3. Strikingly, desialylating the synaptosomes with neuraminidase was not found to enhance galectin-3 binding, indicating that binding in this context may be desialylation-independent. As mentioned previously, there is great interest in understanding how pro-phagocytic tagging of synapses can be targeted specifically to the synapse (but not to the associated neuron). The distinction in binding mechanisms of galectin-3 between synapses and cell bodies suggested here may be of relevance to how this differential tagging is achieved, although the mechanism by which galectin-3 bind to synapses remains unknown. However, the fact that lactose partially inhibited this binding highlights the importance of the lactose-inhibitable galectin-3 carbohydrate-recognition domain in interacting with the synaptic surface, and so implicates synaptic glycans in this binding.

The extent to which galectin-3 plays a role in microglial synaptophagy in developmental or pathological contexts requires further study. As for calreticulin, the facts that i) microglia adopt characteristics of an M1 phenotype during periods of developmental synaptic pruning, and ii) galectin-3 release is enhanced by inflammatory-activating microglia[124,212], suggest that galectin-3 may circulate extracellularly during this developmental pruning. If so, galectin-3 could bind and opsonise synapses for microglial phagocytosis. It should be noted that galectin-3 can induce microglial phagocytosis of non-synaptic targets, including whole cells and neuronal debris[212,675], and so such pro-phagocytic effects may not be specific to synapses. However, it is important to reiterate that phagocytic signalling mechanisms that are well-established to promote microglial phagocytosis of myriad non-synaptic targets (i.e. those controlled by microglial CR3 and TREM2) are somehow specialised to synaptophagy in the context of the developing brain. Thus, despite a more general pro-phagocytic capacity of galectin-3, phagocytosis may be specialised toward synapses during pruning, although this would need investigation. Like calreticulin, function-blocking antibodies against galectin-3 exist and are effective in inhibiting galectin-3-mediated inflammation *in vivo*[675], and so may

be useful for future investigation of a role for galectin-3 in developmental synaptophagy. However, unlike calreticulin, galectin-3 homozygous knockout animals are viable and have been used to study galectin-3 function during neuroinflammation[675]. Such animals would be useful in determining a role for galectin-3 in synaptophagy during development (or indeed pathology) *in vivo*. Regarding the possible role for galectin-3 in pathological synaptic loss: it is noteworthy that galectin-3 has been shown to be upregulated in the brains of AD patients as well as in mouse models of AD[503], and that synaptic loss is one of the earliest hallmarks of AD pathology[575] - meaning galectin-3 could in principle promote AD-associated synaptic loss via microglial synaptophagy. Again, this would require direct testing.

6.3.3. ApoE

ApoE is secreted from both astrocytes and microglia in the brain, and circulates extracellularly in the brain parenchyma to mediate lipid transport between cells, thus regulating lipid homeostasis[632]. As mentioned, apoE exists in three isoforms in humans, and apoE isoform is the strongest genetic risk factor for late-onset AD[640], which is characterised by early synaptic loss[575]. Chung *et al* have shown that apoE influences synaptic pruning by astrocytes, and that this influence is isoform-dependent[728]. In the developing retinogeniculate system, they demonstrate that astrocyte engulfment of axonal projections was inhibited by knocking-in the apoE isoform ε4, but was enhanced by knocking-in ε2. Using a synaptosome-phagocytosis assay, they demonstrated that astrocyte-conditioned medium from ε2 knock-in mice significantly enhanced phagocytosis of synaptosomes by astrocytes, whereas the same medium from ε4 knock-in mice reduced this phagocytosis, compared to medium from apoE-knockout mice. This data is consistent with apoE tagging and opsonising synapses for astrocyte phagocytosis in an isoform-dependent manner, although they did not confirm an opsonisation effect *per se*. However, whether apoE directly binds synapses – and whether any such binding is isoform-dependent – is not clear, and any role for apoE in regulating microglial phagocytosis of synapses has not been reported previously. Through a fluorescence-based binding assay, I show that apoE can associate with synapses down to nanomolar concentrations, and that such association is isoform-dependent, as association of ε2 was significantly higher than ε4 at the same concentration. Furthermore, I show for the first time that apoE association with synapses influences their phagocytosis by microglia, and that this opsonisation is isoform-dependent. For BV-2 microglia, phagocytosis of synaptosomes pre-incubated with ε2 was significantly

greater than phagocytosis of synaptosomes pre-incubated with ε4 - suggesting that in the context of the brain (where apoE will circulate and likely bind synapses), the propensity for phagocytic removal of the bound synapse is indeed influenced by apoE isoform, and this is directly relevant to AD. Moreover, phagocytosis of synaptosomes by primary rat microglia was significantly enhanced by ε2, but was not significantly enhanced by ε4, again consistent with an isoform-dependent opsonisation effect.

With respect to AD, ε4 is the disease-associated isoform of apoE, whilst ε2 is considered protective against AD[640]. AD is characterised by early synaptic loss, yet findings shown here (and also by Chung *et al*[728]) implicate the ε4 isoform as capable of protecting synapses from microglial synaptophagy relative to ε2, which appears paradoxical. In their studies, Chung *et al* also observed accumulation of C1q in the mouse hippocampus in ε4 knock-in mice when compared to ε2 knock-in mice. Given C1q accumulates at synapses in normal ageing[588], they suggest that C1q tags senescent synapses that also accumulate in (and may contribute to) ageing[759]. They propose that the reduced phagocytosis of synapses by astrocytes in the presence of ε4 (when compared to ε2) causes an accumulation of senescent synapses that are then tagged by C1q, which could thus contribute to circuitry decline and AD-associated cognitive deficits[728]. If this is the case, my data open the possibility that such accumulation of senescent synapses due to apoE isoform may also result from impaired microglial (as well as astrocyte) synaptophagy.

It remains unclear how apoE on synapses might signal to microglia, or indeed astrocytes, to regulate synaptophagy. Various receptors for apoE exist, including the phagocytic receptors LRP1 and TREM2, which are both expressed by microglia[477,506,507] and in principle could mediate this phagocytosis. Regarding the isoform-dependency of synapse opsonisation, the reduced association of ε4 with synapses relative to ε2 may be a sufficient explanation. However, isoform-specific binding of apoE to the low-density lipoprotein receptor (LDLR) – related to LRP1 – has been demonstrated[760]. Thus, differential opsonisation capacities for apoE isoforms may also result from differential capacities for activating their phagocytic receptor(s).

6.3.4. Tau

Like apoE, tau is heavily implicated in AD pathology, although typically as a component of the neurofibrillary tangles (NFTs) that accumulate within neurons as a result of tau hyperphosphorylation[761]. However, extracellular tau has also been suggested to contribute to AD pathology[729]. Extracellular tau accumulates in the CSF of AD patients[731], and has been shown to be directly toxic to neurons[762] and may promote the intercellular spread of toxic tau aggregates in tauopathies[729]. Furthermore, extracellular tau is released from synapses, and such release is increased from the synapses of AD brain compared to healthy controls, which is linked to AD-associated synaptic dysfunction[763]. However, how extracellular tau might promote such synaptic dysfunction is now known. I show that extracellular tau can associate with synaptosomes at concentrations down to 10 nM, and this association opsonises the synaptosomes for phagocytosis by primary rat microglia. Thus, extracellular tau may contribute to synaptic loss in AD by promoting microglial synaptophagy, although this would certainly benefit from testing in more physiologically relevant models than those used here, for example in mouse models of tauopathy.

In the absence of pathology, tau secretion into the extracellular space has been documented[762]. Tau has been detected in media conditioned by mixed neuronal cultures from healthy mice, as well as in media conditioned by the human neuronal cell-line SH-SY5Y[764]. Furthermore, tau circulating in the CSF of healthy individuals has also been detected[765]. Thus, extracellular tau may be physiologically relevant, although it is now known what role(s) it may have, or whether it may be released extracellularly in contexts of synaptic pruning.

6.3.5. P2Y receptors

The presence of extracellular nucleotides at synaptic terminals has been well documented[766], and can originate from the synapses themselves[767,768] or from nearby cells like astrocytes[769,770]. Such nucleotides can activate proximal P2Y receptors, which are expressed by both neuronal synapses and immune cells, including astrocytes and microglia[771,772,773]. Activation of P2Y receptors (and also ionotropic P2X receptors) by nucleotides may exert neuromodulatory effects on the synapses, and so are implicated in synaptic plasticity[770,774]. Microglia express both the pyramidinergic receptor $P2Y_6R$[485,430] and also the purinergic receptor $P2Y_{12}R$[709] - and

such receptors have been implicated by us and others in the phagocytosis of diverse targets, including neuronal cells[485]. Furthermore, microglia interact continuously with synapses in the brain[352,353], meaning that microglial $P2Y_6R$ and/or $P2Y_{12}R$ may be activated by nucleotides when proximal to synapses. However, whether such activation might exert any neuromodulatory function, or regulate synaptophagy, is not clear. In this chapter, I show that microglia phagocytose synaptosomes, and this can be inhibited by blocking either $P2Y_6R$ (with MRS2578) or $P2Y_{12}R$ (with PSB0739), or by adding exogenous ADP (the $P2Y_{12}R$ agonist) - consistent with roles for $P2Y_6R$- and $P2Y_{12}R$-signalling in regulating microglial synaptophagy. Furthermore, I show using cerebellar neuronal cultures that synaptic (but not neuronal) loss induced by LPS can be prevented by i) homozygous $P2Y_6R$ knockout, or ii) $P2Y_{12}R$ inhibition by PSB0379. The fact that $P2Y_{12}R$ is expressed exclusively by microglia in the brain[372] directly implicates microglia in mediating this LPS-induced synaptic loss, although they do not confirm that such loss occurs through microglial synaptophagy. Our lab has previously found that blocking or genetically-deleting $P2Y_6R$, or blocking $P2Y_{12}R$, all prevent the microglial phagocytosis of (viable) neurons induced by LPS. My data are consistent with a role for both $P2Y_6R$ and $P2Y_{12}R$ in regulating microglial phagocytosis of synapses in response to a lower LPS dose (that does not cause neuronal loss). This is certainly the most likely explanation, since blocking either $P2Y_6R$ or $P2Y_{12}R$ inhibited microglial phagocytosis of synaptosomes, and microglia are known to phagocytose synapses in neuronal cultures[356,743]. However, this hypothesis could be supported by e.g. i) testing whether LPS-induced synaptic loss is affected by interfering (pharmacologically or genetically) with microglial CR3, a phagocytic receptor known to regulate microglial synaptophagy[32], or ii) testing whether LPS induces microglial phagocytosis of synapses in the cerebellar cultures *per se*, for example by immunostaining against both synaptophysin and the microglial phagolysosomal marker CD68[743], and then measuring co-localisation. Given synaptophysin-positive puncta were significantly reduced after 72 hours of LPS exposure, increased microglial synaptophagy may not be detectable by simply measuring co-localisation of synapses with the phagolysosome at this time-point, as LPS-induced phagocytosis may have occurred well before this time-point. Thus, such experiments may require measuring co-localisation at a range of time-points, and may also benefit from a more precise knowledge of when LPS-induced synaptic loss first occurs in the cerebellar cultures, which should be easy to obtain.

What is the relevance of these findings to microglial synaptophagy during pathology? Regarding $P2Y_6R$, our lab has previously shown *in vitro* that LPS-induced phagocytosis of viable neurons by microglia requires $P2Y_6R$, and *in vivo*, that LPS-induced neuronal loss in the substantia nigra is prevented with $P2Y_6R$ knockout (unpublished). LPS-induced neuroinflammation is commonly used to model Parkinson's disease[775,776], and the loss of dopaminergic neurons that occurs in the substantia nigra during PD is directly linked to the cardinal motor symptoms associated with the disease[777]. PD is also characterised by extensive loss of synapses[592]. Synaptic loss may precede neuronal loss in PD, and indeed, it has been suggested that synaptic loss is the primary contributor to progression of the disease, rather than neuronal loss itself[778]. Thus, my finding that LPS-induced synaptic loss in a neuronal culture model was prevented by $P2Y_6R$ knockout may be relevant to PD. Furthermore, it may be of particular relevance to stages of the disease where synaptic loss but not neuronal loss is occurring, as my model identifies an inflammatory-condition that promotes synaptic loss without detectable neuronal loss. It would be interesting to explore whether LPS-models of PD could be modified to induce synaptic loss without neuronal loss – or else, whether existing models could be analysed at timepoints where synapse loss precedes neuronal loss - and then used to determine whether $P2Y_6R$ regulates this synapse loss *in vivo*. It should also be noted that increasing endotoxin has been identified in brains of neurodegenerative pathologies other than Parkinson's disease, including Alzheimer's disease, and has been suggested to contribute to these pathologies by promoting neuroinflammation, gliosis and phagoptosis[681]. Regardless of how endotoxin may enter the brain during neuropathology (for which there are various hypotheses), it is generally accepted that endotoxin levels rise gradually, rather than reaching a plateau immediately[681]. Given that synaptic loss is induced at a lower concentration of LPS compared to neuronal loss in cerebellar cultures - and that synaptic loss is an early hallmark of multiple neurodegenerative pathologies[779] and may precede neuronal loss[778,780] – my finding that LPS-induced synaptic loss is prevented by $P2Y_6R$ knockout has implications for synaptic loss in neurodegenerative diseases generally, and supports $P2Y_6R$ as a promising therapeutic target in the context of neuropathology.

What about $P2Y_6R$ in developmental synaptic pruning? To my knowledge, no involvement of $P2Y_6R$ in synaptic pruning has been reported. However, $P2Y_6R$ is upregulated in inflammatory-activated microglia *in vitro*[430] and *in vivo*[485], and it seems feasible that $P2Y_6R$ could be expressed by microglia that adopt an M1-like phenotype in the context of

developmental pruning, along with other phagocytic receptors such as CR3[32] and TREM2[356]. If so, $P2Y_6R$ may regulate microglial synaptophagy, although this would require investigation. As mentioned, homozygous $P2Y_6R$ knockout mice are viable and available in our lab, and could be used to further explore a role for $P2Y_6R$ in microglial pruning of synapses during development through methods similar to those employed by Schafer *et al* (for CR3)[32] or Filipello *et al* (for TREM2)[356].

What about $P2Y_{12}R$? I found that phagocytosis of synaptosomes by microglia was inhibited in the presence of the $P2Y_{12}R$ antagonist PSB0739, and also by exogenous ADP. These findings were similar to those obtained regarding microglial phagocytosis of bacteria (Chapter 5), and are consistent with $P2Y_{12}R$ facilitating microglial phagocytosis of synapses through migration and/or process extension toward the synapses. Furthermore, LPS-induced synaptic loss in cerebellar neuronal cultures was inhibited by PSB0739, indicating that microglial $P2Y_{12}R$ is required for this synaptic loss, and consistent with a role for $P2Y_{12}R$ in microglial synaptophagy. Sipe *et al* showed that microglia in the visual cortex exhibit less ramification in $P2Y_{12}R$-knockout mice compared to wild-types, although no differences in process mobility were observed[372]. Monocular deprivation - which induces structural changes in corresponding neural regions of the visual cortex and associated alterations in synaptic plasticity[372] – was also found to increase microglial interactions with, and engulfment of, synapses. Importantly, both the synaptic interactions and engulfment induced by monocular deprivation were absent in $P2Y_{12}R$ knockout mice, directly implicating microglial $P2Y_{12}R$ in modulating synaptic plasticity via synaptophagy. Thus, whilst a role for $P2Y_{12}R$ in microglial synaptophagy in the context of synaptic plasticity seems established, any role for $P2Y_{12}R$ in developmental and pathological synaptophagy is unknown. Unlike $P2Y_6R$ (or calreticulin, or galectin-3), $P2Y_{12}R$ is downregulated by microglial activation[781]. Indeed, microglial expression of $P2Y_{12}R$ in the context of developmental synaptic pruning is minimal[356], bringing the functional relevance of $P2Y_{12}R$ here into question. However, blocking $P2Y_{12}R$ in cerebellar neuronal cultures completely prevented LPS-induced synaptic loss. One possible explanation is that $P2Y_{12}R$ regulates initial migratory responses toward synapses by microglia/ microglial processes to facilitate synaptophagy in contexts of development or inflammation, but is subsequently downregulated. However, it should be noted that no effect of $P2Y_{12}R$-knockout on baseline microglial interactions with, or engulfment of, synapses were observed by Sipe *et al* in the absence of monocular deprivation[372]. A more conclusive answer could be obtained through use

of $P2Y_{12}R$ knockout mice, with which both developmental and pathological synaptophagy by microglia could be explored.

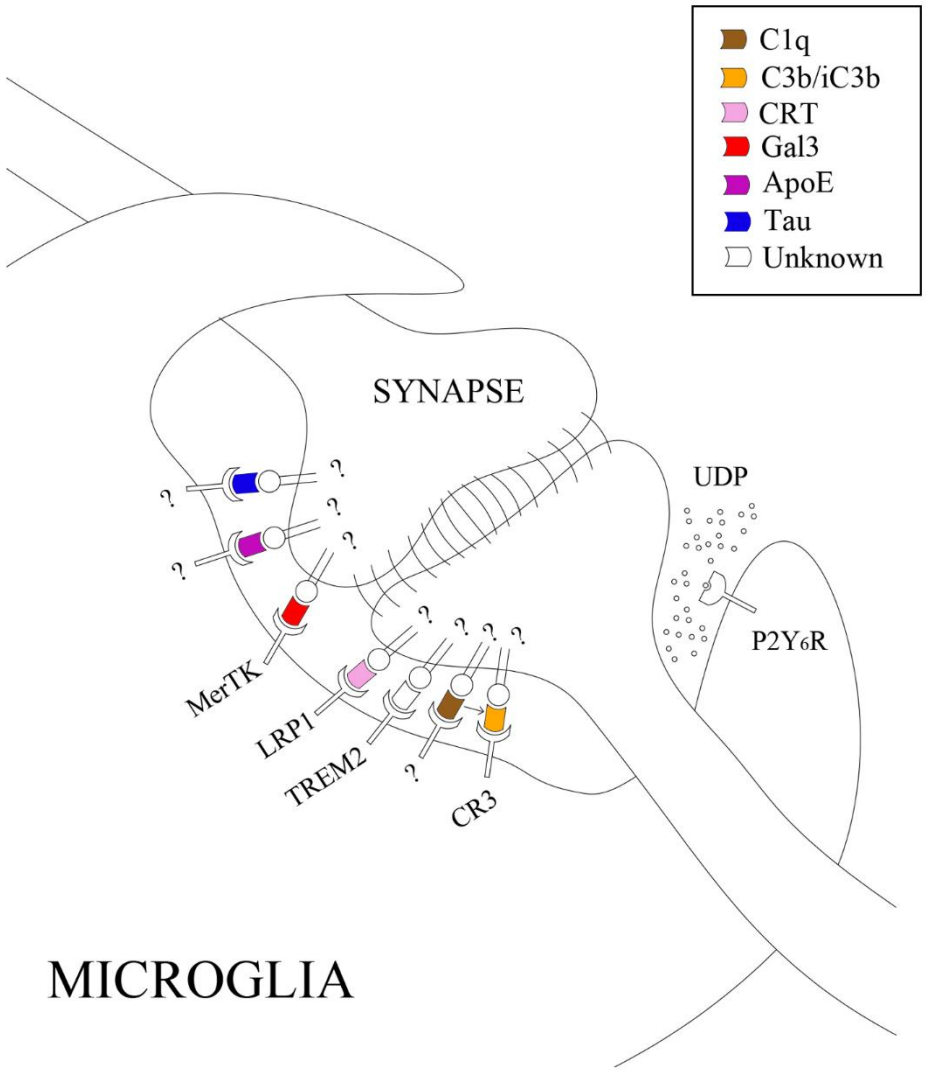

Figure 6.15. Model for microglial phagocytosis of synapses. Microglial phagocytosis of synapses is promoted by a variety of pro-phagocytic signalling mechanisms. CR3 promotes microglial phagocytosis of synapses opsonised with complement component C3, and this can be facilitated by C1q on the synaptic surface[32,222]. TREM2 promotes microglial phagocytosis of synapses through unclear mechanisms[356]. LRP1 and MerTK can both promote microglial phagocytosis of synapses opsonised with calreticulin and galectin-3, respectively. ApoE and tau can opsonise synapses for microglial phagocytosis through unknown mechanisms. Microglial $P2Y_6R$ can also promote phagocytosis of the synapses, possibly by binding extracellular UDP.

CHAPTER VII

CONCLUSIONS & FUTURE PERSPECTIVES

In this work, I report novel roles for multiple known proteins in the regulation of microglial phagocytosis of bacteria and synapses, which are here summarised and reviewed.

7.1. Microglial phagocytosis of bacteria

Microglia are the resident macrophage within the brain, and as such are primarily responsible for detecting and eliminating bacterial pathogens present within the brain parenchyma. In this thesis, I identify calreticulin and galectin-3 as novel opsonins for microglial phagocytosis of bacteria. Both proteins were secreted by inflammatory-activated microglia, and both could bind *E. coli* when in the extracellular space, thus promoting their phagocytic clearance by the microglia. For calreticulin, this phagocytosis was mediated by microglial LRP1. For galectin-3, it was mediated by microglial MerTK. Thus, both calreticulin and galectin-3 present as natural anti-bacterial agents of the brain, and may have therapeutic potential in bacterial infections of the brain. However, it remains to be seen whether these proteins can promote phagocytic clearance of bacteria by microglia *in vivo*, and if their promotion of phagocytosis extends to other bacterial species that have been detected within the healthy brain, or that contribute to brain infection.

Furthermore, I provide evidence that extracellular calreticulin can induce immune activation of microglia, which may be beneficial for phagocytic clearance of microglia but may otherwise be damaging to host tissue. More research is required to elucidate the role of extracellular calreticulin with respect to immune regulation, and it is interesting to speculate that extracellular calreticulin may be released from cells generally during injury (as it is constitutively expressed by all nucleated cells[133]) and so act as an alarmin, although this requires investigation. It may also be the case that extracellular calreticulin promotes phagocytic clearance of bacteria outside the brain to respond to peripheral infection. Indeed, peripheral macrophages have recently been shown to release extracellular calreticulin to

opsonise neutrophils for phagocytic removal by the macrophages[143], and in principle could opsonise bacteria similarly. Whilst I was unable to replicate a calreticulin-opsonisation effect with U937 monocyte cells, this does not mean such an effect does not exist with other peripheral phagocytes (or indeed with other monocyte cells). If this is the case, the therapeutic potential for calreticulin would dramatically expand to peripheral (as well as neural) infection. Moreover, calreticulin-mediated phagocytosis of cellular targets has been reported as immunogenic[656] - that is, it promotes an adaptive immune response against the cell originally phagocytosed. If calreticulin-mediated opsonisation of bacteria is similarly immunogenic, this would further enhance the therapeutic potential of calreticulin, but this would need to be tested. It is appealing to make similar speculations about galectin-3, which has also been detected peripherally during bacterial infection[211], although phagocytosis via galectin-3 is not known to be immunogenic.

Regarding β-amyloid and apolipoprotein E: both proteins are known to be generated by immune cells of the brain[633,634,635,643], and are upregulated during neuroinflammation[637,679,686]. I show that both apoE and β-amyloid are capable of binding and opsonising bacteria for microglial phagocytosis. Interestingly, only the monomeric form of β-amyloid (but not the oligomeric form) bound and opsonised the bacteria to any significant level. β-amyloid oligomerises into fibrillar aggregates during AD pathology, and the presence of bacteria and bacterial-derived endotoxin are all increased in AD brains[681], meaning the reduced capacity for oligomeric β-amyloid to induce phagocytic clearance of bacteria may be relevant to AD. For apoE, the ε2 isoform significantly bound and opsonised the bacteria for microglial phagocytosis, but such effects were not observed with the ε4 isoform. Given ε4 is a primary risk factor for AD (whilst the ε2 isoform is considered neuroprotective)[640], a reduced capacity for ε4 to promote phagocytic clearance of bacteria by microglia may also be relevant to AD. However, as with calreticulin and galectin-3, further research is required to see if these findings translate to the *in vivo* situation.

In this work, I also provide evidence for a novel role of nucleotide signaling in the phagocytic clearance of bacteria by microglia, which is mediated via the microglial receptors $P2Y_6R$ and $P2Y_{12}$. Live *E. coli* were found to activate $P2Y_6R$, and microglia inflammatory-activated by bacterial LPS were found to release extracellular agonist of $P2Y_6R$. Exogenous application of

the $P2Y_6R$ agonist UDP enhanced microglial phagocytosis of bacteria in culture, and this was prevented by blocking $P2Y_6R$. Moreover, LPS-induced phagocytosis of the bacteria by microglia was prevented by eliminating extracellular nucleotide with apyrase, or by blocking $P2Y_6R$. Together, these findings indicate that $P2Y_6R$-signalling mediates the phagocytic clearance of bacteria by microglia, and so $P2Y_6R$ presents as a novel therapeutic target for bacterial infections of the brain. Outside the brain, $P2Y_6R$ is expressed by peripheral immune cells, including macrophages[782], and $P2Y_6R$ is known to promote bacterial clearance by peripheral macrophages in a mouse model of peritonitis[696]. My data support the idea that $P2Y_6R$-mediated clearance of the bacteria in this model was due to phagocytosis. Microglial $P2Y_6R$ has been shown to facilitate phagocytosis of damaged neurons[485], and our lab have found that microglial $P2Y_6R$ is required for the phagoptosis of viable neurons in multiple models of neurodegeneration. Combined with my data, these findings implicate $P2Y_6R$ as a key microglial phagocytic receptor in a variety of contexts. However, given that $P2Y_6R$ is considered detrimental in the neurodegeneration models through its induction of neuronal loss, the therapeutic potential of $P2Y_6R$ in the context of bacterial infections of the brain may be limited if associated tissue damage occurs through its activation. However, this requires investigation. Again, it remains to be seen whether this $P2Y_6R$-dependent microglial phagocytosis of bacteria extends to the *in vivo* situation.

Regarding $P2Y_{12}R$, I also provide preliminary evidence that $P2Y_{12}R$ signalling facilitates microglial phagocytosis of bacteria, possibly by regulating the chemotactic responses to the bacteria by the microglia[118]. The primary agonists for $P2Y_{12}R$ are ATP and ADP[118], and whilst various bacterial strains are known to release these nucleotides extracellularly[701], it has not been confirmed whether bacterial-derived ADP/ATP induces chemotactic responses from microglia via $P2Y_{12}R$. As with $P2Y_6R$, any role for $P2Y_{12}R$ in facilitating bacterial clearance *in vivo* still requires testing. Both $P2Y_6R$- and $P2Y_{12}R$-knockout mouse models are viable[372], and would be the most appropriate tools for such investigation. Whilst $P2Y_{12}R$ is expressed exclusively by microglia in the brain[118], $P2Y_{12}R$ expression has also been detected in peripheral immune cells, including dendritic cells[783] and eosinophils[784]. Thus, in principle, $P2Y_{12}R$ may also facilitate immune responses to bacteria peripherally, such as bacterial clearance via phagocytosis, and this should be investigated.

7.2. Microglial phagocytosis of synapses

Since microglial synaptophagy was first described as a key contributor to the synaptic pruning that occurs during CNS development[354], there has been great interest in discerning the cellular mechanisms that regulate such phagocytic activity. However, our understanding of this regulation is far from complete. In this thesis, I provide evidence for novel roles of several proteins in regulating microglial phagocytosis of synapses – in particular: calreticulin, galectin-3, $P2Y_{12}R$ and $P2Y_6R$. Both calreticulin and galectin-3 were found to bind and opsonise synaptosomes for microglial phagocytosis. As with the bacteria, this was mediated by microglial LRP1 (for calreticulin) and MerTK (for galectin-3). Thus, both calreticulin and galectin-3 present as novel opsonins for synaptophagy, which may play a role in synaptic turnover in the brain, and may also be of relevance in developmental synaptic pruning and pathological synaptic loss.

Whilst it remains to be seen whether either calreticulin or galectin-3 circulate extracellularly in the context of developmental pruning, their detection in the extracellular space during conditions of neuroinflammation[124,675] make a role in pathological synaptic loss entirely possible. Indeed, galectin-3 is known to be upregulated in mouse models of AD, and is enriched in human AD brains[503]. Given synaptic loss is an early hallmark of AD pathology[575] - and that synaptic loss in AD is attributed to microglial synaptophagy[577] - galectin-3 may exacerbate AD pathology by promoting microglial phagocytosis of synapses, although this needs to be tested directly. Once again, future studies should explore the extent to which both calreticulin and galectin-3 can promote microglial phagocytosis of synapses *in vivo*, using either knockout animals or function-blocking antibodies. Such studies could also use *in vitro* models of synaptophagy, such as the neuronal-culture model of inflammatory synaptic loss developed by me and described in Chapter 6. Indeed, preliminary data using this model indicates that calreticulin can induce synaptic loss without associated neuronal loss. If confirmed, such findings would further support a role for calreticulin in microglial synaptophagy. The same model is currently being used to test whether LPS-induced synaptic loss can be prevented by i) blocking LRP1 with RAP; ii) blocking calreticulin with a function-blocking antibody; iii) blocking MerTK with UNC569; and iv) blocking galectin-3 with a function-blocking antibody. Results from these experiments could further elucidate

roles for calreticulin and galectin-3 in microglial-mediated synapse removal, and could prove relevant for both developmental pruning and pathological synaptic loss.

ApoE and tau have both been detected extracellularly in the brain[785,786], and I show that both apoE (specifically the ε2 isoform) and tau bound synaptosomes and opsonised them for phagocytosis by microglia in culture. Thus, these proteins may play a role in synaptic turnover via microglial synaptophagy. As with calreticulin and galectin-3, is it unclear to what extent these proteins are secreted by cells during contexts of developmental synaptic pruning, and so whether these proteins might contribute to such pruning by promoting microglial synaptophagy, which should be investigated. However, both proteins are known to exist extracellularly in the context of AD[731,787], and indeed, both are heavily implicated in AD pathology. Moreover, I was unable to find any significant opsonisation effect by the ε4 isoform of apoE, suggesting a differential capacity for opsonisation of synapses by apoE based on the isoform. Since apoE isoform is the biggest genetic risk factor for AD[640], this finding may also be relevant to AD, and merits further study.

$P2Y_6R$ is expressed by inflammatory-activated microglia[485,430], and so may be expressed by microglia in the context of developmental synaptic pruning, along with other M1-associated phagocytic receptors like CR3[32]. I found that microglial phagocytosis of synaptosomes was inhibited by blocking $P2Y_6R$, and that LPS-induced and microglia-mediated elimination of synapses was absent in neuronal cultures lacking $P2Y_6R$. Our lab has unpublished data establishing a role for $P2Y_6R$ in mediating the neuronal loss caused by microglial phagocytosis of neurons in models of both AD and PD. Given synaptic loss has been observed to precede neuronal loss in these diseases – and that pathological synaptic loss in AD is attributed to microglial synaptophagy[577] – it is interesting to speculate that $P2Y_6R$ may promote such pathological synaptic loss via microglial phagocytosis. This requires further investigation, ideally using *in vivo* models of neurodegenerative disease. If proven correct, this would support $P2Y_6R$ as being a particularly promising therapeutic candidate in the treatment of neurodegeneration.

Regarding $P2Y_{12}R$: I show that blocking $P2Y_{12}R$-signalling inhibited microglial phagocytosis of synaptosomes in culture, and also prevented LPS-induced synaptic loss mediated by microglia in CGC cultures. As with $P2Y_6R$, our lab has found that blocking $P2Y_{12}R$ in the same neuronal cultures treated with a higher LPS dose, or treated with β-amyloid or extracellular tau, prevents the microglial phagocytosis of viable neurons that otherwise results from such treatments. Thus, as for $P2Y_6R$, $P2Y_{12}R$ may be a key mediator of pathological synaptic loss via microglial synaptophagy, and this should be investigated further. Whilst it is less obvious if $P2Y_{12}R$ could play a role in microglial synaptophagy during developmental pruning – as $P2Y_{12}R$ is downregulated in microglia during these periods[356] – this is also possible (particularly given the known role for $P2Y_{12}R$ in mediating plasticity-induced microglial synaptophagy[372]), and should be explored.

As a final comment: the model of inflammatory synaptic loss in neuronal cultures described in Chapter 6 may prove particularly useful in future studies on how pathological microglial-mediated synaptic loss is regulated in the context of neurodegeneration. Inflammatory-activation of the same neuronal cultures by higher doses of LPS induces microglial phagocytosis of viable neurons and neuronal loss, and is used to model neurodegenerative neuronal loss[518,478,491]. This model has helped identify various signalling mechanisms that mediate microglial phagocytosis of live neurons - including VNR-signalling via the opsonin MFG-E8 and neuron-exposed phosphatidylserine[518], LRP1-signalling via neuron-exposed calreticulin[478], and $P2Y_6R$-signalling via extracellular UDP[491]. Such signalling mechanisms are thus implicated in neurodegenerative neuronal loss. My model presents a similarly useful tool to study the mechanisms that regulate synaptic loss by inflammatory-activated microglia, and should be used in a similar fashion. Moreover, the same culture system has also been used to investigate the microglial phagocytosis of viable neurons that is induced by other pathological stimuli, such as TNF-α[521], oligomeric β-amyloid[522] and extracellular tau (unpublished) - and β-amyloid and tau are both used to widely model AD. Given synaptic loss features early in AD pathology[575], it is appealing to speculate that lower doses of these stimuli might induce synaptic loss without neuronal loss in these neuronal cultures, as was the case with LPS. If so, this could expand the use of this model with respect to AD-associated synaptic loss, and be used to identify signalling mechanisms that regulate such loss.

APPENDIX

Provided here are statistical data pertaining to figures found within this thesis, as indicated.

Figure 5.1D

Tukey's multiple comparisons test	Adjusted P Value	Significance
Vehicle:P2Y6R-mCherry 132N1s vs. Vehicle:mCherry 1321N1s	>0.9999	ns
Vehicle:P2Y6R-mCherry 132N1s vs. 0.1 nM:P2Y6R-mCherry 132N1s	0.9964	ns
Vehicle:P2Y6R-mCherry 132N1s vs. 1 nM:P2Y6R-mCherry 132N1s	<0.0001	****
Vehicle:P2Y6R-mCherry 132N1s vs. 10 nM:P2Y6R-mCherry 132N1s	<0.0001	****
Vehicle:P2Y6R-mCherry 132N1s vs. 100 nM:P2Y6R-mCherry 132N1s	<0.0001	****
Vehicle:P2Y6R-mCherry 132N1s vs. 1 µM:P2Y6R-mCherry 132N1s	<0.0001	****
Vehicle:P2Y6R-mCherry 132N1s vs. 10 µM:P2Y6R-mCherry 132N1s	<0.0001	****
Vehicle:mCherry 1321N1s vs. 0.1 nM:mCherry 1321N1s	>0.9999	ns
Vehicle:mCherry 1321N1s vs. 1 nM:mCherry 1321N1s	>0.9999	ns
Vehicle:mCherry 1321N1s vs. 10 nM:mCherry 1321N1s	>0.9999	ns
Vehicle:mCherry 1321N1s vs. 100 nM:mCherry 1321N1s	>0.9999	ns
Vehicle:mCherry 1321N1s vs. 1 µM:mCherry 1321N1s	>0.9999	ns
Vehicle:mCherry 1321N1s vs. 10 µM:mCherry 1321N1s	>0.9999	ns
0.1 nM:P2Y6R-mCherry 132N1s vs. 0.1 nM:mCherry 1321N1s	0.9835	ns
0.1 nM:P2Y6R-mCherry 132N1s vs. 1 nM:P2Y6R-mCherry 132N1s	<0.0001	****
0.1 nM:P2Y6R-mCherry 132N1s vs. 10 nM:P2Y6R-mCherry 132N1s	<0.0001	****
0.1 nM:P2Y6R-mCherry 132N1s vs. 100 nM:P2Y6R-mCherry 132N1s	<0.0001	****
0.1 nM:P2Y6R-mCherry 132N1s vs. 1 µM:P2Y6R-mCherry 132N1s	<0.0001	****
0.1 nM:P2Y6R-mCherry 132N1s vs. 10 µM:P2Y6R-mCherry 132N1s	<0.0001	****
0.1 nM:mCherry 1321N1s vs. 1 nM:mCherry 1321N1s	>0.9999	ns
0.1 nM:mCherry 1321N1s vs. 10 nM:mCherry 1321N1s	>0.9999	ns
0.1 nM:mCherry 1321N1s vs. 100 nM:mCherry 1321N1s	>0.9999	ns
0.1 nM:mCherry 1321N1s vs. 1 µM:mCherry 1321N1s	>0.9999	ns
0.1 nM:mCherry 1321N1s vs. 10 µM:mCherry 1321N1s	>0.9999	ns
1 nM:P2Y6R-mCherry 132N1s vs. 1 nM:mCherry 1321N1s	<0.0001	****
1 nM:P2Y6R-mCherry 132N1s vs. 10 nM:P2Y6R-mCherry 132N1s	<0.0001	****

1 nM:P2Y6R-mCherry 132N1s vs. 100 nM:P2Y6R-mCherry 132N1s	<0.0001	****
1 nM:P2Y6R-mCherry 132N1s vs. 1 µM:P2Y6R-mCherry 132N1s	<0.0001	****
1 nM:P2Y6R-mCherry 132N1s vs. 10 µM:P2Y6R-mCherry 132N1s	<0.0001	****
1 nM:mCherry 1321N1s vs. 10 nM:mCherry 1321N1s	>0.9999	ns
1 nM:mCherry 1321N1s vs. 100 nM:mCherry 1321N1s	>0.9999	ns
1 nM:mCherry 1321N1s vs. 1 µM:mCherry 1321N1s	>0.9999	ns
1 nM:mCherry 1321N1s vs. 10 µM:mCherry 1321N1s	>0.9999	ns
10 nM:P2Y6R-mCherry 132N1s vs. 10 nM:mCherry 1321N1s	<0.0001	****
10 nM:P2Y6R-mCherry 132N1s vs. 100 nM:P2Y6R-mCherry 132N1s	0.233	ns
10 nM:P2Y6R-mCherry 132N1s vs. 1 µM:P2Y6R-mCherry 132N1s	0.1997	ns
10 nM:P2Y6R-mCherry 132N1s vs. 10 µM:P2Y6R-mCherry 132N1s	0.689	ns
10 nM:mCherry 1321N1s vs. 100 nM:mCherry 1321N1s	>0.9999	ns
10 nM:mCherry 1321N1s vs. 1 µM:mCherry 1321N1s	>0.9999	ns
10 nM:mCherry 1321N1s vs. 10 µM:mCherry 1321N1s	>0.9999	ns
100 nM:P2Y6R-mCherry 132N1s vs. 100 nM:mCherry 1321N1s	<0.0001	****
100 nM:P2Y6R-mCherry 132N1s vs. 1 µM:P2Y6R-mCherry 132N1s	>0.9999	ns
100 nM:P2Y6R-mCherry 132N1s vs. 10 µM:P2Y6R-mCherry 132N1s	0.9999	ns
100 nM:P2Y6R-mCherry 132N1s vs. 10 µM:mCherry 1321N1s	<0.0001	****
100 nM:mCherry 1321N1s vs. 1 µM:mCherry 1321N1s	>0.9999	ns
100 nM:mCherry 1321N1s vs. 10 µM:mCherry 1321N1s	>0.9999	ns
1 µM:P2Y6R-mCherry 132N1s vs. 1 µM:mCherry 1321N1s	<0.0001	****
1 µM:P2Y6R-mCherry 132N1s vs. 10 µM:P2Y6R-mCherry 132N1s	0.9996	ns
1 µM:mCherry 1321N1s vs. 10 µM:mCherry 1321N1s	>0.9999	ns

Figure 5.1E

Tukey's multiple comparisons test	**Adjusted P Value**	**Significance**
Vehicle:UMP vs. 10 nM:UMP	>0.9999	ns
Vehicle:UMP vs. 100 nM:UMP	>0.9999	ns
Vehicle:UMP vs. 1 µM:UMP	0.9953	ns
Vehicle:UMP vs. 10 µM:UMP	0.6783	ns
Vehicle:UMP vs. 100 µM:UMP	<0.0001	****
Vehicle:UMP vs. 1 mM:UMP	<0.0001	****
Vehicle:Uridine vs. 1 nM:Uridine	>0.9999	ns
Vehicle:Uridine vs. 10 nM:Uridine	>0.9999	ns
Vehicle:Uridine vs. 100 nM:Uridine	0.9983	ns

Vehicle:Uridine vs. 1 µM:Uridine	>0.9999	ns
Vehicle:Uridine vs. 10 µM:Uridine	0.9973	ns
Vehicle:Uridine vs. 100 µM:Uridine	0.9057	ns
Vehicle:Uridine vs. 1 mM:Uridine	0.9991	ns
1 nM:UMP vs. 10 nM:UMP	>0.9999	ns
1 nM:UMP vs. 100 nM:UMP	>0.9999	ns
1 nM:UMP vs. 1 µM:UMP	0.9974	ns
1 nM:UMP vs. 10 µM:UMP	0.7237	ns
1 nM:UMP vs. 100 µM:UMP	<0.0001	****
1 nM:UMP vs. 1 mM:UMP	<0.0001	****
1 nM:Uridine vs. 10 nM:Uridine	>0.9999	ns
1 nM:Uridine vs. 100 nM:Uridine	>0.9999	ns
1 nM:Uridine vs. 1 µM:Uridine	>0.9999	ns
1 nM:Uridine vs. 10 µM:Uridine	>0.9999	ns
1 nM:Uridine vs. 100 µM:Uridine	0.9991	ns
1 nM:Uridine vs. 1 mM:Uridine	>0.9999	ns
10 nM:UMP vs. 100 nM:UMP	>0.9999	ns
10 nM:UMP vs. 1 µM:UMP	0.9998	ns
10 nM:UMP vs. 10 µM:UMP	0.8465	ns
10 nM:UMP vs. 100 µM:UMP	<0.0001	****
10 nM:UMP vs. 1 mM:UMP	<0.0001	****
10 nM:Uridine vs. 100 nM:Uridine	>0.9999	ns
10 nM:Uridine vs. 1 µM:Uridine	>0.9999	ns
10 nM:Uridine vs. 10 µM:Uridine	>0.9999	ns
10 nM:Uridine vs. 100 µM:Uridine	0.9907	ns
10 nM:Uridine vs. 1 mM:Uridine	>0.9999	ns
100 nM:UMP vs. 1 µM:UMP	0.9997	ns
100 nM:UMP vs. 10 µM:UMP	0.8386	ns
100 nM:UMP vs. 100 µM:UMP	<0.0001	****
100 nM:UMP vs. 1 mM:UMP	<0.0001	****
100 nM:Uridine vs. 1 µM:Uridine	>0.9999	ns
100 nM:Uridine vs. 10 µM:Uridine	>0.9999	ns
100 nM:Uridine vs. 100 µM:Uridine	>0.9999	ns
100 nM:Uridine vs. 1 mM:Uridine	>0.9999	ns
1 µM:UMP vs. 10 µM:UMP	0.9997	ns
1 µM:UMP vs. 100 µM:UMP	<0.0001	****
1 µM:UMP vs. 1 mM:UMP	<0.0001	****
1 µM:Uridine vs. 10 µM:Uridine	>0.9999	ns
1 µM:Uridine vs. 100 µM:Uridine	0.9998	ns
1 µM:Uridine vs. 1 mM:Uridine	>0.9999	ns
10 µM:UMP vs. 100 µM:UMP	<0.0001	****
10 µM:UMP vs. 1 mM:UMP	<0.0001	****
10 µM:UMP vs. 1 mM:Uridine	0.998	ns

Figure 6.7A

Tukey's multiple comparisons test	Adjusted P Value	Summary
Vehicle:ApoE2 vs. 10 nM:ApoE2	0.9939	ns
Vehicle:ApoE2 vs. 100 nM:ApoE2	0.0153	*
Vehicle:ApoE2 vs. 1 µM:ApoE2	<0.0001	****
Vehicle:ApoE4 vs. 10 nM:ApoE4	0.9985	ns
Vehicle:ApoE4 vs. 100 nM:ApoE4	0.1883	ns
Vehicle:ApoE4 vs. 1 µM:ApoE4	<0.0001	****
10 nM:ApoE2 vs. 10 nM:ApoE4	>0.9999	ns
10 nM:ApoE2 vs. 100 nM:ApoE2	0.0632	ns
10 nM:ApoE2 vs. 1 µM:ApoE2	<0.0001	****
10 nM:ApoE4 vs. 100 nM:ApoE4	0.4438	ns
10 nM:ApoE4 vs. 1 µM:ApoE4	<0.0001	****
100 nM:ApoE2 vs. 100 nM:ApoE4	0.8584	ns
100 nM:ApoE2 vs. 1 µM:ApoE2	<0.0001	****
100 nM:ApoE4 vs. 1 µM:ApoE4	<0.0001	****
1 µM:ApoE2 vs. 1 µM:ApoE4	0.0209	*

BIBLIOGRAPHY

1. Stuart, L. M. & Ezekowitz, R. A. B. Phagocytosis: Elegant Complexity. *Immunity* **22**, 539–550 (2005).

2. De Duve, C. *Singularities : landmarks on the pathways of life*. (Cambridge University Press, 2005).

3. Lancaster, C. E., Ho, C. Y., Hipolito, V. E. B., Botelho, R. J. & Terebiznik, M. R. Phagocytosis: What's on the menu? *Biochem. Cell Biol.* **97**, 21–29 (2019).

4. Rabinovitch, M. Professional and non-professional phagocytes: an introduction. *Trends Cell Biol.* **5**, 85–87 (1995).

5. Lekstrom-Himes, J. A. & Gallin, J. I. Immunodeficiency Diseases Caused by Defects in Phagocytes. *N. Engl. J. Med.* **343**, 1703–1714 (2000).

6. Smolle, M. A. & Pichler, M. Inflammation, phagocytosis and cancer: another step in the CD47 act. *J. Thorac. Dis.* **9**, 2279–2282 (2017).

7. Brown, G. C. & Neher, J. J. Eaten alive! Cell death by primary phagocytosis: 'Phagoptosis'. *Trends Biochem. Sci.* **37**, 325–332 (2012).

8. Yutin, N., Wolf, M. Y., Wolf, Y. I. & Koonin, E. V. The origins of phagocytosis and eukaryogenesis. *Biol. Direct* **4**, (2009).

9. Guerrier, S., Plattner, H., Richardson, E., Dacks, J. B. & Turkewitz, A. P. An evolutionary balance: conservation vs innovation in ciliate membrane trafficking. *Traffic* **18**, 18–28 (2017).

10. Richards, O. W. & Davies, R. G. (Richard G. *Imms' General Textbook of Entomology : Volume 2: Classification and Biology*. (Springer Netherlands, 1977).

11. Hsieh, H.-H., Hsu, T.-Y., Jiang, H.-S. & Wu, Y.-C. Integrin α PAT-2/CDC-42 Signaling Is Required for Muscle-Mediated Clearance of Apoptotic Cells in Caenorhabditis elegans. *PLoS Genet.* **8**, e1002663 (2012).

12. Abdu, Y., Maniscalco, C., Heddleston, J. M., Chew, T.-L. & Nance, J. Developmentally programmed germ cell remodelling by endodermal cell cannibalism.

Nat. Cell Biol. **18**, 1302–1310 (2016).

13. Shiratsuchi, A. *et al.* Independent Recognition of *Staphylococcus aureus* by Two Receptors for Phagocytosis in *Drosophila*. *J. Biol. Chem.* **287**, 21663–21672 (2012).

14. Honti, V., Csordás, G., Kurucz, É., Márkus, R. & Andó, I. The cell-mediated immunity of Drosophila melanogaster: Hemocyte lineages, immune compartments, microanatomy and regulation. *Dev. Comp. Immunol.* **42**, 47–56 (2014).

15. Flajnik, M. F. A cold-blooded view of adaptive immunity. *Nat. Rev. Immunol.* **18**, 438–453 (2018).

16. Bonilla, F. A. & Oettgen, H. C. Adaptive immunity. *J. Allergy Clin. Immunol.* **125**, S33–S40 (2010).

17. Lichanska, A. M. & Hume, D. A. Origins and functions of phagocytes in the embryo. *Exp. Hematol.* **28**, 601–11 (2000).

18. Naito, M. *et al.* Development, differentiation, and phenotypic heterogeneity of murine tissue macrophages. *J. Leukoc. Biol.* **59**, 133–138 (1996).

19. Enzan, H. Electron Microscopic Studies of Macrophages in Early Human Yolk Sacs. *Pathol. Int.* **36**, 49–64 (1986).

20. Hume, D. A., Monkley, S. J. & Wainwright, B. J. Detection of c-fms protooncogene in early mouse embryos by whole mount in situ hybridization indicates roles for macrophages in tissue remodelling. *Br. J. Haematol.* **90**, 939–942 (1995).

21. Lichanska, A. M. *et al.* Differentiation of the Mononuclear Phagocyte System During Mouse Embryogenesis: The Role of Transcription Factor PU.1. *Blood* **94**, 127–138 (1999).

22. Matsumoto, Y. & Ikuta, F. Appearance and distribution of fetal brain macrophages in mice. *Cell Tissue Res.* **239**, 271–278 (1985).

23. Franc, N. C., White, K. & Ezekowitz, R. A. B. Phagocytosis and development: back to the future. *Curr. Opin. Immunol.* **11**, 47–52 (1999).

24. Gregory, C. D. & Devitt, A. The macrophage and the apoptotic cell: an innate immune interaction viewed simplistically? *Immunology* **113**, 1 (2004).

25. Szondy, Z., Sarang, Z., Kiss, B., Garabuczi, É. & Köröskényi, K. Anti-inflammatory

Mechanisms Triggered by Apoptotic Cells during Their Clearance. *Front. Immunol.* **8**, 909 (2017).

26. Brüser, A. *et al.* Prostaglandin E 2 glyceryl ester is an endogenous agonist of the nucleotide receptor P2Y 6. 1–15 (2017). doi:10.1038/s41598-017-02414-8

27. Arandjelovic, S. & Ravichandran, K. S. Phagocytosis of apoptotic cells in homeostasis. *Nat. Immunol.* **16**, 907–17 (2015).

28. Hopkinson-Woolley, J., Hughes, D., Gordon, S. & Martin, P. Macrophage recruitment during limb development and wound healing in the embryonic and foetal mouse. *J. Cell Sci.* **107 (Pt 5)**, 1159–67 (1994).

29. Hume, D. A., Perry, V. H. & Gordon, S. Immunohistochemical localization of a macrophage-specific antigen in developing mouse retina: phagocytosis of dying neurons and differentiation of microglial cells to form a regular array in the plexiform layers. *J. Cell Biol.* **97**, 253–257 (1983).

30. Ginhoux, F., Lim, S., Hoeffel, G., Low, D. & Huber, T. Origin and differentiation of microglia. *Front. Cell. Neurosci.* **7**, 45 (2013).

31. Galloway, D. A., Phillips, A. E. M., Owen, D. R. J., Moore, C. S. & Moore, C. S. Phagocytosis in the Brain : Homeostasis and Disease. **10**, 1–15 (2019).

32. Schafer, D. P. *et al.* Microglia Sculpt Postnatal Neural Circuits in an Activity and Complement-Dependent Manner. *Neuron* **74**, 691–705 (2012).

33. Elmore, S. Apoptosis: a review of programmed cell death. *Toxicol. Pathol.* **35**, 495–516 (2007).

34. Rudin, C. M. & Thompson, C. B. B-cell development and maturation. *Semin. Oncol.* **25**, 435–46 (1998).

35. Monks, J. *et al.* Epithelial cells as phagocytes: apoptotic epithelial cells are engulfed by mammary alveolar epithelial cells and repress inflammatory mediator release. *Cell Death Differ.* **12**, 107–114 (2005).

36. Lu, Z. *et al.* Phagocytic activity of neuronal progenitors regulates adult neurogenesis. *Nat. Cell Biol.* **13**, 1076–1083 (2011).

37. Ming, G.-L. & Song, H. Adult neurogenesis in the mammalian brain: significant

answers and significant questions. *Neuron* **70**, 687–702 (2011).

38. Gonçalves, J. T. *et al.* In vivo imaging of dendritic pruning in dentate granule cells. *Nat. Neurosci.* **19**, 788–91 (2016).

39. Hirayama, D., Iida, T. & Nakase, H. The Phagocytic Function of Macrophage-Enforcing Innate Immunity and Tissue Homeostasis. *Int. J. Mol. Sci.* **19**, (2018).

40. Alexander, C. & Rietschel, E. T. Invited review: Bacterial lipopolysaccharides and innate immunity. *J. Endotoxin Res.* **7**, 167–202 (2001).

41. Ginsburg, I. Role of lipoteichoic acid in infection and inflammation. *Lancet. Infect. Dis.* **2**, 171–9 (2002).

42. Brown, G. D. & Gordon, S. A new receptor for β-glucans. *Nature* **413**, 36–37 (2001).

43. Jensen, S. & Thomsen, A. R. Sensing of RNA Viruses: a Review of Innate Immune Receptors Involved in Recognizing RNA Virus Invasion. *J. Virol.* **86**, 2900–2910 (2012).

44. Thompson, M. R., Kaminski, J. J., Kurt-Jones, E. A. & Fitzgerald, K. A. Pattern recognition receptors and the innate immune response to viral infection. *Viruses* **3**, 920–40 (2011).

45. Drummond, R. A., Gaffen, S. L., Hise, A. G. & Brown, G. D. Innate Defense against Fungal Pathogens. *Cold Spring Harb. Perspect. Med.* **5**, (2014).

46. Henneke, P. & Golenbock, D. T. Phagocytosis, innate immunity, and host-pathogen specificity. *J. Exp. Med.* **199**, 1–4 (2004).

47. Gordon, S. Phagocytosis: An Immunobiologic Process. *Immunity* **44**, 463–475 (2016).

48. Greenberg, S. & Grinstein, S. Phagocytosis and innate immunity. *Curr. Opin. Immunol.* **14**, 136–145 (2002).

49. Buckley, R. H. Immunodeficiency Diseases. *JAMA J. Am. Med. Assoc.* **268**, 2797 (1992).

50. Platonov *et al.* Meningococcal disease and polymorphism of FcgammaRIIa (CD32) in late complement component-deficient individuals. *Clin. Exp. Immunol.* **111**, 97–101 (1998).

51. Sanders, L. A. M. *et al.* Fca Receptor Iia (Cd32) Heterogeneity In Patients With Recurrent Bacterial Respiratory Tract Infections. *J. Infect. Dis.* **170**, 854–861 (1994).

52. Wessels, M. R. *et al.* Studies of group B streptococcal infection in mice deficient in complement component C3 or C4 demonstrate an essential role for complement in both innate and acquired immunity. *Proc. Natl. Acad. Sci. U. S. A.* **92**, 11490–4 (1995).

53. Prodeus, A. P., Zhou, X., Maurer, M., Galli, S. J. & Carroll, M. C. Impaired mast cell-dependent natural immunity in complement C3-deficient mice. *Nature* **390**, 172–175 (1997).

54. Fischer, M. B. *et al.* Increased susceptibility to endotoxin shock in complement C3- and C4-deficient mice is corrected by C1 inhibitor replacement. *J. Immunol.* **159**, 976–82 (1997).

55. Marshansky, V. & Futai, M. The V-type H+-ATPase in vesicular trafficking: targeting, regulation and function. *Curr. Opin. Cell Biol.* **20**, 415–426 (2008).

56. Kinchen, J. M. & Ravichandran, K. S. Phagosome maturation: going through the acid test. *Nat. Rev. Mol. Cell Biol.* **9**, 781–795 (2008).

57. Babior, B. M. NADPH oxidase. *Current Opinion in Immunology* **16**, 42–47 (2004).

58. Rosales, C. & Uribe-Querol, E. Phagocytosis: A Fundamental Process in Immunity. *Biomed Res. Int.* **2017**, (2017).

59. Jutras, I. & Desjardins, M. PHAGOCYTOSIS: At the Crossroads of Innate and Adaptive Immunity. *Annu. Rev. Cell Dev. Biol.* **21**, 511–527 (2005).

60. Ramachandra, L., Noss, E., Boom, W. H. & Harding, C. V. Processing of Mycobacterium tuberculosis antigen 85B involves intraphagosomal formation of peptide-major histocompatibility complex II complexes and is inhibited by live bacilli that decrease phagosome maturation. *J. Exp. Med.* **194**, 1421–1432 (2001).

61. Swanson, J. A. & Hoppe, A. D. The coordination of signaling during Fc receptor-mediated phagocytosis. *J. Leukoc. Biol.* **76**, 1093–1103 (2004).

62. van Furth, R. Origin and Kinetics of Mononuclear Phagocytes. *Ann. N. Y. Acad. Sci.* **278**, 161–175 (1976).

63. Geissmann, F. *et al.* Development of monocytes, macrophages, and dendritic cells.

Science **327**, 656–61 (2010).

64. Ogden, C. A. *et al.* C1q and Mannose Binding Lectin Engagement of Cell Surface Calreticulin and Cd91 Initiates Macropinocytosis and Uptake of Apoptotic Cells. *J. Exp. Med.* **194**, 781–796 (2001).

65. Wijeyekoon, R. S. *et al.* Monocyte Function in Parkinson's Disease and the Impact of Autologous Serum on Phagocytosis. *Front. Neurol.* **9**, 870 (2018).

66. Wong, K. L. *et al.* The three human monocyte subsets: Implications for health and disease. *Immunol. Res.* **53**, 41–57 (2012).

67. Gordon, S. & Plüddemann, A. Tissue macrophages: heterogeneity and functions. *BMC Biol.* **15**, 53 (2017).

68. Krenkel, O. & Tacke, F. Liver macrophages in tissue homeostasis and disease. *Nat. Rev. Immunol.* **17**, 306–321 (2017).

69. Yanez, D. A., Lacher, R. K., Vidyarthi, A. & Colegio, O. R. The role of macrophages in skin homeostasis. *Pflugers Arch.* **469**, 455–463 (2017).

70. Bain, C. C. & Schridde, A. Origin, Differentiation, and Function of Intestinal Macrophages. *Front. Immunol.* **9**, 2733 (2018).

71. Byrne, A. J., Mathie, S. A., Gregory, L. G. & Lloyd, C. M. Pulmonary macrophages: key players in the innate defence of the airways. *Thorax* **70**, 1189–96 (2015).

72. Borges da Silva, H. *et al.* Splenic Macrophage Subsets and Their Function during Blood-Borne Infections. *Front. Immunol.* **6**, 480 (2015).

73. Contents, S., Contents, F., An, P. I. & Immunity, I. *The front line of host defense . Garland Science* (Garland Science, 2009).

74. Collin, M., McGovern, N. & Haniffa, M. Human dendritic cell subsets. *Immunology* **140**, 22–30 (2013).

75. Liu, K. *et al.* Origin of dendritic cells in peripheral lymphoid organs of mice. *Nat. Immunol.* **8**, 578–583 (2007).

76. Colonna, M., Trinchieri, G. & Liu, Y.-J. Plasmacytoid dendritic cells in immunity. *Nat. Immunol.* **5**, 1219–1226 (2004).

77. Ruben, J. M. *et al.* Human plasmacytoid dendritic cells acquire phagocytic capacity by TLR9 ligation in the presence of soluble factors produced by renal epithelial cells. *Kidney Int.* **93**, 355–364 (2018).

78. Uciechowski, P. & Rink, L. Neutrophil, Basophil, and Eosinophil Granulocyte Functions in the Elderly. in *Handbook of Immunosenescence* 1–27 (Springer International Publishing, 2018). doi:10.1007/978-3-319-64597-1_22-1

79. Leiding, J. W. Neutrophil Evolution and Their Diseases in Humans. *Front. Immunol.* **8**, 1009 (2017).

80. Lee, W. L., Harrison, R. E. & Grinstein, S. Phagocytosis by neutrophils. *Microbes Infect.* **5**, 1299–1306 (2003).

81. Bar-Shavit, Z. The osteoclast: A multinucleated, hematopoietic-origin, bone-resorbing osteoimmune cell. *J. Cell. Biochem.* **102**, 1130–1139 (2007).

82. Wang, W., Ferguson, D. J. P., Quinn, J. M. W., Simpson, A. H. R. W. & Athanasou, N. A. Osteoclasts are capable of particle phagocytosis and bone resorption. *J. Pathol.* **182**, 92–98 (1997).

83. Chambers, T. J. Phagocytosis and trypsin-resistant glass adhesion by osteoclasts in culture. *J. Pathol.* **127**, 55–60 (1979).

84. Ho, N. *et al.* Mutations of CTSK result in pycnodysostosis via a reduction in cathepsin K protein. *J. Bone Miner. Res.* **14**, 1649–53 (1999).

85. Everts, V., Aronson, D. C. & Beertsen, W. Phagocytosis of bone collagen by osteoclasts in two cases of pycnodysostosis. *Calcif. Tissue Int.* **37**, 25–31 (1985).

86. Shamri, R., Xenakis, J. J. & Spencer, L. A. Eosinophils in innate immunity: an evolving story. *Cell Tissue Res.* **343**, 57–83 (2011).

87. Kato, M. *et al.* Eosinophil infiltration and degranulation in normal human tissue. *Anat. Rec.* **252**, 418–425 (1998).

88. Acharya, K. R. & Ackerman, S. J. Eosinophil granule proteins: form and function. *J. Biol. Chem.* **289**, 17406–15 (2014).

89. Archer, G. T. & Hirsch, J. G. MOTION PICTURE STUDIES ON DEGRANULATION OF HORSE EOSINOPHILS DURING PHAGOCYTOSIS. *J.*

Exp. Med. **118**, 287–294 (1963).

90. Cline, M. J., Hanifin, J. & Lehrer, R. I. Phagocytosis by human eosinophils. *Blood* **32**, 922–34 (1968).

91. Thorne, K. J., Glauert, A. M., Svvennsen, R. J. & Franks, D. Phagocytosis and killing of Trypanosoma dionisii by human neutrophils, eosinophils and monocytes. *Parasitology* **79**, 367–79 (1979).

92. Rengarajan, M., Hayer, A. & Theriot, J. A. Endothelial Cells Use a Formin-Dependent Phagocytosis-Like Process to Internalize the Bacterium Listeria monocytogenes. *PLOS Pathog.* **12**, e1005603 (2016).

93. Grutzendler, J. *et al.* Angiophagy Prevents Early Embolus Washout But Recanalizes Microvessels Through Embolus Extravasation. *Sci. Transl. Med.* **6**, 226–31 (2014).

94. Macara, I. G., Guyer, R., Richardson, G., Huo, Y. & Ahmed, S. M. Epithelial homeostasis. *Curr. Biol.* **24**, R815-25 (2014).

95. Walker, N. I., Bennett, R. E. & Kerr, J. F. R. Cell death by apoptosis during involution of the lactating breast in mice and rats. *Am. J. Anat.* **185**, 19–32 (1989).

96. Kendall, R. T. & Feghali-Bostwick, C. A. Fibroblasts in fibrosis: novel roles and mediators. *Front. Pharmacol.* **5**, 123 (2014).

97. Di Lullo, G. A., Sweeney, S. M., Korkko, J., Ala-Kokko, L. & San Antonio, J. D. Mapping the ligand-binding sites and disease-associated mutations on the most abundant protein in the human, type I collagen. *J. Biol. Chem.* **277**, 4223–31 (2002).

98. Everts, V., Van Der Zee, E., Creemers, L. & Beertsen, W. Phagocytosis and intracellular digestion of collagen, its role in turnover and remodelling. *Histochemical Journal* **28**, 229–245 (1996).

99. Bhide, V. M. *et al.* Collagen phagocytosis by fibroblasts is regulated by decorin. *J. Biol. Chem.* **280**, 23103–13 (2005).

100. Hall, S. E., Savill, J. S., Henson, P. M. & Haslett, C. Apoptotic neutrophils are phagocytosed by fibroblasts with participation of the fibroblast vitronectin receptor and involvement of a mannose/fucose-specific lectin. *J. Immunol.* **153**, 3218–27 (1994).

101. Ravichandran, K. S. Find-me and eat-me signals in apoptotic cell clearance: progress and conundrums. *J. Exp. Med.* **207**, 1807–17 (2010).

102. Medina, C. B. & Ravichandran, K. S. Do not let death do us part: 'find-me' signals in communication between dying cells and the phagocytes. *Cell Death Differ.* **23**, 979–89 (2016).

103. Uhlén, M. *et al.* Tissue-based map of the human proteome. *Science (80-.).* **347**, 1260419–1260419 (2015).

104. Truman, L. A. *et al.* CX3CL1/fractalkine is released from apoptotic lymphocytes to stimulate macrophage chemotaxis. *Blood* **112**, 5026–5036 (2008).

105. Segundo, C. *et al.* Surface molecule loss and bleb formation by human germinal center B cells undergoing apoptosis: role of apoptotic blebs in monocyte chemotaxis. *Blood* **94**, 1012–20 (1999).

106. Bazan, J. F. *et al.* A new class of membrane-bound chemokine with a CX3C motif. *Nature* **385**, 640–644 (1997).

107. Jones, B. A., Beamer, M. & Ahmed, S. Fractalkine/CX3CL1: a potential new target for inflammatory diseases. *Mol. Interv.* **10**, 263–70 (2010).

108. Panek, C. A. *et al.* Differential expression of the fractalkine chemokine receptor (CX3CR1) in human monocytes during differentiation. *Cell. Mol. Immunol.* **12**, 669–680 (2015).

109. Verge, G. M. *et al.* Fractalkine (CX3CL1) and fractalkine receptor (CX3CR1) distribution in spinal cord and dorsal root ganglia under basal and neuropathic pain conditions. *Eur. J. Neurosci.* **20**, 1150–1160 (2004).

110. Hoshiko, M., Arnoux, I., Avignone, E., Yamamoto, N. & Audinat, E. Deficiency of the Microglial Receptor CX3CR1 Impairs Postnatal Functional Development of Thalamocortical Synapses in the Barrel Cortex. *J. Neurosci.* **32**, 15106–15111 (2012).

111. Paolicelli, R. C., Bisht, K. & Tremblay, M.-È. Fractalkine regulation of microglial physiology and consequences on the brain and behavior. *Front. Cell. Neurosci.* **8**, 129 (2014).

112. Law, S.-H. *et al.* An Updated Review of Lysophosphatidylcholine Metabolism in

Human Diseases. *Int. J. Mol. Sci.* **20**, (2019).

113. Lauber, K. *et al.* Apoptotic cells induce migration of phagocytes via caspase-3-mediated release of a lipid attraction signal. *Cell* **113**, 717–30 (2003).

114. Peter, C. *et al.* Migration to Apoptotic "Find-me" Signals Is Mediated via the Phagocyte Receptor G2A. *J. Biol. Chem.* **283**, 5296–5305 (2008).

115. Murakami, N., Yokomizo, T., Okuno, T. & Shimizu, T. G2A Is a Proton-sensing G-protein-coupled Receptor Antagonized by Lysophosphatidylcholine. *J. Biol. Chem.* **279**, 42484–42491 (2004).

116. Hait, N. C., Oskeritzian, C. A., Paugh, S. W., Milstien, S. & Spiegel, S. Sphingosine kinases, sphingosine 1-phosphate, apoptosis and diseases. *Biochim. Biophys. Acta - Biomembr.* **1758**, 2016–2026 (2006).

117. Elliott, M. R. *et al.* Nucleotides released by apoptotic cells act as a find-me signal to promote phagocytic clearance. *Nature* **461**, 282–6 (2009).

118. Haynes, S. E. *et al.* The P2Y12 receptor regulates microglial activation by extracellular nucleotides. *Nat. Neurosci.* **9**, 1512–1519 (2006).

119. Chekeni, F. B. *et al.* Pannexin 1 channels mediate 'find-me' signal release and membrane permeability during apoptosis. *Nature* **467**, 863–7 (2010).

120. Sandilos, J. K. *et al.* Pannexin 1, an ATP Release Channel, Is Activated by Caspase Cleavage of Its Pore-associated C-terminal Autoinhibitory Region. *J. Biol. Chem.* **287**, 11303–11311 (2012).

121. Idzko, M., Ferrari, D. & Eltzschig, H. K. Nucleotide signalling during inflammation. *Nature* **509**, 310–317 (2014).

122. Vilalta, A. & Brown, G. C. Neurophagy, the phagocytosis of live neurons and synapses by glia, contributes to brain development and disease. *FEBS J.* 1–10 (2017). doi:10.1111/febs.14323

123. Li, W. Eat-me signals: Keys to molecular phagocyte biology and "appetite" control. *J. Cell. Physiol.* **227**, 1291 (2012).

124. Cockram, T. O. J., Puigdellívol, M. & Brown, G. C. Calreticulin and Galectin-3 Opsonise Bacteria for Phagocytosis by Microglia. *Front. Immunol.* **10**, 2647–2658

(2019).

125. Borisenko, G. G. *et al.* Macrophage recognition of externalized phosphatidylserine and phagocytosis of apoptotic Jurkat cells--existence of a threshold. *Arch. Biochem. Biophys.* **413**, 41–52 (2003).

126. Martin, S. J. *et al.* Early redistribution of plasma membrane phosphatidylserine is a general feature of apoptosis regardless of the initiating stimulus: inhibition by overexpression of Bcl-2 and Abl. *J. Exp. Med.* **182**, 1545–56 (1995).

127. Verhoven, B., Schlegel, R. A. & Williamson, P. Mechanisms of phosphatidylserine exposure, a phagocyte recognition signal, on apoptotic T lymphocytes. *J. Exp. Med.* **182**, 1597–601 (1995).

128. Bratton, D. L. *et al.* Appearance of phosphatidylserine on apoptotic cells requires calcium-mediated nonspecific flip-flop and is enhanced by loss of the aminophospholipid translocase. *J. Biol. Chem.* **272**, 26159–65 (1997).

129. Krahling, S., Callahan, M. K., Williamson, P. & Schlegel, R. A. Exposure of phosphatidylserine is a general feature in the phagocytosis of apoptotic lymphocytes by macrophages. *Cell Death Differ.* **6**, 183–189 (1999).

130. Hanayama, R. *et al.* Identification of a factor that links apoptotic cells to phagocytes. *Nature* **417**, 182–187 (2002).

131. van der Meer, J. H. M., van der Poll, T. & van ‘t Veer, C. TAM receptors, Gas6, and protein S: roles in inflammation and hemostasis. *Blood* **123**, 2460–2469 (2014).

132. Caberoy, N. B., Zhou, Y. & Li, W. Tubby and tubby-like protein 1 are new MerTK ligands for phagocytosis. *EMBO J.* **29**, 3898–3910 (2010).

133. Clark, R. A. *et al.* Regulation of calreticulin expression during induction of differentiation in human myeloid cells. Evidence for remodeling of the endoplasmic reticulum. *J. Biol. Chem.* **277**, 32369–78 (2002).

134. Hammond, C., Braakman, I. & Helenius, A. Role of N-linked oligosaccharide recognition, glucose trimming, and calnexin in glycoprotein folding and quality control. *Proc. Natl. Acad. Sci. U. S. A.* **91**, 913–917 (1994).

135. Gardai, S. J. *et al.* Cell-surface calreticulin initiates clearance of viable or apoptotic

cells through trans-activation of LRP on the phagocyte. *Cell* **123**, 321–34 (2005).

136. Schcolnik-Cabrera, A. *et al.* Calreticulin in phagocytosis and cancer: opposite roles in immune response outcomes. *Apoptosis* **24**, 245–255 (2019).

137. Martins, I. *et al.* Surface-exposed calreticulin in the interaction between dying cells and phagocytes. *Ann. N. Y. Acad. Sci.* **1209**, 77–82 (2010).

138. Chao, M. P. *et al.* Calreticulin is the dominant pro-phagocytic signal on multiple human cancers and is counterbalanced by CD47. *Sci. Transl. Med.* **2**, (2010).

139. Garg, A. D. *et al.* A novel pathway combining calreticulin exposure and ATP secretion in immunogenic cancer cell death. *EMBO J.* **31**, 1062–1079 (2012).

140. Païdassi, H. *et al.* Investigations on the c1q-calreticulin-phosphatidylserine interactions yield new insights into apoptotic cell recognition. *J. Mol. Biol.* **408**, 277–290 (2011).

141. Vandivier, R. W. *et al.* Role of Surfactant Proteins A, D, and C1q in the Clearance of Apoptotic Cells In Vivo and In Vitro: Calreticulin and CD91 as a Common Collectin Receptor Complex. *J. Immunol.* **169**, 3978–3986 (2002).

142. Stuart, G. R., Lynch, N. J., Day, A. J., Schwaeble, W. J. & Sim, R. B. The C1q and collectin binding site within C1q receptor (cell surface calreticulin). *Immunopharmacology* **38**, 73–80 (1997).

143. Feng, M. *et al.* Programmed cell removal by calreticulin in tissue homeostasis and cancer. *Nat. Commun.* **9**, 3194 (2018).

144. Hart, S. P., Smith, J. R. & Dransfield, I. Phagocytosis of opsonized apoptotic cells: roles for 'old-fashioned' receptors for antibody and complement. *Clin. Exp. Immunol.* **135**, 181–5 (2004).

145. Stevens, B. *et al.* The Classical Complement Cascade Mediates CNS Synapse Elimination. *Cell* **131**, 1164–1178 (2007).

146. Walport, M. J. Complement. *N. Engl. J. Med.* **344**, 1058–1066 (2001).

147. Dunkelberger, J. R. & Song, W.-C. Complement and its role in innate and adaptive immune responses. *Cell Res.* **20**, 34–50 (2010).

148. Kraus, D., Medof, M. E. & Mold, C. Complementary recognition of alternative pathway activators by decay-accelerating factor and factor H. *Infect. Immun.* **66**, 399–

405 (1998).

149. Stossel, T. P., Field, R. J., Gitlin, J. D., Alper, C. A. & Rosen, F. S. The opsonic fragment of the third component of human complement (C3). *J. Exp. Med.* **141**, 1329–47 (1975).

150. Martin, U. *et al.* The human C3a receptor is expressed on neutrophils and monocytes, but not on B or T lymphocytes. *J. Exp. Med.* **186**, 199–207 (1997).

151. Fearon, D. T. Identification of the membrane glycoprotein that is the C3b receptor of the human erythrocyte, polymorphonuclear leukocyte, B lymphocyte, and monocyte. *J. Exp. Med.* **152**, 20–30 (1980).

152. Zwirner, J. *et al.* Blood- and skin-derived monocytes/macrophages respond to C3a but not to C3a(desArg) with a transient release of calcium via a pertussis toxin-sensitive signal transduction pathway. *Eur. J. Immunol.* **27**, 2317–2322 (1997).

153. Helmy, K. Y. *et al.* CRIg: A macrophage complement receptor required for phagocytosis of circulating pathogens. *Cell* **124**, 915–927 (2006).

154. van Lookeren Campagne, M., Wiesmann, C. & Brown, E. J. Macrophage complement receptors and pathogen clearance. *Cell. Microbiol.* **9**, 2095–2102 (2007).

155. Païdassi, H. *et al.* C1q Binds Phosphatidylserine and Likely Acts as a Multiligand-Bridging Molecule in Apoptotic Cell Recognition. *J. Immunol.* **180**, 2329–2338 (2008).

156. Botto, M. *et al.* Homozygous C1q deficiency causes glomerulonephritis associated with multiple apoptotic bodies. *Nat. Genet.* **19**, 56–59 (1998).

157. Navratil, J. S., Korb, L. C. & Ahearn, J. M. Systemic lupus erythematosus and complement deficiency: clues to a novel role for the classical complement pathway in the maintenance of immune tolerance. *Immunopharmacology* **42**, 47–52 (1999).

158. Shao, W.-H. & Cohen, P. L. Disturbances of apoptotic cell clearance in systemic lupus erythematosus. *Arthritis Res. Ther.* **13**, 202 (2011).

159. Janeway, C. J., Travers, P., Walport, M. & Al., E. The destruction of antibody-coated pathogens via Fc receptors. *Immunobiol. Immune Syst. Heal. Dis.* 1–6 (2001). doi:10.1128/CMR.00046-08

160. Aderem, A. & Underhill, D. M. Mechanisms of phagocytosis in macrophages. *Annu. Rev. Immunol.* **17**, 593–623 (1999).

161. Takai, T., Li, M., Sylvestre, D., Clynes, R. & Ravetch, J. V. FcR γ chain deletion results in pleiotrophic effector cell defects. *Cell* **76**, 519–529 (1994).

162. Maglione, P. J., Xu, J., Casadevall, A. & Chan, J. Fcγ Receptors Regulate Immune Activation and Susceptibility during *Mycobacterium tuberculosis* Infection. *J. Immunol.* **180**, 3329–3338 (2008).

163. Masuda, A. *et al.* Fcgamma receptor regulation of Citrobacter rodentium infection. *Infect. Immun.* **76**, 1728–37 (2008).

164. Price, B. E. *et al.* Anti-phospholipid autoantibodies bind to apoptotic, but not viable, thymocytes in a beta 2-glycoprotein I-dependent manner. *J. Immunol.* **157**, 2201–8 (1996).

165. Hart, S. P., Alexander, K. M. & Dransfield, I. Immune complexes bind preferentially to Fc gamma RIIA (CD32) on apoptotic neutrophils, leading to augmented phagocytosis by macrophages and release of proinflammatory cytokines. *J. Immunol.* **172**, 1882–7 (2004).

166. Litvack, M. L., Post, M. & Palaniyar, N. IgM promotes the clearance of small particles and apoptotic microparticles by macrophages. *PLoS One* **6**, e17223 (2011).

167. Kim, S. J., Gershov, D., Ma, X., Brot, N. & Elkon, K. B. I-PLA $_2$ Activation during Apoptosis Promotes the Exposure of Membrane Lysophosphatidylcholine Leading to Binding by Natural Immunoglobulin M Antibodies and Complement Activation. *J. Exp. Med.* **196**, 655–665 (2002).

168. Janeway, C., Travers, P., Walport, M. & Shlomchik, M. *Immunobiology: The Immune System in Health and Disease. 5th edition.* (Garland Science, 2001).

169. Weis, W. I., Taylor, M. E. & Drickamer, K. The C-type lectin superfamily in the immune system. *Immunol. Rev.* **163**, 19–34 (1998).

170. Lu, J., Teh, C., Kishore, U. & Reid, K. B. . Collectins and ficolins: sugar pattern recognition molecules of the mammalian innate immune system. *Biochim. Biophys. Acta - Gen. Subj.* **1572**, 387–400 (2002).

171. Drickamer, K. Engineering galactose-binding activity into a C-type mannose-binding protein. *Nature* **360**, 183–186 (1992).

172. Matsushita, M., Endo, Y., Fujita, T., Timpl, R. & Reid, K. B. Cutting edge: complement-activating complex of ficolin and mannose-binding lectin-associated serine protease. *J. Immunol.* **164**, 2281–4 (2000).

173. Jack, D. L., Klein, N. J. & Turner, M. W. Mannose-binding lectin: targeting the microbial world for complement attack and opsonophagocytosis. *Immunol. Rev.* **180**, 86–99 (2001).

174. Jack, D. L., Lee, M. E., Turner, M. W., Klein, N. J. & Read, R. C. Mannose-binding lectin enhances phagocytosis and killing of *Neisseria meningitidis* by human macrophages. *J. Leukoc. Biol.* **77**, 328–336 (2005).

175. Lu, J. & Le, Y. Ficolins and the Fibrinogen-like Domain. *Immunobiology* **199**, 190–199 (1998).

176. Matsushita, M. *et al.* A Novel Human Serum Lectin with Collagen- and Fibrinogen-like Domains That Functions as an Opsonin. *J. Biol. Chem.* **271**, 2448–2454 (1996).

177. Bidula, S., Sexton, D. W. & Schelenz, S. Ficolins and the Recognition of Pathogenic Microorganisms: An Overview of the Innate Immune Response and Contribution of Single Nucleotide Polymorphisms. *J. Immunol. Res.* **2019**, 1–13 (2019).

178. Ren, Y., Ding, Q. & Zhang, X. Ficolins and infectious diseases. *Virol. Sin.* **29**, 25–32 (2014).

179. Matsushita, M. & Fujita, T. The role of Ficolins in innate immunity. *Immunobiology* **205**, 490–497 (2002).

180. Taira, S., Kodama, N., Matsushita, M. & Fujita, T. Opsonic function and concentration of human serum ficolin/P35. *Fukushima J. Med. Sci.* **46**, 13–23 (2000).

181. Luo, F. *et al.* Ficolin-2 defends against virulent Mycobacteria tuberculosis infection in vivo, and its insufficiency is associated with infection in humans. *PLoS One* **8**, e73859 (2013).

182. Lu, J., Le, Y., Kon, O. L., Chan, J. & Lee, S. H. Biosynthesis of human ficolin, and Escherichia coli-binding protein, by monocytes: Comparison with the synthesis of two

macrophage-specific proteins, C1q and the mannose receptor. *Immunology* **89**, 289–294 (1996).

183. Teh, C., Le, Y., Lee, S. H. & Lu, J. M-ficolin is expressed on monocytes and is a lectin binding to N-acetyl-D-glucosamine and mediates monocyte adhesion and phagocytosis of Escherichia coli. *Immunology* **101**, 225–32 (2000).

184. Du Clos, T. W. Pentraxins: structure, function, and role in inflammation. *ISRN Inflamm.* **2013**, 379040 (2013).

185. Abernethy, T. J. & Avery, O. T. The occurrence during acute infections of a protein not normally present in the blood: I. distribution of the reactive protein in patients' sera and the effect of calcium on the flocculation reaction with c polysaccharide of pneumococcus. *J. Exp. Med.* **73**, 173–182 (1941).

186. Volanakis, J. E. & Kaplan, M. H. Specificity of C-Reactive Protein for Choline Phosphate Residues of Pneumococcal C-Polysaccharide. *Exp. Biol. Med.* **136**, 612–614 (1971).

187. Li, Y. P., Mold, C. & Du Clos, T. W. Sublytic complement attack exposes C-reactive protein binding sites on cell membranes. *J. Immunol.* **152**, 2995–3005 (1994).

188. Hind, C. R. K., Collins, P. M., Baltz, M. L. & Pepys, M. B. Human serum amyloid P component, a circulating lectin with specificity for the cyclic 4,6-pyruvate acetal of galactose. Interactions with various bacteria. *Biochem. J.* **225**, 107–111 (1985).

189. Noursadeghi, M. *et al.* Role of serum amyloid P component in bacterial infection: Protection of the host or protection of the pathogen. *Proc. Natl. Acad. Sci. U. S. A.* **97**, 14584–14589 (2000).

190. Pepys, M. B., Dyck, R. F., de Beer, F. C., Skinner, M. & Cohen, A. S. Binding of serum amyloid P-component (SAP) by amyloid fibrils. *Clin. Exp. Immunol.* **38**, 284–293 (1979).

191. Mold, C., Baca, R. & Du Clos, T. W. Serum Amyloid P Component and C-Reactive Protein Opsonize Apoptotic Cells for Phagocytosis through Fcγ Receptors. *J. Autoimmun.* **19**, 147–154 (2002).

192. Kaplan, M. H. & Volanakis, J. E. Interaction of C-reactive protein complexes with the complement system. I. Consumption of human complement associated with the

reaction of C-reactive protein with pneumococcal C-polysaccharide and with the choline phosphatides, lecithin and sphingomyelin. *J. Immunol.* **112**, 2135–47 (1974).

193. Culley, F. J., McAdam, K. P. W. J., Raynes, J. G., Harris, R. A. & Kaye, P. M. C-reactive protein binds to a novel ligand on Leishmania donovani and increases uptake into human macrophages. *J. Immunol.* **156**, 4691–4696 (1996).

194. Gershov, D., Kim, S., Brot, N. & Elkon, K. B. C-Reactive protein binds to apoptotic cells, protects the cells from assembly of the terminal complement components, and sustains an antiinflammatory innate immune response: implications for systemic autoimmunity. *J. Exp. Med.* **192**, 1353–64 (2000).

195. Yi, Y.-S. Functional Role of Milk Fat Globule-Epidermal Growth Factor VIII in Macrophage-Mediated Inflammatory Responses and Inflammatory/Autoimmune Diseases. *Mediators Inflamm.* **2016**, (2016).

196. Abe, T. *et al.* Regulation of osteoclast homeostasis and inflammatory bone loss by MFG-E8. *J. Immunol.* **193**, 1383–91 (2014).

197. Neniskyte, U. & Brown, G. C. Lactadherin/MFG-E8 is essential for microglia-mediated neuronal loss and phagoptosis induced by amyloid β. *J. Neurochem.* **126**, 312–317 (2013).

198. Miyasaka, K., Hanayama, R., Tanaka, M. & Nagata, S. Expression of milk fat globule epidermal growth factor 8 in immature dendritic cells for engulfment of apoptotic cells. *Eur. J. Immunol.* **34**, 1414–1422 (2004).

199. Miksa, M. *et al.* Fractalkine-Induced MFG-E8 Leads to Enhanced Apoptotic Cell Clearance by Macrophages. *Mol. Med.* **13**, 553–560 (2007).

200. Andersen, M. H., Graversen, H., Fedosov, S. N., Petersen, T. E. & Rasmussen, J. T. Functional Analyses of Two Cellular Binding Domains of Bovine Lactadherin †. *Biochemistry* **39**, 6200–6206 (2000).

201. Finnemann, S. C., Bonilha, V. L., Marmorstein, A. D. & Rodriguez-Boulan, E. Essential role for MFG-E8 as ligand for αvβ5 integrin in diurnal retinal phagocytosis. *Proc. Natl. Acad. Sci. U. S. A.* **104**, 12005–12010 (2007).

202. Yamaguchi, H. *et al.* Milk fat globule EGF factor 8 in the serum of human patients of systemic lupus erythematosus. *J. Leukoc. Biol.* **83**, 1300–1307 (2008).

203. Asano, K. *et al.* Masking of Phosphatidylserine Inhibits Apoptotic Cell Engulfment and Induces Autoantibody Production in Mice. *J. Exp. Med.* **200**, 459–467 (2004).

204. Dasgupta, S. K. & Thiagarajan, P. The role of lactadherin in the phagocytosis of phosphatidylserine-expressing sickle red blood cells by macrophages. *Haematologica* **90**, 1267–8 (2005).

205. Atabai, K. *et al.* Mfge8 diminishes the severity of tissue fibrosis in mice by binding and targeting collagen for uptake by macrophages. *J. Clin. Invest.* **119**, 3713–3722 (2009).

206. Nagata, K. *et al.* Identification of the product of growth arrest-specific gene 6 as a common ligand for Axl, Sky, and Mer receptor tyrosine kinases. *J. Biol. Chem.* **271**, 30022–7 (1996).

207. Nakano, T. *et al.* Cell adhesion to phosphatidylserine mediated by a product of growth arrest-specific gene 6. *J. Biol. Chem.* **272**, 29411–4 (1997).

208. Zagórska, A., Través, P. G., Lew, E. D., Dransfield, I. & Lemke, G. Diversification of TAM receptor tyrosine kinase function. *Nat. Immunol.* **15**, 920–8 (2014).

209. Tsou, W.-I. *et al.* Receptor tyrosine kinases, TYRO3, AXL, and MER, demonstrate distinct patterns and complex regulation of ligand-induced activation. *J. Biol. Chem.* **289**, 25750–63 (2014).

210. Grommes, C. *et al.* Regulation of microglial phagocytosis and inflammatory gene expression by Gas6 acting on the Axl/Mer family of tyrosine kinases. *J. Neuroimmune Pharmacol.* **3**, 130–40 (2008).

211. Díaz-Alvarez, L. & Ortega, E. The Many Roles of Galectin-3, a Multifaceted Molecule, in Innate Immune Responses against Pathogens. *Mediators Inflamm.* **2017**, 1–10 (2017).

212. Nomura, K., Vilalta, A., Allendorf, D. H., Hornik, T. C. & Brown, G. C. Activated Microglia Desialylate and Phagocytose Cells via Neuraminidase, Galectin-3, and Mer Tyrosine Kinase. *J. Immunol.* **198**, 4792–4801 (2017).

213. Liu, F. T. *et al.* Expression and function of galectin-3, a beta-galactoside-binding lectin, in human monocytes and macrophages. *Am. J. Pathol.* **147**, 1016–28 (1995).

214. Hughes, R. C. Secretion of the galectin family of mammalian carbohydrate-binding proteins. *Biochim. Biophys. Acta* **1473**, 172–85 (1999).

215. Karlsson, A. *et al.* Galectin-3 functions as an opsonin and enhances the macrophage clearance of apoptotic neutrophils. *Glycobiology* **19**, 16–20 (2008).

216. Caberoy, N. B., Alvarado, G., Bigcas, J.-L. & Li, W. Galectin-3 is a new MerTK-specific eat-me signal. *J. Cell. Physiol.* **227**, 401–407 (2012).

217. Galvan, M. D., Greenlee-Wacker, M. C. & Bohlson, S. S. C1q and phagocytosis: the perfect complement to a good meal. *J. Leukoc. Biol.* **92**, 489–497 (2012).

218. Merino, S. *et al.* Activation of the complement classical pathway (C1q binding) by mesophilic Aeromonas hydrophila outer membrane protein. *Infect. Immun.* **66**, 3825–31 (1998).

219. Klickstein, L. B., Barbashov, S. F., Liu, T., Jack, R. M. & Nicholson-Weller, A. Complement receptor type 1 (CR1, CD35) is a receptor for C1q. *Immunity* **7**, 345–55 (1997).

220. Païdassi, H. *et al.* Investigations on the C1q–Calreticulin–Phosphatidylserine Interactions Yield New Insights into Apoptotic Cell Recognition. *J. Mol. Biol.* **408**, 277–290 (2011).

221. Linnartz, B., Kopatz, J., Tenner, a. J. & Neumann, H. Sialic Acid on the Neuronal Glycocalyx Prevents Complement C1 Binding and Complement Receptor-3-Mediated Removal by Microglia. *J. Neurosci.* **32**, 946–952 (2012).

222. Bialas, A. R. & Stevens, B. TGF-β signaling regulates neuronal C1q expression and developmental synaptic refinement. *Nat. Neurosci.* **16**, 1773–82 (2013).

223. Alvarez-Dominguez, C., Carrasco-Marin, E. & Leyva-Cobian, F. Role of complement component C1q in phagocytosis of Listeria monocytogenes by murine macrophage-like cell lines. *Infect. Immun.* **61**, 3664–72 (1993).

224. Yuste, J. *et al.* Impaired opsonization with C3b and phagocytosis of Streptococcus pneumoniae in sera from subjects with defects in the classical complement pathway. *Infect. Immun.* **76**, 3761–3770 (2008).

225. Nicholson, A., Brade, V., Lee, G. D., Shin, H. S. & Mayer, M. M. Kinetic studies of

the formation of the properdin system enzymes on zymosan: evidence that nascent C3b controls the rate of assembly. *J. Immunol.* **112**, 1115–23 (1974).

226. Lewis, L. A. *et al.* Defining targets for complement components C4b and C3b on the pathogenic neisseriae. *Infect. Immun.* **76**, 339–50 (2008).

227. Bohlson, S. S., O'Conner, S. D., Hulsebus, H. J., Ho, M. M. & Fraser, D. A. Complement, C1Q, and C1q-related molecules regulate macrophage polarization. *Front. Immunol.* **5**, 1–7 (2014).

228. Takizawa, F., Tsuji, S. & Nagasawa, S. Enhancement of macrophage phagocytosis upon iC3b deposition on apoptotic cells. *FEBS Lett.* **397**, 269–72 (1996).

229. Hawley, K. L. *et al.* Serum C3 Enhances Complement Receptor 3-Mediated Phagocytosis of Borrelia burgdorferi. *Int. J. Biol. Sci.* **11**, 1269–71 (2015).

230. Rubin-Bejerano, I., Abeijon, C., Magnelli, P., Grisafi, P. & Fink, G. R. Phagocytosis by human neutrophils is stimulated by a unique fungal cell wall component. *Cell Host Microbe* **2**, 55–67 (2007).

231. Cohen, J. H. *et al.* The C3b/C4b receptor (CR1, CD35) on erythrocytes: methods for study of the polymorphisms. *Mol. Immunol.* **36**, 819–25

232. Rosales, C. & Uribe-Querol, E. Phagocytosis: A Fundamental Process in Immunity. *Biomed Res. Int.* **2017**, 1–18 (2017).

233. Yan, J. *et al.* Critical role of Kupffer cell CR3 (CD11b/CD18) in the clearance of IgM-opsonized erythrocytes or soluble beta-glucan. *Immunopharmacology* **46**, 39–54 (2000).

234. Kubagawa, H. *et al.* Nomenclature of Toso, Fas Apoptosis Inhibitory Molecule 3, and IgM FcR. *J. Immunol.* **194**, 4055–4057 (2015).

235. Nadesalingam, J., Dodds, A. W., Reid, K. B. M. & Palaniyar, N. Mannose-Binding Lectin Recognizes Peptidoglycan via the N -Acetyl Glucosamine Moiety, and Inhibits Ligand-Induced Proinflammatory Effect and Promotes Chemokine Production by Macrophages . *J. Immunol.* **175**, 1785–1794 (2005).

236. Polotsky, V. Y., Fischer, W., Ezekowitz, R. A. & Joiner, K. A. Interactions of human mannose-binding protein with lipoteichoic acids. *Infect. Immun.* **64**, 380–3 (1996).

237. Kilpatrick, D. C. Phospholipid-binding activity of human mannan-binding lectin. *Immunol. Lett.* **61**, 191–5 (1998).

238. Malhotra, R., Thiel, S., Reid, K. B. & Sim, R. B. Human leukocyte C1q receptor binds other soluble proteins with collagen domains. *J. Exp. Med.* **172**, 955–959 (1990).

239. Ghiran, I. *et al.* Complement Receptor 1/Cd35 Is a Receptor for Mannan-Binding Lectin. *J. Exp. Med.* **192**, 1797–1808 (2000).

240. Kuhlman, M., Joiner, K. & Ezekowitz, R. A. B. The human mannose-binding protein functions as an opsonin. *J. Exp. Med.* **169**, 1733–1745 (1989).

241. Brouwer, N. *et al.* Mannose-binding lectin (MBL) facilitates opsonophagocytosis of yeasts but not of bacteria despite MBL binding. *J. Immunol.* **180**, 4124–32 (2008).

242. Jäkel, A., Reid, K. B. M. & Clark, H. Surfactant protein A (SP-A) binds to phosphatidylserine and competes with annexin V binding on late apoptotic cells. *Protein Cell* **1**, 188–97 (2010).

243. Kuroki, Y. & Akino, T. Pulmonary surfactant protein A (SP-A) specifically binds dipalmitoylphosphatidylcholine. *J. Biol. Chem.* **266**, 3068–3073 (1991).

244. Chaby, R., Garcia-Verdugo, I., Espinassous, Q. & Augusto, L. A. Interactions between LPS and lung surfactant proteins. *J. Endotoxin Res.* **11**, 181–185 (2005).

245. Gardai, S. *et al.* By binding SIRPα or calreticulin/CD91, lung collectins act as dual function surveillance molecules to suppress or enhance inflammation. *Elsevier*

246. Ding, J., Umstead, T. M., Floros, J. & Phelps, D. S. Factors affecting SP-A-mediated phagocytosis in human monocytic cell lines. *Respir. Med.* **98**, 637–650 (2004).

247. Kabha, K. *et al.* SP-A enhances phagocytosis of Klebsiella by interaction with capsular polysaccharides and alveolar macrophages. *Am. J. Physiol. Cell. Mol. Physiol.* **272**, L344–L352 (1997).

248. Schagat, T. L., Wofford, J. A. & Wright, J. R. Surfactant Protein A Enhances Alveolar Macrophage Phagocytosis of Apoptotic Neutrophils. *J. Immunol.* **166**, 2727–2733 (2001).

249. de Wetering, J. K. van *et al.* Characteristics of Surfactant Protein A and D Binding to Lipoteichoic Acid and Peptidoglycan, 2 Major Cell Wall Components of Gram-

Positive Bacteria. *J. Infect. Dis.* **184**, 1143–1151 (2001).

250. Allen, M. J., Voelker, D. R. & Mason, R. J. Interactions of surfactant proteins A and D with Saccharomyces cerevisiae and Aspergillus fumigatus. *Infect. Immun.* **69**, 2037–44 (2001).

251. Ofek, I. *et al.* Surfactant protein D enhances phagocytosis and killing of unencapsulated phase variants of Klebsiella pneumoniae. *Infect. Immun.* **69**, 24–33 (2001).

252. Restrepo, C. I., Dong, Q., Savov, J., Mariencheck, W. I. & Wright, J. R. Surfactant Protein D Stimulates Phagocytosis of *Pseudomonas aeruginosa* by Alveolar Macrophages. *Am. J. Respir. Cell Mol. Biol.* **21**, 576–585 (1999).

253. Geunes-Boyer, S. *et al.* Surfactant protein D increases phagocytosis of hypocapsular Cryptococcus neoformans by murine macrophages and enhances fungal survival. *Infect. Immun.* **77**, 2783–94 (2009).

254. Kuraya, M., Ming, Z., Liu, X., Matsushita, M. & Fujita, T. Specific binding of L-ficolin and H-ficolin to apoptotic cells leads to complement activation. *Immunobiology* **209**, 689–697 (2005).

255. Honoré, C. *et al.* Tethering of Ficolin-1 to cell surfaces through recognition of sialic acid by the fibrinogen-like domain. *J. Leukoc. Biol.* **88**, 145–158 (2010).

256. Jensen, K. *et al.* M-ficolin is present in Aspergillus fumigatus infected lung and modulates epithelial cell immune responses elicited by fungal cell wall polysaccharides. *Virulence* **8**, 1870–1879 (2017).

257. Kjaer, T. R. *et al.* M-ficolin binds selectively to the capsular polysaccharides of Streptococcus pneumoniae serotypes 19B and 19C and of a Streptococcus mitis strain. *Infect. Immun.* **81**, 452–9 (2013).

258. Zhang, J. *et al.* Secreted M-Ficolin Anchors onto Monocyte Transmembrane G Protein-Coupled Receptor 43 and Cross Talks with Plasma C-Reactive Protein to Mediate Immune Signaling and Regulate Host Defense. *J. Immunol.* **185**, 6899–6910 (2010).

259. Marnell, L. L., Mold, C., Volzer, M. A., Burlingame, R. W. & Du Clos, T. W. C-reactive protein binds to Fc gamma RI in transfected COS cells. *J. Immunol.* **155**,

2185–93 (1995).

260. Bharadwaj, D., Stein, M.-P., Volzer, M., Mold, C. & Clos, T. W. Du. The Major Receptor for C-Reactive Protein on Leukocytes Is Fcγ Receptor II. *J. Exp. Med.* **190**, 585–590 (1999).

261. Lu, J. *et al.* Recognition and functional activation of the human IgA receptor (FcalphaRI) by C-reactive protein. *Proc. Natl. Acad. Sci. U. S. A.* **108**, 4974–9 (2011).

262. Lu, J. *et al.* Structural recognition and functional activation of FcγR by innate pentraxins. *Nature* **456**, 989–992 (2008).

263. Mold, C., Gresham, H. D., Du Clos, T. W. & Du Clos, T. W. Serum amyloid P component and C-reactive protein mediate phagocytosis through murine Fc gamma Rs. *J. Immunol.* **166**, 1200–5 (2001).

264. Noursadeghi, M. *et al.* Role of serum amyloid P component in bacterial infection: Protection of the host or protection of the pathogen. *Proc. Natl. Acad. Sci. U. S. A.* **97**, 14584–14589 (2000).

265. Hind, C. R. K., Collins, P. M., Baltz, M. L. & Pepys, M. B. Human serum amyloid P component, a circulating lectin with specificity for the cyclic 4,6-pyruvate acetal of galactose. Interactions with various bacteria. *Biochem. J.* **225**, 107–111 (1985).

266. Ying, S. C., Gewurz, A. T., Jiang, H. & Gewurz, H. Human serum amyloid P component oligomers bind and activate the classical complement pathway via residues 14-26 and 76-92 of the A chain collagen-like region of C1q. *J. Immunol.* **150**, 169–76 (1993).

267. Anderson, H. A. *et al.* Serum-derived protein S binds to phosphatidylserine and stimulates the phagocytosis of apoptotic cells. *Nat. Immunol.* **4**, 87–91 (2003).

268. Nandrot, E. F. Opposite Roles of MerTK Ligands Gas6 and Protein S During Retinal Phagocytosis. in 577–583 (Springer, Cham, 2018). doi:10.1007/978-3-319-75402-4_70

269. Caberoy, N. B., Alvarado, G. & Li, W. Tubby regulates microglial phagocytosis through MerTK. *J. Neuroimmunol.* **252**, 40–48 (2012).

270. Caberoy, N. B., Maiguel, D., Kim, Y. & Li, W. Identification of tubby and tubby-like

protein 1 as eat-me signals by phage display. *Exp. Cell Res.* **316**, 245–57 (2010).

271. Russ, A. *et al.* Blocking "don't eat me" signal of CD47-SIRPα in hematological malignancies, an in-depth review. *Blood Reviews* **32**, 480–489 (2018).

272. Fujioka, Y. *et al.* A novel membrane glycoprotein, SHPS-1, that binds the SH2-domain-containing protein tyrosine phosphatase SHP-2 in response to mitogens and cell adhesion. *Mol. Cell. Biol.* **16**, 6887–99 (1996).

273. Dugas, V., Beauchamp, C., Chabot-Roy, G., Hillhouse, E. E. & Lesage, S. Implication of the CD47 pathway in autoimmune diabetes. *J. Autoimmun.* **35**, 23–32 (2010).

274. Oldenborg, P.-A. *et al.* Role of CD47 as a Marker of Self on Red Blood Cells. *Science (80-.).* **288**, 2051–2054 (2000).

275. Campbell, I. G., Freemont, P. S., Foulkes, W. & Trowsdale, J. An ovarian tumor marker with homology to vaccinia virus contains an IgV-like region and multiple transmembrane domains. *Cancer Res.* **52**, 5416–20 (1992).

276. Chao, M. P. *et al.* Therapeutic Antibody Targeting of CD47 Eliminates Human Acute Lymphoblastic Leukemia. *Cancer Res.* **71**, 1374–1384 (2011).

277. Kim, D. *et al.* Anti-CD47 antibodies promote phagocytosis and inhibit the growth of human myeloma cells. *Leukemia* **26**, 2538–2545 (2012).

278. Majeti, R. *et al.* CD47 Is an Adverse Prognostic Factor and Therapeutic Antibody Target on Human Acute Myeloid Leukemia Stem Cells. *Cell* **138**, 286–299 (2009).

279. Willingham, S. B. *et al.* The CD47-signal regulatory protein alpha (SIRPa) interaction is a therapeutic target for human solid tumors. *Proc. Natl. Acad. Sci.* **109**, 6662–6667 (2012).

280. Lyons, A. *et al.* Analysis of the Impact of CD200 on Phagocytosis. *Mol. Neurobiol.* **54**, 5730–5739 (2017).

281. Hayakawa, K. *et al.* CD200 restrains macrophage attack on oligodendrocyte precursors via toll-like receptor 4 downregulation. *J. Cereb. Blood Flow Metab.* **36**, 781–93 (2016).

282. Koning, N., Swaab, D. F., Hoek, R. M. & Huitinga, I. Distribution of the Immune Inhibitory Molecules CD200 and CD200R in the Normal Central Nervous System and

Multiple Sclerosis Lesions Suggests Neuron-Glia and Glia-Glia Interactions. *J. Neuropathol. Exp. Neurol.* **68**, 159–167 (2009).

283. Broderick, C. *et al.* Constitutive Retinal CD200 Expression Regulates Resident Microglia and Activation State of Inflammatory Cells during Experimental Autoimmune Uveoretinitis. *Am. J. Pathol.* **161**, 1669–1677 (2002).

284. Griffiths, M. R., Gasque, P. & Neal, J. W. The regulation of the CNS innate immune response is vital for the restoration of tissue homeostasis (repair) after acute brain injury: a brief review. *Int. J. Inflam.* **2010**, 151097 (2010).

285. Rosenblum, M. D. *et al.* CD200 is a novel p53-target gene involved in apoptosis-associated immune tolerance. *Blood* **103**, 2691–2698 (2004).

286. Barkal, A. A. *et al.* CD24 signalling through macrophage Siglec-10 is a target for cancer immunotherapy. *Nature* **572**, 392–396 (2019).

287. Cesari, M., Pahor, M. & Incalzi, R. A. Plasminogen activator inhibitor-1 (PAI-1): a key factor linking fibrinolysis and age-related subclinical and clinical conditions. *Cardiovasc. Ther.* **28**, e72-91 (2010).

288. Mesters, R. M., Flörke, N., Ostermann, H. & Kienast, J. Increase of plasminogen activator inhibitor levels predicts outcome of leukocytopenic patients with sepsis. *Thromb. Haemost.* **75**, 902–7 (1996).

289. Prabhakaran, P. *et al.* Elevated levels of plasminogen activator inhibitor-1 in pulmonary edema fluid are associated with mortality in acute lung injury. *Am. J. Physiol. Cell. Mol. Physiol.* **285**, L20–L28 (2003).

290. Takeshita, K. *et al.* Increased Expression of Plasminogen Activator Inhibitor-1 in Cardiomyocytes Contributes to Cardiac Fibrosis after Myocardial Infarction. *Am. J. Pathol.* **164**, 449–456 (2004).

291. Park, Y.-J. *et al.* PAI-1 inhibits neutrophil efferocytosis. *Proc. Natl. Acad. Sci. U. S. A.* **105**, 11784–9 (2008).

292. Jeon, H. *et al.* Plasminogen activator inhibitor type 1 regulates microglial motility and phagocytic activity. *J. Neuroinflammation* **9**, 637 (2012).

293. Horn, L., Hui, R. & Millward, M. Treatment of Pulmonary Adenocarcinoma With

Immune Checkpoint Inhibitors. *Pulm. Adenocarcinoma Approaches to Treat.* 151–171 (2019). doi:10.1016/B978-0-323-55433-6.00010-9

294. Gordon, S. R. *et al.* PD-1 expression by tumour-associated macrophages inhibits phagocytosis and tumour immunity. *Nature* **545**, 495–499 (2017).

295. Huang, X. *et al.* PD-1 expression by macrophages plays a pathologic role in altering microbial clearance and the innate inflammatory response to sepsis. *Proc. Natl. Acad. Sci. U. S. A.* **106**, 6303–8 (2009).

296. Zhu, J. *et al.* Protein Interacting C-Kinase 1 Modulates Surface Expression of P2Y6 Purinoreceptor, Actin Polymerization and Phagocytosis in Microglia. *Neurochem. Res.* **41**, 795–803 (2016).

297. Li, L., Dong, M. & Wang, X.-G. The Implication and Significance of Beta 2 Microglobulin: A Conservative Multifunctional Regulator. *Chin. Med. J. (Engl).* **129**, 448–55 (2016).

298. Barkal, A. A. *et al.* Engagement of MHC class I by the inhibitory receptor LILRB1 suppresses macrophages and is a target of cancer immunotherapy. *Nat. Immunol.* **19**, 76–84 (2018).

299. Vimr, E. R., Kalivoda, K. A., Deszo, E. L. & Steenbergen, S. M. Diversity of microbial sialic acid metabolism. *Microbiol. Mol. Biol. Rev.* **68**, 132–53 (2004).

300. Zhang, X.-H. *et al.* Desialylation is associated with apoptosis and phagocytosis of platelets in patients with prolonged isolated thrombocytopenia after allo-HSCT. *J. Hematol. Oncol.* **8**, 116 (2015).

301. Bhide, G. P. & Colley, K. J. Sialylation of N-glycans: mechanism, cellular compartmentalization and function. *Histochem. Cell Biol.* **147**, 149–174 (2017).

302. Schwarzkopf, M. *et al.* Sialylation is essential for early development in mice. *Proc. Natl. Acad. Sci.* **99**, 5267–5270 (2002).

303. Macauley, M. S., Crocker, P. R. & Paulson, J. C. Siglec-mediated regulation of immune cell function in disease. *Nat. Rev. Immunol.* **14**, 653–66 (2014).

304. Claude, J., Linnartz-Gerlach, B., Kudin, A. P., Kunz, W. S. & Neumann, H. Microglial CD33-related Siglec-E inhibits neurotoxicity by preventing the phagocytosis-

associated oxidative burst. *J. Neurosci.* **33**, 18270–6 (2013).

305. Lübbers, J., Rodríguez, E. & van Kooyk, Y. Modulation of Immune Tolerance via Siglec-Sialic Acid Interactions. *Front. Immunol.* **9**, 2807 (2018).

306. Wang, Q. *et al.* Desialylation Induces Apoptosis and Phagocytosis of Platelets in Patients with Prolonged Isolated Thrombocytopenia after Allogeneic Hematopoietic Stem Cell Transplantation. *Blood* **124**, 432–432 (2014).

307. Toshimori, K., Araki, S., Öra, C. & Eddy, E. M. Loss of Sperm Surface Sialic Acid Induces Phagocytosis: An Assay with a Monoclonal Antibody T21, Which Recognizes a 54K Sialoglycoprotein. *Arch. Androl.* **27**, 79–86 (1991).

308. Shi, Y. *et al.* Protein-tyrosine kinase Syk is required for pathogen engulfment in complement-mediated phagocytosis. *Blood* **107**, 4554–4562 (2006).

309. Newman, S. L., Mikus, L. K. & Tucci, M. A. Differential requirements for cellular cytoskeleton in human macrophage complement receptor- and Fc receptor-mediated phagocytosis. *J. Immunol.* **146**, 967–74 (1991).

310. Allen, L. A. H. & Aderem, A. Molecular definition of distinct cytoskeletal structures involved in complement- and Fc receptor-mediated phagocytosis in macrophages. *J. Exp. Med.* **184**, 627–637 (1996).

311. Yan, M., Collins, R. F., Grinstein, S. & Trimble, W. S. Coronin-1 Function Is Required for Phagosome Formation. *Mol. Biol. Cell* **16**, 3077–3087 (2005).

312. Bamburg, J. R. & Bernstein, B. W. Roles of ADF/cofilin in actin polymerization and beyond. *F1000 Biology Reports* **2**, (2010).

313. Nag, S., Larsson, M., Robinson, R. C. & Burtnick, L. D. Gelsolin: The tail of a molecular gymnast. *Cytoskeleton* **70**, 360–384 (2013).

314. Fairn, G. D. & Grinstein, S. How nascent phagosomes mature to become phagolysosomes. *Trends in Immunology* **33**, 397–405 (2012).

315. Levin, R., Grinstein, S. & Canton, J. The life cycle of phagosomes: formation, maturation, and resolution. *Immunol. Rev.* **273**, 156–179 (2016).

316. Rink, J., Ghigo, E., Kalaidzidis, Y. & Zerial, M. Rab conversion as a mechanism of progression from early to late endosomes. *Cell* **122**, 735–749 (2005).

317. Harrison, R. E., Bucci, C., Vieira, O. V, Schroer, T. A. & Grinstein, S. Phagosomes fuse with late endosomes and/or lysosomes by extension of membrane protrusions along microtubules: role of Rab7 and RILP. *Mol. Cell. Biol.* **23**, 6494–506 (2003).

318. Antonin, W. A SNARE complex mediating fusion of late endosomes defines conserved properties of SNARE structure and function. *EMBO J.* **19**, 6453–6464 (2000).

319. Masson, P. L., Heremans, J. F. & Schonne, E. Lactoferrin, an iron-binding protein in neutrophilic leukocytes. *J. Exp. Med.* **130**, 643–58 (1969).

320. Skaar, E. P. The battle for iron between bacterial pathogens and their vertebrate hosts. *PLoS Pathog.* **6**, e1000949 (2010).

321. Nauseef, W. M. Myeloperoxidase in human neutrophil host defence. *Cell. Microbiol.* **16**, 1146–1155 (2014).

322. Harry, G. J. Microglia during development and aging. *Pharmacol. Ther.* **139**, 313–326 (2013).

323. Aguzzi, A., Barres, B. A. & Bennett, M. L. Microglia: Scapegoat, Saboteur, or Something Else ? *Science (80-.).* **339**, 156–161 (2013).

324. Chan, W. Y., Kohsaka, S. & Rezaie, P. The origin and cell lineage of microglia—New concepts. *Brain Res. Rev.* **53**, 344–354 (2007).

325. Salter, M. W. & Beggs, S. Sublime microglia: Expanding roles for the guardians of the CNS. *Cell* **158**, 15–24 (2014).

326. Brown, G. C. & Neher, J. J. Microglial phagocytosis of live neurons. *Nat. Publ. Gr.* **15**, 209–216 (2014).

327. Brown, G. C. & Vilalta, A. How microglia kill neurons. *Brain Res.* **1628**, 288–297 (2015).

328. Dubbelaar, M. L., Kracht, L., Eggen, B. J. L. & Boddeke, E. W. G. M. The Kaleidoscope of Microglial Phenotypes. *Front. Immunol.* **9**, 1753 (2018).

329. Bachiller, S. *et al.* Microglia in neurological diseases: A road map to brain-disease dependent-inflammatory response. *Front. Cell. Neurosci.* **12**, 1–17 (2018).

330. Li, Q. & Barres, B. A. Microglia and macrophages in brain homeostasis and disease.

Nat. Rev. Immunol. **18**, 225–242 (2018).

331. Ajami, B., Bennett, J. L., Krieger, C., Tetzlaff, W. & Rossi, F. M. V. Local self-renewal can sustain CNS microglia maintenance and function throughout adult life. *Nat. Neurosci.* **10**, 1538–1543 (2007).

332. Thion, M. S., Ginhoux, F. & Garel, S. Microglia and early brain development: An intimate journey. *Science* **362**, 185–189 (2018).

333. Wlodarczyk, A. *et al.* A novel microglial subset plays a key role in myelinogenesis in developing brain. *EMBO J.* **36**, 3292–3308 (2017).

334. Nakanishi, M. *et al.* Microglia-derived interleukin-6 and leukaemia inhibitory factor promote astrocytic differentiation of neural stem/progenitor cells. *Eur. J. Neurosci.* **25**, 649–658 (2007).

335. Lenz, K. M. & Nelson, L. H. Microglia and Beyond: Innate Immune Cells As Regulators of Brain Development and Behavioral Function. *Front. Immunol.* **9**, 698 (2018).

336. Cunningham, C. L., Martínez-Cerdeño, V. & Noctor, S. C. Microglia regulate the number of neural precursor cells in the developing cerebral cortex. *J. Neurosci.* **33**, 4216–33 (2013).

337. Marín-Teva, J. L. *et al.* Microglia promote the death of developing Purkinje cells. *Neuron* **41**, 535–47 (2004).

338. Li, Q. *et al.* Developmental Heterogeneity of Microglia and Brain Myeloid Cells Revealed by Deep Single-Cell RNA Sequencing. *Neuron* **101**, 207-223.e10 (2019).

339. Ueno, M. *et al.* Layer V cortical neurons require microglial support for survival during postnatal development. *Nat. Neurosci.* **16**, 543–551 (2013).

340. Swinnen, N. *et al.* Complex invasion pattern of the cerebral cortex bymicroglial cells during development of the mouse embryo. *Glia* **61**, 150–163 (2013).

341. Squarzoni, P. *et al.* Microglia Modulate Wiring of the Embryonic Forebrain. *Cell Rep.* **8**, 1271–1279 (2014).

342. Pont-Lezica, L. *et al.* Microglia shape corpus callosum axon tract fasciculation: functional impact of prenatal inflammation. *Eur. J. Neurosci.* **39**, 1551–1557 (2014).

343. Lim, S.-H. *et al.* Neuronal Synapse Formation Induced by Microglia and Interleukin 10. *PLoS One* **8**, e81218 (2013).

344. Parkhurst, C. *et al.* Microglia promote learning-dependent synapse formation through brain-derived neurotrophic factor. *Elsevier*

345. Rakic, P., Bourgeois, J.-P., Eckenhoff, M. F., Zecevic, N. & Goldman-Rakic, P. S. Concurrent overproduction of synapses in diverse regions of the primate cerebral cortex. *Science (80-.).* **232**, 232–236 (1986).

346. Johnson-Venkatesh, E. M., Khan, M. N., Murphy, G. G., Sutton, M. A. & Umemori, H. Excitability governs neural development in a hippocampal region-specific manner. *Development* **142**, 3879–91 (2015).

347. Huttenlocher, P. R. & Dabholkar, A. S. Regional differences in synaptogenesis in human cerebral cortex. *J. Comp. Neurol.* **387**, 167–178 (1997).

348. Keown, C. L. *et al.* Local functional overconnectivity in posterior brain regions is associated with symptom severity in autism spectrum disorders. *Cell Rep.* **5**, 567–572 (2013).

349. Chung, W.-S., Allen, N. J. & Eroglu, C. Astrocytes Control Synapse Formation, Function, and Elimination. *Cold Spring Harb. Perspect. Biol.* **7**, a020370 (2015).

350. Pocock, J. M. & Kettenmann, H. Neurotransmitter receptors on microglia. *Trends Neurosci.* **30**, 527–535 (2007).

351. Kettenmann, H., Kirchhoff, F. & Verkhratsky, A. Microglia: New Roles for the Synaptic Stripper. *Neuron* **77**, 10–18 (2013).

352. Wake, H., Moorhouse, A. J., Jinno, S., Kohsaka, S. & Nabekura, J. Resting Microglia Directly Monitor the Functional State of Synapses In Vivo and Determine the Fate of Ischemic Terminals. *J. Neurosci.* **29**, 3974–3980 (2009).

353. Tremblay, M. E., Lowery, R. L. & Majewska, A. K. Microglial interactions with synapses are modulated by visual experience. *PLoS Biol.* **8**, (2010).

354. Paolicelli, R. C. *et al.* Synaptic pruning by microglia is necessary for normal brain development. *Science* **333**, 1456–1458 (2011).

355. Linnartz-Gerlach, B., Schuy, C., Shahraz, A., Tenner, A. J. & Neumann, H. Sialylation

of neurites inhibits complement-mediated macrophage removal in a human macrophage-neuron Co-Culture System. *Glia* **64**, 35–47 (2016).

356. Filipello, F. *et al.* The Microglial Innate Immune Receptor TREM2 Is Required for Synapse Elimination and Normal Brain Article The Microglial Innate Immune Receptor TREM2 Is Required for Synapse Elimination and Normal Brain Connectivity. *Immunity* **48**, 979-991.e8 (2018).

357. Lehrman, E. K. *et al.* CD47 Protects Synapses from Excess Microglia- Mediated Pruning during Development Article CD47 Protects Synapses from Excess Microglia-Mediated Pruning during Development. *Neuron* **100**, 120-134.e6 (2018).

358. Zhan, Y. *et al.* Deficient neuron-microglia signaling results in impaired functional brain connectivity and social behavior. *Nat. Neurosci.* **17**, 400–406 (2014).

359. Magnus, T., Chan, A., Linker, R. A., Toyka, K. V. & Gold, R. Astrocytes Are Less Efficient in the Removal of Apoptotic Lymphocytes than Microglia Cells: Implications for the Role of Glial Cells in the Inflamed Central Nervous System. *J. Neuropathol. Exp. Neurol.* **61**, 760–766 (2002).

360. Galloway, D. A., Phillips, A. E. M., Owen, D. R. J. & Moore, C. S. Phagocytosis in the Brain: Homeostasis and Disease. *Front. Immunol.* **10**, 790 (2019).

361. Sierra, A., Abiega, O., Shahraz, A. & Neumann, H. Janus-faced microglia: beneficial and detrimental consequences of microglial phagocytosis. *Front. Cell. Neurosci.* **7**, 6 (2013).

362. Sierra, A. *et al.* Microglia shape adult hippocampal neurogenesis through apoptosis-coupled phagocytosis. *Cell Stem Cell* **7**, 483–95 (2010).

363. Safaiyan, S. *et al.* Age-related myelin degradation burdens the clearance function of microglia during aging. *Nat. Neurosci.* **19**, 995–998 (2016).

364. Yin, J., Valin, K. L., Dixon, M. L. & Leavenworth, J. W. The Role of Microglia and Macrophages in CNS Homeostasis, Autoimmunity, and Cancer. *J. Immunol. Res.* **2017**, 1–12 (2017).

365. Hsieh, J. *et al.* IGF-I instructs multipotent adult neural progenitor cells to become oligodendrocytes. *J. Cell Biol.* **164**, 111–22 (2004).

366. Fontainhas, A. M. *et al.* Microglial Morphology and Dynamic Behavior Is Regulated by Ionotropic Glutamatergic and GABAergic Neurotransmission. *PLoS One* **6**, e15973 (2011).

367. Dissing-Olesen, L. *et al.* Activation of neuronal NMDA receptors triggers transient ATP-mediated microglial process outgrowth. *J. Neurosci.* **34**, 10511–27 (2014).

368. Eyo, U. B. *et al.* Neuronal Hyperactivity Recruits Microglial Processes via Neuronal NMDA Receptors and Microglial P2Y12 Receptors after Status Epilepticus. *J. Neurosci.* **34**, 10528–10540 (2014).

369. Singh, A. & Abraham, W. C. Astrocytes and synaptic plasticity in health and disease. *Exp. Brain Res.* **235**, 1645–1655 (2017).

370. Wu, Y., Dissing-Olesen, L., MacVicar, B. A. & Stevens, B. Microglia: Dynamic Mediators of Synapse Development and Plasticity. *Trends Immunol.* **36**, 605–613 (2015).

371. Stellwagen, D. & Malenka, R. C. Synaptic scaling mediated by glial TNF-α. *Nature* **440**, 1054–1059 (2006).

372. Sipe, G. O. *et al.* Microglial P2Y12 is necessary for synaptic plasticity in mouse visual cortex. *Nat. Commun.* **7**, (2016).

373. Rogers, J. T. *et al.* CX3CR1 Deficiency Leads to Impairment of Hippocampal Cognitive Function and Synaptic Plasticity. *J. Neurosci.* **31**, 16241–16250 (2011).

374. Koeglsperger, T. *et al.* Impaired glutamate recycling and GluN2B-mediated neuronal calcium overload in mice lacking TGF-β1 in the CNS. *Glia* **61**, 985–1002 (2013).

375. Louveau, A., Harris, T. H. & Kipnis, J. Revisiting the Mechanisms of CNS Immune Privilege. *Trends Immunol.* **36**, 569–577 (2015).

376. Branton, W. G. *et al.* Brain microbial populations in HIV/AIDS: α-proteobacteria predominate independent of host immune status. *PLoS One* **8**, e54673 (2013).

377. Servick, K. Do gut bacteria make a second home in our brains? *Science* (2018). doi:10.1126/science.aaw0147

378. Nau, R., Ribes, S., Djukic, M. & Eiffert, H. Strategies to increase the activity of microglia as efficient protectors of the brain against infections. *Front. Cell. Neurosci.*

8, 1–13 (2014).

379. Zysk, G. *et al.* Pneumolysin Is the Main Inducer of Cytotoxicity to Brain Microvascular Endothelial Cells Caused by Streptococcus pneumoniae. *Infect. Immun.* **69**, 845–852 (2001).

380. Kim, K. S. Mechanisms of microbial traversal of the blood-brain barrier. *Nat. Rev. Microbiol.* **6**, 625–34 (2008).

381. Lehnardt, S. *et al.* Activation of innate immunity in the CNS triggers neurodegeneration through a Toll-like receptor 4-dependent pathway. *Proc. Natl. Acad. Sci. U. S. A.* **100**, 8514–8519 (2003).

382. Park, B. S. & Lee, J. O. Recognition of lipopolysaccharide pattern by TLR4 complexes. *Experimental and Molecular Medicine* **45**, e66–e66 (2013).

383. Schröder, N. W. J. *et al.* Lipoteichoic Acid (LTA) of S. pneumoniae and S. aureus Activates Immune Cells via Toll-like Receptor (TLR)-2, Lipopolysaccharide (LPS) binding protein (LBP) and CD14 while TLR-4 and MD-2 are not Involved. *J. Biol. Chem.* **278**, 15587–94 (2003).

384. Ribes, S. *et al.* Resistance of the Brain to Escherichia coli K1 Infection Depends on MyD88 Signaling and the Contribution of Neutrophils and Monocytes. *Infect. Immun.* **81**, 1810–1819 (2013).

385. Kielian, T. *et al.* MyD88-dependent signals are essential for the host immune response in experimental brain abscess. *J. Immunol.* **178**, 4528–37 (2007).

386. Koedel, U. *et al.* MyD88 is required for mounting a robust host immune response to Streptococcus pneumoniae in the CNS. *Brain* **127**, 1437–1445 (2004).

387. Torres, M. *et al.* MyD88 is crucial for the development of a protective CNS immune response to Toxoplasma gondii infection. *J. Neuroinflammation* **10**, 19 (2013).

388. Oshiumi, H. *et al.* The TLR3/TICAM-1 Pathway Is Mandatory for Innate Immune Responses to Poliovirus Infection. *J. Immunol.* **187**, 5320–5327 (2011).

389. Abe, Y. *et al.* The toll-like receptor 3-mediated antiviral response is important for protection against poliovirus infection in poliovirus receptor transgenic mice. *J. Virol.* **86**, 185–94 (2012).

390. Sabouri, A. H. *et al.* TLR signaling controls lethal encephalitis in WNV-infected brain. *Brain Res.* **1574**, 84–95 (2014).

391. Koutsouras, G. W., Ramos, R. L. & Martinez, L. R. Role of microglia in fungal infections of the central nervous system. *Virulence* **8**, 705–718 (2017).

392. Gres, V., Kolter, J., Erny, D. & Henneke, P. The role of CNS macrophages in streptococcal meningoencephalitis. *J. Leukoc. Biol.* **106**, 209–218 (2019).

393. Thorsdottir, S., Henriques-Normark, B. & Iovino, F. The role of microglia in bacterial meningitis: Inflammatory response, experimental models and new neuroprotective therapeutic strategies. *Front. Microbiol.* **10**, 1–8 (2019).

394. Davies, B. W. *et al.* DNA damage and reactive nitrogen species are barriers to Vibrio cholerae colonization of the infant mouse intestine. *PLoS Pathog.* **7**, e1001295 (2011).

395. Arvin, B., Neville, L. F., Barone, F. C. & Feuerstein, G. Z. The role of inflammation and cytokines in brain injury. *Neurosci. Biobehav. Rev.* **20**, 445–452 (1996).

396. Ribes, S. *et al.* Toll-Like Receptor Prestimulation Increases Phagocytosis of Escherichia coli DH5 and Escherichia coli K1 Strains by Murine Microglial Cells. *Infect. Immun.* **77**, 557–564 (2009).

397. Ribes, S. *et al.* Toll-like receptor stimulation enhances phagocytosis and intracellular killing of nonencapsulated and encapsulated Streptococcus pneumoniae by murine microglia. *Infect. Immun.* **78**, 865–71 (2010).

398. Ribes, S. *et al.* The viral TLR3 agonist poly(I:C) stimulates phagocytosis and intracellular killing of Escherichia coli by microglial cells. *Neurosci. Lett.* **482**, 17–20 (2010).

399. Ribes, S. *et al.* The nucleotide-binding oligomerization domain-containing-2 ligand muramyl dipeptide enhances phagocytosis and intracellular killing of Escherichia coli K1 by Toll-like receptor agonists in microglial cells. *J. Neuroimmunol.* **252**, 16–23 (2012).

400. Arcuri, C., Mecca, C., Bianchi, R., Giambanco, I. & Donato, R. The Pathophysiological Role of Microglia in Dynamic Surveillance, Phagocytosis and Structural Remodeling of the Developing CNS. *Front. Mol. Neurosci.* **10**, 1–22 (2017).

401. Veerhuis, R., Nielsen, H. M. & Tenner, A. J. Complement in the brain. *Mol. Immunol.* **48**, 1592–603 (2011).

402. Tian, L., Ma, L., Kaarela, T. & Li, Z. Neuroimmune crosstalk in the central nervous system and its significance for neurological diseases. *J. Neuroinflammation* **9**, 155 (2012).

403. Weinstein, J. R. *et al.* IgM-Dependent Phagocytosis in Microglia Is Mediated by Complement Receptor 3, Not Fcα/μ Receptor. *J. Immunol.* **195**, 5309–17 (2015).

404. Lunnon, K. *et al.* Systemic inflammation modulates Fc receptor expression on microglia during chronic neurodegeneration. *J. Immunol.* **186**, 7215–24 (2011).

405. Klein, M. *et al.* Innate Immunity to Pneumococcal Infection of the Central Nervous System Depends on Toll-Like Receptor (TLR) 2 and TLR4. *J. Infect. Dis.* **198**, 1028–1036 (2008).

406. Ribes, S. *et al.* Intraperitoneal prophylaxis with CpG oligodeoxynucleotides protects neutropenic mice against intracerebral Escherichia coli K1 infection. *J. Neuroinflammation* **11**, 14 (2014).

407. Schetters, S. T. T., Gomez-Nicola, D., Garcia-Vallejo, J. J. & Van Kooyk, Y. Neuroinflammation: Microglia and T Cells Get Ready to Tango. *Front. Immunol.* **8**, 1905 (2017).

408. Korn, T. & Kallies, A. T cell responses in the central nervous system. *Nat. Rev. Immunol.* **17**, 179–194 (2017).

409. Buttini, M., Limonta, S. & Boddeke, H. W. G. M. Peripheral administration of lipopolysaccharide induces activation of microglial cells in rat brain. *Neurochem. Int.* **29**, 25–35 (1996).

410. Cunha, C., Gomes, C., Vaz, A. R. & Brites, D. Exploring New Inflammatory Biomarkers and Pathways during LPS-Induced M1 Polarization. *Mediators Inflamm.* **2016**, 6986175 (2016).

411. Dalpke, A. H. *et al.* Immunostimulatory CpG-DNA Activates Murine Microglia. *J. Immunol.* **168**, 4854–4863 (2002).

412. Zhang, L., Zhang, J. & You, Z. Switching of the Microglial Activation Phenotype Is a

Possible Treatment for Depression Disorder. *Front. Cell. Neurosci.* **12**, 306 (2018).

413. Hammond, T. R. *et al.* Single-Cell RNA Sequencing of Microglia throughout the Mouse Lifespan and in the Injured Brain Reveals Complex Cell-State Changes. *Immunity* **50**, 253-271.e6 (2019).

414. Orihuela, R., McPherson, C. A. & Harry, G. J. Microglial M1/M2 polarization and metabolic states. *Br. J. Pharmacol.* **173**, 649–65 (2016).

415. Hanisch, U.-K. K. & Kettenmann, H. Microglia: active sensor and versatile effector cells in the normal and pathologic brain. *Nat. Neurosci.* **10**, 1387–1394 (2007).

416. Butovsky, O. *et al.* Identification of a unique TGF-β–dependent molecular and functional signature in microglia. *Nat. Neurosci.* **17**, 131–143 (2014).

417. Brionne, T. C., Tesseur, I., Masliah, E. & Wyss-Coray, T. Loss of TGF-beta 1 leads to increased neuronal cell death and microgliosis in mouse brain. *Neuron* **40**, 1133–45 (2003).

418. Hoek, R. M. *et al.* Down-Regulation of the Macrophage Lineage Through Interaction with OX2 (CD200). *Science (80-.).* **290**, 1768–1771 (2000).

419. Barakat, R. & Redzic, Z. Differential cytokine expression by brain microglia/macrophages in primary culture after oxygen glucose deprivation and their protective effects on astrocytes during anoxia. *Fluids Barriers CNS* **12**, 6 (2015).

420. Fiebich, B. L., Batista, C. R. A., Saliba, S. W., Yousif, N. M. & de Oliveira, A. C. P. Role of microglia TLRs in neurodegeneration. *Front. Cell. Neurosci.* **12**, 329 (2018).

421. Wlodarczyk, A. *et al.* A novel microglial subset plays a key role in myelinogenesis in developing brain. *EMBO J.* **36**, 3292–3308 (2017).

422. Grabert, K. *et al.* Microglial brain region−dependent diversity and selective regional sensitivities to aging. *Nat. Neurosci.* **19**, 504–516 (2016).

423. Prajeeth, C. K. *et al.* Effector molecules released by Th1 but not Th17 cells drive an M1 response in microglia. *Brain. Behav. Immun.* **37**, 248–259 (2014).

424. Takeda, K. & Akira, S. TLR signaling pathways. *Semin. Immunol.* **16**, 3–9 (2004).

425. Hu, X. & Ivashkiv, L. B. Cross-regulation of Signaling Pathways by Interferon-γ: Implications for Immune Responses and Autoimmune Diseases. *Immunity* **31**, 539–

550 (2009).

426. Netea, M. G., van de Veerdonk, F. L., van der Meer, J. W. M., Dinarello, C. A. & Joosten, L. A. B. Inflammasome-Independent Regulation of IL-1-Family Cytokines. *Annu. Rev. Immunol.* **33**, 49–77 (2015).

427. Zhou, L. & Zhu, D.-Y. Neuronal nitric oxide synthase: Structure, subcellular localization, regulation, and clinical implications. *Nitric Oxide* **20**, 223–230 (2009).

428. Segal, A. W. The function of the NADPH oxidase of phagocytes and its relationship to other NOXs in plants, invertebrates, and mammals. *Int. J. Biochem. Cell Biol.* **40**, 604 (2008).

429. Subramaniam, S. R. & Federoff, H. J. Targeting Microglial Activation States as a Therapeutic Avenue in Parkinson's Disease. *Front. Aging Neurosci.* **9**, 1–18 (2017).

430. Yang, X. *et al.* Microglia P2Y6 receptor is related to Parkinson's disease through neuroinflammatory process. *J. Neuroinflammation* **14**, 1–12 (2017).

431. Chauhan, P., Hu, S., Sheng, W. S., Prasad, S. & Lokensgard, J. R. Modulation of Microglial Cell Fcγ Receptor Expression Following Viral Brain Infection. *Sci. Rep.* **7**, 41889 (2017).

432. Ponomarev, E. D., Shriver, L. P. & Dittel, B. N. CD40 Expression by Microglial Cells Is Required for Their Completion of a Two-Step Activation Process during Central Nervous System Autoimmune Inflammation. *J. Immunol.* **176**, 1402–1410 (2006).

433. Vijitruth, R. *et al.* Cyclooxygenase-2 mediates microglial activation and secondary dopaminergic cell death in the mouse MPTP model of Parkinson's disease. *J. Neuroinflammation* **3**, 6 (2006).

434. Streit, W. J., Mrak, R. E. & Griffin, W. S. T. Microglia and neuroinflammation: a pathological perspective. *J. Neuroinflammation* **1**, 14 (2004).

435. Cherry, J. D., Olschowka, J. A. & O'Banion, M. K. Neuroinflammation and M2 microglia: The good, the bad, and the inflamed. *J. Neuroinflammation* **11**, 1–15 (2014).

436. Bao, K. & Reinhardt, R. L. The differential expression of IL-4 and IL-13 and its impact on type-2 immunity. *Cytokine* **75**, 25–37 (2015).

437. Martinez, F. O. & Gordon, S. The M1 and M2 paradigm of macrophage activation: Time for reassessment. *F1000Prime Rep.* **6**, 1–13 (2014).

438. Desgeorges, T., Caratti, G., Mounier, R., Tuckermann, J. & Chazaud, B. Glucocorticoids Shape Macrophage Phenotype for Tissue Repair. *Front. Immunol.* **10**, 1591 (2019).

439. Franco, R. & Fernández-Suárez, D. Alternatively activated microglia and macrophages in the central nervous system. *Prog. Neurobiol.* **131**, 65–86 (2015).

440. Mori, S., Maher, P. & Conti, B. Neuroimmunology of the interleukins 13 and 4. *Brain Sci.* **6**, E18 (2016).

441. Lobo-Silva, D., Carriche, G. M., Castro, A. G., Roque, S. & Saraiva, M. Balancing the immune response in the brain: IL-10 and its regulation. *J. Neuroinflammation* **13**, 297 (2016).

442. Varin, A. & Gordon, S. Alternative activation of macrophages: Immune function and cellular biology. *Immunobiology* **214**, 630–641 (2009).

443. Gadani, S. P., Cronk, J. C., Norris, G. T. & Kipnis, J. IL-4 in the Brain: A Cytokine To Remember. *J. Immunol.* **189**, 4213–4219 (2012).

444. Cherry, J. D., Olschowka, J. A. & O'Banion, M. K. Neuroinflammation and M2 microglia: the good, the bad, and the inflamed. *J. Neuroinflammation* **11**, 98 (2014).

445. Butovsky, O., Talpalar, A. E., Ben-Yaakov, K. & Schwartz, M. Activation of microglia by aggregated β-amyloid or lipopolysaccharide impairs MHC-II expression and renders them cytotoxic whereas IFN-γ and IL-4 render them protective. *Mol. Cell. Neurosci.* **29**, 381–393 (2005).

446. Chao, C. C., Hu, S. & Peterson, P. K. Modulation of human microglial cell superoxide production by cytokines. *J. Leukoc. Biol.* **58**, 65–70 (1995).

447. Lyons, A. *et al.* Decreased neuronal CD200 expression in IL-4-deficient mice results in increased neuroinflammation in response to lipopolysaccharide. *Brain. Behav. Immun.* **23**, 1020–1027 (2009).

448. Roesch, S., Rapp, C., Dettling, S. & Herold-Mende, C. When Immune Cells Turn Bad-Tumor-Associated Microglia/Macrophages in Glioma. *Int. J. Mol. Sci.* **19**, (2018).

449. Lenz, K. M. & Nelson, L. H. Microglia and Beyond: Innate Immune Cells As Regulators of Brain Development and Behavioral Function. *Front. Immunol.* **9**, 698 (2018).

450. Keren-Shaul, H. *et al.* A Unique Microglia Type Associated with Restricting Development of Alzheimer's Disease. *Cell* **169**, 1276-1290.e17 (2017).

451. Choi, H., Choi, Y., Hwang, D. W. & Lee, D. S. Reconfiguration of neuronal subpopulation associated with disease-associated microglia in human Alzheimer's disease brain. *bioRxiv* 522987 (2019). doi:10.1101/522987

452. Mazaheri, F. *et al.* Distinct roles for BAI1 and TIM-4 in the engulfment of dying neurons by microglia. *Nat. Commun.* **5**, 4046 (2014).

453. Mori, K. *et al.* Brain-specific angiogenesis inhibitor 1 (BAI1) is expressed in human cerebral neuronal cells. *Neurosci. Res.* **43**, 69–74 (2002).

454. Sokolowski, J. D. *et al.* Brain-specific angiogenesis inhibitor-1 expression in astrocytes and neurons: Implications for its dual function as an apoptotic engulfment receptor. *Brain. Behav. Immun.* **25**, 915–921 (2011).

455. Park, D. *et al.* BAI1 is an engulfment receptor for apoptotic cells upstream of the ELMO/Dock180/Rac module. *Nature* **450**, 430–434 (2007).

456. Marker, D. F. *et al.* LRRK2 kinase inhibition prevents pathological microglial phagocytosis in response to HIV-1 Tat protein. *J. Neuroinflammation* **9**, 261 (2012).

457. Hsiao, C.-C., van der Poel, M., van Ham, T. J. & Hamann, J. Macrophages Do Not Express the Phagocytic Receptor BAI1/ADGRB1. *Front. Immunol.* **10**, 962 (2019).

458. Ehlers, M. R. W. CR3: a general purpose adhesion-recognition receptor essential for innate immunity. *Microbes Infect.* **2**, 289–294 (2000).

459. Pena-Ortega, F. Pharmacological Tools to Activate Microglia and their Possible use to Study Neural Network Patho-physiology. *Curr. Neuropharmacol.* **15**, 595–619 (2017).

460. Czirr, E. *et al.* Microglial complement receptor 3 regulates brain Aβ levels through secreted proteolytic activity. *J. Exp. Med.* **214**, 1081–1092 (2017).

461. Anderson, S. R. *et al.* Complement Targets Newborn Retinal Ganglion Cells for Phagocytic Elimination by Microglia. *J. Neurosci.* **39**, 2025–2040 (2019).

462. Kaur, C., Too, H. F. & Ling, E. A. Phagocytosis of Escherichia coli by amoeboid microglial cells in the developing brain. *Acta Neuropathol.* **107**, 204–208 (2004).

463. Rotshenker, S. Microglia and Macrophage Activation and the Regulation of Complement-Receptor-3 (CR3/MAC-1)-Mediated Myelin Phagocytosis in Injury and Disease. *J. Mol. Neurosci.* **21**, 65–72 (2003).

464. Shi, Q. *et al.* Complement C3 deficiency protects against neurodegeneration in aged plaque-rich APP / PS1 mice. **6295**, 1–14 (2017).

465. Conde, J. R. & Streit, W. J. Microglia in the Aging Brain. *J. Neuropathol. Exp. Neurol.* **65**, 199–203 (2006).

466. Bournazos, S. & Ravetch, J. V. Fcγ Receptor Function and the Design of Vaccination Strategies. *Immunity* **47**, 224–233 (2017).

467. Quan, Y., Möller, T. & Weinstein, J. R. Regulation of Fcgamma receptors and immunoglobulin G-mediated phagocytosis in mouse microglia. *Neurosci. Lett.* **464**, 29–33 (2009).

468. Ulvestad, E. *et al.* Fc Receptors for IgG on Cultured Human Microglia Mediate Cytotoxicity and Phagocytosis of Antibody-coated Targets. *J. Neuropathol. Exp. Neurol.* **53**, 27–36 (1994).

469. Sanders, L. A. M. *et al.* Human immunoglobulin G (IgG) Fc receptor IIA (CD32) polymorphism and IgG2- mediated bacterial phagocytosis by neutrophils. *Infect. Immun.* **63**, 73–81 (1995).

470. Kusner, D. J., Hall, C. F. & Jackson, S. Fc gamma receptor-mediated activation of phospholipase D regulates macrophage phagocytosis of IgG-opsonized particles. *J. Immunol.* **162**, 2266–74 (1999).

471. Fuller, J. P., Stavenhagen, J. B. & Teeling, J. L. New roles for Fc receptors in neurodegeneration-the impact on Immunotherapy for Alzheimer's Disease. *Front. Neurosci.* **8**, 235 (2014).

472. Yang, L. *et al.* LRP1 modulates the microglial immune response via regulation of JNK and NF-κB signaling pathways. *J. Neuroinflammation* **13**, 304 (2016).

473. Gardai, S. J. *et al.* Cell-Surface Calreticulin Initiates Clearance of Viable or Apoptotic

Cells through trans-Activation of LRP on the Phagocyte. *Cell* **123**, 321–334 (2005).

474. Nilsson, A., Vesterlund, L. & Oldenborg, P.-A. Macrophage expression of LRP1, a receptor for apoptotic cells and unopsonized erythrocytes, can be regulated by glucocorticoids. *Biochem. Biophys. Res. Commun.* **417**, 1304–1309 (2012).

475. Fancy, R. M. *et al.* Cell Surface Calreticulin-LRP1 Binding and its Role in Apoptotic Cell Engulfment. *Biophys. J.* **114**, 464a-465a (2018).

476. Chao, M. P. *et al.* Calreticulin is the dominant pro-phagocytic signal on multiple human cancers and is counterbalanced by CD47. *Sci. Transl. Med.* **2**, 63–94 (2010).

477. Marzolo, M. P., von Bernhardi, R., Bu, G. & Inestrosa, N. C. Expression of ?2-macroglobulin receptor/low density lipoprotein receptor-related protein (LRP) in rat microglial cells. *J. Neurosci. Res.* **60**, 401–411 (2000).

478. Fricker, M., Oliva-Martín, M. J. & Brown, G. C. Primary phagocytosis of viable neurons by microglia activated with LPS or Aβ is dependent on calreticulin/LRP phagocytic signalling. *J. Neuroinflammation* **9**, 196 (2012).

479. Gaultier, A. *et al.* Low-density lipoprotein receptor-related protein 1 is an essential receptor for myelin phagocytosis. *J. Cell Sci.* **122**, 1155–62 (2009).

480. Brifault, C., Gilder, A. S., Laudati, E., Banki, M. & Gonias, S. L. Shedding of Membrane-associated LDL Receptor-related Protein-1 from microglia amplifies and sustains neuroinflammation. *J. Biol. Chem.* **292**, 18699–18712 (2017).

481. Zhu, H. *et al.* The expression and clinical significance of different forms of Mer receptor tyrosine kinase in systemic lupus erythematosus. *J. Immunol. Res.* **2014**, 431896 (2014).

482. Scott, R. S. *et al.* Phagocytosis and clearance of apoptotic cells is mediated by MER. *Nature* **411**, 207–211 (2001).

483. Neher, J. J. *et al.* Phagocytosis executes delayed neuronal death after focal brain ischemia. *Proc. Natl. Acad. Sci. U. S. A.* **110**, E4098-107 (2013).

484. Healy, L. M. *et al.* MerTK Is a Functional Regulator of Myelin Phagocytosis by Human Myeloid Cells. *J. Immunol.* **196**, 3375–84 (2016).

485. Koizumi, S. *et al.* UDP acting at P2Y6 receptors is a mediator of microglial

phagocytosis. *Nature* **446**, 1091–5 (2007).

486. Communi, D., Parmentier, M. & Boeynaems, J.-M. M. Cloning, Functional Expression and Tissue Distribution of the Human P2Y6Receptor. *Biochem. Biophys. Res. Commun.* **222**, 303–308 (1996).

487. Kim, B. *et al.* Uridine 5'-diphosphate induces chemokine expression in microglia and astrocytes through activation of the P2Y6 receptor. *J. Immunol.* **186**, 3701–9 (2011).

488. Kobayashi, K. *et al.* Neurons and glial cells differentially express P2Y receptor mRNAs in the rat dorsal root ganglion and spinal cord. *J. Comp. Neurol.* **498**, 443–454 (2006).

489. Steculorum, S. M. *et al.* Hypothalamic UDP Increases in Obesity and Promotes Feeding via P2Y6-Dependent Activation of AgRP Neurons. *Cell* **162**, 1404–1417 (2015).

490. Koizumi, S., Ohsawa, K., Inoue, K. & Kohsaka, S. Purinergic receptors in microglia: Functional modal shifts of microglia mediated by P2 and P1 receptors. *Glia* **61**, 47–54 (2013).

491. Neher, J. J., Neniskyte, U., Hornik, T. & Brown, G. C. Inhibition of UDP/P2Y6 purinergic signaling prevents phagocytosis of viable neurons by activated microglia in vitro and in vivo. *Glia* **62**, 1463–1475 (2014).

492. DeKruyff, R. H. *et al.* T Cell/Transmembrane, Ig, and Mucin-3 Allelic Variants Differentially Recognize Phosphatidylserine and Mediate Phagocytosis of Apoptotic Cells. *J. Immunol.* **184**, 1918–1930 (2010).

493. Meyers, J. H., Sabatos, C. A., Chakravarti, S. & Kuchroo, V. K. The TIM gene family regulates autoimmune and allergic diseases. *Trends Mol. Med.* **11**, 362–9 (2005).

494. Wong, K. *et al.* Phosphatidylserine receptor Tim-4 is essential for the maintenance of the homeostatic state of resident peritoneal macrophages. *Proc. Natl. Acad. Sci.* **107**, 8712–8717 (2010).

495. Bu, X., Zhu, B., Umetsu, D., DeKruyff, R. & Freeman, G. TIM-4 mediated phagocytosis of apoptotic cells induces regulatory cytokine secretion by mouse peritoneal macrophages. *J. Immunol.* **184**, 136.47 (2010).

496. Bu, X., DeKruyff, R., Umetsu, D. & Freeman, G. TIM-3- and TIM-4-mediated phagocytosis of apoptotic cells induces cytokine production in peritoneal macrophages. *J. Immunol.* **186**, 100.55 (2011).

497. Ulland, T. K. & Colonna, M. TREM2 — a key player in microglial biology and Alzheimer disease. *Nat. Rev. Neurol.* **14**, 667–675 (2018).

498. Zhao, Y. *et al.* TREM2 Is a Receptor for β-Amyloid that Mediates Microglial Function. *Neuron* **97**, 1023-1031.e7 (2018).

499. Daws, M. R. *et al.* Pattern recognition by TREM-2: binding of anionic ligands. *J. Immunol.* **171**, 594–9 (2003).

500. Shirotani, K. *et al.* Aminophospholipids are signal-transducing TREM2 ligands on apoptotic cells. *Sci. Rep.* **9**, 7508 (2019).

501. Kawabori, M. *et al.* Triggering Receptor Expressed on Myeloid Cells 2 (TREM2) Deficiency Attenuates Phagocytic Activities of Microglia and Exacerbates Ischemic Damage in Experimental Stroke. *J. Neurosci.* **35**, 3384 (2015).

502. Lessard, C. B. *et al.* High-affinity interactions and signal transduction between Aβ oligomers and TREM 2. *EMBO Mol. Med.* **10**, e9027 (2018).

503. Boza-Serrano, A. *et al.* Galectin-3, a novel endogenous TREM2 ligand, detrimentally regulates inflammatory response in Alzheimer's disease. *Acta Neuropathol.* **138**, 251–273 (2019).

504. Atagi, Y. *et al.* Apolipoprotein E is a ligand for triggering receptor expressed on myeloid cells 2 (TREM2). *J. Biol. Chem.* **290**, 26043–26050 (2015).

505. Konishi, H. & Kiyama, H. Microglial TREM2/DAP12 Signaling: A Double-Edged Sword in Neural Diseases. *Front. Cell. Neurosci.* **12**, 206 (2018).

506. Takahashi, K., Rochford, C. D. P. & Neumann, H. Clearance of apoptotic neurons without inflammation by microglial triggering receptor expressed on myeloid cells-2. *J. Exp. Med.* **201**, 647–657 (2005).

507. Kiialainen, A., Hovanes, K., Paloneva, J., Kopra, O. & Peltonen, L. Dap12 and Trem2, molecules involved in innate immunity and neurodegeneration, are co-expressed in the CNS. *Neurobiol. Dis.* **18**, 314–322 (2005).

508. Poliani, P. L. *et al.* TREM2 sustains microglial expansion during aging and response to demyelination. *J. Clin. Invest.* **125**, 2161–2170 (2015).

509. Cantoni, C. *et al.* TREM2 regulates microglial cell activation in response to demyelination in vivo. *Acta Neuropathol.* **129**, 429–447 (2015).

510. Horton, M. A. The αvβ3 integrin "vitronectin receptor". *Int. J. Biochem. Cell Biol.* **29**, 721–725 (1997).

511. Hynes, R. O. Integrins: versatility, modulation, and signaling in cell adhesion. *Cell* **69**, 11–25 (1992).

512. Felding-Habermann, B. & Cheresh, D. A. Vitronectin and its receptors. *Curr. Opin. Cell Biol.* **5**, 864–868 (1993).

513. Milner, R. & Campbell, I. L. The extracellular matrix and cytokines regulate microglial integrin expression and activation. *J. Immunol.* **170**, 3850–8 (2003).

514. Hanayama, R. *et al.* Identification of a factor that links apoptotic cells to phagocytes. *Nature* **417**, 182–187 (2002).

515. Hermann, P. *et al.* The vitronectin receptor and its associated CD47 molecule mediates proinflammatory cytokine synthesis in human monocytes by interaction with soluble CD23. *J. Cell Biol.* **144**, 767–75 (1999).

516. Milner, R. *et al.* Fibronectin- and Vitronectin-Induced Microglial Activation and Matrix Metalloproteinase-9 Expression Is Mediated by Integrins α5β1 and αvβ5. *J. Immunol.* **178**, 8158–8167 (2007).

517. Kim, H. *et al.* Potential role of fibronectin in microglia/macrophage activation following cryoinjury in the rat brain: An immunohistochemical study. *Brain Res.* **1502**, 11–19 (2013).

518. Neher, J. J. *et al.* Inhibition of Microglial Phagocytosis Is Sufficient To Prevent Inflammatory Neuronal Death. *J. Immunol.* **186**, 4973–4983 (2011).

519. Fricker, M. *et al.* MFG-E8 Mediates Primary Phagocytosis of Viable Neurons during Neuroinflammation. *J. Neurosci.* **32**, 2657–2666 (2012).

520. Hornik, T. C., Vilalta, A. & Brown, G. C. Activated microglia cause reversible apoptosis of pheochromocytoma cells , inducing their cell death by phagocytosis

Keywords. *J. Cell Sci.* **129**, 65–79 (2015).

521. Neniskyte, U., Vilalta, A. & Brown, G. C. Tumour necrosis factor alpha-induced neuronal loss is mediated by microglial phagocytosis. *FEBS Lett.* **588**, 2952–2956 (2014).

522. Neniskyte, U., Neher, J. J. & Brown, G. C. Neuronal death induced by nanomolar amyloid β is mediated by primary phagocytosis of neurons by microglia. *J. Biol. Chem.* **286**, 39904–39913 (2011).

523. Zhao, L. *et al.* Microglial phagocytosis of living photoreceptors contributes to inherited retinal degeneration. *EMBO Mol. Med.* **7**, 1179–97 (2015).

524. Siew, J. J. & Chern, Y. Microglial Lectins in Health and Neurological Diseases. *Front. Mol. Neurosci.* **11**, 158 (2018).

525. Crocker, P. R., Paulson, J. C. & Varki, A. Siglecs and their roles in the immune system. *Nat. Rev. Immunol.* **7**, 255–266 (2007).

526. Bornhöfft, K. F., Goldammer, T., Rebl, A. & Galuska, S. P. Siglecs: A journey through the evolution of sialic acid-binding immunoglobulin-type lectins. *Dev. Comp. Immunol.* **86**, 219–231 (2018).

527. Nitschke, L. The role of CD22 and other inhibitory co-receptors in B-cell activation. *Current Opinion in Immunology* **17**, 290–297 (2005).

528. Tedder, T. F., Poe, J. C. & Haas, K. M. CD22: A multifunctional receptor that regulates B lymphocyte survival and signal transduction. *Advances in Immunology* **88**, 1–50 (2005).

529. Lizcano, A. *et al.* Erythrocyte sialoglycoproteins engage Siglec-9 on neutrophils to suppress activation. *Blood* **129**, 3100–3110 (2017).

530. Nutku, E., Aizawa, H., Hudson, S. A. & Bochner, B. S. Ligation of Siglec-8: a selective mechanism for induction of human eosinophil apoptosis. *Blood* **101**, 5014–5020 (2003).

531. Griciuc, A. *et al.* Alzheimer's disease risk gene CD33 inhibits microglial uptake of amyloid beta. *Neuron* **78**, 631–43 (2013).

532. Hayakawa, T. *et al.* A human-specific gene in microglia. *Science* **309**, 1693 (2005).

533. Wang, Y. & Neumann, H. Alleviation of Neurotoxicity by Microglial Human Siglec-11. *J. Neurosci.* **30**, 3482–3488 (2010).

534. Cao, H. *et al. SIGLEC16* encodes a DAP12-associated receptor expressed in macrophages that evolved from its inhibitory counterpart *SIGLEC11* and has functional and non-functional alleles in humans. *Eur. J. Immunol.* **38**, 2303–2315 (2008).

535. Gautier, E. L. *et al.* Gene-expression profiles and transcriptional regulatory pathways that underlie the identity and diversity of mouse tissue macrophages. *Nat. Immunol.* **13**, 1118–1128 (2012).

536. Claude, J., Linnartz-Gerlach, B., Kudin, A. P., Kunz, W. S. & Neumann, H. Microglial CD33-Related Siglec-E Inhibits Neurotoxicity by Preventing the Phagocytosis-Associated Oxidative Burst. *J. Neurosci.* **33**, 18270–18276 (2013).

537. Kopatz, J. *et al.* Siglec-h on activated microglia for recognition and engulfment of glioma cells. *Glia* **61**, 1122–1133 (2013).

538. Barclay, A. N. & Brown, M. H. The SIRP family of receptors and immune regulation. *Nat. Rev. Immunol.* **6**, 457–464 (2006).

539. Zhang, H., Li, F., Yang, Y., Chen, J. & Hu, X. SIRP/CD47 signaling in neurological disorders. *Brain Res.* **1623**, 74–80 (2015).

540. Yamao, T. *et al.* Negative Regulation of Platelet Clearance and of the Macrophage Phagocytic Response by the Transmembrane Glycoprotein SHPS-1. *J. Biol. Chem.* **277**, 39833–39839 (2002).

541. Okazawa, H. *et al.* Negative regulation of phagocytosis in macrophages by the CD47-SHPS-1 system. *J. Immunol.* **174**, 2004–11 (2005).

542. Smith, R. E. *et al.* A novel MyD-1 (SIRP-1α) signaling pathway that inhibits LPS-induced TNFα production by monocytes. *Blood* **102**, 2532–2540 (2003).

543. Liu, Y. *et al.* Signal Regulatory Protein (SIRPα), a Cellular Ligand for CD47, Regulates Neutrophil Transmigration. *J. Biol. Chem.* **277**, 10028–10036 (2002).

544. Gitik, M., Liraz-Zaltsman, S., Oldenborg, P.-A., Reichert, F. & Rotshenker, S. Myelin down-regulates myelin phagocytosis by microglia and macrophages through

interactions between CD47 on myelin and SIRPα (signal regulatory protein-α) on phagocytes. *J. Neuroinflammation* **8**, 24 (2011).

545. Chang, G. H.-F., Barbaro, N. M. & Pieper, R. O. Phosphatidylserine-dependent phagocytosis of apoptotic glioma cells by normal human microglia, astrocytes, and glioma cells. *Neuro. Oncol.* **2**, 174–183 (2000).

546. Kulprathipanja, N. V & Kruse, C. A. Microglia phagocytose alloreactive CTL-damaged 9L gliosarcoma cells. *J. Neuroimmunol.* **153**, 76–82 (2004).

547. Galarneau, H., Villeneuve, J., Gowing, G., Julien, J.-P. & Vallieres, L. Increased Glioma Growth in Mice Depleted of Macrophages. *Cancer Res.* **67**, 8874–8881 (2007).

548. Mucke, L. & Selkoe, D. J. Neurotoxicity of amyloid β-protein: Synaptic and network dysfunction. *Cold Spring Harb. Perspect. Med.* **2**, a006338 (2012).

549. Ziegler-Waldkirch, S. & Meyer-Luehmann, M. The role of glial cells and synapse loss in mouse models of Alzheimer's disease. *Front. Cell. Neurosci.* **12**, 1–8 (2018).

550. Paresce, D. M., Ghosh, R. N. & Maxfield, F. R. Microglial cells internalize aggregates of the Alzheimer's disease amyloid beta-protein via a scavenger receptor. *Neuron* **17**, 553–65 (1996).

551. Liu, Y. *et al.* LPS receptor (CD14): a receptor for phagocytosis of Alzheimer's amyloid peptide. *Brain* **128**, 1778–1789 (2005).

552. Liu, S. *et al.* TLR2 Is a Primary Receptor for Alzheimer's Amyloid β Peptide To Trigger Neuroinflammatory Activation. *J. Immunol.* **188**, 1098–1107 (2012).

553. Stys, P. K., Zamponi, G. W., van Minnen, J. & Geurts, J. J. G. Will the real multiple sclerosis please stand up? *Nat. Rev. Neurosci.* **13**, 507–514 (2012).

554. Nielsen, H. H. *et al.* Enhanced Microglial Clearance of Myelin Debris in T Cell-Infiltrated Central Nervous System. *J. Neuropathol. Exp. Neurol.* **68**, 845–856 (2009).

555. Bogie, J. F., Stinissen, P., Hellings, N. & Hendriks, J. J. Myelin-phagocytosing macrophages modulate autoreactive T cell proliferation. *J. Neuroinflammation* **8**, 85 (2011).

556. Olah, M. *et al.* Identification of a microglia phenotype supportive of remyelination.

Glia **60**, 306–21 (2012).

557. Mariani, M. M. & Kielian, T. Microglia in infectious diseases of the central nervous system. *Journal of Neuroimmune Pharmacology* **4**, 448–461 (2009).

558. Iovino, F., Seinen, J., Henriques-Normark, B. & van Dijl, J. M. How Does Streptococcus pneumoniae Invade the Brain? *Trends Microbiol.* **24**, 307–315 (2016).

559. Diesselberg, C. *et al.* Activin A increases phagocytosis of Escherichia coli K1 by primary murine microglial cells activated by toll-like receptor agonists. *J. Neuroinflammation* **15**, 175 (2018).

560. Redlich, S., Ribes, S., Schütze, S., Czesnik, D. & Nau, R. Palmitoylethanolamide stimulates phagocytosis of Escherichia coli K1 and Streptococcus pneumoniae R6 by microglial cells. *J. Neuroimmunol.* **244**, 32–34 (2012).

561. Redlich, S., Ribes, S., Schütze, S. & Nau, R. Palmitoylethanolamide stimulates phagocytosis of Escherichia coli K1 by macrophages and increases the resistance of mice against infections. *J. Neuroinflammation* **11**, 108 (2014).

562. Alvis Miranda, H., Castellar-Leones, S. M., Elzain, M. A. & Moscote-Salazar, L. R. Brain abscess: Current management. *J. Neurosci. Rural Pract.* **4**, S67-81 (2013).

563. Prasad, K. N. *et al.* Analysis of microbial etiology and mortality in patients with brain abscess. *J. Infect.* **53**, 221–227 (2006).

564. Brook, I. Microbiology and antimicrobial treatment of orbital and intracranial complications of sinusitis in children and their management. *Int. J. Pediatr. Otorhinolaryngol.* **73**, 1183–1186 (2009).

565. Kielian, T., Mayes, P. & Kielian, M. Characterization of microglial responses to Staphylococcus aureus: effects on cytokine, costimulatory molecule, and Toll-like receptor expression. *J. Neuroimmunol.* **130**, 86–99 (2002).

566. Esen, N. & Kielian, T. Central role for MyD88 in the responses of microglia to pathogen-associated molecular patterns. *J. Immunol.* **176**, 6802–11 (2006).

567. Boekhoff, T. M. A. *et al.* Microglial Contribution to Secondary Injury Evaluated in a Large Animal Model of Human Spinal Cord Trauma. *J. Neurotrauma* **29**, 1000–1011 (2012).

568. Domínguez-Punaro, M. de la C. *et al.* In vitro characterization of the microglial inflammatory response to Streptococcus suis, an important emerging zoonotic agent of meningitis. *Infect. Immun.* **78**, 5074–85 (2010).

569. Wolf, S. A., Boddeke, H. W. G. M. & Kettenmann, H. Microglia in Physiology and Disease. *Annu. Rev. Physiol.* **79**, 619–643 (2017).

570. Graeber, M. B., Scheithauer, B. W. & Kreutzberg, G. W. Microglia in brain tumors. *Glia* **40**, 252–259 (2002).

571. Roesch, S., Rapp, C., Dettling, S. & Herold-Mende, C. When Immune Cells Turn Bad-Tumor-Associated Microglia/Macrophages in Glioma. *Int. J. Mol. Sci.* **19**, (2018).

572. Hou, Y. *et al.* Ageing as a risk factor for neurodegenerative disease. *Nat. Rev. Neurol.* **15**, 565–581 (2019).

573. Norden, D. M. & Godbout, J. P. Review: microglia of the aged brain: primed to be activated and resistant to regulation. *Neuropathol. Appl. Neurobiol.* **39**, 19–34 (2013).

574. Leza, J. C. *et al.* Inflammation in schizophrenia: A question of balance. *Neurosci. Biobehav. Rev.* **55**, 612–26 (2015).

575. Lee, E. & Chung, W. S. Glial control of synapse number in healthy and diseased brain. *Front. Cell. Neurosci.* **13**, 1–8 (2019).

576. Australia, D., Baker, S., Banerjee, S. & others. Alzheimer's Disease International: World Alzheimer Report 2019: Attitudes to Dementia. 2019. *Alzheimer's Dis. Int. London* 11–12 (2019).

577. Rajendran, L. & Paolicelli, R. C. Microglia-Mediated Synapse Loss in Alzheimer's Disease. *J. Neurosci.* **38**, 2911–2919 (2018).

578. Tomiyama, T. *et al.* A Mouse Model of Amyloid Oligomers: Their Contribution to Synaptic Alteration, Abnormal Tau Phosphorylation, Glial Activation, and Neuronal Loss In Vivo. *J. Neurosci.* **30**, 4845–4856 (2010).

579. Mitew, S., Kirkcaldie, M. T. K., Dickson, T. C. & Vickers, J. C. Altered synapses and gliotransmission in Alzheimer's disease and AD model mice. *Neurobiol. Aging* **34**, 2341–51 (2013).

580. Koffie, R. M. *et al.* Oligomeric amyloid associates with postsynaptic densities and

correlates with excitatory synapse loss near senile plaques. *Proc. Natl. Acad. Sci.* **106**, 4012–4017 (2009).

581. Decker, H. *et al.* N-Methyl-d-aspartate receptors are required for synaptic targeting of Alzheimer's toxic amyloid-β peptide oligomers. *J. Neurochem.* **115**, 1520–1529 (2010).

582. Capetillo-Zarate, E. *et al.* High-resolution 3D reconstruction reveals intra-synaptic amyloid fibrils. *Am. J. Pathol.* **179**, 2551–8 (2011).

583. Györffy, B. A. *et al.* Local apoptotic-like mechanisms underlie complementmediated synaptic pruning. *Proc. Natl. Acad. Sci. U. S. A.* **115**, 6303–6308 (2018).

584. Reichwald, J., Danner, S., Wiederhold, K.-H. & Staufenbiel, M. Expression of complement system components during aging and amyloid deposition in APP transgenic mice. *J. Neuroinflammation* **6**, 35 (2009).

585. Fonseca, M. I., Zhou, J., Botto, M. & Tenner, A. J. Absence of C1q Leads to Less Neuropathology in Transgenic Mouse Models of Alzheimer's Disease. *J. Neurosci.* **24**, 6457–6465 (2004).

586. Hong, S. *et al.* Complement and microglia mediate early synapse loss in Alzheimer mouse models. *Science (80-.).* **352**, 712–716 (2016).

587. Dejanovic, B. *et al.* Changes in the Synaptic Proteome in Tauopathy and Rescue of Tau-Induced Synapse Loss by C1q Antibodies. *Neuron* **100**, 1322-1336.e7 (2018).

588. Stephan, A. H. *et al.* A Dramatic Increase of C1q Protein in the CNS during Normal Aging. *J. Neurosci.* **33**, 13460–13474 (2013).

589. Petralia, R. S., Mattson, M. P. & Yao, P. J. Communication breakdown: the impact of ageing on synapse structure. *Ageing Res. Rev.* **14**, 31–42 (2014).

590. Guerreiro, R. & Bras, J. The age factor in Alzheimer's disease. *Genome Med.* **7**, 106 (2015).

591. Shi, Q. *et al.* Complement C3-Deficient Mice Fail to Display Age-Related Hippocampal Decline. *J. Neurosci.* **35**, 13029–13042 (2015).

592. Bellucci, A. *et al.* Review: Parkinson's disease: from synaptic loss to connectome dysfunction. *Neuropathol. Appl. Neurobiol.* **42**, 77–94 (2016).

593. Schulz-Schaeffer, W. J. The synaptic pathology of α-synuclein aggregation in dementia with Lewy bodies, Parkinson's disease and Parkinson's disease dementia. *Acta Neuropathol.* **120**, 131–143 (2010).

594. Austin, S. A., Floden, A. M., Murphy, E. J. & Combs, C. K. α-synuclein expression modulates microglial activation phenotype. *J. Neurosci.* **26**, 10558–10563 (2006).

595. Clare, R., King, V. G., Wirenfeldt, M. & Vinters, H. V. Synapse Loss in Dementias. *J. Neurosci. Res.* **88**, 2083 (2010).

596. Baker, M. *et al.* Mutations in progranulin cause tau-negative frontotemporal dementia linked to chromosome 17. *Nature* **442**, 916–919 (2006).

597. Paushter, D. H., Du, H., Feng, T. & Hu, F. The lysosomal function of progranulin, a guardian against neurodegeneration. *Acta Neuropathol.* **136**, 1–17 (2018).

598. Lui, H. *et al.* Progranulin Deficiency Promotes Circuit-Specific Synaptic Pruning by Microglia via Complement Activation. *Cell* **165**, 921–35 (2016).

599. Woollacott, I. O. C. & Rohrer, J. D. The clinical spectrum of sporadic and familial forms of frontotemporal dementia. *J. Neurochem.* **138**, 6–31 (2016).

600. Kirkbride, J. B. *et al.* Incidence of Schizophrenia and Other Psychoses in England, 1950–2009: A Systematic Review and Meta-Analyses. *PLoS One* **7**, e31660 (2012).

601. McGrath, J., Saha, S., Chant, D. & Welham, J. Schizophrenia: a concise overview of incidence, prevalence, and mortality. *Epidemiol. Rev.* **30**, 67–76 (2008).

602. Cannon, T. D. *et al.* Cortex mapping reveals regionally specific patterns of genetic and disease-specific gray-matter deficits in twins discordant for schizophrenia. *Proc. Natl. Acad. Sci. U. S. A.* **99**, 3228–3233 (2002).

603. Garey, L. J. *et al.* Reduced dendritic spine density on cerebral cortical pyramidal neurons in schizophrenia. *J. Neurol. Neurosurg. Psychiatry* **65**, 446–453 (1998).

604. Silva-Gómez, A. B., Rojas, D., Juárez, I. & Flores, G. Decreased dendritic spine density on prefrontal cortical and hippocampal pyramidal neurons in postweaning social isolation rats. *Brain Res.* **983**, 128–136 (2003).

605. Sekar, A. *et al.* Schizophrenia risk from complex variation of complement component 4. *Nature* **530**, 177–183 (2016).

606. Weinreb, R. N., Aung, T. & Medeiros, F. A. The pathophysiology and treatment of glaucoma: a review. *JAMA* **311**, 1901–11 (2014).

607. Howell, G. R. *et al.* Molecular clustering identifies complement and endothelin induction as early events in a mouse model of glaucoma. *J. Clin. Invest.* **121**, 1429–1444 (2011).

608. Williams, P. A. *et al.* Inhibition of the classical pathway of the complement cascade prevents early dendritic and synaptic degeneration in glaucoma. *Mol. Neurodegener.* **11**, 26 (2016).

609. Chancey, C., Grinev, A., Volkova, E. & Rios, M. The global ecology and epidemiology of West Nile virus. *Biomed Res. Int.* **2015**, 376230 (2015).

610. Vasek, M. J. *et al.* A complement–microglial axis drives synapse loss during virus-induced memory impairment. *Nature* **534**, 538–543 (2016).

611. Spiegel, R. & Horovitz, Y. Neurologic manifestations of West Nile virus infection. in *New Immunology Research Developments* 201–218 (2008).

612. Avdoshina, V., Bachis, A. & Mocchetti, I. Synaptic dysfunction in human immunodeficiency virus type-1-positive subjects: inflammation or impaired neuronal plasticity? *J. Intern. Med.* **273**, 454–65 (2013).

613. Zhang, X. *et al.* Extracellular ADP facilitates monocyte recruitment in bacterial infection via ERK signaling. *Cell. Mol. Immunol.* **15**, 58–73 (2018).

614. Blasi, E., Barluzzi, R., Bocchini, V., Mazzolla, R. & Bistoni, F. Immortalization of murine microglial cells by a v-raf / v-myc carrying retrovirus. *J. Neuroimmunol.* **27**, 229–237 (1990).

615. Pontén, J. & Macintyre, E. H. Long term culture of normal and neoplastic human glia. *Acta Pathol. Microbiol. Scand.* **74**, 465–486 (1968).

616. Sundström, C. & Nilsson, K. Establishment and characterization of a human histiocytic lymphoma cell line (U-937). *Int. J. Cancer* **17**, 565–577 (1976).

617. Greene, L. A. & Tischler, A. S. Establishment of a noradrenergic clonal line of rat adrenal pheochromocytoma cells which respond to nerve growth factor. *Proc. Natl. Acad. Sci.* **73**, 2424–2428 (1976).

618. Hornik, T. C., Neniskyte, U. & Brown, G. C. Inflammation induces multinucleation of Microglia via PKC inhibition of cytokinesis, generating highly phagocytic multinucleated giant cells. *J. Neurochem.* **128**, 650–661 (2014).

619. Kinsner, A. *et al.* Inflammatory neurodegeneration induced by lipoteichoic acid from Staphylococcus aureus is mediated by glia activation, nitrosative and oxidative stress, and caspase activation. *J. Neurochem.* **95**, 1132–1143 (2005).

620. Dunkley, P. R., Jarvie, P. E. & Robinson, P. J. A rapid percoll gradient procedure for preparation of synaptosomes. *Nat. Protoc.* **3**, 1718–1728 (2008).

621. Daniel, J. a, Malladi, C. S., Kettle, E., McCluskey, A. & Robinson, P. J. Analysis of synaptic vesicle endocytosis in synaptosomes by high-content screening. *Nat. Protoc.* **7**, 1439–55 (2012).

622. Tinevez, J.-Y. *et al.* TrackMate: An open and extensible platform for single-particle tracking. *Methods* **115**, 80–90 (2017).

623. Sezonov, G., Joseleau-Petit, D. & D'Ari, R. Escherichia coli physiology in Luria-Bertani broth. *J. Bacteriol.* **189**, 8746–8749 (2007).

624. Deczkowska, A. *et al.* Perspective Disease-Associated Microglia : A Universal Immune Sensor of Neurodegeneration. *Cell* **173**, 1073–1081 (2018).

625. Danilczyk, U. G., Cohen-Doyle, M. F. & Williams, D. B. Functional relationship between calreticulin, calnexin, and the endoplasmic reticulum luminal domain of calnexin. *J. Biol. Chem.* **275**, 13089–97 (2000).

626. Pandya, U. *et al.* The Biophysical Interaction of the Danger-Associated Molecular Pattern (DAMP) Calreticulin with the Pattern-Associated Molecular Pattern (PAMP) Lipopolysaccharide. *Int. J. Mol. Sci.* **20**, 408 (2019).

627. Bajor, A. *et al.* Modulatory role of calreticulin as chaperokine for dendritic cell-based immunotherapy. *Clin. Exp. Immunol.* **165**, 220–234 (2011).

628. Bak, S. P., Amiel, E., Walters, J. J. & Berwin, B. Calreticulin requires an ancillary adjuvant for the induction of efficient cytotoxic T cell responses. *Mol. Immunol.* **45**, 1414–23 (2008).

629. Ho, M. K. & Springer, T. A. Mac-2, a novel 32,000 Mr mouse macrophage

subpopulation-specific antigen defined by monoclonal antibodies. *J. Immunol.* **128**, 1221–8 (1982).

630. Burguillos, M. A. *et al.* Microglia-Secreted Galectin-3 Acts as a Toll-like Receptor 4 Ligand and Contributes to Microglial Article Acts as a Toll-like Receptor 4 Ligand and Contributes to Microglial Activation. *CellReports* **10**, 1626–1638 (2015).

631. Mey, A., Leffler, H., Hmama, Z., Normier, G. & Revillard, J. P. The animal lectin galectin-3 interacts with bacterial lipopolysaccharides via two independent sites. *J. Immunol.* **156**, 1572–7 (1996).

632. Mahley, R. W. Central Nervous System Lipoproteins: ApoE and Regulation of Cholesterol Metabolism. *Arterioscler. Thromb. Vasc. Biol.* **36**, 1305–15 (2016).

633. Boyles, J. K., Pitas, R. E., Wilson, E., Mahley, R. W. & Taylor, J. M. Apolipoprotein E associated with astrocytic glia of the central nervous system and with nonmyelinating glia of the peripheral nervous system. *J. Clin. Invest.* **76**, 1501–1513 (1985).

634. Nakai, M., Kawamata, T., Taniguchi, T., Maeda, K. & Tanaka, C. Expression of apolipoprotein E mRNA in rat microglia. *Neurosci. Lett.* **211**, 41–44 (1996).

635. Polazzi, E. *et al.* Neuronal Regulation of Neuroprotective Microglial Apolipoprotein E Secretion in Rat In Vitro Models of Brain Pathophysiology. *J. Neuropathol. Exp. Neurol.* **74**, 818–834 (2015).

636. Mahley, R. W. & Rall, S. C. Apolipoprotein E: Far More Than a Lipid Transport Protein. *Annu. Rev. Genomics Hum. Genet.* **1**, 507–537 (2000).

637. Ophir, G. *et al.* Human apoE3 but not apoE4 rescues impaired astrocyte activation in apoE null mice. *Neurobiol. Dis.* **12**, 56–64 (2003).

638. Kober, D. L. & Brett, T. J. TREM2-Ligand Interactions in Health and Disease. *J. Mol. Biol.* **429**, 1607–1629 (2017).

639. Rensen, P. C. *et al.* Human recombinant apolipoprotein E redirects lipopolysaccharide from Kupffer cells to liver parenchymal cells in rats In vivo. *J. Clin. Invest.* **99**, 2438–2445 (1997).

640. Liu, C.-C., Liu, C.-C., Kanekiyo, T., Xu, H. & Bu, G. Apolipoprotein E and Alzheimer

disease: risk, mechanisms and therapy. *Nat. Rev. Neurol.* **9**, 106–18 (2013).

641. Brothers, H. M., Gosztyla, M. L. & Robinson, S. R. The Physiological Roles of Amyloid-β Peptide Hint at New Ways to Treat Alzheimer's Disease. *Front. Aging Neurosci.* **10**, 118 (2018).

642. Gosztyla, M. L., Brothers, H. M. & Robinson, S. R. Alzheimer's Amyloid-β is an Antimicrobial Peptide: A Review of the Evidence. *J. Alzheimer's Dis.* **62**, 1495–1506 (2018).

643. Haass, C., Hung, A. Y. & Selkoe, D. J. Processing of beta-amyloid precursor protein in microglia and astrocytes favors an internal localization over constitutive secretion. *J. Neurosci.* **11**, 3783–93 (1991).

644. Sheng, J. G. *et al.* Lipopolysaccharide-induced-neuroinflammation increases intracellular accumulation of amyloid precursor protein and amyloid β peptide in APPswe transgenic mice. *Neurobiol. Dis.* **14**, 133–145 (2003).

645. Kumar, D. K. V. *et al.* Amyloid-β peptide protects against microbial infection in mouse and worm models of Alzheimer's disease. *Sci. Transl. Med.* **8**, 340–72 (2016).

646. Li, Y. *et al.* Galectin-3 Is a Negative Regulator of Lipopolysaccharide-Mediated Inflammation. *J. Immunol.* **181**, 2781–2789 (2008).

647. Miksa, M., Komura, H., Wu, R., Shah, K. G. & Wang, P. A novel method to determine the engulfment of apoptotic cells by macrophages using pHrodo succinimidyl ester. *J. Immunol. Methods* **342**, 71–77 (2009).

648. Ting-Beall, H. P., Lee, A. S. & Hochmuth, R. M. Effect of cytochalasin D on the mechanical properties and morphology of passive human neutrophils. *Ann. Biomed. Eng.* **23**, 666–71

649. Sim, R. B. *et al.* Interaction of C1q and the Collectins with the Potential Receptors Calreticulin (cClqR/Collectin Receptor) and Megalin. *Immunobiology* **199**, 208–224 (1998).

650. Martins, I. *et al.* Surface-exposed calreticulin in the interaction between dying cells and phagocytes. *Ann. N. Y. Acad. Sci.* **1209**, 77–82 (2010).

651. Gray, A. J. *et al.* The mitogenic effects of the Bβ chain of fibrinogen are mediated

through cell surface calreticulin. *J. Biol. Chem.* **270**, 26602–26606 (1995).

652. White, T. K., Zhu, Q. & Tanzer, M. L. Cell Surface Calreticulin Is a Putative Mannoside Lectin Which Triggers Mouse Melanoma Cell Spreading. *J. Biol. Chem.* **270**, 15926–15929 (1995).

653. van den Berg, R. H., Faber-Krol, M., van Es, L. A. & Daha, M. R. Regulation of the function of the first component of complement by human C1q receptor. *Eur. J. Immunol.* **25**, 2206–2210 (1995).

654. Zhang, Y. *et al.* Oxidative Stress–Induced Calreticulin Expression and Translocation: New Insights into the Destruction of Melanocytes. *J. Invest. Dermatol.* **134**, 183–191 (2014).

655. Obeid, M. *et al.* Calreticulin exposure dictates the immunogenicity of cancer cell death. *Nat. Med.* **13**, 54–61 (2007).

656. Obeid, M. *et al.* Calreticulin exposure is required for the immunogenicity of γ-irradiation and UVC light-induced apoptosis. *Cell Death Differ.* **14**, 1848–1850 (2007).

657. Goicoechea, S., Pallero, M. A., Eggleton, P., Michalak, M. & Murphy-Ullrich, J. E. The anti-adhesive activity of thrombospondin is mediated by the N-terminal domain of cell surface calreticulin. *J. Biol. Chem.* **277**, 37219–28 (2002).

658. Wiersma, V. R., Michalak, M., Abdullah, T. M., Bremer, E. & Eggleton, P. Mechanisms of translocation of ER chaperones to the cell surface and immunomodulatory roles in cancer and autoimmunity. **5**, 1–14 (2015).

659. Krysko, D. V., Ravichandran, K. S. & Vandenabeele, P. Macrophages regulate the clearance of living cells by calreticulin. *Nat. Commun.* **9**, 4644 (2018).

660. Ni, M. *et al.* Serum Levels of Calreticulin in Correlation with Disease Activity in Patients with Rheumatoid Arthritis. *J. Clin. Immunol.* **33**, 947–953 (2013).

661. Kapoor, M. et al. Interactions of Substrate with Calreticulin, an Endoplasmic Reticulum Chaperone. **278**, 6194–6200 (2003).

662. Orr, A. W. *et al.* Low density lipoprotein receptor-related protein is a calreticulin coreceptor that signals focal adhesion disassembly. *J. Cell Biol.* **161**, 1179–89 (2003).

663. Mantuano, E. *et al.* LDL receptor-related protein-1 regulates NFκB and microRNA-155 in macrophages to control the inflammatory response. *Proc. Natl. Acad. Sci. U. S. A.* **113**, 1369–74 (2016).

664. Yang, D., Han, Z. & Oppenheim, J. J. Alarmins and immunity. *Immunol. Rev.* **280**, 41–56 (2017).

665. Schcolnik-Cabrera, A. *et al.* Calreticulin in phagocytosis and cancer: opposite roles in immune response outcomes. *Apoptosis* **24**, 245–255 (2019).

666. Wang, J., Gao, Z. P., Qin, S., Liu, C. B. & Zou, L. L. Calreticulin is an effective immunologic adjuvant to tumor-associated antigens. *Exp. Ther. Med.* **14**, 3399–3406 (2017).

667. Fermino, M. L. *et al.* LPS-Induced Galectin-3 Oligomerization Results in Enhancement of Neutrophil Activation. *PLoS One* **6**, e26004 (2011).

668. Gupta, S. K., Masinick, S., Garrett, M. & Hazlett, L. D. Pseudomonas aeruginosa lipopolysaccharide binds galectin-3 and other human corneal epithelial proteins. *Infect. Immun.* **65**, 2747–53 (1997).

669. Zhang, W. *et al.* Discovery of Mer Specific Tyrosine Kinase Inhibitors for the Treatment and Prevention of Thrombosis. *J. Med. Chem.* **56**, 9693–9700 (2013).

670. Christoph, S. *et al.* UNC569, a Novel Small-Molecule Mer Inhibitor with Efficacy against Acute Lymphoblastic Leukemia *In Vitro* and *In Vivo*. *Mol. Cancer Ther.* **12**, 2367–2377 (2013).

671. Graham, D. K., Dawson, T. L., Mullaney, D. L., Snodgrass, H. R. & Earp, H. S. Cloning and mRNA expression analysis of a novel human protooncogene, c-mer. *Cell Growth Differ.* **5**, 647–57 (1994).

672. Behrens, E. M. *et al.* The mer receptor tyrosine kinase: expression and function suggest a role in innate immunity. *Eur. J. Immunol.* **33**, 2160–2167 (2003).

673. Williams, B. J. C., Craven, R. R., Earp, H. S., Kawula, T. H. & Matsushima, G. K. TAM receptors are dispensable in the phagocytosis and killing of bacteria. *Cell. Immunol.* **259**, 128–134 (2009).

674. Dong, R. *et al.* Galectin-3 as a novel biomarker for disease diagnosis and a target for

therapy (Review). *Int. J. Mol. Med.* **41**, 599–614 (2018).

675. Yip, P. K. *et al.* Galectin-3 released in response to traumatic brain injury acts as an alarmin orchestrating brain immune response and promoting neurodegeneration. *Sci. Rep.* **7**, 1–13 (2017).

676. Park, A.-M., Hagiwara, S., Hsu, D. K., Liu, F.-T. & Yoshie, O. Galectin-3 Plays an Important Role in Innate Immunity to Gastric Infection by Helicobacter pylori. *Infect. Immun.* **84**, 1184–1193 (2016).

677. Farnworth, S. L. *et al.* Galectin-3 Reduces the Severity of Pneumococcal Pneumonia by Augmenting Neutrophil Function. *Am. J. Pathol.* **172**, 395–405 (2008).

678. Van Oosten, M. *et al.* Apolipoprotein E Protects Against Bacterial Lipopolysaccharide-induced Lethality. *J. Biol. Chem.* **276**, 8820–8824 (2001).

679. Main, B. S. *et al.* Apolipoprotein E4 impairs spontaneous blood brain barrier repair following traumatic brain injury. *Mol. Neurodegener.* **13**, 17 (2018).

680. Pane, K. *et al.* A new cryptic cationic antimicrobial peptide from human apolipoprotein E with antibacterial activity and immunomodulatory effects on human cells. *FEBS J.* **283**, 2115–2131 (2016).

681. Brown, G. C. The endotoxin hypothesis of neurodegeneration. *J. Neuroinflammation* **16**, 1–10 (2019).

682. Emery, D. C. *et al.* 16S rRNA Next Generation Sequencing Analysis Shows Bacteria in Alzheimer ' s Post-Mortem Brain. **9**, 1–13 (2017).

683. Ilievski, V. *et al.* Chronic oral application of a periodontal pathogen results in brain inflammation, neurodegeneration and amyloid beta production in wild type mice. *PLoS One* **13**, e0204941 (2018).

684. Zhan, X. *et al.* Gram-negative bacterial molecules associate with Alzheimer disease pathology. *Neurology* **87**, 2324–2332 (2016).

685. Murphy, M. P., LeVine, H. & III. Alzheimer's disease and the amyloid-beta peptide. *J. Alzheimers. Dis.* **19**, 311–23 (2010).

686. Bitting, L., Naidu, A., Cordell, B. & Murphy, G. M. β-Amyloid Peptide Secretion by a Microglial Cell Line Is Induced by β-Amyloid-(25–35) and Lipopolysaccharide. *J.*

Biol. Chem. **271**, 16084–16089 (1996).

687. Mönning, U. *et al.* Synthesis and secretion of Alzheimer amyloid beta A4 precursor protein by stimulated human peripheral blood leucocytes. *FEBS Lett.* **277**, 261–6 (1990).

688. Spitzer, P. *et al.* Phagocytosis and LPS alter the maturation state of β-amyloid precursor protein and induce different Aβ peptide release signatures in human mononuclear phagocytes. *J. Neuroinflammation* **7**, 59 (2010).

689. Pulze, L. *et al.* NET amyloidogenic backbone in human activated neutrophils. *Clin. Exp. Immunol.* **183**, 469–79 (2016).

690. Gosselin, D. *et al.* An environment-dependent transcriptional network specifies human microglia identity. *Science* **356**, (2017).

691. Rothaug, M., Becker-Pauly, C. & Rose-John, S. The role of interleukin-6 signaling in nervous tissue. *Biochimica et Biophysica Acta - Molecular Cell Research* **1863**, 1218–1227 (2016).

692. von Kügelgen, I. & Hoffmann, K. Pharmacology and structure of P2Y receptors. *Neuropharmacology* **104**, 50–61 (2016).

693. von Kugelgen, I. & Harden, T. K. Molecular Pharmacology, Physiology, and Structure of the P2Y Receptors. in *Advances in Pharmacology* **61**, 373–415 (2011).

694. Robaye, B., Boeynaems, J. M. & Communi, D. Slow desensitization of the human P2Y6 receptor. *Eur. J. Pharmacol.* **329**, 231–236 (1997).

695. Bian, J. *et al.* P2Y6 Receptor-Mediated Spinal Microglial Activation in Neuropathic Pain. *Pain Res. Manag.* **2019**, 1–10 (2019).

696. Zhang, Z. *et al.* P2Y6 Agonist Uridine 5'-Diphosphate Promotes Host Defense against Bacterial Infection via Monocyte Chemoattractant Protein-1-Mediated Monocytes/Macrophages Recruitment. *J. Immunol.* **186**, 5376–5387 (2011).

697. Takayama, F., Hayashi, Y., Wu, Z., Liu, Y. & Nakanishi, H. Diurnal dynamic behavior of microglia in response to infected bacteria through the UDP-P2Y6 receptor system. *Sci. Rep.* **6**, 30006 (2016).

698. Mildner, A., Huang, H., Radke, J., Stenzel, W. & Priller, J. P2Y $_{12}$ receptor is

expressed on human microglia under physiological conditions throughout development and is sensitive to neuroinflammatory diseases. *Glia* **65**, 375–387 (2017).

699. Honda, S. *et al.* Extracellular ATP or ADP induce chemotaxis of cultured microglia through Gi/o-coupled P2Y receptors. *J. Neurosci.* **21**, 1975–1982 (2001).

700. De Simone, R. *et al.* TGF-β and LPS modulate ADP-induced migration of microglial cells through P2Y1 and P2Y12 receptor expression. *J. Neurochem.* **115**, 450–459 (2010).

701. Mempin, R. *et al.* Release of extracellular ATP by bacteria during growth. *BMC Microbiol.* **13**, 301 (2013).

702. Gounaris, K. Nucleotidase cascades are catalyzed by secreted proteins of the parasitic nematode Trichinella spiralis. *Infect. Immun.* **70**, 4917–24 (2002).

703. White, C. & McGeown, J. G. Carbachol triggers RyR-dependent Ca(2+) release via activation of IP(3) receptors in isolated rat gastric myocytes. *J. Physiol.* **542**, 725–33 (2002).

704. Gajardo-Gómez, R., Labra, V. C. & Orellana, J. A. Connexins and Pannexins: New Insights into Microglial Functions and Dysfunctions. *Front. Mol. Neurosci.* **9**, 86 (2016).

705. Giaume, C., Leybaert, L., Naus, C. C. & Saez, J. C. Connexin and pannexin hemichannels in brain glial cells: Properties, pharmacology, and roles. *Front. Pharmacol.* **4**, 1–17 (2013).

706. Krick, S. *et al.* Dual Oxidase 2 (Duox2) Regulates Pannexin 1-mediated ATP Release in Primary Human Airway Epithelial Cells via Changes in Intracellular pH and Not H2O2 Production. *J. Biol. Chem.* **291**, 6423–6432 (2016).

707. D'Ambrosi, N., Iafrate, M., Saba, E., Rosa, P. & Volonté, C. Comparative analysis of P2Y4 and P2Y6 receptor architecture in native and transfected neuronal systems. *Biochim. Biophys. Acta - Biomembr.* **1768**, 1592–1599 (2007).

708. Garcia, R. A. *et al.* P2Y6 receptor potentiates pro-inflammatory responses in macrophages and exhibits differential roles in atherosclerotic lesion development. *PLoS One* **9**, (2014).

709. Haynes, S. E. *et al.* The P2Y12 receptor regulates microglial activation by extracellular nucleotides. *Nat. Neurosci.* **9**, 1512–1519 (2006).

710. Madry, C. *et al.* Microglial Ramification, Surveillance, and Interleukin-1β Release Are Regulated by the Two-Pore Domain K+ Channel THIK-1. *Neuron* **97**, 299-312.e6 (2018).

711. Qin, J. *et al.* TLR-Activated Gap Junction Channels Protect Mice against Bacterial Infection through Extracellular UDP Release. *J. Immunol.* **196**, 1790–1798 (2016).

712. Sil, P. *et al.* P2Y6 Receptor Antagonist MRS2578 Inhibits Neutrophil Activation and Aggregated Neutrophil Extracellular Trap Formation Induced by Gout-Associated Monosodium Urate Crystals. *J. Immunol.* **198**, 428–442 (2017).

713. Nakano, M. *et al.* UDP/P2Y6 receptor signaling regulates IgE-dependent degranulation in human basophils. *Allergol. Int.* **66**, 574–580 (2017).

714. Hansen, A. *et al.* The P2Y6 Receptor Mediates Clostridium difficile Toxin-Induced CXCL8/IL-8 Production and Intestinal Epithelial Barrier Dysfunction. *PLoS One* **8**, e81491 (2013).

715. Mamedova, L. K., Joshi, B. V, Gao, Z. G., Von Kügelgen, I. & Jacobson, K. A. Diisothiocyanate derivatives as potent, insurmountable antagonists of P2Y6 nucleotide receptors. *Biochem. Pharmacol.* **67**, 1763–1770 (2004).

716. Ziegner, U. H. M. *et al.* Progressive Neurodegeneration in Patients with Primary Immunodeficiency Disease on IVIG Treatment. *Clin. Immunol.* **102**, 19–24 (2002).

717. D'hondt, C., Ponsaerts, R., De Smedt, H., Bultynck, G. & Himpens, B. Pannexins, distant relatives of the connexin family with specific cellular functions? *BioEssays* **31**, 953–974 (2009).

718. Mikolajewicz, N., Zimmermann, E. A., Willie, B. M. & Komarova, S. V. Mechanically stimulated ATP release from murine bone cells is regulated by a balance of injury and repair. *Elife* **7**, e37812 (2018).

719. Sackin, H. Mechanosensitive Channels. *Annu. Rev. Physiol.* **57**, 333–353 (1995).

720. Velasco-Estevez, M. *et al.* Infection Augments Expression of Mechanosensing Piezo1 Channels in Amyloid Plaque-Reactive Astrocytes. *Front. Aging Neurosci.* **10**, 332

(2018).

721. Bavi, N. *et al.* Principles of Mechanosensing at the Membrane Interface. in 85–119 (Springer, Singapore, 2017). doi:10.1007/978-981-10-6244-5_4

722. Cox, C. D. *et al.* Removal of the mechanoprotective influence of the cytoskeleton reveals PIEZO1 is gated by bilayer tension. *Nat. Commun.* **7**, 10366 (2016).

723. Cinar, E. *et al.* Piezo1 regulates mechanotransductive release of ATP from human RBCs. *Proc. Natl. Acad. Sci. U. S. A.* **112**, 11783–8 (2015).

724. Miyamoto, T. *et al.* Functional Role for Piezo1 in Stretch-evoked Ca^{2+} Influx and ATP Release in Urothelial Cell Cultures. *J. Biol. Chem.* **289**, 16565–16575 (2014).

725. Ayna, G. *et al.* ATP release from dying autophagic cells and their phagocytosis are crucial for inflammasome activation in macrophages. *PLoS One* **7**, e40069 (2012).

726. Tanaka, K., Choi, J., Cao, Y. & Stacey, G. Extracellular ATP acts as a damage-associated molecular pattern (DAMP) signal in plants. *Front. Plant Sci.* **5**, 446 (2014).

727. Iwase, T. *et al.* Isolation and Identification of ATP-Secreting Bacteria from Mice and Humans. *J. Clin. Microbiol.* **48**, 1949–1951 (2010).

728. Chung, W.-S. *et al.* Novel allele-dependent role for APOE in controlling the rate of synapse pruning by astrocytes. *Proc. Natl. Acad. Sci.* **113**, 10186–10191 (2016).

729. Yamada, K. Extracellular Tau and Its Potential Role in the Propagation of Tau Pathology. *Front. Neurosci.* **11**, 667 (2017).

730. Olsson, A. *et al.* Simultaneous measurement of β-amyloid(1-42), total Tau, and phosphorylated Tau (Thr181) in cerebrospinal fluid by the xMAP technology. *Clin. Chem.* **51**, 336–345 (2005).

731. Blennow, K. *et al.* tau protein in cerebrospinal fluid - A biochemical marker for axonal degeneration in Alzheimer disease? *Mol. Chem. Neuropathol.* **26**, 231–245 (1995).

732. Pankratov, Y., Lalo, U., Verkhratsky, A. & North, R. A. Vesicular release of ATP at central synapses. *Pflugers Arch. Eur. J. Physiol.* **452**, 589–597 (2006).

733. Morgan, I. G. Synaptosomes and cell separation. *Neuroscience* **1**, 159–165 (1976).

734. Whittaker, V. P. Thirty years of synaptosome research. *J. Neurocytol.* **22**, 735–42

(1993).

735. Polosa, P. L. & Attardi, G. Distinctive pattern and translational control of mitochondrial protein synthesis in rat brain synaptic endings. *J. Biol. Chem.* **266**, 10011–7 (1991).

736. Dunkley, P. R. & Robinson, P. J. Depolarization-dependent protein phosphorylation in synaptosomes: mechanisms and significance. *Prog. Brain Res.* **69**, 273–93 (1986).

737. Ashton, A. C. & Ushkaryov, Y. A. Properties of synaptic vesicle pools in mature central nerve terminals. *J. Biol. Chem.* **280**, 37278–88 (2005).

738. Byun, Y. G. & Chung, W. S. A novel in vitro live-imaging assay of astrocyte-mediated phagocytosis using pH indicator-conjugated synaptosomes. *J. Vis. Exp.* **2018**, (2018).

739. Byun, Y. G. & Chung, W.-S. In Vitro Engulfment Assay to Measure Phagocytic Activity of Astrocytes Using Synaptosomes. in 155–168 (Humana Press, New York, NY, 2019). doi:10.1007/978-1-4939-9068-9_11

740. Abud, E. M. *et al.* iPSC-Derived Human Microglia-like Cells to Study Neurological Diseases. *Neuron* **94**, 278-293.e9 (2017).

741. Keaney, J., Gasser, J., Gillet, G., Scholz, D. & Kadiu, I. Inhibition of Bruton's Tyrosine Kinase Modulates Microglial Phagocytosis: Therapeutic Implications for Alzheimer's Disease. *J. Neuroimmune Pharmacol.* **14**, 448–461 (2019).

742. Chung, W.-S. *et al.* Astrocytes mediate synapse elimination through MEGF10 and MERTK pathways. *Nature* **504**, 394–400 (2013).

743. Dejanovic, B. *et al.* Changes in the Synaptic Proteome in Tauopathy and Rescue of Tau-Induced Synapse Loss by C1q Antibodies. *Neuron* **100**, 1322-1336.e7 (2018).

744. Gylys, K. H., Fein, J. A., Yang, F. & Cole, G. M. Enrichment of presynaptic and postsynaptic markers by size-based gating analysis of synaptosome preparations from rat and human cortex. *Cytometry* **60A**, 90–96 (2004).

745. Dodd, P. R. *et al.* Optimization of freezing, storage, and thawing conditions for the preparation of metabolically active synaptosomes from frozen rat and human brain. *Neurochem. Pathol.* **4**, 177–98 (1986).

746. Pereira, M. E. A. A rapid and sensitive assay for neuraminidase using peanut lectin

hemagglutination: Application to Vibrio cholera and Trypanosoma cruzi. *J. Immunol. Methods* **63**, 25–34 (1983).

747. Eyo, U. B. *et al.* P2Y12R-Dependent Translocation Mechanisms Gate the Changing Microglial Landscape. *Cell Rep.* **23**, 959–966 (2018).

748. Sheppard, O., Coleman, M. P. & Durrant, C. S. Lipopolysaccharide-induced neuroinflammation induces presynaptic disruption through a direct action on brain tissue involving microglia-derived interleukin 1 beta. *J. Neuroinflammation* **16**, 1–13 (2019).

749. Grabrucker, A., Vaida, B., Bockmann, J. & Boeckers, T. M. Synaptogenesis of hippocampal neurons in primary cell culture. *Cell Tissue Res.* **338**, 333–341 (2009).

750. Sellgren, C. M. *et al.* Increased synapse elimination by microglia in schizophrenia patient-derived models of synaptic pruning. *Nat. Neurosci.* **22**, 374–385 (2019).

751. Cohen, J., Wilkin, G. P. & Wilkin, G. P. *Neural cell culture : a practical approach*. (IRL Press at Oxford University Press, 1995).

752. Thiel, G. Synapsin I, Synapsin II, and Synaptophysin: Marker Proteins of Synaptic Vesicles. *Brain Pathol.* **3**, 87–95 (1993).

753. Kolos, Y. A., Grigoriyev, I. P. & Korzhevskyi, D. E. A synaptic marker synaptophysin. *Morfologiia (Saint Petersburg, Russia)* **147**, 78–82 (2015).

754. Linnartz-Gerlach, B., Schuy, C., Shahraz, A., Tenner, A. J. & Neumann, H. Sialylation of neurites inhibits complement-mediated macrophage removal in a human macrophage-neuron Co-Culture System. *Glia* (2015). doi:10.1002/glia.22901

755. Gratuze, M., Leyns, C. E. G. & Holtzman, D. M. New insights into the role of TREM2 in Alzheimer's disease. *Mol. Neurodegener.* **13**, 66 (2018).

756. Duus, K. *et al.* Direct interaction between CD91 and C1q. *FEBS J.* **277**, 3526–3537 (2010).

757. Mesaeli, N. *et al.* Calreticulin is essential for cardiac development. *J. Cell Biol.* **144**, 857–68 (1999).

758. Herz, J., Clouthier, D. E. & Hammer, R. E. LDL receptor-related protein internalizes and degrades uPA-PAI-1 complexes and is essential for embryo implantation. *Cell* **71**,

411–21 (1992).

759. Burke, S. N. & Barnes, C. A. Senescent synapses and hippocampal circuit dynamics. *Trends Neurosci.* **33**, 153–61 (2010).

760. Yamamoto, T., Choi, H. W. & Ryan, R. O. Apolipoprotein E isoform-specific binding to the low-density lipoprotein receptor. *Anal. Biochem.* **372**, 222–6 (2008).

761. Brion, J.-P. Neurofibrillary Tangles and Alzheimer's Disease. *Eur. Neurol.* **40**, 130–140 (1998).

762. Sebastián-Serrano, Á., de Diego-García, L. & Díaz-Hernández, M. The Neurotoxic Role of Extracellular Tau Protein. *Int. J. Mol. Sci.* **19**, (2018).

763. Sokolow, S. *et al.* Pre-synaptic C-terminal truncated tau is released from cortical synapses in Alzheimer's disease. *J. Neurochem.* **133**, 368–379 (2015).

764. Karch, C. M., Jeng, A. T. & Goate, A. M. Extracellular Tau levels are influenced by variability in Tau that is associated with tauopathies. *J. Biol. Chem.* **287**, 42751–62 (2012).

765. Blennow, K. & Zetterberg, H. The past and the future of Alzheimer's disease CSF biomarkers—a journey toward validated biochemical tests covering the whole spectrum of molecular events. *Front. Neurosci.* **9**, 345 (2015).

766. Sperlágh, B. & Vizi, E. S. The role of extracellular adenosine in chemical neurotransmission in the hippocampus and Basal Ganglia: pharmacological and clinical aspects. *Curr. Top. Med. Chem.* **11**, 1034–46 (2011).

767. Dunwiddie, T. V. & Hoffer, B. J. Adenine nucleotides and synaptic transmission in the in vitro rat hippocampus. *Br. J. Pharmacol.* **69**, 59–68 (1980).

768. Burnstock, G. Physiology and Pathophysiology of Purinergic Neurotransmission. *Physiol. Rev.* **87**, 659–797 (2007).

769. Lalo, U. *et al.* Exocytosis of ATP From Astrocytes Modulates Phasic and Tonic Inhibition in the Neocortex. *PLoS Biol.* **12**, e1001747 (2014).

770. Lalo, U., Palygin, O., Verkhratsky, A., Grant, S. G. N. & Pankratov, Y. ATP from synaptic terminals and astrocytes regulates NMDA receptors and synaptic plasticity through PSD-95 multi-protein complex. *Sci. Rep.* **6**, 33609 (2016).

771. Boué-Grabot, E. & Pankratov, Y. Modulation of Central Synapses by Astrocyte-Released ATP and Postsynaptic P2X Receptors. *Neural Plast.* **2017**, 1–11 (2017).

772. Guzman, S. J. & Gerevich, Z. P2Y Receptors in Synaptic Transmission and Plasticity: Therapeutic Potential in Cognitive Dysfunction. *Neural Plast.* **2016**, 1–12 (2016).

773. Abbracchio, M. P. & Ceruti, S. Roles of P2 receptors in glial cells: focus on astrocytes. *Purinergic Signal.* **2**, 595–604 (2006).

774. Khakh, B. S. & North, R. A. Neuromodulation by Extracellular ATP and P2X Receptors in the CNS. *Neuron* **76**, 51–69 (2012).

775. Liu, M. & Bing, G. Lipopolysaccharide animal models for Parkinson's disease. *Parkinsons. Dis.* **2011**, 327089 (2011).

776. Nava Catorce, M. & Gevorkian, G. LPS-induced Murine Neuroinflammation Model: Main Features and Suitability for Pre-clinical Assessment of Nutraceuticals. *Curr. Neuropharmacol.* **14**, 155–164 (2016).

777. Surmeier, D. J. Determinants of dopaminergic neuron loss in Parkinson's disease. *FEBS J.* **285**, 3657–3668 (2018).

778. Reeve, A. K. *et al.* Mitochondrial dysfunction within the synapses of substantia nigra neurons in Parkinson's disease. *npj Park. Dis.* **4**, 9 (2018).

779. Henstridge, C. M., Tzioras, M. & Paolicelli, R. C. Glial Contribution to Excitatory and Inhibitory Synapse Loss in Neurodegeneration. *Front. Cell. Neurosci.* **13**, 63 (2019).

780. Hilton, K. J., Cunningham, C., Reynolds, R. A. & Perry, V. H. Early Hippocampal Synaptic Loss Precedes Neuronal Loss and Associates with Early Behavioural Deficits in Three Distinct Strains of Prion Disease. *PLoS One* **8**, e68062 (2013).

781. Koizumi, S., Ohsawa, K., Inoue, K. & Kohsaka, S. Purinergic receptors in microglia: Functional modal shifts of microglia mediated by P2 and P1 receptors. *Glia* **61**, 47–54 (2013).

782. Bar, I. *et al.* Knockout Mice Reveal a Role for $P2Y_6$ Receptor in Macrophages, Endothelial Cells, and Vascular Smooth Muscle Cells. *Mol. Pharmacol.* **74**, 777–784 (2008).

783. Ben Addi, A., Cammarata, D., Conley, P. B., Boeynaems, J.-M. & Robaye, B. Role of

the P2Y 12 Receptor in the Modulation of Murine Dendritic Cell Function by ADP. *J. Immunol.* **185**, 5900–5906 (2010).

784. Muniz, V. S. *et al.* Purinergic P2Y12 Receptor Activation in Eosinophils and the Schistosomal Host Response. *PLoS One* **10**, e0139805 (2015).

785. Liao, F., Yoon, H. & Kim, J. Apolipoprotein e metabolism and functions in brain and its role in Alzheimer's disease. *Current Opinion in Lipidology* **28**, 60–67 (2017).

786. Jagust, W. Is amyloid-β harmful to the brain? Insights from human imaging studies. *Brain* **139**, 23–30 (2016).

787. Pirttilä, T. *et al.* Apolipoprotein E (apoE) levels in brains from Alzheimer disease patients and controls. *Brain Res.* **722**, 71–77 (1996).